

CR 114631
AVAILABLE TO THE PUBLIC

FINAL REPORT

EFFECTIVENESS EVALUATION OF STOL
TRANSPORT OPERATIONS

by

Ellis F. Hitt, Juergen M. H. Bruckner,
Vincent J. Drago, Ronald A. Brown,
Fred G. Rea and Richard F. Porter

February 20, 1973

Prepared under Contract No. NAS2-6889 by
BATTELLE
Columbus Laboratories
505 King Avenue
Columbus, Ohio 43201

for

AMES RESEARCH CENTER
NATIONAL AERONAUTICS AND SPACE ADMINISTRATION

TABLE OF CONTENTS

	Page
SUMMARY	1
INTRODUCTION	2
Study Ground Rules	3
NASA Study Ground Rules	3
METHODOLOGY DEVELOPMENT	5
Overall STOL OPS Concept and Computational Methods	5
Deterministic Models	9
Airport Model	9
Powered-Lift STOL Performance Model	11
Expected Value Models	14
Aircraft Navigation, Guidance, and Control Variance	
Analysis Model	14
Reliability Model	17
Maintainability Model	18
Monte Carlo Model	21
Definition of Operational Environment	22
Route Network Connecting City Pairs Served	22
Phases of Flight	32
Schedule	37
Externally Blown Flap STOL Aircraft	37
Air Traffic Mix and Density	37
Air Traffic Control	43
Navigation Aids	47
Weather	50
Mission Performance Measures	50
User Categories and Assumed Information Needs	50
STOL Mission Performance Measures	56
Mission Performance Goals	57
Systems Functions, Subfunctions, and Modes	59
Navigation, Guidance, Control Subfunctions	61
Takeoff/Landing	64
Climbout/Approach	64
Cruise	64
Hazard Avoidance	64
Communications	64
Systems Management	64
Constraints	65
Aircraft	65
Airport	65
Approach/Landing Performance Limits	65
Causes of Excessive Deviations	66

TABLE OF CONTENTS
(Continued)

	Page
Present Performance Monitoring Methods	67
Implementation of Monitors in the Simulation	67
Lateral Constraint Limits	67
Vertical Constraint Limits	67
Horizontal Position Time/Control	67
MLS Acquisition Window	67
Navigation Aids	71
ATC Standards and Operating Procedures	71
Airline Imposed Constraints	71
Development of Base-Line Functional Requirements and Initial System Operating Procedures	73
Base-Line Avionics Configuration	73
State Estimation Function	91
Command Generation/Execution Functions	95
Hazard Avoidance Function	95
Communication Function	95
Systems Management Function	95
Safe Flight Function	95
Implementation of Functions in Monte Carlo Program	102
Man-Machine Task Allocations	102
Takeoff/Climb	102
Cruise	103
Final Approach/Landing	103
Commonalities Among Mission Phases	106
Division of Crew Duties	106
Mode Selection	111
Base-line Modes Switching Logic	111
System Operating Procedures	112
Details of Information Flow With STOL OPS	114
Input	114
Nominal Flight	114
Monte Carlo	114
Output	114
SAMPLE RESULTS FROM APPLICATION OF STOL OPS TO CANDIDATE STOL SYSTEM CONFIGURATION	123
ANGCAP Results	123
STOL OPS Monte Carlo Results	140
Case 1	140
Case 2	146
Case 3	146
Case 4	146
Examples of Experiments Needed Based on Limited STOL OPS Applications	159

TABLE OF CONTENTS
(Continued)

	Page
CONCLUDING REMARKS160
RECOMMENDATIONS161
REFERENCES164

APPENDIX A

OPERATIONAL ENVIRONMENT166
Airport Model166
Landing168
Taxi Into Gate Area168
Refuel168
Passenger Enplanement168
Cargo Load/Unload168
Taxi Out to Takeoff Runway168
Takeoff168
Weather168
Traffic Forecast Development169
Development of 1980 Air Traffic Forecast for San Jose Municipal170
Development of 1980 Air Traffic Forecast for Sacramento Executive172
Development of 1980 Air Traffic Forecast for Orange County175
Airport Capacity Model178
Capacity Model Computer Code179
REFERENCES184

APPENDIX B

POWERED LIFT STOL PERFORMANCE MODEL185
Nomenclature185
Description188
Input Data200
Discrete Parameters200
Data Tables200
Output208

APPENDIX C

AIRCRAFT NAVIGATION ERROR ANALYSIS210
Analysis for Continuous Systems213

TABLE OF CONTENTS
(Continued)

	Page
Analysis for Discrete Systems219
Measurement Error Models222
VOR Error Model222
DME Error Model222
Air Data System Error Models223
MLS Error Model232
REFERENCES233

APPENDIX D

GUIDANCE/CONTROL FUNCTIONS ANALYSIS234
REFERENCES238

APPENDIX E

AIRCRAFT NAVIGATION GUIDANCE CONTROL ANALYSIS PROGRAM (ANGCAP)	
DESCRIPTION AND EXAMPLE OF RESULTS239
Program Description239
Linear Models240
Input Data Description240
Radio Navigation Aids242
Microwave Landing System Definitions242
Default Data Values242
En Route Waypoints244
Determination of Waypoints For Transition to Final	
Approach and Landing247
Turn Onto Common Path Maneuver247
Sidestep Maneuver251
Approach Waypoints260
Typical ANGCAP Output261
Detailed Cruise Output261
REFERENCES279

APPENDIX F

CREW PERFORMANCE280
Review of Crew Performance Estimation Methods280
REFERENCES283

TABLE OF CONTENTS
(Continued)

Page

LIST OF FIGURES

FIGURE 1.	STOL OPS ROUTINE FLOW DIAGRAM.	5
FIGURE 2.	FLOW CHART OF A MONTE CARLO SIMULATION BETWEEN TWO SUCCESSIVE DECISION POINTS	7
FIGURE 3.	NUMBER OF MONTE CARLO RUNS VERSUS CONFIDENCE LEVEL WHERE THE MAXIMUM ALLOWABLE DIFFERENCE BETWEEN THE TRUE AND ESTIMATED PROBABILITIES IS 5 PERCENT OF n/N	8
FIGURE 4.	INTERRELATIONSHIP OF MAJOR STOL OPS MODELS	10
FIGURE 5.	CLIMB PROFILES	15
FIGURE 6.	COMPARISON OF BETA AND EXPONENTIAL PROBABILITY DENSITY FUNCTIONS.	20
FIGURE 7a.	FRONT OF FAA AIRPORT MASTER RECORD FOR SAN JOSE MUNICIPAL.	23
FIGURE 7b.	BACK OF FAA AIRPORT MASTER RECORD FOR SAN JOSE MUNICIPAL.	24
FIGURE 8a.	FRONT OF FAA AIRPORT MASTER RECORD FOR SACRAMENTO EXECUTIVE.	25
FIGURE 8b.	BACK OF FAA AIRPORT MASTER RECORD FOR SACRAMENTO EXECUTIVE.	26
FIGURE 9a.	FRONT OF FAA AIRPORT MASTER RECORD FOR ORANGE COUNTY	27
FIGURE 9b.	BACK OF FAA AIRPORT MASTER RECORD FOR ORANGE COUNTY	28
FIGURE 10.	INPUT DATA DESCRIBING SAN JOSE MUNICIPAL (SJC) AIRPORT.	29
FIGURE 11.	INPUT DATA DESCRIBING SACRAMENTO EXECUTIVE (SAC) AIRPORT.	30
FIGURE 12.	INPUT DATA DESCRIBING ORANGE COUNTY (SNA) AIRPORT.	31
FIGURE 13.	PREFLIGHT/TAXI-OUT/TAKEOFF CLIMB FLIGHT PHASES	33
FIGURE 14.	TYPICAL CRUISE PHASE HORIZONTAL FLIGHT PLAN.	35
FIGURE 15.	APPROACH/LANDING FLIGHT PLAN	36
FIGURE 16.	TAXI-IN FLIGHT PHASE	37
FIGURE 17.	MISSION PROFILE - SINGLE FLIGHT LEG.	39
FIGURE 18.	INPUT DATA DESCRIBING SCHEDULE AND FLIGHT PATH	40
FIGURE 19.	GROUND TRACK OF NOMINAL VFR FLIGHT PATH FOR ROUTE NETWORK.	41
FIGURE 20.	DOUGLAS EBF STOL	42
FIGURE 21.	FORECAST OF 1980 DAILY AIR TRAFFIC OPERATIONS BY TYPE AND TIME OF DAY FOR SAN JOSE MUNICIPAL (SJC)	44

LIST OF FIGURES
(Continued)

	Page
FIGURE 22. FORECAST OF 1980 DAILY AIR TRAFFIC OPERATIONS BY TYPE AND TIME OF DAY FOR SACRAMENTO EXECUTIVE (SAC) .	45
FIGURE 23. FORECAST OF 1980 DAILY AIR TRAFFIC OPERATIONS BY TYPE AND TIME OF DAY FOR ORANGE COUNTY (SNA).	46
FIGURE 24. FLIGHT PHASES AND AIR TRAFFIC CONTROL FUNCTIONS . . .	48
FIGURE 25. RADIO NAVIGATION GROUND STATION DATA.	49
FIGURE 26. BLOCK DIAGRAM OF NAVIGATION GUIDANCE, AND CONTROL FUNCTION INTERACTIONS	62
FIGURE 27. LATERAL CONSTRAINT LIMITS	69
FIGURE 28. VERTICAL CONSTRAINT LIMITS.	70
FIGURE 29. BLOCK DIAGRAM DEPICTING MAJOR ELEMENTS AND INTER-ACTIONS OF AN ADVANCED STOL AVIONICS SYSTEM	79
FIGURE 30. LISTING OF INPUT DATA FOR STOL AIRCRAFT AND ONBOARD SYSTEMS	80
FIGURE 31. STATE ESTIMATION FUNCTION SUBFUNCTIONS AND MODES. . .	92
FIGURE 32. COMMAND GENERATION/EXECUTION FUNCTION SUBFUNCTIONS AND MODES	96
FIGURE 33. HAZARD AVOIDANCE FUNCTION SUBFUNCTIONS AND MODES. . .	97
FIGURE 34. COMMUNICATION FUNCTION SUBFUNCTIONS AND MODES . . .	99
FIGURE 35. SYSTEMS MANAGEMENT FUNCTION SUBFUNCTION AND MODES . .	100
FIGURE 36. SAFE FLIGHT FUNCTION.	101
FIGURE 37. TIME LINE HISTORY OF ANTICIPATED SYSTEM CONTROL ACTIVITY DURING TAKEOFF	104
FIGURE 38. TIME HISTORY OF ANTICIPATED CONTROL ACTIVITY DURING LANDING.	107
FIGURE 39. PREFLIGHT MONTE CARLO ROUTINE	115
FIGURE 40. TAXI-OUT MONTE CARLO ROUTINE.	116
FIGURE 41. TAKE OFF MONTE CARLO ROUTINE.	117
FIGURE 42. CLIMB MONTE CARLO ROUTINE	117
FIGURE 43. EN ROUTE MONTE CARLO ROUTINE.	118
FIGURE 44. LANDING MONTE CARLO ROUTINE	119
FIGURE 45. MONTE CARLO VARIABLES	121
FIGURE 46. MONTE CARLO EVENTS.	122
FIGURE 47. MONTE CARLO MODE USAGE.	122
FIGURE 48. SAMPLE PORTION OF ONE PAGE OF ANGCAP OUTPUT DURING FLIGHT FROM SAN JOSE TO SACRAMENTO.	124
FIGURE 49. SUMMARY RESULTS OUTPUT FROM ANGCAP KALMAN FILTER UPDATE.	126
FIGURE 50. NOMINAL GROUND TRACK OF IFR FLIGHT PATH FOR CASES 1, 7, and 13 of FIGURE 49	127

LIST OF FIGURES
(Continued)

		Page
FIGURE 51.	NOMINAL GROUND TRACK OF IFR FLIGHT PATH AND ESTIMATED CROSSTRACK DEVIATION FOR KALMAN FILTER UPDATE	128
FIGURE 52.	PLOT OF 4 NM AIRWAY WIDTH AND 3σ CROSSTRACK ACTUAL DEVIATION FOR KALMAN FILTER UPDATE USING $\rho/\theta, \rho$ MEASUREMENTS	129
FIGURE 53.	PLOT OF NOMINAL IFR FLIGHT PATH AND 3σ CROSSTRACK ESTIMATED DEVIATION FOR KALMAN FILTER UPDATE USING $\rho/\theta, \theta$ MEASUREMENTS.	131
FIGURE 54.	PLOT OF 4 NM AIRWAY WIDTH AND 3σ CROSSTRACK ACTUAL DEVIATION FOR KALMAN FILTER UPDATE USING ρ, ρ MEASUREMENTS	132
FIGURE 55.	PLOT OF NOMINAL IFR FLIGHT PATH AND 3σ CROSSTRACK ACTUAL DEVIATION FOR KALMAN FILTER UPDATE USING ρ/θ MEASUREMENTS	133
FIGURE 56.	PLOT OF NOMINAL IFR FLIGHT PATH AND 3σ CROSSTRACK ESTIMATED DEVIATION FOR POSITION FIX UPDATE USING ρ/θ MEASUREMENTS	134
FIGURE 57.	SUMMARY RESULTS OUTPUT FROM ANGCAP FOR KALMAN FILTER UPDATE	135
FIGURE 58.	PLOT OF NOMINAL IFR FLIGHT PATH AND 3σ CROSSTRACK ESTIMATED DEVIATION FOR KALMAN FILTER UPDATE USING, θ, θ MEASUREMENTS	136
FIGURE 59.	PLOT OF 3σ CROSSTRACK ACTUAL AND ESTIMATED DEVIATIONS FOR POSITION FIX UPDATE USING θ MEASUREMENT.	137
FIGURE 60.	PLOT OF 4 NM AIRWAY WIDTH AND 3σ CROSSTRACK ACTUAL DEVIATION FOR KALMAN FILTER UPDATE USING ρ MEASUREMENT.	138
FIGURE 61.	PLOT OF 4 NM WIDE AIRWAY AND 1σ CROSSTRACK ACTUAL DEVIATION USING NO EXTERNAL MEASUREMENTS.	139
FIGURE 62.	EXAMPLE OF STOL OPS RESULTS FOR NOMINAL DEMONSTRATION CASE	143
FIGURE 63.	EXAMPLE OF STOL OPS RESULTS FOR NOMINAL DEMONSTRATION CASE WITH NO IN ROUTE WINDS	153
FIGURE 64.	EXAMPLE OF STOL OPS RESULTS FOR NOMINAL DEMONSTRATION CASE ASSUMING 100% IFR WEATHER.	155
FIGURE 65.	EXAMPLE OF STOL OPS RESULTS FOR DEMONSTRATION CASE WITH INCREASE OF SNA VFR CAPACITY TO 140 MOVEMENTS/HOUR	157

LIST OF FIGURES
(Continued)

Page

APPENDIX A

FIGURE A-1. INPUT DATA FOR A TYPICAL AIRPORT 167
FIGURE A-2. FORECAST OF 1980 DAILY AIR TRAFFIC OPERATIONS
BY TYPE AND TIME OF DAY FOR SAN JOSE MUNICIPAL(SJC). 173
FIGURE A-3. FORECAST OF 1980 DAILY AIR TRAFFIC OPERATIONS
BY TYPE AND TIME OF DAY FOR SACRAMENTO EXECUTIVE
(SAC). 174
FIGURE A-4. FORECAST OF 1980 DAILY AIR TRAFFIC OPERATIONS BY
TYPE AND TIME OF DAY FOR ORANGE COUNTY (SNA) 176
FIGURE A-5. EXAMPLE OF CAPACITY MODEL RESULTS FOR SNA. 180

APPENDIX B

FIGURE B-1. FLOW CHART OF SUBROUTINE ARCFT 191
FIGURE B-2. FLOW CHART FOR SUBROUTINE ATMS 193
FIGURE B-3. FLOW CHART FOR FUNCTION FULFLO 193
FIGURE B-4. FLOW CHART FOR FUNCTION AFC. 193
FIGURE B-5. SAMPLE PAGE OF TYPICAL OUTPUT FROM SUBROUTINE
ARCFT. 209

APPENDIX C

FIGURE C-1. TYPICAL AIR DATA COMPUTATION 226
FIGURE C-2. ERROR IN ALTITUDE VERSUS PRESSURE ERROR. 230

APPENDIX E

FIGURE E-1. DESCRIPTION OF THE AIRPORTS, RADIO NAVIGATION AIDS,
AND MLS SYSTEMS. 241
FIGURE E-2. DEFAULT VALUES 245
FIGURE E-3. NAVIGATION ERROR COEFFICIENTS. 246
FIGURE E-4. CRUISE (EN ROUTE) WAYPOINTS. 248
FIGURE E-5. VERTICAL AND HORIZONTAL PLANE FLIGHT PROFILES
IN TERMINAL AREA 249
FIGURE E-6. HORIZONTAL INTERCEPT GEOMETRY. 250
FIGURE E-7. TURN INITIATION HORIZONTAL PLANE COORDINATES FOR
RT = 1335 FEET AND INTERCEPT ANGLES SHOWN. 253

LIST OF FIGURES
(Continued)

	Page
FIGURE E-8a. GENERALIZED ROLL TURN MANEUVER	254
FIGURE E-8b. COMPONENTS OF CORRECTIVE TURN MANEUVER (REFERENCE E-1)	254
FIGURE E-9. EXAMPLE OF MLS ACQUISITION AND TURN ONTO COMMON PATH.	256
FIGURE E-10. PUSHOVER MANEUVER	257
FIGURE E-11a. SAMPLE OF ANGCAP OUTPUT FOR LEG 1, CASE 1	262
FIGURE E-12. SUMMARY OF SAMPLE ANGCAP OUTPUT OF FIGURE E-11.	274
FIGURE E-13. SUMMARY OF ANGCAP OUTPUT FOR ALL LEGS--FIVE KALMAN FILTER UPDATES AND ONE POSITION FIX UPDATE	275
FIGURE E-13b. SUMMARY OF ANGCAP OUTPUT FOR ALL LEGS--TWO KALMAN FILTER UPDATES AND THREE POSITION FIX UPDATES	276

LIST OF TABLES

	Page
TABLE 1. COMPUTED AIRCRAFT PERFORMANCE PARAMETERS AS A FUNCTION OF FLIGHT MODE INDICATOR	13
TABLE 2. PERCENTAGE FREQUENCY OF WIND DIRECTION AND SPEED	51
TABLE 3. CEILING VERSUS VISIBILITY	52
TABLE 4. SUBCATEGORIES OF PUBLIC SECTOR.	53
TABLE 5. SUBCATEGORIES OF PRIVATE SECTOR	55
TABLE 6. DEFINITION OF MAJOR STATE VECTORS	60
TABLE 7. COMBINATIONS OF SUBFUNCTIONS FOR NAVIGATION, GUIDANCE, AND CONTROL	63
TABLE 8. ALTITUDE AND DISTANCE LIMITATIONS	72
TABLE 9. EQUIPMENT REQUIRED FOR IFR DISPATCH (FAR PARTS 25.1303 and 121.303).	74
TABLE 10. AIRBORNE EQUIPMENT REQUIREMENTS CATEGORIES I AND II	75
TABLE 11. BASELINE STOL AVIONICS.	76
TABLE 12. ATA 100 SYSTEM LISTING.	87
TABLE 13. ATA SUBSYSTEM LISTING	89
TABLE 14. INFORMATION REQUIREMENTS FOR CRUISE PHASE	105
TABLE 15. SUMMATION OF PARAMETERS CONTROLLED IN THE FLIGHT PHASES.	108
TABLE 16. DIVERSION OF CREW DUTIES FOR CATEGORY I OR VFR WEATHER	109
TABLE 17. DIVISION OF CREW DUTIES FOR CATEGORY II or III WEATHER APPROACH AND	110
TABLE 18. SUGGESTED EXERCISE	162
TABLE 19. SUGGESTED TASKS	163

APPENDIX B

TABLE B-1. MAXIMUM LIFT COEFFICIENT VERSUS MACH NUMBER FOR FLAPS UP.	200
TABLE B-2. MAXIMUM NET THRUST AS A FUNCTION OF MACH NUMBER AND ALTITUDE.	201
TABLE B-3. MINIMUM NET THRUST AS A FUNCTION OF MACH NUMBER AND ALTITUDE.	201
TABLE B-4. PROFILE DRAG COEFFICIENT VERSUS MACH NUMBER FLAPS UP.	202
TABLE B-5. $\frac{\partial C_D}{\partial C_L}$ - VERSUS MACH NUMBER, FLAPS UP.	202
TABLE B-6. $\frac{\partial C_D}{\partial C_L^2}$ - VERSUS MACH NUMBER, FLAPS UP.	203

LIST OF TABLES

	Page
TABLE B-7. NORMALIZED FUEL FLOW AS A FUNCTION OF MACH NUMBER AND NORMALIZED NET THRUST	203
TABLE B-8. MAXIMUM GROSS THRUST VERSUS TRUE AIRSPEED	204
TABLE B-9. MINIMUM GROSS THRUST VERSUS TRUE AIRSPEED	204
TABLE B-10. RATIO OF RAM DRAG COEFFICIENT TO GROSS THRUST COEFFICIENT, AS A FUNCTION OF TRUE AIRSPEED	204
TABLE B-11. LANDING CONFIGURATION ANGLE OF ATTACK AS A FUNCTION OF LIFT COEFFICIENT AND GROSS THRUST COEFFICIENT. . .	205
TABLE B-12. GROSS AXIAL FORCE COEFFICIENT AS A FUNCTION OF GROSS THRUST AND ANGLE OF ATTACK, LANDING CONFIGURATION . .	205
TABLE B-13. TAKE-OFF CONFIGURATION ANGLE OF ATTACK AS A FUNCTION OF LIFT COEFFICIENT AND GROSS THRUST COEFFICIENT. . .	206
TABLE B-14. GROSS AXIAL FORCE COEFFICIENT AS A FUNCTION OF GROSS THRUST COEFFICIENT AND ANGLE OF ATTACK, TAKEOFF CONFIGURATION	206
TABLE B-15. MAXIMUM LIFT COEFFICIENT IN THE LANDING CONFIGURATION AS A FUNCTION OF GROSS THRUST COEFFICIENT	207
TABLE B-16. MAXIMUM LIFT COEFFICIENT IN THE TAKEOFF CONFIGURATIONS AS A FUNCTION OF GROSS THRUST COEFFICIENT	207
TABLE B-17. GROSS THRUST COEFFICIENT REQUIRED TO ATTAIN SPECIFIED MAXIMUM LIFT COEFFICIENT, LANDING CONFIGURATION . . .	207
TABLE B-18. GROSS THRUST COEFFICIENT REQUIRED TO ATTAIN SPECIFIED MAXIMUM LIFT COEFFICIENT, TAKEOFF CONFIGURATION . . .	208
TABLE B-19. LIFT COEFFICIENT DURING GROUND ROLL, IN TAKEOFF CONFIGURATION, AS A FUNCTION OF GROSS THRUST COEFFICIENT	208

APPENDIX C

TABLE C-1. TYPICAL BAROMETRIC ALTIMETER ERROR MODELS	228
--	-----

LIST OF TABLES

Page

APPENDIX E

TABLE E-1.	TYPICAL TURN INITIATION COORDINATES REFERENCED TO COMMON PATH WAYPOINT.	252
TABLE E-2.	TYPICAL RESULTS RELATING TURN INITIATION AND MLS ACQUISITION	257
TABLE E-3.	EXAMPLE OF FINAL APPROACH WAYPOINTS WITH 90° INTERCEPT	260

B

EFFECTIVENESS EVALUATION OF STOL TRANSPORT OPERATIONS

By Ellis F. Hitt, Juergen M. H. Bruckner,
Vincent J. Drago, Ronald A. Brown,
Fred G. Rea, Richard F. Porter

BATTELLE
Columbus Laboratories

SUMMARY

A short-takeoff and landing (STOL) systems simulation model has been developed and implemented in a computer code (known as STOL OPS) which permits evaluation of the operation of a STOL aircraft and its avionics in a commercial airline operating environment. STOL OPS concentrates on the avionics functions of navigation, guidance, control, communication, hazard avoidance, and systems management. External world factors influencing the operation of the STOL aircraft include each airport and its geometry, air traffic at each airport, air traffic control equipment and procedures, weather (including winds and visibility), and the flight path between each airport served by the route.

The development of the STOL OPS program provides NASA a set of computer programs which can be used for detailed analysis of a STOL aircraft and its avionics and permit establishment of system requirements as a function of airline mission performance goals. While the principal thrust of the effort reported herein was development of the STOL OPS program, tentative results are presented for the California corridor scenario used to check out the program.

Extensive exercise cases must be run for a wide variety of STOL scenarios prior to specification of conclusive system criteria. The tentative results derived with the present version of the STOL OPS program have indicated need for additional experimental and modelling effort. Substantial effort should be devoted to establishment and maintenance of a data bank for avionics subsystems.

INTRODUCTION

The objective of this project was to develop and apply an overall STOL systems simulation model to assist in developing the data base needed to establish systems criteria and operational procedures for STOL transport operations. The focus of the simulation effort was on avionics functions such as navigation, guidance, control, and flight management in an airline route operation. The multiplicity of applicable STOL system concepts and the related functions, performance criteria, and specifications preclude sole dependence on an experimental approach because of the great number of points that would be required. Experiments will be costly and must be used selectively in those areas or directions shown by analysis and simulation to be the most promising. The present simulation will permit the assessment of various STOL avionics configurations, air traffic control equipment and standards, and operational procedures, and assist in the identification of developmental alternatives which are most suitable for their particular technological and operational application in the existing political and economic environment.

Material relevant to STOL transportation was carefully reviewed to ascertain the parameters necessary to characterize the operational environment and the interactions of the STOL aircraft with its environment. Previous success in the development of an avionics system simulation model and a computer program that implemented this model (ref. 1) suggested to NASA that this previously developed avionics system simulation model could be adapted to permit application to the STOL mission. The adaptation involved removal of certain deterministic and stochastic system models and development of others. These mathematical models, and the computer programs that implement them, permit evaluation of the mission performance of a single STOL aircraft and its avionics in a realistic environment descriptive of the mission being simulated.

The simulation tools have been developed to permit detailed simulation of the specific STOL aircraft of interest as it operates over a route network typical of that expected for a commercial STOL operation. The interaction of that aircraft with the external world and the internal functions required to fly that aircraft are simulated in detail. The external world factors include: each airport and its geometry; the operation of other aircraft at each airport; air traffic control equipment, procedures, and standards; weather, including visibility and winds; the flight path between each airport served by the route; and other factors. Each of these external world factors is described in detail in this report. Internal to the aircraft being simulated in detail are the avionics system functions of navigation, guidance, control, communications, hazard avoidance, and systems management. In addition, the details of factors necessary for flight of the aircraft including inflight procedures and ground servicing procedures

are simulated.

The development of the STOL Operations (STOL OPS) computer program provides NASA a set of computer programs which can be used for detailed analysis of a STOL aircraft and its avionics and permit establishment of system requirements as a function of airline mission performance goals. While the principal thrust of the effort reported herein was development of the STOL OPS program, tentative results are presented for the scenario used to check out the program. Extensive exercise cases must be run for a wide variety of STOL scenarios prior to specification of conclusive system criteria. The tentative results derived with the present version of the STOL OPS program have indicated need for additional experimental and modelling effort. The present version of the program and hence the results are a function of the study ground rules.

Study Ground Rules

The ground rules used for this study were mutually agreed upon by NASA Ames Research Center and Battelle, and are based on associated NASA studies and experience.

NASA Study Ground Rules.-The STOL aircraft to be simulated is a 100 passenger externally blown flap vehicle designed for a 2,000 foot field length (ref. 2).

The time frame and the initial definition of the operational environment to be considered should be 1980. The air traffic environment is forecast for that time frame. Assumptions were made that only minimal airport configuration changes from present day configurations would occur before 1980, that the ATC radio navigation aids would be unchanged from their present locations and performance, and that the microwave landing system (MLS), SC-117 Configuration G (ref. 3), would be operational at each of the airports.

The scenario assumed for development of the simulation was service in the California corridor. This service was assumed to be between San Jose Municipal Airport (SJC), Sacramento Executive Airport (SAC), and Orange County Airport (SNA) at Santa Ana.

Weather in 1980 was assumed to be similar to historical weather data available for each of the sites under consideration.

ATC rules and procedures were assumed to be virtually identical to present day standards. Also, it was assumed that area navigation (RNAV) would be approved for operational usage.

Current airborne equipment requirements for Categories I and II operation (ref. 4) were assumed to apply. It was further assumed that avionics and operating procedures covered by Federal Air Regulations, Part 25 and Part 121 (refs. 5 and 6) would still apply.

METHODOLOGY DEVELOPMENT

Overall STOL OPS Concept and Computational Methods

The STOL Operations (STOL OPS) program developed in this study is made up of a number of computer routines that implement various mathematical models necessary for the simulation of STOL transport operations. These models include deterministic models and stochastic system models. The stochastic system models include both expected value models and Monte Carlo models. A simple diagram illustrating the basic operations of the STOL Operations (STOL OPS) computer program is depicted in Figure 1.

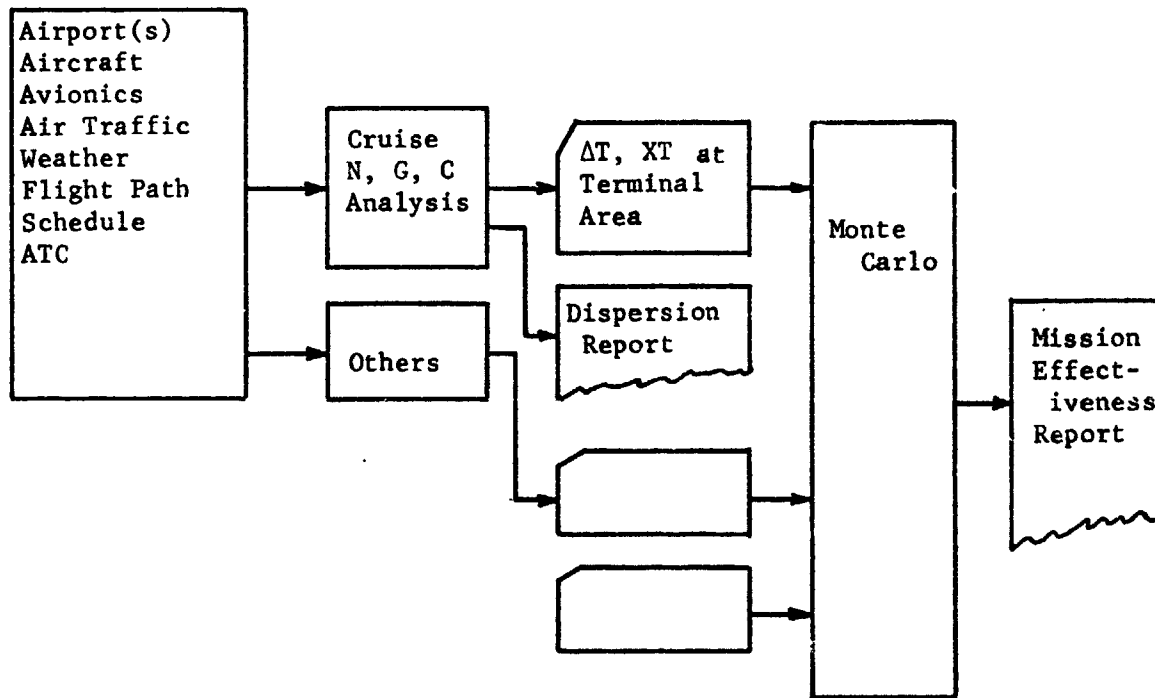


FIGURE 1. STOL OPS ROUTINE FLOW DIAGRAM

Input data describing the airports, the aircraft being simulated, its avionics, the air traffic, the weather, the flight path flown, the aircraft's operation schedule, and the air traffic control equipment, procedures, and standards are processed to provide various reports. Some of this processing is performed by intermediate programs such as the Aircraft Navigation Guidance Control Analysis Program (ANGCAP). These intermediate programs produce individual reports as well as preprocessed data utilized in the Monte Carlo simulation routine.

The mission effectiveness report depicted in Figure 1 is the principal output of the STOL OPS Program. This report presents the results of the evaluations of the STOL aircraft and its avionics and associated operating procedures for the operational environment being simulated. The effectiveness evaluation consists of the statistical results representing various mission performance measures, discussed in a later section of this report, as processed by the logic implemented in the Monte Carlo routines.

The advantage of the Monte Carlo method is that it can readily handle systems of large dimensions, which also involve complex decision logic. The decision logic can be made to correspond with that involved in the actual flight of the aircraft. In addition, no linearizing assumptions are needed, no sophisticated mathematics are required in formulating the analysis planned, and the analogy between the computational algorithm and the physical event being simulated is quite direct. The major disadvantage of the Monte Carlo method is that the simulation of complex situations may be very costly in computer time, especially if a high confidence level in the results is desired for remote events.

Conceptually, the Monte Carlo method is straightforward when applied to the type of simulation being considered in this study. All the conditions that prevail on a mission or flight leg, or at least their appropriate descriptive statistical parameters, are known. Conceptually, the scenario is divided into series of small steps of time. At the end of each step, an assessment is made as to what stochastic event actually transpired during the elemental time span. On the basis of what occurred, the decision logic specifies the next course of action to be taken. This sequence of steps is illustrated in Figure 2. The whole procedure is then repeated a number of times. Results of each Monte Carlo run are binary events, i.e., either the event happened or did not happen. For example, in any given Monte Carlo run, either the aircraft is dispatched or the flight is cancelled. The probability of an event is given by the ratio n/N where N is the number of Monte Carlo runs and n is the number of times the event occurred in N trials. The number of runs, N , necessary to obtain a given accuracy with a desired confidence level is a function that can be computed by integrating the Gaussian distribution (ref. 7) if both n and $N - n$ are greater than the number 5 and N is greater than the number 30. Typical results for a range of confidence levels and for a maximum allowable error of 5% of n/N are shown in Figure 3.

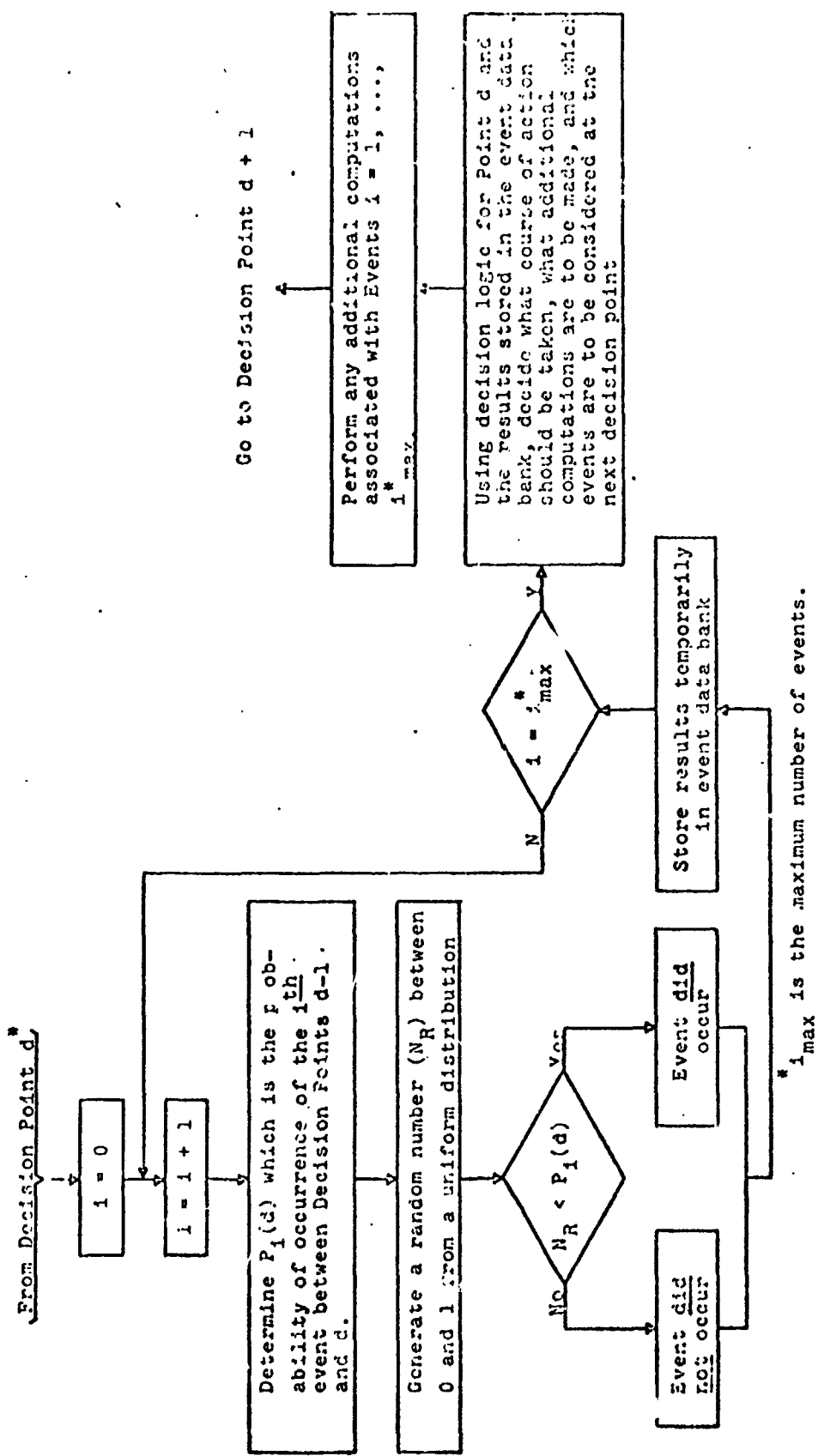


FIGURE 2. FLOW CHART OF A MONTE CARLO SIMULATION BETWEEN TWO SUCCESSIVE DECISION POINTS

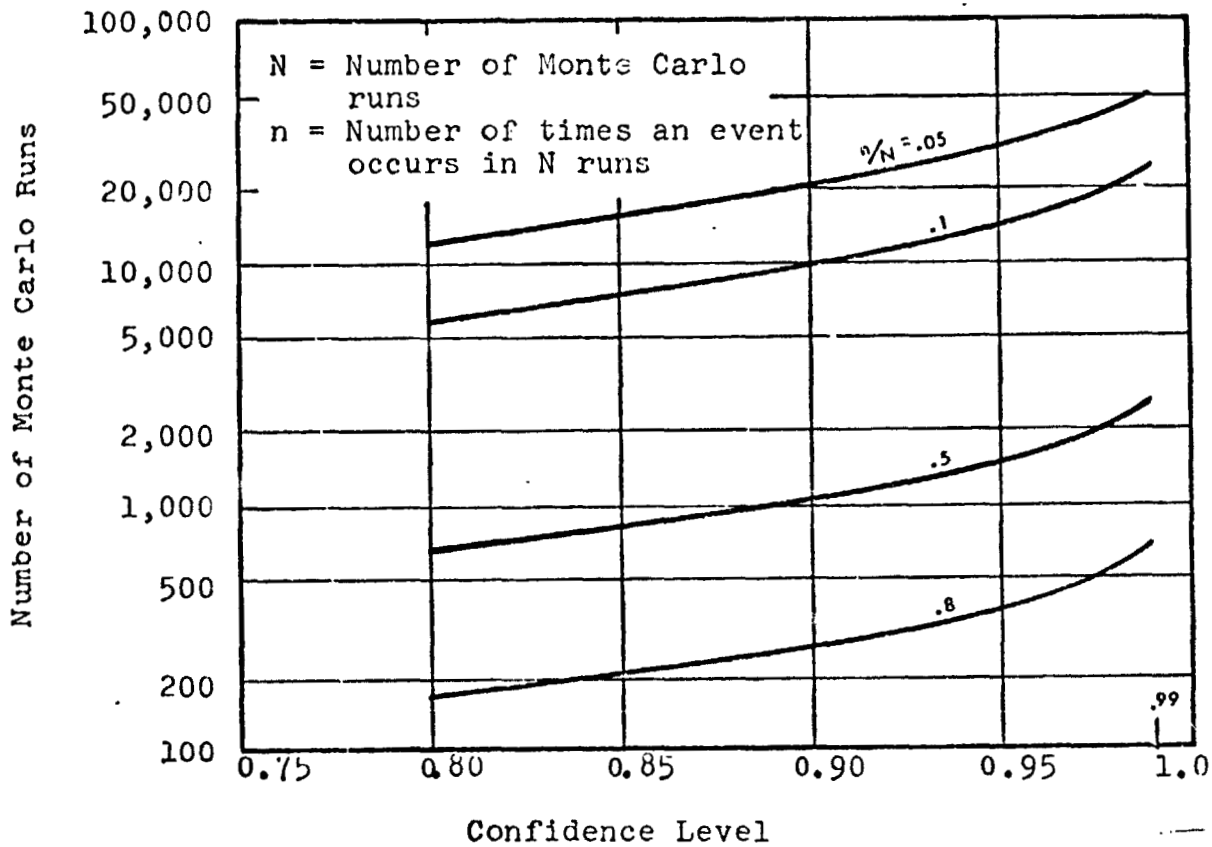


FIGURE 3. NUMBER OF MONTE CARLO RUNS VERSUS CONFIDENCE LEVEL WHERE THE MAXIMUM ALLOWABLE DIFFERENCE BETWEEN THE TRUE AND ESTIMATED PROBABILITIES IS 5 PERCENT OF n/N

It can be seen from Figure 3 that it will usually require between 1,000 and 10,000 Monte Carlo runs to obtain reasonable accuracies at a high confidence level (say greater than 90%). In a complex scenario, the number of decision points in each Monte Carlo run may be of the order of 50 per flight leg. If the calculation associated with a decision point are lengthy, then the computer cost involved with one simulation can become quite significant. One obvious manner in which computational time per Monte Carlo run can be reduced is to precalculate the $P_i(d)$ and the "additional computations" mentioned in Figure 2. These precalculated quantities are stored in a data bank and extracted at the appropriate time during a Monte Carlo run. The main objection to performing extensive calculations outside the Monte Carlo routine is that some of the flexibility in handling scenario's and/or decision logic associated with the avionics is lost. The alternatives allowed by the decision logic must be somewhat restrictive to prevent the storage requirements of the data bank utilized by the Monte Carlo routine from becoming excessive. In addition, the computer time involved in obtaining the precalculated quantities could become so great as to defeat the usefulness of this approach.

A more comprehensive description of the mathematical models and computation methodology follows. Figure 4 has been developed as an aid to the understanding of the interrelationships between the primary models.

Deterministic Models.-The principal deterministic models are the airport and powered lift STOL performance models. Each of these is briefly described below.

Airport Model: The airport model allows a detailed simulation of ground operations at any airport for which input data are provided. The input data are contained in three arrays. The first array contains the information that is needed to describe specific points of interest in the airport, e.g., runway endpoint, turnoff points, navigation aids locations, etc. Each point is described by user designated point number, and X and Y position. The X and Y position is relative to an origin at the control tower with a positive X axis east, and the positive Y axis north. A second array contains specific information for each runway, such as orientation, length, width, and turnoff points. The third array describes all the taxi paths between a runway and terminal building area. The airport model is made up of the following subroutines.

Landing: The landing routine is called at touchdown of the aircraft. Input to this routine is a runway designation, point of touchdown and aircraft touchdown weight. A constant deceleration of 10 ft/sec^2 is used to calculate runway time and distance required to slow down to the taxi velocity. Once it has been determined that the aircraft has reached a safe turnoff velocity, the aircraft will turn off onto the nearest taxiway. The distance and time from touchdown to turnoff will be calculated.

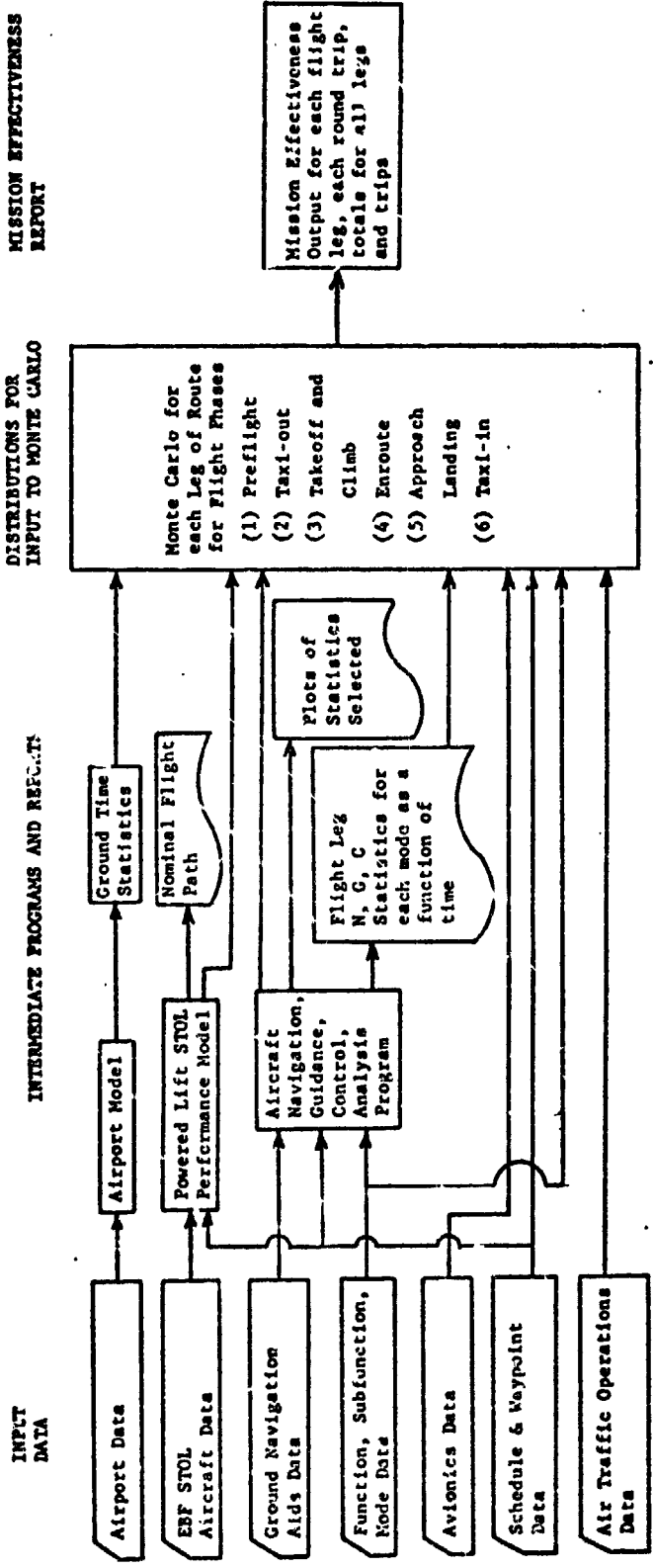


FIGURE 4. INTERRELATIONSHIP OF MAJOR STOL OPS MODELS

Taxi In: Based upon the turnoff that is chosen, the taxi-in routine describes the appropriate taxi path from data contained in the taxi array. The aircraft is assumed to taxi in at a constant velocity. Conflicts in intersections are not modelled.

Deplaning: The deplane routine calculates time consumed by passengers deplaning the aircraft. Once the aircraft has reached the gate, there is a set time delay to allow both the flight and ground crews time to prepare for deplanement. It is assumed that the passengers deplane at a constant rate while fueling is under way. Since deplaning time is less than fueling time, this routine has been omitted in the Monte Carlo. If fueling is not required at each stop, this routine is needed.

Fuel: The fuel required is determined from the nominal flight path. The time to refuel equals the pounds of fuel loaded divided by the fueling rate.

Boarding: The boarding routine calculates the time for passengers to board. It is assumed that passengers board in a 10-minute mean time with a 2-minute \log distribution.

Cargo Load/Unload: The cargo load routine assumes a 10-minute mean with a two minute \log distribution. It is further assumed that cargo can be loaded and unloaded during deplaning, fueling, and boarding. Therefore, the time to unload and load the cargo is compared to the time of these three events. If the load/unload time is greater than these three times and greater than the scheduled ground time, the additional time is calculated and a delay is attributed to cargo loading/unloading.

Taxi Out: The desired takeoff runway is provided as input data in the taxi-out routine and the appropriate taxi path to that runway is described from data in the taxi array. The taxi-out time is calculated in a manner similar to taxi-in time.

Takeoff: The takeoff routine calculates the time incurred during the takeoff phase. This includes runway-occupancy time and delays due to other traffic.

Detailed Description of Airport Models: The details involved in the development of equations comprising the airport models are contained in Appendix A of this report.

Powered-Lift STOL Performance Model: A computer routine has been developed to model the performance of the general class of powered-lift STOL transport aircraft. The input variables to this routine are:

H, altitude as a function of time
V, true airspeed as a function of time
W, weight
PHI, maximum bank angle
IF, an integer which denotes one of three possible flap deflections
GAM, flight path angle with respect to air mass (if appropriate)
VWDOT, head-on component of wind gradient
MI, an integer which identifies the desired operating mode.

The flight mode indicator, MI, has eight possible values and specifies output quantities to be computed as shown in Table 1.

Any segment of a desired flight profile can be computed by selecting the appropriate flight mode. The following paragraphs describe the manner in which each flight mode can be used.

If M=1 is selected, maximum thrust is determined from stored data as a function of Mach number and altitude and used to accelerate the aircraft along the selected flight path angle. MI=4 is similar, except that minimum thrust is implied.

If M=2 or 3 is selected, maximum available thrust is used while the equivalent airspeed (EAS) or Mach number, respectively, is held constant. The use of MI=5 or 6 is similar except that minimum thrust is employed.

Setting MI=7 or 8 implies flight at constant equivalent airspeed or Mach number, respectively, at a specified flight path angle (which can be zero for level cruise). The appropriate thrust setting is determined internally in the routine. If the desired path angle is beyond the performance capability of the aircraft, the specified flight path angle is disregarded and maximum performance is computed.

The flap configuration is determined by the value of the flap deflection integer, IF. Values of 0, 1 and 2 denote flaps up, takeoff flaps, and landing flaps, respectively. Takeoff flap settings are changed at 150 knots indicated airspeed. On approach, takeoff flap settings are used from 150 knots to V_{approach} at which time landing flap settings are used. For either of the latter two, the use of MI=7 or 8 requires an iteration on angle of attack and engine thrust to satisfy the lift coefficient and net axial force requirements for equilibrium. This iteration is automatically performed internally in the routine.

TABLE 1. COMPUTED AIRCRAFT PERFORMANCE PARAMETERS AS
A FUNCTION OF FLIGHT MODE INDICATOR

MI	Specified				Computed			
	GAM	Max Thrust	Min Thrust	Constant EAS	Constant Mach. No.	VDOT	WDOT	GAM
1	X	X				X	X	
2		X		X			X	X
3		X			X		X	X
4	X		X			X	X	
5			X	X			X	X
6			X		X		X	X
7	X			X			X	
8	X				X		X	

Figure 5 illustrates climb profiles computed with this routine for the McDonnell Douglas 100 passenger, 2000 feet field length, EBF airplane for two initial weights. For these sample calculations, the aircraft subroutine was used in conjunction with a standard integration routine.

Each time the aircraft performance routine is used, a check is made to insure that the required lift coefficient is within the capabilities of the aircraft for the flap position selected.

Analytical approximations are used for all atmospheric data to simulate standard conditions. For the aircraft data, 16 tables are used, although all of these are never required for any one selected operating mode and flap position.

Detailed presentation of the mathematical models comprising the aircraft performance routine are presented in Appendix B. This appendix lists the input data, the equations and flow logic, and typical output of this model. The powered-lift STOL performance model is used to generate the nominal flight path. The results of this nominal are used to define the nominal waypoints and flight times. The nominal flight times are computed only once and then stored for use by the Monte Carlo routine. The Monte Carlo routine then need only specify the segments over which the flight is to occur based upon the operating schedule and avionics availability. The nominal flight times for the segments are then immediately available to the Monte Carlo routine.

Expected Value Models.-The principal expected value models are the aircraft navigation, guidance, and control variance analysis, reliability, and maintainability models. Each of these are briefly described below.

Aircraft Navigation, Guidance, and Control Variance Analysis Model: Mathematical models have been derived to implement state estimation error analysis techniques and guidance/control analysis methods discussed in detail in Appendices C and D. The FORTRAN computer code implementing these models is discussed in detail in Appendix E. This code is executable as a separate program for detailed analysis studies. In addition to detailed printout, the code generates matrices for later access by the Monte Carlo program. Thus, the aircraft navigation, guidance, and control analysis code may be thought of as a separate program or a preprocessor to minimize execution time required in the large Monte Carlo code.

The user must supply data describing the location of the ground navigation aids and their performance as well as the flight path geometry of the aircraft with respect to each of these navigation stations. In addition,

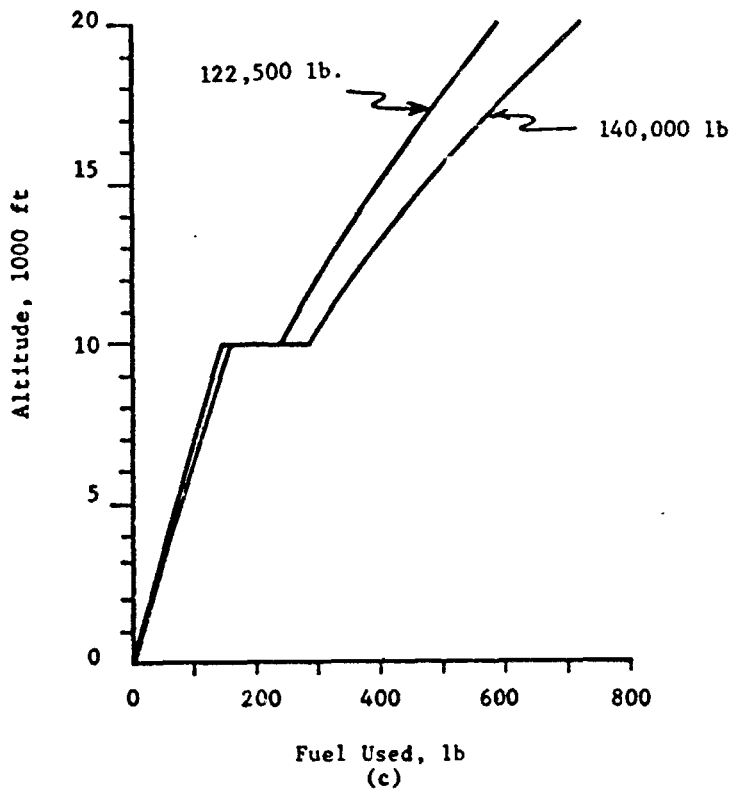
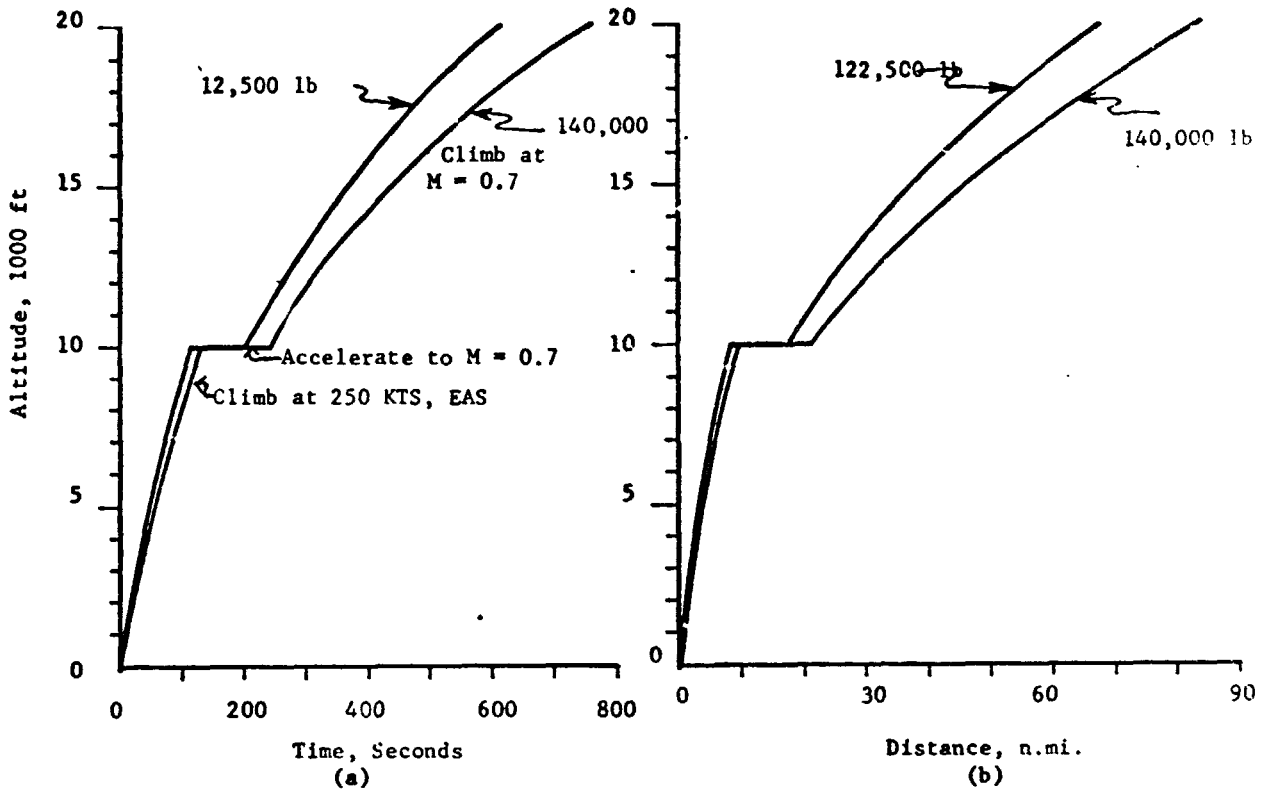


FIGURE 5. CLIMB PROFILES

the user must define the avionics equipment utilized for each of the functions, subfunctions, and modes. The navigation guidance and control system configuration assumed in the error analysis code has been structured to be general to permit investigation of a variety of subfunctions and modes. No distinction is made in the code between automatic and manual command generation or state estimation. It is assumed that state estimation is performed by receiving periodic position updates. Between updates, position is estimated by extrapolating from the last position estimate using an estimate of the aircraft's velocity. The model is similar to that developed by Bryson in ref. 8.

The error sources considered are time correlated velocity estimation errors, time correlated altimeter error, and pure bias and white noise for each of the range and bearing readings from up to two VOR/DME stations. While the data bank has a capacity for storing information on a large number of VOR/DME stations, it is assumed that, at most only two stations are used simultaneously during any portion of the flight. The basic system models are developed as discussed in ref. 8 and resulting variance equations are propagated as discussed in detail in Appendices C and D. While ref. 8 emphasizes air data as a means of performing velocity estimation, inertial systems could provide this information.

If an inertial system is to be considered, only the data values need to be changed. This neglects some effects unique to inertial systems, such as the Schuler period*. Since updating occurs relatively rapidly compared with the Schuler period of 84 minutes, the effect of neglecting the Schuler period will be negligible.

Both the measurement and updating models are completely general so that alternative measurement schemes may be studied. For example, consider using range (ρ) only information from two stations (ρ, ρ). In this case, there would only be two measurements to process. Also, discrepancies between true and model measurement matrices may be included.

The update routine provides the capability of alternative methods of computing the gain. For example, if a Kalman filter is not included, a simple least-squares method might be used to compute the gains. Also, an arbitrary position fix might be used; then the measurement information would completely replace previous position estimation. The option is also provided to vary the frequency of the updates at times specified by the user.

*Period of a pendulum whose natural frequency is equivalent to that of a physical pendulum whose length is equal to the radius (R) of the Earth, $T = 2\pi\sqrt{R/g} \approx 84$ minutes.

While the analysis of a Kalman filtered system required including bias errors of states, the Monte Carlo simulation of the flight of the aircraft using the state estimation scheme requires far fewer states. Thus, covariances which are a subset of the total 18 by 18 covariance of the navigation analysis program are stored and used once during the approach/landing phase in conjunction with the random number generator to generate position and velocity errors over random sample aircraft flight in the Monte Carlo program.

The aircraft navigation, guidance, and control variance analysis program (ANGCAP) provides a method of detailed investigation of state estimation using periodic updates from a wide range of measurements and utilizing a wide range of methods of computing update gains. This analysis detail does not increase execution time of the Monte Carlo analysis program, yet the capability is provided for performing Monte Carlo analysis of any of the analyzed state estimation schemes.

The aircraft state covariance at the end of each flight is catalogued in a master file for use in the plotting routine. The covariance matrix is available for each subfunction and mode and consists of the cross track position deviation, the altitude deviation, and the along-track time deviation specified in terms of early or late arrival at the end of the flight segment period.

A plot of the covariance of the navigation errors and aircraft deviation can also be provided over any route segment. In this manner, if an analysis of the en route navigation system (consisting of the on-board avionics, desired flight path, and the available airborne and ground navigation aids) is desired, only this portion of the program need be run.

Examples of the output of this program and plots available from the program are presented in a later section of this report.

Reliability Model: The operational status of the STOL aircraft and its avionics is obtained in the simulation by computing the probability of failure at several points in time. An exponential failure model is assumed so that the probability of failure in time Δt is given by

$$P_{\text{fail}}(\Delta t) = 1 - e^{-\Delta t / \text{MTBF}} \quad (1)$$

where MTBF = mean time between failure.

During a Monte Carlo execution, the reliability model determines (by a random sample from the reliability distribution) the time of the failure for each of the components of interest. If the simulated time is less than the component failure time, the Monte Carlo routine proceeds with the component active. When the simulated time is equal to the component failure time, a flag is set in the Monte Carlo routine to make the component fail. When a failure is detected, the system functions are searched to determine the effect of the failure. The flight then continues normally, reverts to a back-up mode of operation, or in the event of a failure of a critical subsystem, performs an unscheduled landing.

Maintainability Model: Airline operation normally assumes a maintenance policy involving replacement of a line replaceable unit, rather than repair of an avionics black box on the aircraft. One way to model equipment replacement would be to specify a mean time to replace (MTR) parameter and use an exponential probability distribution to obtain random replacement times. This is the technique used to model failures, and has been found to be an adequate model for most failure phenomena. However, the exponential model has two serious inadequacies with respect to replacement times:

- (1) Unrealistically small and large times can occur since the exponential distribution is defined from $t = 0$ to $t = \text{infinity}$.
- (2) Repair time cannot be concentrated about some mean value as would be the case for simply replacing an avionics "black box" that is known to have failed.

A probability distribution that overcomes the above limitations is the beta distribution. The beta probability density function is given by

$$f(t; \gamma, \eta, t_0, t_1) = \frac{1}{t_1 - t_0} \frac{\Gamma(\gamma + \eta)}{\Gamma(\gamma)\Gamma(\eta)} \left[\frac{t - t_0}{t_1 - t_0} \right]^{\gamma-1} \left[\frac{t_1 - t}{t_1 - t_0} \right]^{\eta-1}, \quad t_0 < t < t_1 \quad (2)$$

$$= 0, \quad t < t_0 \text{ or } t > t_1,$$

where $\Gamma(\alpha)$ is the gamma function

$$\Gamma(\alpha) = \int_0^{\infty} x^{\alpha-1} e^{-x} dx \quad (3)$$

Figure 6 shows the beta density function on the range $t_0 = 10$ minutes to $t_1 = 20$ minutes with a mean time of 15 minutes. The exponential distribution with MTR = 15 minutes is also shown for comparison. The mean and variance of the beta distribution are

$$\bar{t} = \frac{\gamma t_1 - \eta t_0}{\eta + \gamma} \quad (4)$$

$$\sigma_t^2 = \frac{\eta \gamma}{(\eta + \gamma)^2 (\eta + \gamma + 1)} (t_1 - t_0)^2 \quad (5)$$

For the case $\eta = \gamma$ as shown in Figure 6, Equations (4) and (5) are

$$\bar{t} = 1/2 (t_1 - t_0) \quad (6)$$

$$\sigma_t^2 = \frac{1}{4(2\eta + 1)} (t_1 - t_0)^2 \quad (7)$$

For convenience, let σ_t^2 be given by

$$\sigma_t^2 = \frac{1}{P_f} (t_1 - t_0)^2 \quad (8)$$

where P_f = peaking factor, a measure of the concentration of repair time about the mean time, \bar{t} .

Note from Figure 6 that for $\eta/\gamma=1$, a uniform density results, and thus

$$\bar{t} = 1/2(t_1 - t_0)$$

and

$$P_f = 12$$

would represent a uniform density function.

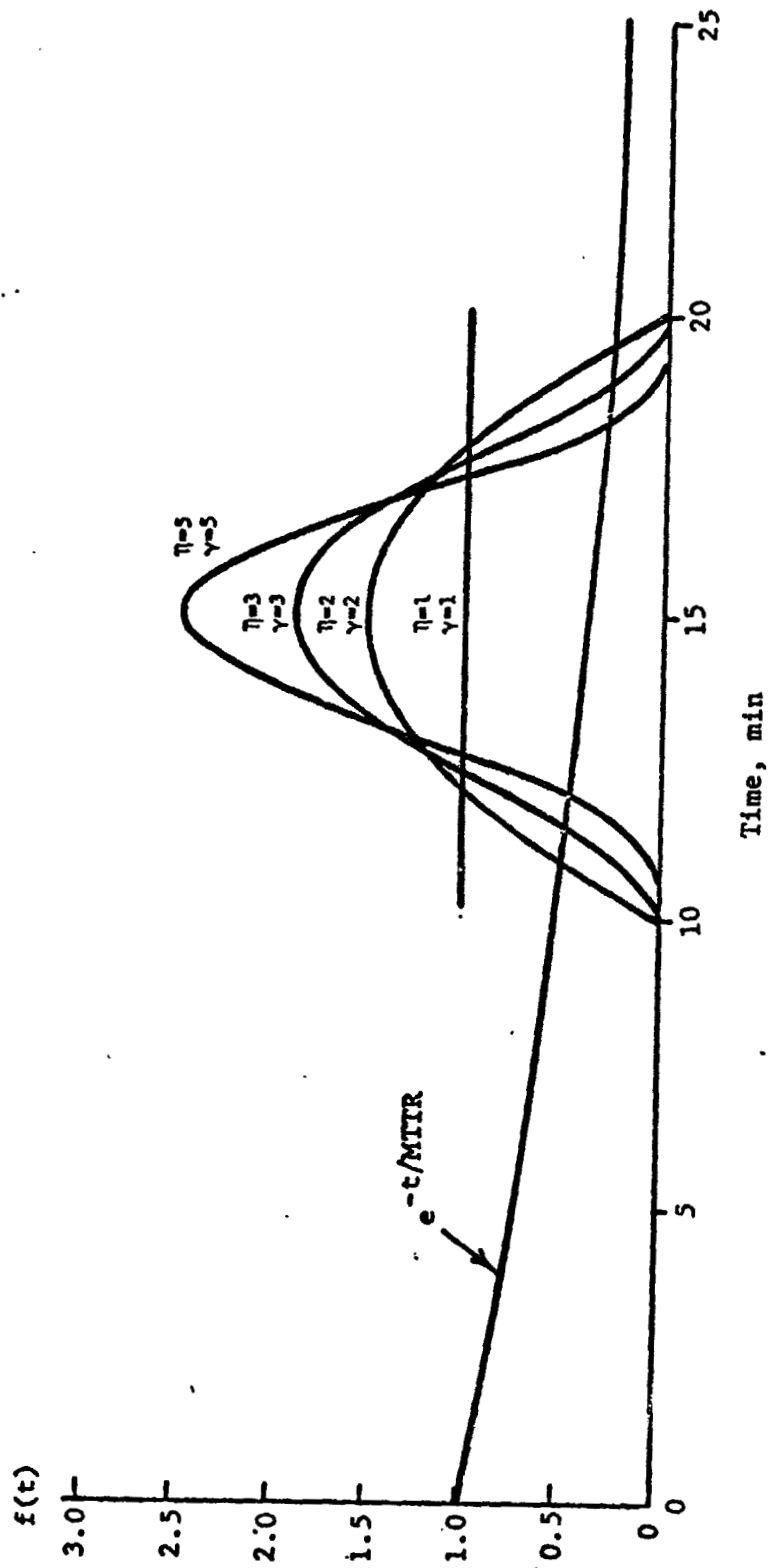


FIGURE 6. COMPARISON OF BETA AND EXPONENTIAL PROBABILITY DENSITY FUNCTIONS

To completely define the beta density function, one must specify the four parameters:

- \bar{t} = expected repair time
- t_0 = minimum repair time
- t_1 = maximum repair time
- P_f = peaking factor time.

The parameters η and γ in the beta function are then given by

$$\eta = \frac{1}{\sigma_t^2} \left(\frac{t_1 - \bar{t}}{t_1 - t_0} \right) \left\{ (t_1 - \bar{t})(\bar{t} - t_0) \sigma_t^2 \right\} \quad (9)$$

$$\gamma = \frac{\bar{t} - t_0}{t_1 - \bar{t}} \eta \quad (10)$$

Although the repair model defined above places an additional burden on the user in specifying the required parameters, it is believed that the increased flexibility obtained from the beta distribution justifies that burden.

In order to use the program, it is necessary that the required data; t_1 , t_0 , t , and P_f for the STOL subsystems be provided.

Monte Carlo Model. - The Monte Carlo model basically implements for each phase of a routine flight the specific logic and decisions that are made during that phase of the flight. A computer implementation of the model samples the probabilistic event specified between the decision points of the scenario a large number of times.

The use of the Monte Carlo routine may be best described by example. The routine examines the schedule to determine the next flight segment. Based upon the system availability from the reliability model of the required dispatch items, the aircraft departure time is computed. (The particular route leg flown is based upon the specified way points to the next airport.) Once a leg is chosen, the nominal flight time is obtained from the table generated by the aircraft performance model. The sample deviations from the nominal (cross track position, altitude, and time) are obtained from the master file of distributions described by the covariance matrix for that segment and navigation mode.

In the terminal area, the weather categories and avionic systems availability determine the capability to land or whether diversion to a different airport is required. If a landing can be accomplished, the aircraft performance model provides a nominal time to final approach while the aircraft navigation-guidance-control analysis program statistics and traffic statistics provide the time deviations from the nominal period. During the final approach, the aircraft performance model provides the nominal time and position for touchdown while the deviation from nominal provides statistics on whether a missed approach was required or the landing was successfully accomplished. The airport model provides nominal time and deviations at gate arrival, and prepares for the next departure.

The output of the Monte Carlo routine is a mission effectiveness report. The details of this output are provided in a later section of this report.

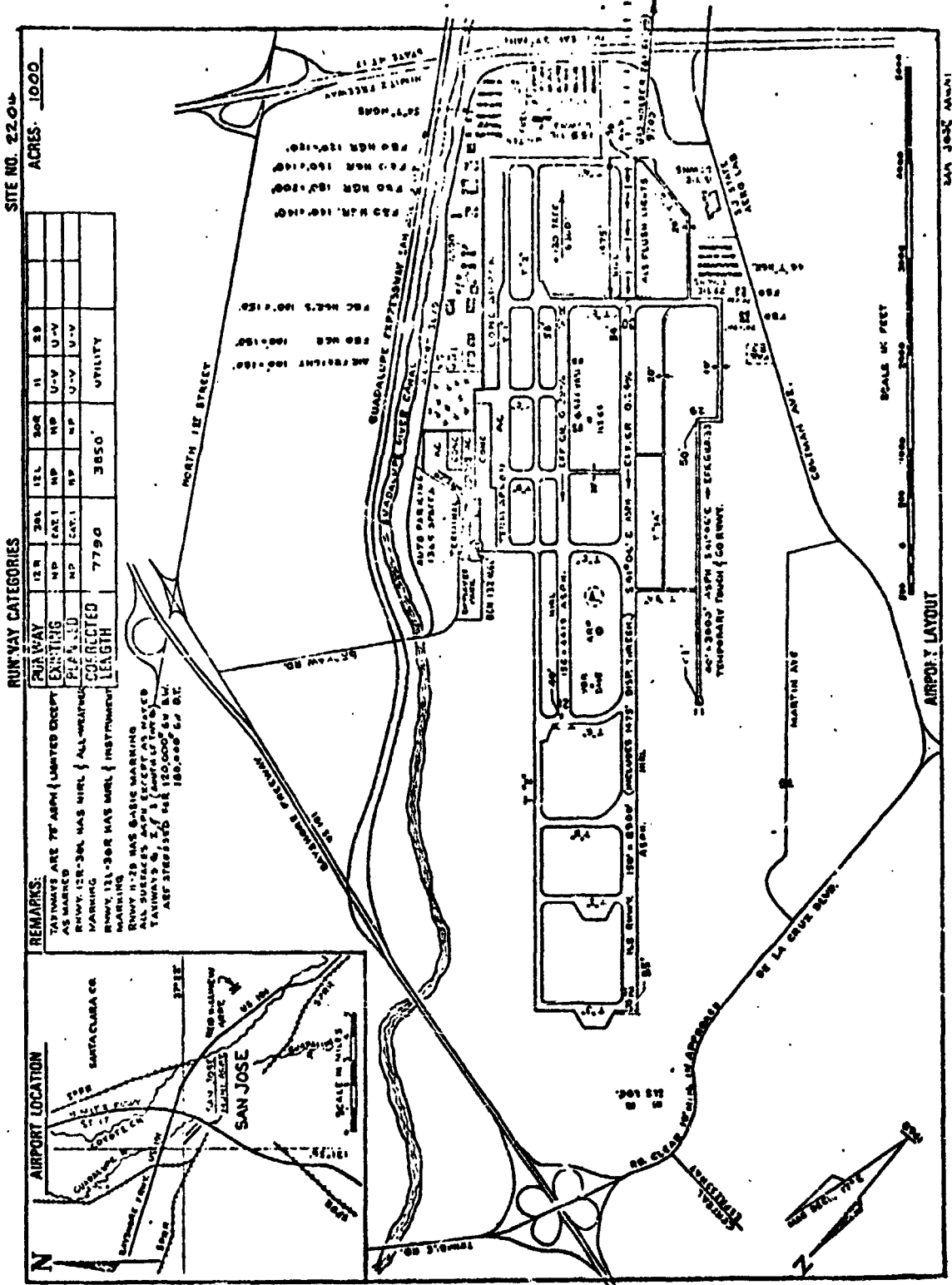
Definition of Operational Environment

While the set of mathematical models that describe the operational environment are completely general, the input data describing the operational environment should normally be referenced to some time frame. For the purposes of program check out, NASA directed that operational environment data represent 1980. The primary factors considered in defining the operational environment are the:

- (1) City pairs served
- (2) Airports used
- (3) Aircraft used
- (4) Air traffic mix and density for each airport
- (5) ATC equipment, procedures, and standards
- (6) Weather .

A discussion of each of these follows.

Route Network Connecting City Pairs Served.-The simulation can be applied to nearly any route network. NASA-Ames decided that the operational environment to be used for purposes of demonstrating the program should be the California corridor. The initial simulation considers service between San Jose, Sacramento, and Santa Ana. It was agreed that this service would utilize San Jose Municipal airport (SJC), Sacramento Executive airport (SAC), and Orange County airport (SNA). Figures 7, 8 and 9 are copies of FAA Form 5010-1 for each of these airports. Figures 10, 11, and 12 are copies of the present form of the input data for each of these airports respectively.

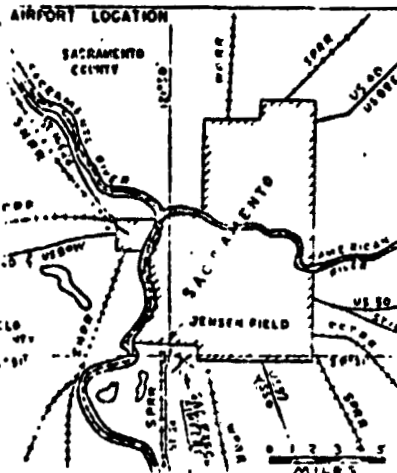


b. Back

FIGURE 7. (CONTINUED)

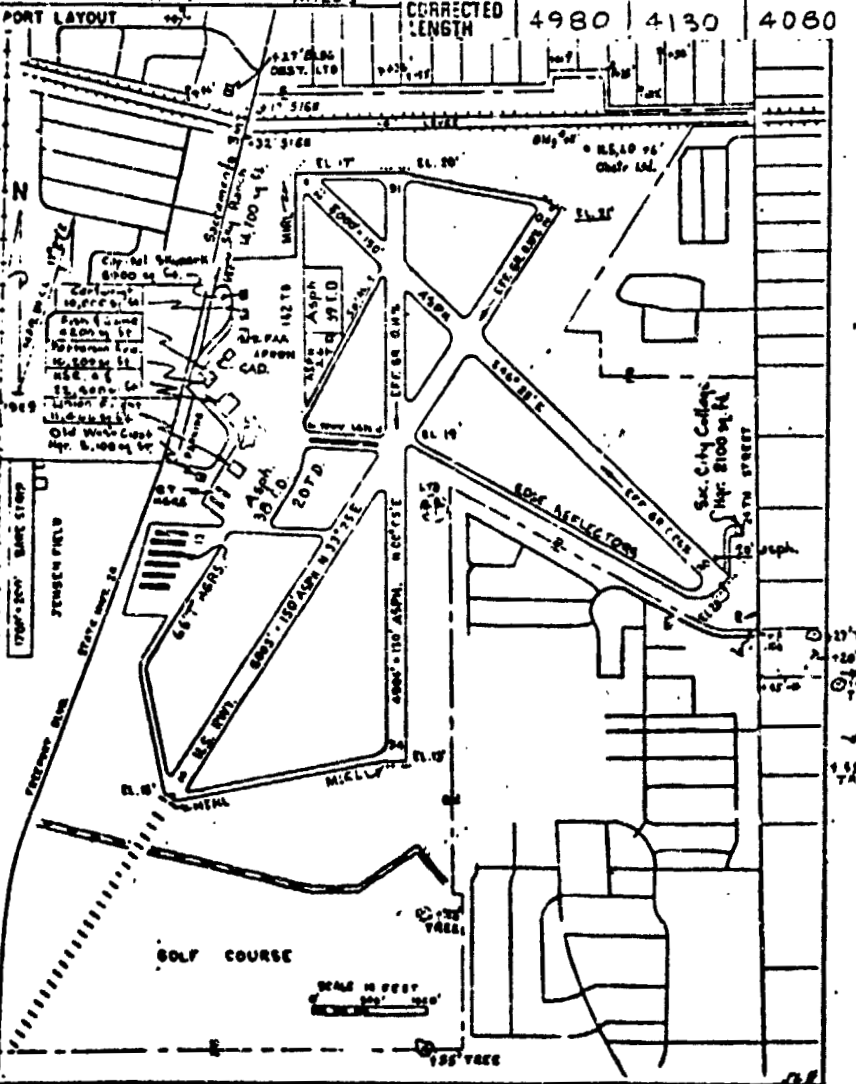
SACRAMENTO MUNI.

SITE NO. 2127
ACRES 168



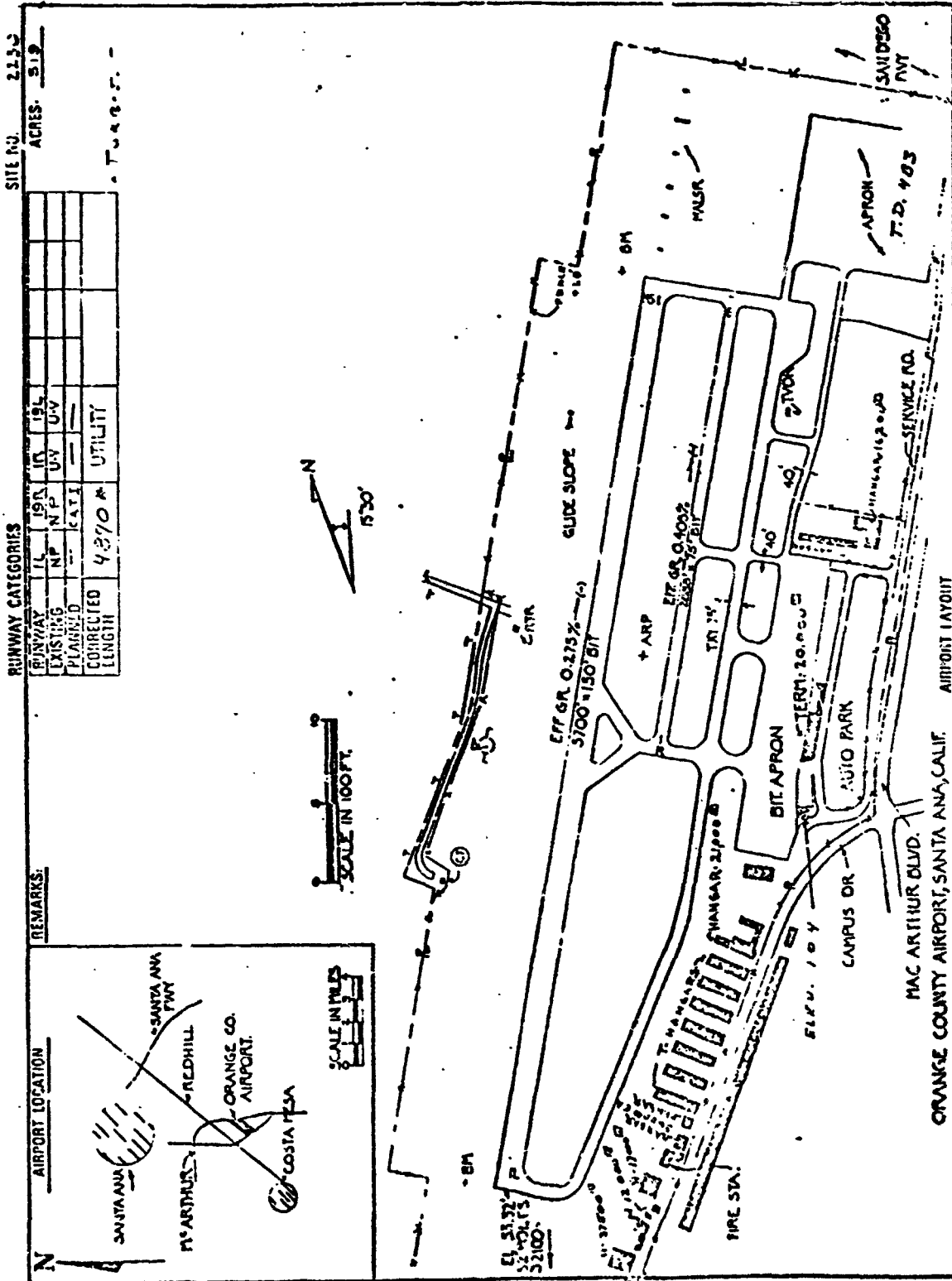
- REMARKS:
1. All buildings not marked are hangers.
 2. All taxiways not lighted here reflectors installed.
 3. All taxiways are 50' wide, asph.
 4. All roads and railroads approximately the same elevation as the runways.
 5. Wind Cone and Tetrahedron are lighted.
 6. Residential areas surround the airport.
 7. All aprons have asph surfacing.
 8. Runway Markings: 2-20 "Instrument" 16-34 and 12-30 "Basic".
 9. RWY 2-20 has high intensity runway lights. RWYS 16-34 and 12-30 have medium intensity runway lights.

RUNWAY	2	20	12	30	16	34
EXISTING	CA	NP	ND	ND	ND	ND
PLANNED	CA	NP	ND	ND	ND	ND



b. Back

FIGURE 8. (CONTINUED)



b. Back

FIGURE 9. (CONTINUED)

SAN JOSE

*** GENERAL INFORMATION ***

CODE NAME-SJC LATITUDE-37 23 0.0 LONGITUDE-121 55 0.0 ALTITUDE(FT)- 570. CONTROLLED AIRSPACE RADIUS(INH)- 15.
 REFERENCE POINT NO. 1 2 3 4 5 6 7 8 9 10
 DISTANCE EAST NRT TOWER -3333. 1053. -1823. 7. 1500. 150. -700. -155.
 DISTANCE NORTH NRT TOWER -2500. -400. -2500. 700. -1350. -3500. -2050. -3200. -552. -3058.
 REFERENCE POINT NO. 11 12 13 14 15 16
 DISTANCE EAST NRT TOWER 400. -1500. -500. 100. 700. -250.
 DISTANCE NORTH NRT TOWER -1700. 950. -350. -750. -1250. -150.

*** RUNWAY INFORMATION ***

RUNWAY NO. 1 HEADING(DEG) 110. TAKEOFF CLIMB ALT.(FT) 1500. TURNOFFS 1 2
 REF. PT. 2 LENGTH(FT) 3500. CLIDE SLOPE(DEC) 2. REFERENCE POINT 5 1
 WIDTH(FT) 60. COMMON PATH(INH) 2. TURNOFF VELOCITY(KTS) 20. 20.
 RUNWAY NO. 2 HEADING(DEG) 123. TAKEOFF CLIMB ALT.(FT) 1500. TURNOFFS 1 2 3 4
 REF. PT. 5 LENGTH(FT) 4419. CLIDE SLOPE(DEC) 7. REFERENCE POINT 9 10 11 3
 WIDTH(FT) 150. COMMON PATH(INH) 2. TURNOFF VELOCITY(KTS) 20. 20. 20. 20.
 RUNWAY NO. 3 HEADING(DEG) 390. TAKEOFF CLIMB ALT.(FT) 1500. TURNOFFS 1 2
 REF. PT. 3 LENGTH(FT) 3000. CLIDE SLOPE(DEC) 7. REFERENCE POINT 5 2
 WIDTH(FT) 60. COMMON PATH(INH) 2. TURNOFF VELOCITY(KTS) 20. 20.
 RUNWAY NO. 4 HEADING(DEG) 300. TAKEOFF CLIMB ALT.(FT) 1500. TURNOFFS 1 2 3 4
 REF. PT. 3 LENGTH(FT) 4419. CLIDE SLOPE(DEC) 7. REFERENCE POINT 11 10 9 4
 WIDTH(FT) 150. COMMON PATH(INH) 2. TURNOFF VELOCITY(KTS) 20. 20. 20. 20.

*** MISCELLANEOUS INFORMATION ***

GATE REFERENCE POINT- 10
 TAXICUOLE NO. TAXICUOLE SEQUENCE
 1- 1- 3- 7- 16-
 2- 2- 5- 9- 16-
 3- 3- 7- 16-
 4- 4- 12- 12- 16-
 5- 5- 9- 16-
 6- 6- 14- 16-
 7- 7- 14- 16-
 8- 8- 14- 16-
 9- 9- 14- 16-

FIGURE 10. INPUT DATA DESCRIBING SAN JOSE MUNICIPAL (SJC) AIRPORT

SACRAMENTO EXECUTIVE

*** GENERAL INFORMATION ***

CODE NAME-SAC LATITUDE= 34 24 0.0 LONGITUDE=121 30 0.0 ALTITUDE(FT)= 219. CONTROLLED AIRSPACE RADIUS(MI)= 15.0
 REFERENCE POINT NO. 1
 DISTANCE EAST MRY TOWER 100. 250. 1300. 1300. 2600. 2600. 750. 6
 DISTANCE NORTH MRY TOWER 2000. 2000. 2000. 2000. 2000. 2000. 2000. 7
 REFERENCE POINT NO. 2
 DISTANCE EAST MRY TOWER 11 12 500. 500.
 DISTANCE NORTH MRY TOWER -750. 0. 1500.

*** RUNWAY INFORMATION ***

RUNWAY NO. 1 HEADINGS(DEC) 120. TAKEOFF CLIMB ALT.(FT) 1500. TURNOFFS
 REF. PT. 1 LENGTH(FT) 500. GLIDE SLOPE(DEC) 2. REFERENCE POINT
 WIDTH(FT) 150. COMMON PATH(MI) 2. TURNOFF VELOCITY(KTS) 20.
 RUNWAY NO. 2 HEADINGS(DEC) 163. TAKEOFF CLIMB ALT.(FT) 1500. TURNOFFS
 REF. PT. 3 LENGTH(FT) 494. GLIDE SLOPE(DEC) 7. REFERENCE POINT
 WIDTH(FT) 150. COMMON PATH(MI) 2. TURNOFF VELOCITY(KTS) 20. 20.
 RUNWAY NO. 3 HEADINGS(DEC) 21. TAKEOFF CLIMB ALT.(FT) 1500. TURNOFFS
 REF. PT. 6 LENGTH(FT) 600. GLIDE SLOPE(DEC) 7. REFERENCE POINT
 WIDTH(FT) 150. COMMON PATH(MI) 2. TURNOFF VELOCITY(KTS) 20. 20. 20.
 RUNWAY NO. 4 HEADINGS(DEC) 203. TAKEOFF CLIMB ALT.(FT) 1500. TURNOFFS
 REF. PT. 7 LENGTH(FT) 600. GLIDE SLOPE(DEC) 7. REFERENCE POINT
 WIDTH(FT) 150. COMMON PATH(MI) 2. TURNOFF VELOCITY(KTS) 20. 20. 20.
 RUNWAY NO. 5 HEADINGS(DEC) 305. TAKEOFF CLIMB ALT.(FT) 1500. TURNOFFS
 REF. PT. 2 LENGTH(FT) 500. GLIDE SLOPE(DEC) 7. REFERENCE POINT
 WIDTH(FT) 150. COMMON PATH(MI) 2. TURNOFF VELOCITY(KTS) 20.
 RUNWAY NO. 6 HEADINGS(DEC) 347. TAKEOFF CLIMB ALT.(FT) 1500. TURNOFFS
 REF. PT. 8 LENGTH(FT) 496. GLIDE SLOPE(DEC) 7. REFERENCE POINT
 WIDTH(FT) 150. COMMON PATH(MI) 2. TURNOFF VELOCITY(KTS) 20. 20. 20.

*** MISCELLANEOUS INFORMATION ***

TAIRROUTE NO. 12
 TAXIRROUTE SEQUENCE
 1 1-13-12
 2 2-5-12
 3 3-1-13-12
 4 4-6-9-11-12
 5 5-12
 6 6-7-3-1-13-12
 7 7-8-9-10-11-12
 8 8-12

FIGURE 11. INPUT DATA DESCRIBING SACRAMENTO EXECUTIVE (SAC) AIRPORT.

ORANGE COUNTY

*** GENERAL INFORMATION ***

COAC NAME-SNA LATITUDE- 33.36 0.0 LONGITUDE-117 50 0.0 ALTITUDE(FT)- 945. CONTROLLED AIRSPACE. RADIUS(IN)- 15.

REFERENCE POINT NO. 1 2 3 4 5 6 7 8
 DISTANCE EAST WRT TOWER 1453. 3033. 2250. 3300. 2500. 1800. 2750. 2000.
 DISTANCE NORTH WRT TOWER 100. 2000. 1453. 2500. 1250. 0. 1200. -150.

*** RUNWAY INFORMATION ***

RUNWAY NO. 1 HEADING(DEC) 12. TAKEOFF CLIMB ALT.(FT) 1500. TURNOFFS 1 2
 REF. PT. 1 LENGTH(FT) 2888. GLIDE SLOPE(DEC) 7. REFERENCE POINT 3 2
 WIDTH(FT) 75. COMMON PATH(IN) 2. TURNOFF VELOCITY(KTS) 20. 20.

RUNWAY NO. 2 HEADING(DEC) 190. TAKEOFF CLIMB ALT.(FT) 1500. TURNOFFS 1 2
 REF. PT. 2 LENGTH(FT) 2388. GLIDE SLOPE(DEC) 7. REFERENCE POINT 3 1
 WIDTH(FT) 75. COMMON PATH(IN) 2. TURNOFF VELOCITY(KTS) 20. 23.

*** MISCELLANEOUS INFORMATION ***

CATZ REFERENCE POINT- 7

TAIRROUTE NO. TAIRROUTE SEQUENCE

1 1- 8- 7-
 2 2- 4- 5- 7-
 3 3- 7-

FIGURE 12. INPUT DATA DESCRIBING ORANGE COUNTY (SNA) AIRPORT

It was assumed that the route network would be flown clockwise with the earliest flight scheduled for departure at 7:00 a.m. with operations ceasing at 11:30 p.m. The flight path between individual airports is a function of the performance of the aircraft whose flight is being simulated and the navigation, guidance and control equipment and procedures being utilized. Careful consideration is given to ATC rules describing air space utilization and speed and altitude relationships in generating the flight path between airports. The flight between two airports is considered to be one leg of the route network. The flight path is defined in terms of way points which are referenced to ground navigation aids in terms of range, bearing, altitude, and aircraft velocity. These way points are extracted from the output of the powered lift STOL performance model. Each leg of the route network is made up of six flight phases.

Phases of Flight: The six phases of flight considered to make up one leg of the route network are:

- (1) Preflight
- (2) Taxi out
- (3) Takeoff/climb
- (4) Cruise
- (5) Approach/land
- (6) Taxi in .

The preflight phase is considered to begin as soon as the aircraft reaches the gate from the previous leg. During the preflight phase ground servicing, maintenance, and flight plan filing and approval are accomplished. In addition, the aircraft systems are checked out prior to entering the next flight phase.

The taxi-out flight phase begins when the aircraft departs the gate. During this phase of the flight all internal system functions, including systems management, communication, navigation, guidance, control, and hazard avoidance, are conducted. External environment factors influencing the operation of the aircraft include the airport's geometry, movement of other aircraft, weather and ATC equipment and operating procedures.

The takeoff phase is considered to be complete when the aircraft is airborne and reaches a specified altitude determined by input data. Figure 13 depicts this flight phase and the two previous flight phases.

The cruise phase flight begins when the aircraft completes its climb to cruise altitude. The cruise altitude is a function of the length of the flight leg between two airports, the aircraft's performance, and ATC instrument flight rules (IFR). During cruise, the aircraft performs internal

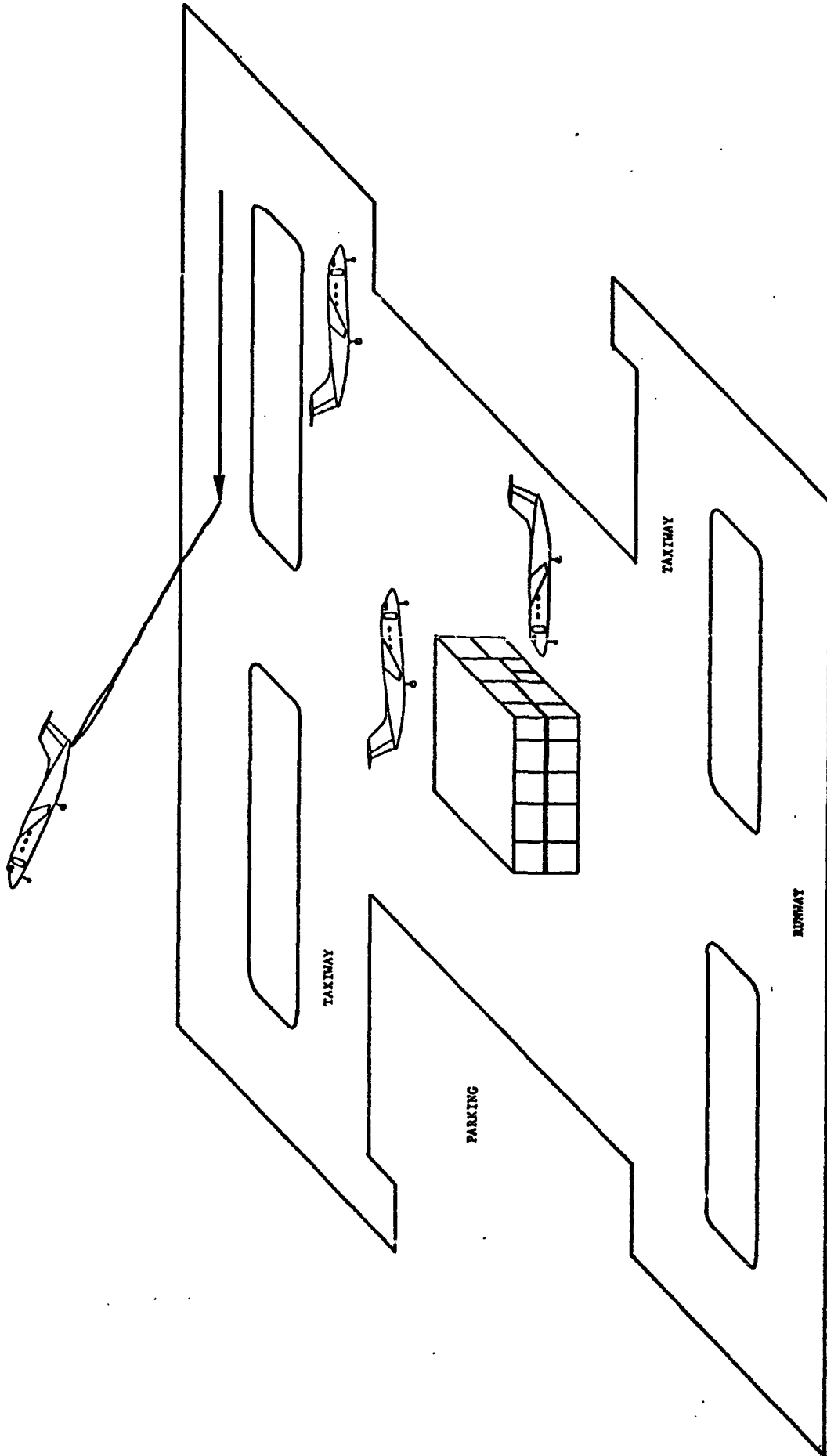


FIGURE 13. PREFLIGHT/TAXI OUT/TAKEOFF-CLIMB
FLIGHT PHASES

functions of systems management, navigation, guidance, control, communications, and hazard avoidance. The external environment influencing the operation of the aircraft includes the routes to the destination airport and the alternate airport, ATC equipment and flight rules, weather, and other aircraft. The actual flight path flown on any leg is selected by the user subject to the constraints of aircraft performance and ATC rules.

If RNAV equipment is available it is theoretically possible to fly a great circle route between two airports. In reality, if RNAV is assumed, the aircraft should fly the cruise phase using an RNAV route designed in accordance with the suggestions of the Airline Area Navigation Subcommittee (ref. 9). It is also possible to fly a non-RNAV route by utilizing conventional VOR/DME navigation and flying radials between VORTAC's. The actual cruise flight path is subject to user selection of data.

For proper operation of the navigation, guidance and control analysis program, it is necessary to define a waypoint at each heading, altitude, or aircraft velocity change. It is also necessary to define a waypoint at each change from one navigation aid to another navigation aid. Further details concerning the definition of the waypoints and the resulting flight path are given in Appendices E and B. Figure 14 depicts a typical cruise phase flight path in the horizontal plane.

The approach and landing phase begins at initiating of descent from cruise altitude to the approach altitude. The location of the waypoint which defines initiation of descent is a function of the cruise altitude, the approach altitude, and the aircraft's performance as well as ATC rules governing the speed as a function of altitude. The descent may be phased with an intermediate altitude between the cruise altitude and approach altitude. It is possible that a delay balancing fix waypoint (ref. 9) will be defined which requires holding due to air traffic delay. It is assumed that the aircraft always flies over an initial approach, or feeder, fix in the terminal area. The altitude at that phase is a function of the altitude of the planned glide slope intercept. The final approach phase waypoint located on the extended runway centerline must be specified. The location of this waypoint is a function of the desired altitude and glide slope intercept, the glide slope selected, the aircraft's performance, the weather, and the accuracy of the navigation, guidance and control functions. Detailed discussion of the transition to final approach/landing is included in Appendix E. Figure 15 depicts a typical approach/landing flight path. Once the aircraft touches down it is considered to have entered the final phase of the leg.

Taxi in is the sixth phase of a leg of flight between two airports. During the taxi-in, the aircraft internal functions of systems management, navigation, guidance, control, communications, and hazard avoidance are performed. External environment factors influencing the taxi of the aircraft include the airport geometry and other surface traffic as depicted

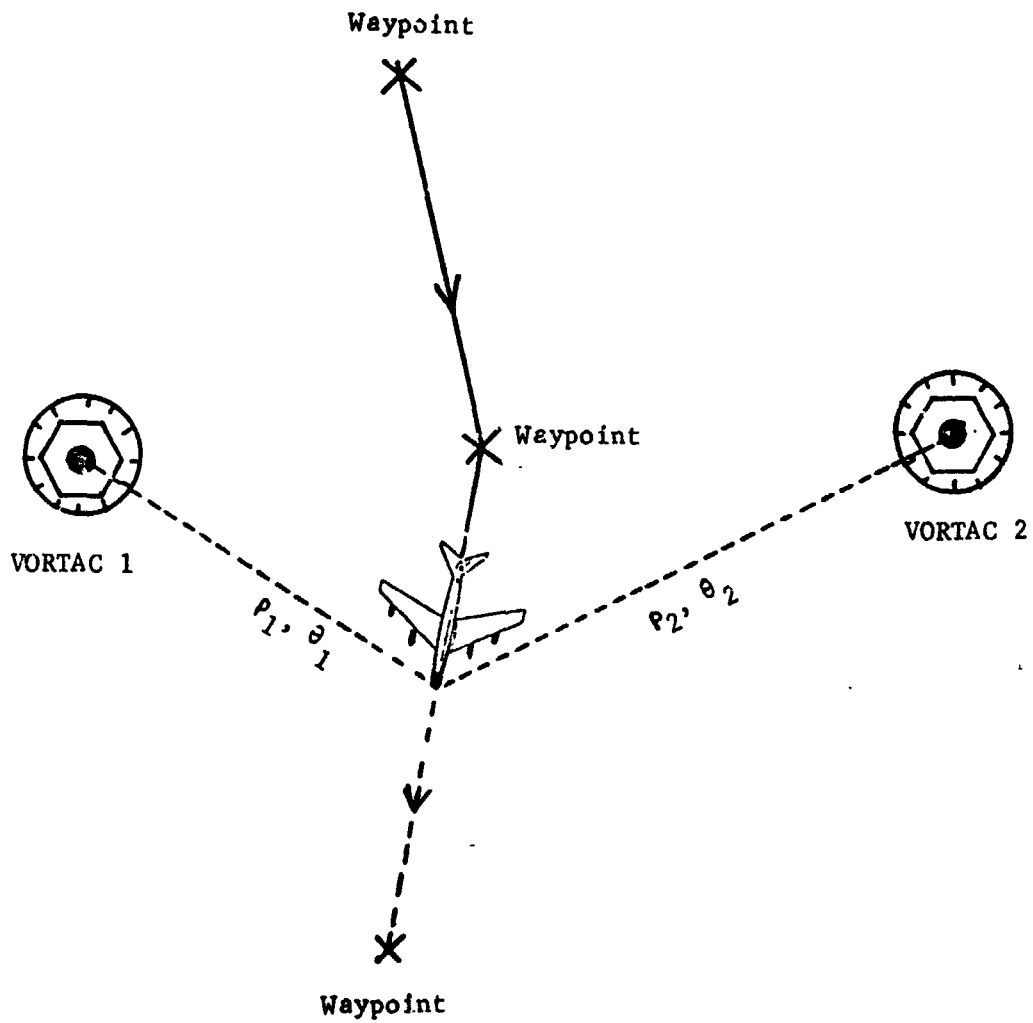


FIGURE 14. TYPICAL CRUISE PHASE HORIZONTAL FLIGHT PATH

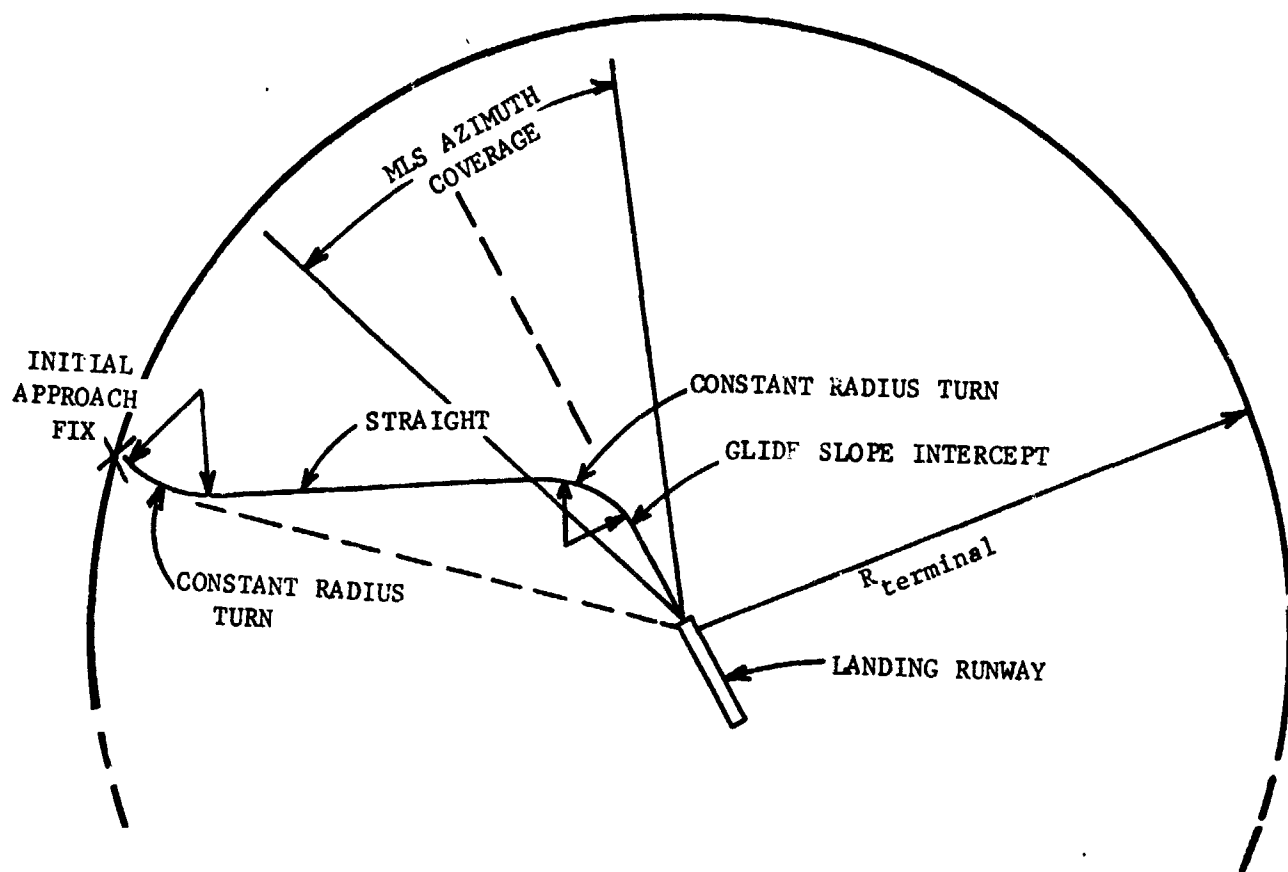


FIGURE 15. APPROACH/LANDING FLIGHT PATH

in Figure 16. The taxi-in phase is considered to have been completed when the aircraft arrives at the gate. The preflight phase of the next leg begins with aircraft arrival at the gate. Figure 17 depicts the previously described mission profile for a single flight leg. This figure depicts the possibility of diversion to an alternate field, an event possible due to loss of an avionics function or weather conditions being below the minima the aircraft's avionics are certificated for during landing.

The route network involves flying each leg as described. The flight path around the entire route network is represented by a number of waypoints as well as the schedule.

Schedule.-Figure 18 depicts the schedule for a closed route network, with the aircraft departing San Jose Municipal at 7 a.m., landing at Sacramento Executive at 7:30 a.m. and departing at 7:50 a.m., landing at Santa Ana (Orange County) at 9 a.m. and departing at 9:30 a.m., with landing at San Jose at 10:35. The waypoints which define the flight are expressed in terms of distance and bearing to various VOR/DME stations, altitude, and air speed.

Figure 19 indicates a desired or nominal ground track for a radial flight and the locations of the VOR/DME stations used. Note that this is not a good flight track for an area navigation flight, since the flight track passes over the VOR/DME stations in nearly all instances. If the use of RNAV or a Kalman filter is specified for the navigation function, mathematical models implemented in the aircraft navigation, guidance, and control analysis program prohibit use of an update from a particular station during the time the flight track is within 3,000 feet of that station. The waypoints are not repeated if the same flight path is flown for each round trip around the route network. Figure 18 lists the schedule information for each round trip around the route network. For the schedule shown, four complete round trips would be flown during one day of operation.

Externally Blown Flap STOL Aircraft.-Figure 20 depicts the 100 passenger externally blown flap aircraft designed for 2,000 foot field length. This aircraft was selected by NASA Ames Research Center as the STOL transport to be simulated. The aircraft is powered by Allison PD287-3 engines, with a design cruise speed of Mach 0.7. The mission range is 500 nautical miles with a STOL takeoff gross weight of a 142,600 pounds. Detail of the simulation of the externally blown flap aircraft including description of input data, processing, and output are presented in Appendix B.

Air Traffic Mix and Density.-In order to derive meaningful results, input data are required giving the air traffic mix and density for each of the city pairs making up the route network. As a minimum, this mix and density should be broken into the scheduled operations as a function of the time of day and the distribution of the unscheduled operations as a function of time of day. Further, the classes of the aircraft making up the

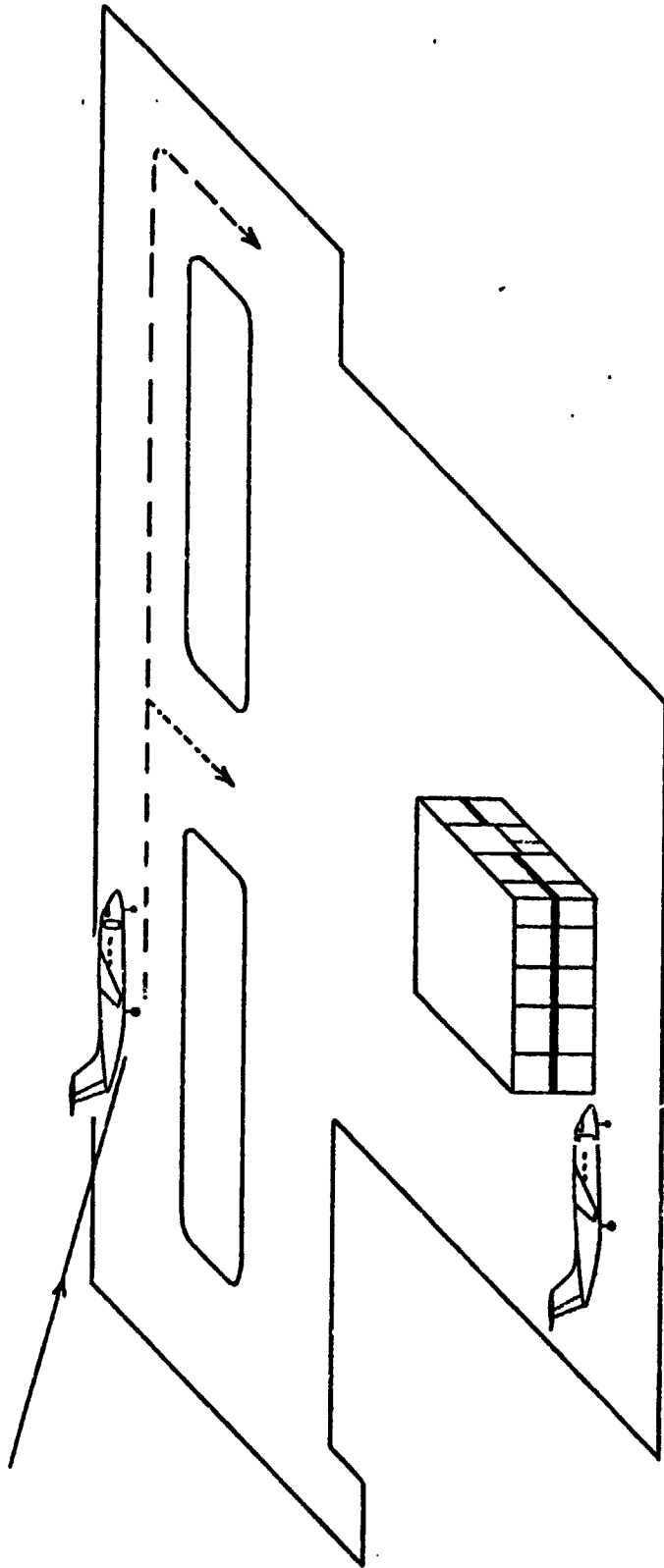


FIGURE 16. TAXI-IN FLIGHT PHASE

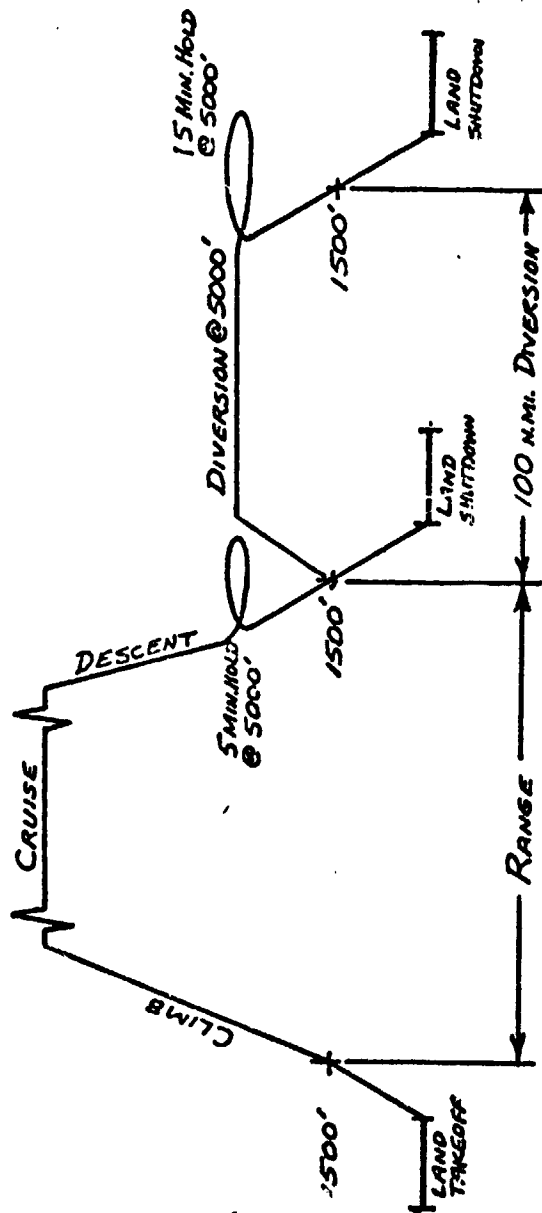


FIGURE 17. MISSION PROFILE - SINGLE FLIGHT LEG

SCHEDULE

WAYPOINTS

DEPARTURE AIRPORT	GATE	TAKEOFF AIRPORT	ARRIVAL AIRPORT	LANDING AIRPORT	GATE	ARRIVAL	DISTANCE (NM)	BEARING (DEG)	VOR/DME STATION	ALTITUDE (FT)	AIRSPEED (KTS)
SJC	7.8	7.5	SAC	7.10	7.35	18.	175.	9.	J	11000.	400.
SAC	8.2	8.5	SNA	9.10	9.15	30.	0.	0.	5	11000.	400.
						0.			5	9000.	250.
						18.	113.	113.	5	21000.	420.
						0.	0.	0.	6	21000.	420.
						48.	124.	124.	6	21000.	420.
						0.	0.	0.	7	21000.	420.
						42.	141.	141.	7	21000.	420.
						0.	0.	0.	8	21000.	420.
						30.	148.	148.	8	21000.	420.
						0.	0.	0.	9	21000.	420.
						15.	88.	88.	9	21000.	420.
						10.	319.	319.	10	21000.	420.
						0.	0.	0.	10	9000.	250.
SNA	9.40	9.45	SJC	10.45	10.50	0.	0.	0.	10	20000.	420.
						31.	235.	235.	10	20000.	420.
						0.	0.	0.	11	20000.	420.
						27.	316.	316.	11	20000.	420.
						0.	0.	0.	12	20000.	420.
						40.	312.	312.	12	20000.	420.
						0.	0.	0.	13	20000.	420.
						42.	308.	308.	13	20000.	420.
						30.	1-2.	1-2.	11	20000.	420.
						0.	0.	0.	1	10000.	250.
SJC	11.15	11.24	SAC	11.45	11.50	0.	0.	0.	10	20000.	420.
SAC	12.15	12.24	SNA	13.25	13.30	31.	235.	235.	10	20000.	420.
SNA	13.45	14.0	SJC	15.0	15.5	0.	0.	0.	11	20000.	420.
SJC	15.30	15.35	SAC	16.0	16.5	27.	316.	316.	11	20000.	420.
SAC	16.30	16.35	SNA	17.40	17.45	0.	0.	0.	12	20000.	420.
SNA	18.15	18.15	SJC	19.15	19.20	40.	312.	312.	12	20000.	420.
SJC	19.45	19.50	SAC	20.15	20.20	0.	0.	0.	13	20000.	420.
SAC	20.45	21.50	SNA	21.55	22.0	42.	308.	308.	13	20000.	420.
SNA	22.25	22.30	SJC	23.30	23.35	30.	1-2.	1-2.	11	20000.	420.

FIGURE 18. INPUT DATA DESCRIBING SCHEDULE AND FLIGHT PATH

NOMINAL AIRCRAFT PATH

CASE 1 6 11

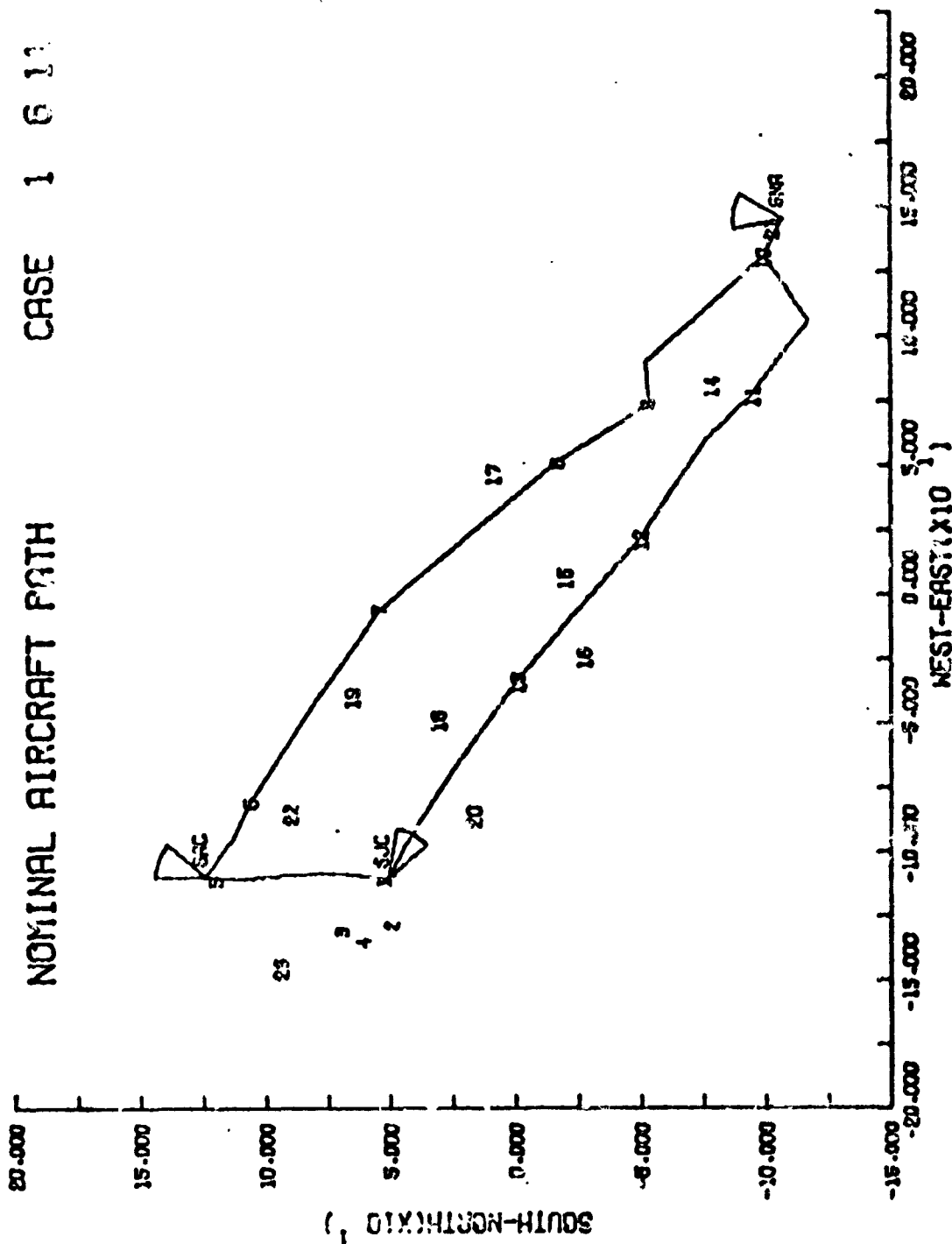


FIGURE 15. GROUND TRACK OF NOMINAL VFR FLIGHT PATH FOR ROUTE NETWORK

BASEPOINT PARAMETRIC AIRCRAFT

EXTERNALLY-BLOWN FLAP

PASSENGERS: 100

FIELD LENGTH (FT): 2000

FOUR VP PROPFAN ENGINES

ALLISON PD287-3

BYPASS RATIO 17.4

PRESSURE RATIO 1.25

SLS THRUST 24,200 LB

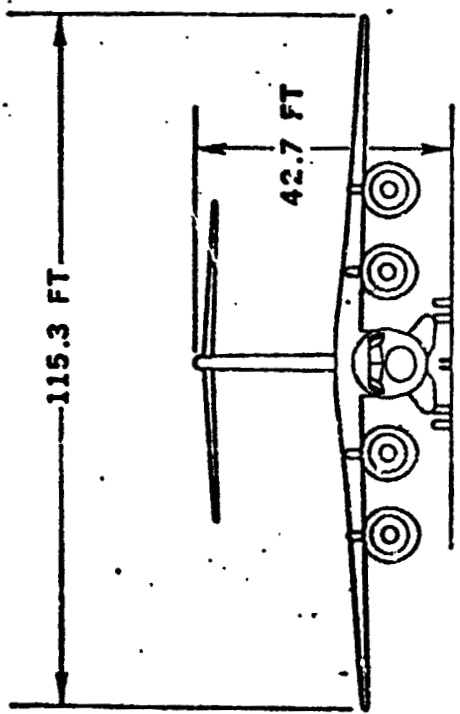
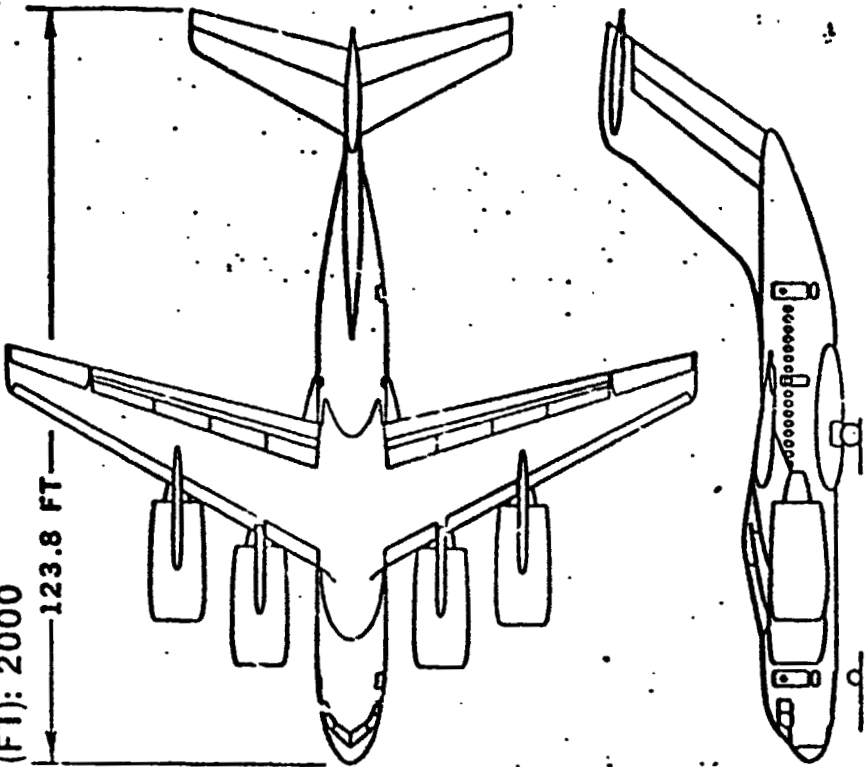


FIGURE 20. DOUGLAS EBF STOL

scheduled and unscheduled operations is needed. In the model implemented in the program, scheduled and unscheduled operations were combined by aircraft type as a function of the time of day. Figures 21, 22, and 23 present the results of a forecast for 1980 daily air traffic operations by type and time of day for San Jose Municipal (SJC), for Sacramento Executive and Orange County, respectively. The development of these forecasts for each of these airports is discussed in Appendix A. Since the results of the forecast are input data, different forecasts can be used by merely changing the input data.

Air Traffic Control.-The air traffic control system consists of various navigation aids, flight rules and standards, and operational procedures. Various documents (ref. 9, 10, 11 and 12) were reviewed to assist in defining the ATC environment.

Air space utilization must be considered in construction of flight paths to be used for the airports of interest. Nearly all major city pairs to be served by SIOL will involve a terminal control area (TCA) for at least one city of the city pair. Terminal control areas are prescribed in part 71 of the Federal Aviation Regulations (FAR). The primary limitation imposed by a terminal control area is that speed of all instrument flight rule (IFR) aircraft is restricted to less than 250 knots below 10,000 feet (ref. 11). The top of the TCA airspace is being expanded to 12,500 feet for some terminal control areas. All aircraft are controlled and separated by ATC in a terminal control area. The specific factor that is considered in the definition of the terminal area air traffic control environment is the separation criteria for aircraft in the terminal area. This is restricted to the separation of consecutive aircraft along the common path on final approach in the current ATC model in the program. Various studies are being performed to determine what these criteria should be. The results of these studies can be implemented by changing the input data to that value from the present 3 nautical miles. Since the terminal control radius and ceiling vary depending on the specific city, it is necessary to have available the terminal control area charts for the cities considered in the simulation. Currently, a terminal control area chart for Los Angeles is being used and that for San Francisco is being obtained. At present, Sacramento is not a terminal control area.

It can be assumed that the transition controller will properly route the en route traffic to the approach controller for the airport. The terminal area separation criteria are a function of not only the specific air traffic control procedures and equipment, but also a function of the aircraft mix and density and specific aircraft characteristics as well as the airport characteristics. Since the model of the terminal area environment allows variations in separation criteria in terms of distance and time between consecutive aircraft movements over the same flight path, it is necessary that data on the approach speed of all aircraft operating at each airport be provided as input data. Typical approach speeds for the

SJC DAILY SCHEDULE OF AIRCRAFT OPERATIONS
1980 TIME FRAME

44

DAY	HOUR OF DAY	DC-8		B-727		LIGHT TWIN		LIGHT SINGLE		STOL	
		TYPE		TYPE		TYPE		TYPE		TYPE	
	6.00-6.59	0.		1.		12.		80.		0.	
	7.00-7.59	3.		6.		12.		80.		3.	
	8.00-8.59	7.		9.		12.		60.		4.	
	9.00-9.59	8.		9.		12.		80.		4.	
	10.00-10.59	1.		3.		12.		80.		1.	
	11.00-11.59	7.		7.		12.		80.		2.	
	12.00-12.59	1.		3.		12.		80.		0.	
	13.00-13.59	3.		4.		12.		80.		1.	
	14.00-14.59	2.		3.		12.		80.		0.	
	15.00-15.59	3.		4.		12.		80.		0.	
	16.00-16.59	4.		5.		12.		80.		1.	
	17.00-17.59	8.		10.		12.		80.		3.	
	18.00-18.59	4.		7.		12.		80.		4.	
	19.00-19.59	5.		9.		11.		55.		4.	
	20.00-20.59	8.		10.		10.		35.		2.	
	21.00-21.59	8.		9.		9.		20.		1.	
	22.00-22.59	6.		7.		8.		10.		0.	
	23.00-23.59	0.		1.		6.		4.		0.	

CLASSIFICATION APPROACH SPEED

DC-8 TYPE OVER 119 KTS
 B-727 TYPE 100 KTS - 119 KTS
 LIGHT TWIN TYPE 80 KTS - 99 KTS
 LIGHT SINGLE TYPE UNDER 80 KTS
 STOL TYPE ALL STOL TRANSPORTS

FIGURE 21. FORECAST OF 1980 DAILY AIR TRAFFIC OPERATIONS
BY TYPE AND TIME OF DAY FOR SAN JOSE MUNICIPAL (SJC)

SAC DAILY SCHEDULE OF AIRCRAFT OPERATIONS

HOUR OF DAY	DC-8		B-727		LIGHT TWIN		LIGHT SINGLE		SIOL	
	TYPE	TYPE	TYPE	TYPE	TYPE	TYPE	TYPE	TYPE	TYPE	TYPE
5.00-5.59	0.	0.	0.	0.	4.	4.	4.	4.	0.	0.
7.00-7.59	0.	0.	3.	3.	4.	4.	4.	4.	0.	0.
8.00-8.59	0.	0.	6.	6.	4.	4.	4.	4.	5.	5.
9.00-9.59	0.	0.	7.	7.	4.	4.	4.	4.	4.	4.
10.00-10.59	0.	0.	1.	1.	4.	4.	4.	4.	1.	1.
11.00-11.59	0.	0.	6.	6.	4.	4.	4.	4.	2.	2.
12.00-12.59	0.	0.	1.	1.	4.	4.	4.	4.	0.	0.
13.00-13.59	0.	0.	3.	3.	4.	4.	4.	4.	1.	1.
14.00-14.59	0.	0.	2.	2.	4.	4.	4.	4.	0.	0.
15.00-15.59	0.	0.	3.	3.	4.	4.	4.	4.	0.	0.
16.00-16.59	0.	0.	3.	3.	4.	4.	4.	4.	1.	1.
17.00-17.59	0.	0.	7.	7.	4.	4.	4.	4.	3.	3.
18.00-18.59	0.	0.	2.	2.	4.	4.	4.	4.	5.	5.
19.00-19.59	0.	0.	4.	4.	4.	4.	4.	4.	4.	4.
20.00-20.59	0.	0.	7.	7.	4.	4.	4.	4.	2.	2.
21.00-21.59	0.	0.	8.	8.	2.	2.	2.	2.	1.	1.
22.00-22.59	0.	0.	6.	6.	2.	2.	2.	2.	5.	5.
23.00-23.59	0.	0.	0.	0.	2.	2.	2.	2.	0.	0.

FIGURE 22. FORECAST OF 1980 DAILY AIR TRAFFIC OPERATIONS

BY TYPE AND TIME OF DAY FOR SACRAMENTO EXECUTIVE (SAC)

REPRODUCIBILITY OF THE ORIGINAL PAGE IS POOR.

SNA DAILY SCHEDULE OF AIRCRAFT OPERATIONS
1980 TIME FRAME

HOUR OF DAY	DC-8		B-727		LIGHT TWIN		LIGHT SINGLE		SIOL	
	TYPE	0.	TYPE	1.	TYPE	22.	TYPE	90.	TYPE	0.
6:00-6:59	0.	0.	1.	1.	22.	22.	90.	90.	0.	0.
7:00-7:59	0.	0.	6.	6.	22.	22.	90.	90.	4.	4.
8:00-8:59	0.	0.	10.	10.	22.	22.	90.	90.	6.	6.
9:00-9:59	0.	0.	9.	9.	22.	22.	90.	90.	5.	5.
10:00-10:59	0.	0.	3.	3.	22.	22.	90.	90.	2.	2.
11:00-11:59	0.	0.	6.	6.	22.	22.	90.	90.	3.	3.
12:00-12:59	0.	0.	3.	3.	22.	22.	90.	90.	1.	1.
13:00-13:59	0.	0.	4.	4.	22.	22.	90.	90.	2.	2.
14:00-14:59	0.	0.	3.	3.	22.	22.	90.	90.	1.	1.
15:00-15:59	0.	0.	4.	4.	22.	22.	90.	90.	1.	1.
16:00-16:59	0.	0.	5.	5.	22.	22.	90.	90.	2.	2.
17:00-17:59	0.	0.	9.	9.	22.	22.	90.	90.	4.	4.
18:00-18:59	0.	0.	8.	8.	22.	22.	90.	90.	6.	6.
19:00-19:59	0.	0.	10.	10.	15.	15.	80.	80.	5.	5.
20:00-20:59	0.	0.	11.	11.	10.	10.	60.	60.	3.	3.
21:00-21:59	0.	0.	8.	8.	5.	5.	40.	40.	2.	2.
22:00-22:59	0.	0.	7.	7.	4.	4.	17.	17.	1.	1.
23:00-23:59	0.	0.	1.	1.	3.	3.	10.	10.	0.	0.

CLASSIFICATION APPROACH SPEED

DC-8 TYPE OVER 119 KTS
 B-727 TYPE 100 KTS - 119 KTS
 LIGHT TWIN TYPE 80 KTS - 99 KTS
 LIGHT SINGLE TYPE UNDER 80 KTS
 SIOL TYPE ALL SIOL TRANSPORTS

FIGURE 23. FORECAST OF 1980 DAILY AIR TRAFFIC OPERATIONS BY TYPE AND TIME OF DAY FOR ORANGE COUNTY (SNA)

present jet aircraft are given in reference 12. These data were used to group the aircraft into categories as a function of approach speed as discussed in the previous section of this report.

Figure 24 depicts the typical air traffic control functions in the terminal area at each end of a typical flight leg.

En route airspace regulations are primarily related to choice of flight altitude as a function of heading. For IFR operation, flight altitude en route is to be at odd thousands of feet for headings of 0 to 180 degrees. Even thousands of feet of altitude are to be used for headings from 180 degrees to 360 degrees. Area positive control (APC) airspace regulation must be followed for all IFR flights above 10,000 feet on the West Coast between San Francisco and San Diego (ref. 11). For operation within this area or any other positive control area, the aircraft must be operated under IFR specified flight levels assigned by ATC and equipped with instruments required for IFR operations.

It was assumed that the simulation should include the suggested planning principles for RNAV if an RNAV route is assumed to be flown using an RNAV equipped aircraft (ref. 9). RNAV route widths en route are assumed to be 4 nautical miles. Since the output of the aircraft navigation, guidance/control analysis program is used by the plotting code, the option is available to plot the estimated and actual 3σ deviations versus the 4 n.mi. route width. Since the route width is an input data parameter to the plotting code, different route widths can be utilized.

Navigation Aids: As stated in the guidelines, it was assumed that only existing en route navigation aids should be used. As previously stated, the actual VOR/DME stations used depend upon the user selection of the appropriate station as a function of the desired or nominal ground track. Figure 25 is a listing of the VOR/DME stations with the numbers corresponding to the numbers plotted in Figure 19. These aids have been entered into the program to permit use in the navigation, guidance and control analysis program. These data were taken from references 14 and 15.

As previously noted, a microwave landing system (MLS) was assumed to be operational at each of the airports. The navigation, guidance and control analysis program models the microwave landing system in terms of its azimuth, elevation, and coverage as well as the errors in each of the measurements. In addition, the siting of the MLS configuration of the airport can be changed by changing input data. This permits simulation of a variety of MLS configurations and permits trade-off of MLS siting, common path length, and estimated and actual deviations as an aircraft enters the terminal area as discussed in further detail in Appendix E.

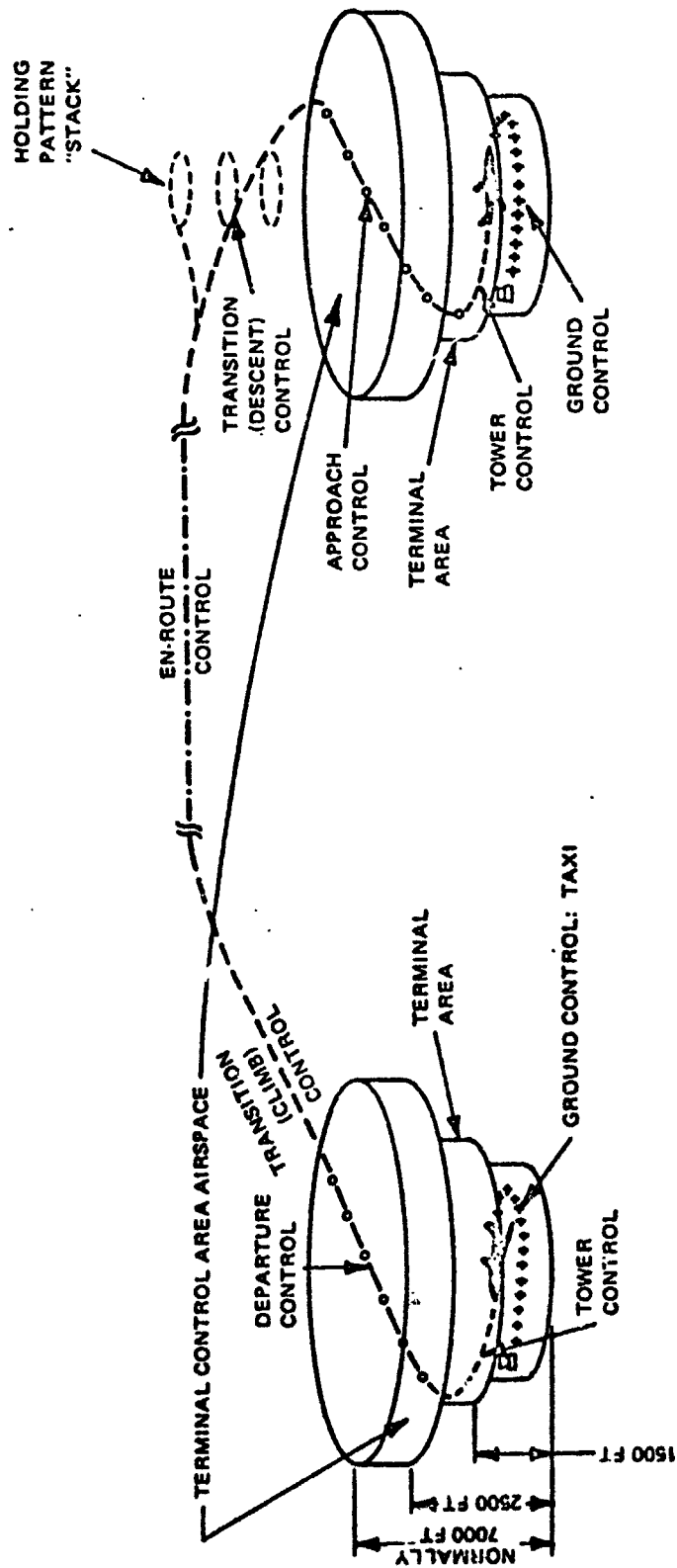


FIGURE 24. FLIGHT PHASES AND AIR TRAFFIC CONTROL FUNCTIONS

INPUT DATA FROM NAFEC, ANA-251, AND AIRWAY FACILITIES SERVICE, AAF-240

NO.	NAME	CLASS	LATITUDE	LONGITUDE	ELEVATION	MAG. VAR.
1	SAN JOSE	L-VOR/DME	37 21 53.0	121 55 45.0	50.	17.
2	WOODSIDE	L-VOR/DME	37 23 51.0	122 16 49.0	2213.	17.
3	OAKLAND	M-VOR/DME	37 43 33.6	122 13 21.0	10.	17.
4	SAN FRANCISCO	L-VOR/DME	37 36 50.0	122 21 24.0	10.	17.
5	SACRAMENTO	M-VOR/DME	38 26 37.4	121 33 2.0	10.	17.
6	LIDSEY	M-VOR/DME	38 4 28.8	121 0 10.1	240.	17.
7	FRESNO	M-VOR/DME	36 53 12.4	119 48 11.0	341.	17.
8	REDFIELD	M-VOR/DME	35 29 4.6	119 5 46.9	550.	16.
9	GERMAN (F)	M-VOR/DME	34 48 15.0	118 51 45.0	4239.	16.
10	SEAL BEACH (F)	L-VOR/DME	33 47 30.0	118 3 30.0	30.	16.
11	VENTURA (E)	M-VOR/DME	34 7 0.0	119 3 0.0	500.	16.
12	FELLOWS	L-VOR/DME	35 5 25.2	119 51 52.6	3870.	16.
13	PRIEST	M-VOR/DME	34 8 25.2	120 39 50.1	3840.	16.
14	FILLMORE (E)	M-VOR/DME	34 21 30.0	118 52 45.0	1000.	16.
15	AVENAL	M-VOR/DME	35 38 49.2	119 58 39.4	710.	16.
16	PASO ROBLES	L-VOR/DME	35 40 21.0	120 37 33.7	820.	16.
17	PORTERVILLE	L-VOR/DME	35 54 47.2	119 1 11.6	580.	16.
18	LCS RAVES	L-VOR/DME	36 42 55.8	120 46 39.6	2060.	17.
19	PERCEN	L-VGR	37 13 9.9	120 23 57.3	180.	17.
20	SALINAS	M-VOR/DME	36 39 49.9	121 36 7.6	180.	17.
21	SANTA ANA	L-VOR	33 40 43.2	117 51 45.0	40.	15.
22	STACKTON	M-VOR/DME	37 50 1.2	121 10 13.3	40.	17.
23	NAPA	L-VOR/DME	38 10 45.9	122 22 19.4	0.	17.

VOR RME
MISO (MR) 851.0 447.0
MTR (MR) 4.4 6.9

FIGURE 25. RADIO NAVIGATION GROUND STATION DATA

Weather.-Sample copies of surface wind summaries were obtained from the National Climatic Center at Asheville, North Carolina. Table 2 (a copy of these data) presents the percentage frequency of wind direction and speeds during the various years is indicated for the specific time period shown. Similar surface wind information is available for all hours by month and all months and all hours.

Table 3 presents a summary of ceiling versus visibility data for the same station, the same years, month, and time period. Data will be extracted for the appropriate time periods and used in the program to determine whether the ceiling and visibility permit VFR flight or require acquisition of the MLS and specific avionics for a safe landing. These data can also be acquired from the National Climatic Center.

Checkout of the program and the sample case runs, results of which are presented in a later section of this report, were performed using the sample data for all hours for the month of January.

En route winds are modeled as described in Appendix C. Data for the en route wind statistics were extracted from ref. 8.

Mission Performance Measures

The measures of effectiveness used in this study are the STOL Mission performance measures and STOL system function performance measures. STOL mission performance measures could be specified a number of ways. The performance measures acceptable to one user of the information, which will result from this and other studies, might be considered of little value to other users. As a result, it is quite important that any mission performance measures specified be meaningful to as many users as possible. Before discussing the STOL mission performance measures formulated in this study, it is necessary to discuss the categories of users of the information and their information needs. In many cases, knowledge of these needs aided in defining appropriate performance measures.

User Categories and Assumed Information Needs.-Users of this information can be placed into either of two broad categories which shall be defined as the (1) public and (2) private sectors. These categories can be further subdivided according to the users' responsibility or viewpoint.

It is suggested that the public sector be subdivided as shown in Table 4.

23116
STATION

SANTA ANA, CALIFORNIA, MCAS

46-47.60-61.66-69

46-47.60-61.66-69

1969

JAN

1968

ALL WEATHER

CLASS

0000-0200

TIME PERIOD

TABLE 2. PERCENTAGE FREQUENCY OF WIND DIRECTION AND SPEED (FROM HOURLY OBSERVATIONS)

5702 SURFACE WINDS JAN 68

SPEED (KNOTS) DIR.	DATE												MEAN WIND SPEED		
	1-3	4-6	7-10	11-14	17-21	22-27	28-33	34-40	41-47	48-55	56	%			
N	.7			.2										.2	5.5
NNE	.5	.7			.2										.6
NE	1.2	2.1	.5	.7	.9	.2									4.1
NNE	1.6	4.6	5	.2	.2										3.6
E	3.5	9.1	2.9	.2	.2										7.2
ESE	.7	3.0	1.4												3.4
SE	2.1	2.8	.9	.2	.2										3.1
SE	.2	.7	.9	.2	.2										6.0
S	.2	.7	1.6												7.7
SSW															7.2
SW			.2												2.0
WSW	.2	.2													2.2
W		.9	.7												1.9
WNW	.6				.2										1.6
W		1.2	.7	.2											7.3
NNW	.2	.2		.2											.7
WNW		.2		.2											1.7
CLM															49.0
	11.6	25.5	9.7	8.1	1.6	.5									100.0
															431

TOTAL NUMBER OF OBSERVATIONS

d

TABLE 3. CEILING VERSUS VISIBILITY

92114 SANTA ANA, CALIFORNIA MCAS 46-57.50-61.66-69 JAN 68 0000-0200

PERCENTAGE FREQUENCY OF OCCURRENCE (FROM HOURLY OBSERVATIONS)

Table with columns for CEILING (FEET) and VISIBILITY (STATUTE MILES) from 0 to 10. Rows represent various ceiling heights from 47.0 to 55.7 feet.

TOTAL NUMBER OF OBSERVATIONS 433

NAVWHA SEVCOM

TABLE 4. SUBCATEGORIES OF PUBLIC SECTOR

Federal Government
Department of Transportation
Federal Aviation Administration
Civil Aeronautics Board
NASA
Department of Defense
State and Local Government
State Aviation Department
Local and Regional Planning Groups
City Government
Airport Authority
General Public
Passengers

At the Federal Government level, the Department of Transportation (DOT) is assumed to be primarily concerned with the viability of STOL compared with other modes of short haul transportation. If STOL is viable, it is assumed that DOT would be concerned with the investment required by the Federal Government to assist in implementing commercial STOL. Although this project is not directly concerned with estimating the investment required to assist in implementing STOL, it is concerned with identifying action which must take place, including technology development, if STOL is to become viable.

The Federal Aviation Administration (FAA) can be assumed to be concerned with maximizing the number of passenger movements with a specific probability of safety within a given cost constraint. Since this study is not concerned with estimating capacity of airports but instead determining how capacity affects a flight of this STOL aircraft in terms of avionics requirements, the type of capacity information of most use to FAA will not be forthcoming. Analysis of capacity as affected by the STOL aircraft could require modeling the movement of all aircraft using that airport in great detail, an effort clearly beyond the scope of this study. The cost constraint was not addressed in this study. FAA is vitally interested in a determining investment required to implement commercial STOL with the advent of the Airport and Airways Development Act of 1970. This investment would be a function of air routes, air traffic control and navigational aids, and specific airport facility requirements.

The Civil Aeronautics Board (CAB) is assumed to be primarily concerned with demand and indirectly, airline profitability. Having the power to grant new routes or deny applications to abandon existing service, they would require information that would assist them in making decisions which have direct impact on STOL viability.

NASA, whose primary role is advancement of technology, is primarily concerned with knowing the technology developments required to make STOL viable which includes economic goals. In addition, NASA requires information related to the technology alternatives which, if developed, could contribute to the desired viability. The cost of each of these alternatives will be needed by NASA to assist in determination of the resources required.

While the Department of Defense (DOD) requires much of the same information needed by NASA, different mission performance measures might be appropriate due to the unique characteristics of the military application of STOL. The system criteria which will result from this evaluation will not likely be representative of DOD STOL system criteria because of the difference in the scenario. The present statement of work makes no allowance for investigation of DOD applications and, therefore, no specific military mission performance measures were developed.

State and local government information needs will be less technical than those of the Federal Government with respect to the STOL vehicle itself. In general, their principal concern will be with the economics and the required regulatory actions.

State aviation departments principal concern will be the investment required by the state government if STOL can be shown to have a positive influence on regional development. The state aviation departments may share in the financing of new facilities requested by local governments.

Local and regional planning groups will need information related to STOL impact on regional development to aid in their planning, and establish reasonable land use plans. The investment required by local governments to provide needed facilities would be valuable information. Economic impact on the area would also be of interest.

City governments will be interested in obtaining information that would assist in determining the potential impact of STOL on the cities, viz. information that would assist in determination of the economic influence, and the costs of (1) providing airport access, (2) acquisition of land and development of airport facilities, (3) safety services including fire and police protection, and (4) the operation of the airport. Cities must also concern themselves with the probable degree of general public acceptance since there is opposition, in many cases by a well meaning minority of the the populace, to air transportation because of noise and purported environmental damage. Prior to the enactment of regulatory legislation, an examination of all available information should be made to determine the need for and form of such legislation.

Local airport authorities are concerned primarily with the construction of facilities and operation of the airport. Their information needs are more technical than those of other local governmental agencies since they must oversee the design and construction of the needed facilities as well as operate the facilities once they are in being. Physical layout, sizing, etc are of vital interest. Some information of this type did result from this study.

The general public, including the user as well as the nonuser, is primarily interested in any form of transportation only as it impacts them individually. The nonuser makes up the majority of the general public now and for the immediate future. Potentially, STOL will provide a limited number of nonusers with jobs once in operation. A slightly greater number would be employed during the construction of new facilities. These nonusers realize a direct economic benefit from STOL. The majority of the populace would not realize such a direct economic benefit. Their view of STOL would depend upon its visibility in the form of new taxes or bond levies to construct and operate the facilities, its safety, and the impact on each individual in terms of the disturbance it creates with their normal life style. If STOL is quiet, nonpolluting, financially self-supporting, and does not disturb the life style of the general populace, they would be minimally interested in information pertaining to STOL.

The potential passenger who might use STOL would be most concerned with information pertaining to the reliability of this mode of short haul transportation, the comfort, the total trip time, the frequency of service and the cost. This study will produce much of this information but will not deal with cost during this phase.

Table 5 lists subcategories of users of the information, which will result from this and other studies, considered to be in the private sector.

TABLE 5. SUBCATEGORIES OF PRIVATE SECTOR

Airlines
Airframe Manufacturers
Avionics Manufacturers

Airlines are concerned with demand, route structure, and the required aircraft characteristics to service the demand and route structure while making a profit. This study will not determine demand and desired route structure. These were specified by NASA ARC. The study has provided information related to STOL operational considerations.

Air-frame manufacturers are vitally interested in determining whether there is a market for STOL and, if so, the characteristics the aircraft must possess. Much work has been done in an attempt to answer these questions and this study, as well as others, provide additional information of the type needed by airframe manufacturers.

Avionics manufacturers require information concerning the characteristics STOL avionics systems should possess as well as the required characteristics. This study provides information concerning only market for STOL avionics.

The information user categories and their general information needs were considered in defining the STOL mission performance measures presented below. Additional work may be required in the future as performance measures developed is related to information needs of the foregoing groups wherever practical.

STOL Mission Performance Measures.-Mission performance measures for STOL have been defined to satisfy the information needs of the various interested groups discussed in the foregoing section. As discussed in a later section of this report, a Monte Carlo routine developed for the six flight phases provides the cumulative statistics resulting from defining the legs making up the route network a selected number of times. These statistics for the specific mission performance measures model include:

- (1) Equipment-repair time
- (2) Fuel-loading time
- (3) Passenger-loading time
- (4) Total ground time
- (5) Gate-departure delays
- (6) Dispatch reliability (defined as the probability of starting the scheduled flight without incurring a cancellation or delay of more than 15 minutes because of a system or component nonavailability)
- (7) Takeoff delays
- (8) Takeoff runway occupancy time
- (9) Takeoff runway distance used
- (10) Unscheduled landings
- (11) Missed approaches
- (12) Diversions to alternate
- (13) Landing runway occupancy time

- (14) Landing runway distance used
- (15) Gate arrival time deviation
- (16) Landing time delays
- (17) Initial fuel load
- (18) Initial takeoff weight
- (19) Fuel consumed
- (20) Canceled flights
- (21) Scheduled flights flown.

These mission performance measures are functions of lower level system function performance measures which are discussed in a later section of this report. For example, missed approaches can be due to system function failures such as loss of a particular subsystem required for safe landing under a given weather condition; state estimation errors, command generation errors, command execution errors; conflict with other air traffic at that airport; and aircraft performance constraints. The specific relationship of the STOL mission performance measures to the system function performance measures are included in the Monte Carlo routines for the six flight phases.

Mission Performance Goals. -Mission performance goals which must be specified as numerical values include the desired dispatch reliability, permitted flight cancellations, and the definition of deviations which are permitted for each phase of flight. These deviations may be described in terms of airway route widths for the cruise phase, terminal area path constraints, and time deviations at waypoints for four-dimension (4-D) or fixed time of arrival (FTA) guidance. Specification of a desired dispatch reliability requires the designer to allocate that goal to the various subsystems and estimate required inflight reliability and ground maintenance parameter goals.

Reference 2 states that flight cancellation automatically occurs if an aircraft is delayed 3 hours. The reason for selection of this value was not given. It is felt that the elapsed time past scheduled departure, at which point the cancellation occurs, could be a function of the time the next flight is scheduled to leave the city to be served. The number of operations listed for each of the airports considered in this study do not currently have associated with them the cities served by these operations. Review of Reference 18 indicates that departure delays are attributed to the various ATIS 100 systems. For the present, a flight will not be considered to be delayed if it departs within 15 minutes of the scheduled departure time. Dispatch reliability is defined as

$$P_{\text{Dispatch}} = P_{\text{Reliable}} + (1 - P_{\text{Reliable}}) (P_{\text{Replace}})$$

where

P_{Dispatch} = probability of dispatch

P_{Reliable} = probability that all required systems were operating at the time of gate arrival

P_{Replace} = the probability that the replacement time for required subsystem is less than the scheduled ground time plus 15 minutes.

Using the beta probability density function for replacement or repair, if the maximum replacement time specified for each subsystem is less than scheduled ground time plus 15 minutes, P_{Replace} will always be one. If the maximum replacement time is greater than the scheduled ground time plus 15 minutes, P_{Replace} may likely be less than one.

For the purpose of exercising the program, a dispatch reliability goal of 98% was assumed. The results of synthesizing the avionics to meet this goal are presented in a later section of this report. It is presently assumed that the aircraft minimum equipment list (MEL) is determined by a data item for each of the subsystems contained in the data bank. This is consistent with the equipment required for IFR dispatch by FAR parts 25.1303 and 121.303. Reference 18 states that a maintainability "goal" is to design an airplane which not only has a low direct maintenance cost, but can also operate day in and day out without delay and cancellation and will not be required to be taken out of service for maintenance except at times of low traffic density, such as periods of a few hours on one or two week nights. This goal may not be completely obtainable, but it is certainly approachable and is a realistic goal toward which the airplane designer can direct his maintainability efforts. This goal is hereafter referred to as his "optimum maintainability". To allow maintenance work to be concentrated to a few evening hours separated by several days, three major aspects of maintainability must be provided for in the design of the airplane:

- (1) Postponement of maintenance for several days after the moment the need arises.
- (2) Rapid repair or replacement to permit the aircraft to be repaired during a scheduled station stop
- (3) Prediction of impending failures to permit replacement or repair at a planned maintenance period in advance of actual failure.

This reference further states that

"Dispatch with components inoperative permits achievement of optimum maintenance at selected areas without schedule interruptions, but has its penalties and is not applicable to all components. The penalties in weight, cost, and 'switching systems' are equally obvious. On the most recent designs, such as the DC-9, dispatch inoperative consideration started with an analysis of all system components to determine the need and practicability of inoperative dispatch. To avoid the penalties of direct duplication, design modifications can be made to permit functions to be performed by secondary, but existing, means when the primary means is inoperative."

This concept parallels the concept of the modes for each of the functions as considered in STOL OPS.

Dispatch reliability goals have also been expressed in which the allowance for repair time has been specified as one hour. In these cases, a probability of replacement or repair of 99.75% in the scheduled ground time plus one hour might correspond to a dispatch reliability of 99% with only 15 minutes allowed, after which time the nondispatch is counted as a delay.

Systems Functions, Subfunctions, and Modes

A STOL system function is defined as an operation or action required to conduct the STOL mission. Avionics system functions include state estimation (navigation), command generation (guidance), command execution (control), communication, hazard avoidance, and systems management. A particular function may be performed in a variety of modes, which connotes specific combinations of avionics hardware subsystems and software. The specific mode that is utilized in performing a function is dependent upon the available hardware/software mechanization. For example, if the state estimation function is done automatically, defined as the subfunction of automatic navigation, the onboard computer would sample a variety of state measurements provided either sequentially or simultaneously. If a particular state measurement is unreliable due to measurement uncertainties or hardware subsystem failures, in automatic navigation the software logic causes reversion to a backup mode and processed only those measurements available. Crew selection of state estimation modes requires various manual navigation subfunctions to be defined. Whatever the function, subfunctions permit automatic or manual modes.

Before continuing the discussion of system functions and performance measures, it is appropriate to define specific parameters to be computed in the program. Table 6 contains a definition of the major state vectors used throughout this work.

TABLE 6. DEFINITION OF MAJOR STATE VECTORS

\underline{x}_n	\triangleq	nominal state vector, nominal flight profile as a function of time
\underline{x}_a	\triangleq	actual state vector, flight profile flown by aircraft as a function of time
\underline{x}_e	\triangleq	estimated state vector, derived by processing state measurement sensor outputs
$\underline{x}_a - \underline{x}_n$	\triangleq	\underline{d}_a actual deviation vector, represents ability of aircraft from performance point of view to maintain \underline{x}_n
$\underline{x}_e - \underline{x}_n$	\triangleq	\underline{d}_c , computed deviation, vector input to command generation function
$\underline{x}_e - \underline{x}_a$	$=$	\underline{e} , state estimation error
\underline{d}_c	$=$	$\underline{e} + \underline{d}_a$

The performance measure for the state estimation function is the state estimation error, \underline{e} , as defined in Table 6. This error represents the statistical uncertainty in the state (position, velocity, and time) estimates.

The performance measure for command generation could possibly be the computed deviation, \underline{d}_c , defined in Table 6 if a manual mode is utilized. Higher order modes involving solution of guidance algorithms may require different performance measures depending upon the algorithm to be solved. In all modes, the value of \underline{d}_c will be dependent upon the air traffic control procedures being simulated. For example, if positive air traffic control is utilized, which is probable at airports operating near capacity, then \underline{d}_c is dependent on ATC's estimate of the vehicle state and nominal

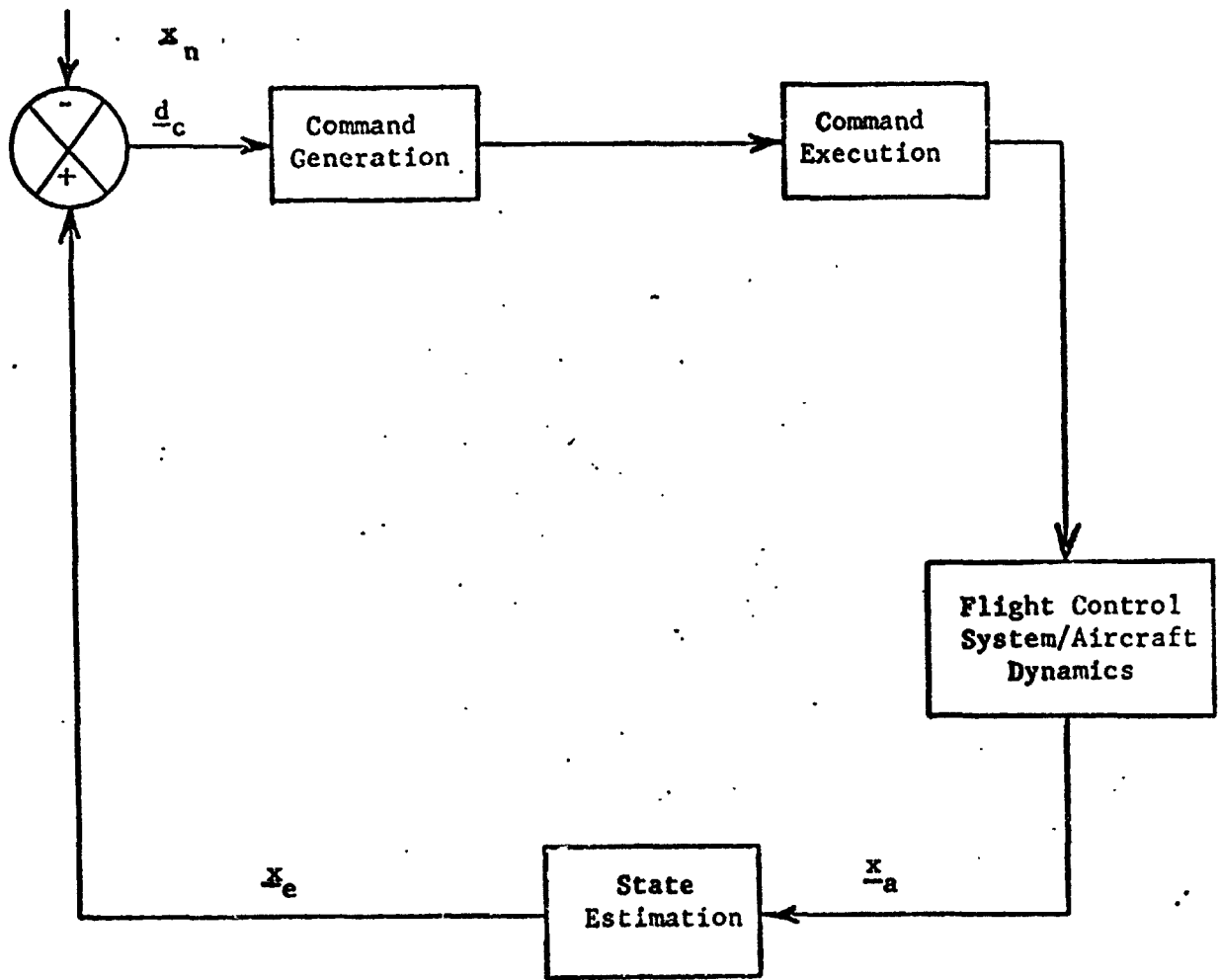
flight path. In the case where air traffic control surveillance might not be available, the crew would have to rely upon d_c computed onboard the aircraft for the command generation function.

Since d_c is the input to the guidance/control algorithms whose solutions result in performance of the command execution (control) function, the appropriate system performance measure for the control function is dependent upon the control algorithm. Since the form of this algorithm will depend upon whether fixed time of arrival (FTA) (4-D navigation/guidance), or variable time of arrival (VTA) (3-D navigation/guidance or 2-D navigation guidance) is used, the command execution function performance measure can, in general, be stated to include only the accuracy with which a system responds to the command generation. In the case of the FTA guidance algorithm, the command execution function performance measure is a time deviation at one or more specific points along the flight path.

In the case of the VTA guidance algorithm, the appropriate performance measures for the command execution function is more difficult to discretely define along the entire flight path. At the end of the flight path, the aircraft must be able to execute a successful landing. In this case, for the VTA algorithm, the control function performance measure could be based upon a variety of parameters which may be dependent upon weather. For example, if the weather conditions require use of an MLS for landing, the cross track and altitude deviations at the MLS acquisition must be such that a landing can be safely executed without violating the performance constraints of the aircraft on the first approach. This effectively defines a window, as discussed in Appendix E, that the combination of navigation, guidance, and control deviations cannot exceed if a successful landing is to be made on the first approach. If the weather conditions are VFR, the control function performance measure could be the deviations at decision height and touchdown dispersions. Figure 26 is a block diagram depicting the interactions between the state estimation, command generation, and command execution functions.

If the crew selects a manual subfunction, this requires selection of the specific manual mode also. It is recognized that the selection of the automatic or manual subfunction is normally a function of flight phase, i.e., takeoff, cruise, descent, and landing. Primary functions that involve change of subfunction from automatic to manual and vice versa, as a function of flight phase, are (1) navigation, (2) guidance, and (3) control.

Navigation, Guidance, Control Subfunctions.—The subfunctions for navigation, guidance, and control are automatic and manual. Table 7 shows all the possible combinations of these subfunctions.



Legend

- \underline{x}_a Δ actual state vector
- \underline{x}_e Δ estimated state vector
- \underline{x}_n Δ nominal state vector
- \underline{d}_c Δ computed deviation vector

FIGURE 26. BLOCK DIAGRAM OF NAVIGATION, GUIDANCE, AND CONTROL FUNCTION INTERACTIONS

TABLE 7. COMBINATIONS OF SUBFUNCTIONS FOR NAVIGATION, GUIDANCE, AND CONTROL

Configuration Function	Acceptable				Unacceptable			
	1	2	3	4	5	6	7	8
Navigation	A	A	A	M	A	M	M	M
Guidance	A	A	M	M	M	M	A	A
Control	A	M	M	M	A	A	A	M

The first four represent legitimate configurations. As an illustration, Configuration 1 could represent an area navigation (RNAV) system coupled through an autopilot. Configuration 2 could represent the same RNAV coupled through the flight director and pilot. Configuration 3 could represent the case where the pilot has to fly raw deviation from a VOR receiver. That is, he would not have the benefit of a flight director computer to provide steering commands. Another possible mode for Configuration 1 is the case where there is no RNAV computer and the aircraft has to fly VOR radials in cruise. This mode can be classed as fully automatic but does not have the flexibility of the mode described earlier for Configuration 1.

Configurations 5 and 6 are comparable to Configurations 3 and 4 except that control is automatic. These could represent cases where the pilot has to determine which direction to fly (manual guidance) but uses heading hold or control wheel steering autopilot modes for control. Configurations 5 and 6 are legitimate. However, they should have essentially the same performance characteristics as Configurations 3 and 4. Thus, Configurations 5 and 6 are classified as unacceptable conditions and the possible modes which they might represent are incorporated in Configurations 3 and 4.

Configurations 7 and 8 are unacceptable because automatic guidance is not feasible if there is only manual navigation.

In running the evaluation program, it is assumed that the most automated subfunction will be used. That is, if automatic equipment is available and working, it is assumed that the pilot will utilize the equipment. This may not always be the case in practice, but it should be true that if the automated equipment is required because of a particular weather condition or flight profile, the pilot will use it.

Some comments about the impact of the various acceptable configurations are appropriate for each phase of flight.

Takeoff/Landing: Subfunction availability will dictate whether or not a takeoff or landing is possible for a particular weather condition. In addition to subfunction availability, proper redundancy must exist for the existing weather category.

Climbout/Approach: The degree of automation will dictate the complexity of paths which can be followed for these phases of flight. That is, with present day conventional ILS equipment and autopilots, an aircraft could not operate in a dense environment requiring precise curved paths for climbout and descent without an interruption of the ATC pattern. This could cause schedule delays and missed approaches depending on when mode reversions occur and the traffic density.

Cruise: The degree of automation will also dictate the types of paths which can be flown for this phase of flight. For example, if an RNAV computer fails, the aircraft must revert to flying VOR radials. If other types of failures occur (such as both VOR's), the aircraft may no longer be able to fly RNAV paths or VOR radials. In this case, the pilot may have to declare an emergency and divert to another airport, depending on weather conditions.

Hazard Avoidance.-The hazard avoidance function primarily involves avoiding conditions that can impose a hazard to the aircraft. These conditions are weather, other aircraft, obstruction to flight such as terrain and natural features, as well as man-made structures. The primary performance measure that is used is the probability of receiving a hazard avoidance warning in time to make the appropriate maneuver to avoid the hazard. Equipment involved in the hazard avoidance function is discussed in a later section.

Communications.-The communications function performance measure has been modeled as the probability of being able to conduct successful voice or digital data link communications. Since the radio navigation receivers serve as input state measurement sensors, they are not considered part of the communication function unless the same receiver/transmitter is used for voice communications as well as radial navigation.

Systems Management.-The primary systems management function performance measures are fuel management and schedule delay. To properly evaluate delay both at gate departure and takeoff, all of the successful aircraft functions required for dispatch and flight progression are monitored in the Monte Carlo program to assess the impact of failure rates and maintainability parameters on performance.

Constraints

A variety of parameters act as constraining factors. Many of these parameters are dependent upon the scenario being simulated. The constraining parameters include those related to: (1) the aircraft, (2) the airport, (3) the approach/landing performance limits, (4) the weather, and (5) the navigation aids. As the simulation is exercised, it will be possible to identify additional constraints beyond those described below. These additional constraints may include those due to joint CTOL and STOL operation, if the same runway is utilized, as well as those due to airport configurations. Since two quite different types of constraints are involved, physical and procedural, it can be expected that constraints will be continually identified as the simulation is exercised for differing scenarios. The aircraft and airport constraints described below are implemented in the Monte Carlo program whereas the approach/landing performance limits are not.

Aircraft. - The physical aircraft constraints include (1) operating empty weight, (2) maximum fuel capacity, (3) maximum gross takeoff weight, (4) maximum gross landing weight, (5) maximum takeoff thrust, (6) physical dimensions including wing span, length, height, and gear foot print, (7) aircraft operating ceiling, (8) aircraft performance including rate of climb, rate of sink, braking, etc., and (9) real-world realizable MTBF and maintainability parameters for onboard systems including avionics.

Airport. - The physical configuration of the airport is a significant constraining factor in that the configuration has a significant influence on the number of operations that may be conducted per hour at that airport under various weather conditions for the air traffic mix and density utilizing that airport. In addition the location of the airport in itself effectively creates a constraint due to weather conditions in that locality. The number of scheduled and unscheduled operations performed at the airport as a function of time of day also act as a constraint on the flight of a single STOL aircraft being simulated in detail in this study. The combination of foregoing factors ultimately determines the delays to be expected by the STOL aircraft because of the foregoing airport related parameters.

Approach/Landing Performance Limits. - Realistic performance limits or constraints during the approach and landing phase are described below. If the aircraft path and time errors exceed those limits, a missed approach should be executed. There are several reasons for choosing, or being directed, to execute a missed approach:

- (1) If the terminal airspace is tightly controlled and the aircraft is expected to fly a specific path, then large deviations could create a collision hazard with other aircraft.

- (2) If the traffic control has sophisticated sequencing and metering capabilities, then the aircraft is expected to maintain precise time control. Excessive deviation is cause for directing a missed approach.
- (3) The most obvious reason for executing a missed approach is if the lateral or vertical performance in the last few hundred feet of altitude is such that an unsafe landing could result.

Each of the above is discussed in the following paragraphs and a recommended format for approach/landing performance limits is presented.

Causes of Excessive Deviations: Excessive deviations result from two sources: system failures and "poor" fault-free performance. The pilot can fit into either category with blunders appearing like failures and sloppy tracking looking like poor performance. Failures in critical system elements that are detected will cause a missed approach at the time of detection. Undetected failures will cause go-around when the adverse performance becomes obvious. It should be noted that before an aircraft-control system can be certified, it must be shown that detected and undetected failures yield only a very remote probability of hazard (on the order of 10^{-7} to 10^{-9}). For Category I and II type landing systems, this remote probability is provided by insisting on pilot visibility for the final landing stage. For Category III, it is through multiple redundant systems. By the same token, it must be assumed that the same assurance of remote probability of hazard due to failures will be provided for all operations in the terminal area. Thus, for purposes of the simulation, it can be assumed that all critical failures are detected in the terminal area and that if a missed approach is warranted, it is executed at time of failure. (It should be noted that some terminal area avionics may fail prior to reaching the terminal area but go undetected until used. To account for these cases, failure exposure time should be total flight time, but a portion of the terminal avionics equipment failures reflecting undetected failures should be treated as if they occur in the terminal area even though they occurred earlier.)

"Poor" fault-free performance (poor is in quotes because it does not necessarily reflect poor design or pilot performance) results, generally, from noise state estimation, large external disturbances, or excess maneuvering requirements. Noisy state estimation is a matter of fact with present ILS and terminal VOR/DME's. The new microwave landing system promises to relieve most of these problems. External disturbances include steady wind, turbulence, and windshear. Large deviations can also occur if the turn onto the final course is close enough to touchdown that overshoots have insufficient time to settle.

It is this "poor" performance which must be monitored in some manner to determine whether a missed approach is warranted.

Present Performance Monitoring Methods: Performance in the approach/landing phase is presently monitored as follows. For a Category I or II landing, the monitoring is with surveillance radar in the horizontal plane, with localizer deviation aboard the aircraft and with pilot visibility at the decision height. The surveillance radar is too crude to provide much more than gross monitoring. The pilot is controlling with the localizer deviation and he monitors that deviation to avoid large errors. It should be noted that he smooths what he observes when the signal is noisy. For example, when another aircraft overflies the localizer, it often causes large oscillatory deviations and in some cases radio flag warnings. However, the pilot recognizes these symptoms for what they are and smooths them unless he is close to the decision height. Precision monitoring is accomplished at the decision height when the pilot must visually verify that he can safely land or execute a missed approach.

For a Category III landing, reliance is placed on the integrity of the control system and the ground navigation aids. If the pilot notes that the control signals are sufficiently nulled and there are no failure indications in either the aircraft or ground equipment, the landing proceeds. There are variations in how the integrity monitoring is performed. For example, the DC-10 used an independent monitor which models the aircraft and control system and projects the landing point. The L-1011 uses quadruple redundant systems and verifies that all systems agree. In addition, excess ILS deviation monitors are activated as the aircraft approaches touchdown. The purpose of both techniques is to detect failures and look for gross control errors.

Prior to reaching the final landing path, monitoring is provided with the surveillance radar and whatever navigation equipment is being used onboard the aircraft.

Implementation of Monitors in the Simulation: There are two purposes for describing performance limits in the simulation.

- (1) To describe the true aircraft/control limits in the final landing stage.
- (2) To determine the impact on schedule performance of a given set of limits monitored by an actual sensor.

The first objective implies monitoring aircraft performance with respect to true performance while the second implies monitoring with respect to some state sensor or combination of sensors. The limits for the second objective will necessarily be tighter than those for the first to allow for estimation errors.

Accurate performance limits should include constraints on position, velocity and acceleration (or altitude). However, it is believed that continuous assessment of position will provide adequate monitoring.

The recommended formats for lateral and vertical performance limits are assumed independent. This is felt to be reasonable because of the relatively minor coupling between lateral and longitudinal axes and because of the usual separation of lateral and longitudinal control systems.

Lateral Constraint Limits: Figure 27 shows the lateral format. Over the distance d_1 , there is a small angle restriction representing performance required for a safe landing. This distance could reflect approximately the last 30 seconds of flight. The origin of the angles θ_1 and θ_2 is at the localizer and projected MLS azimuth location. This is logical because it reflects gradually tightened performance as the aircraft approaches touchdown and allows a reasonable error at touchdown. In addition, θ_1 is an actual measurement and, thus, is the most likely measurement to use as a monitor. θ_2 reflects performance limits necessary to avoid obstacles on the final approach. Present regulations restrict obstacle height as a function of angular deviation from the runway centerline. The distance d_3 supplies a monitor of lateral position in the terminal area sufficient to avoid a collision hazard.

Vertical Constraint Limits: Vertical limits, Figure 28, are similar to the lateral limits with θ_1 , θ_2 , and Z_2 corresponding to θ_1 , θ_2 , and d_3 respectively. Over the distance d_1 , a constant altitude error is used to reflect the transfer from a glide slope measurement to altitude which occurs with automatic landing systems and effectively with manual landing. The altitude at the distance d_1 from the transmitter is 50 - 100 feet.

Horizontal Position Time/Control: Time control can be implemented as control within a continuously moving slot or control to discrete waypoints. In any event, the purpose is to achieve precise landing time and safe separation on the common path. Again, two forms of monitoring are desirable. First, the actual landing time should be assessed to determine whether it is within acceptable limits. If not, it can be assumed that a go-around would have been executed. This would be a fairly wide limit giving the aircraft as much leeway as possible. A second limit can be placed on the estimated time error at specific waypoints or continuously. The method of implementation should depend on the form of time control.

MLS Acquisition Window: Prior to beginning the final approach subject to the foregoing constraints, it is necessary to acquire the microwave landing system if the weather conditions are Category 1 or lower. Appendix E presents a discussion of the transition to final approach and landing

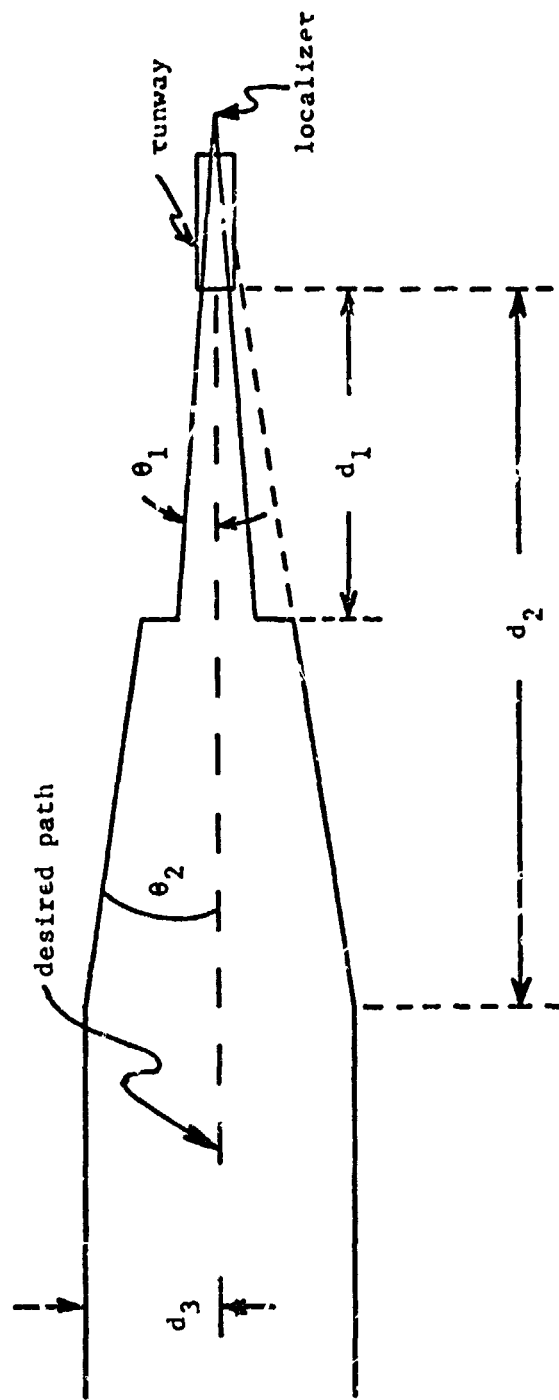


FIGURE 27. LATERAL CONSTRAINT LIMITS

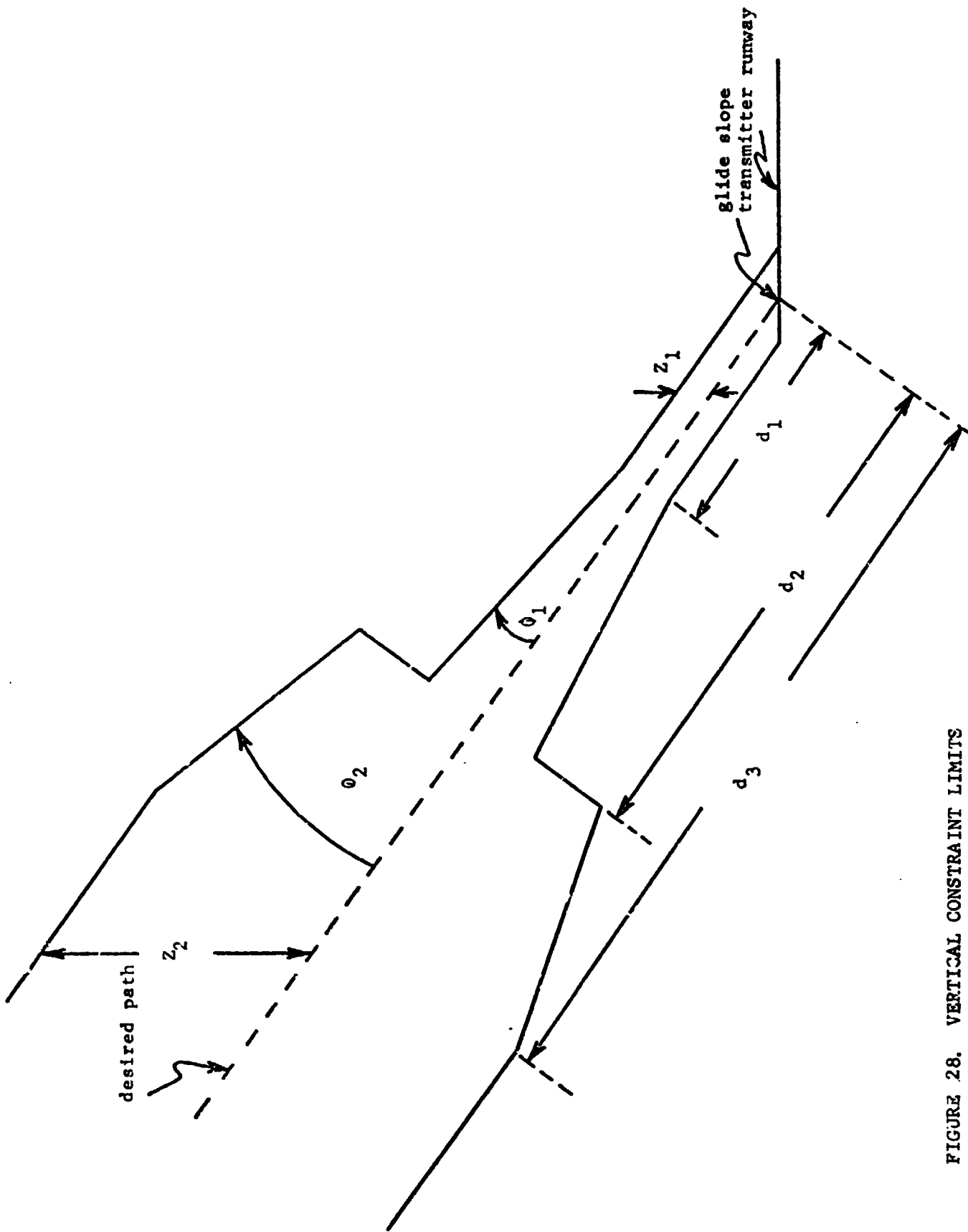


FIGURE 28. VERTICAL CONSTRAINT LIMITS

and the relationship of the location and size of the MLS acquisition window to the estimated and actual deviations in terms of cross track, altitude, and time.

Navigation Aids. - As discussed in a later section of this report, the use of ground-based radio navigation aids for state estimation is highly desirable. Figure 25 lists the radio navigation ground station data for the aids previously depicted along the route network shown in Figure 19. Note that each of these aids has a definite location and is denoted by a class L or H. Data defining the coverage for each class have been extracted from Reference 13 and are presented in Table 8.

Data on the MLS navigation aids coverage and accuracy were taken from Reference 3. MLS location and availability are input variables also. It is possible by data specification to have the glide slope and localizer colocated or separated. The mean-time between outages and mean-time to repair the MLS are estimated values and are input data.

ATC Standards and Operating Procedures. - The previously discussed ATC regulations may be considered as constraints. These include the speed limitations as a function of altitude, the flight altitudes as a function of heading, the en route airway width, the sequencing and metering in the terminal area, the ATC common path separation, and a common path length. In addition, the maximum capacity of each runway may be considered a constraint.

Airline Imposed Constraints. - While the allowable time after scheduled gate departure before delay is counted as an input variable, the airframe manufacturer might view that time as a constraint. This time is normally determined by the airline operator. In addition the elapsed time past scheduled gate departure, at which time a decision to cancel a flight is reached, may be considered a constraint.

TABLE 8. ALTITUDE AND DISTANCE LIMITATIONS

VOR/VORTAC/TACAN NAVAIDS		
Normal Usable Altitudes and Radius Distances		
<u>Class</u>	<u>Altitudes, ft</u>	<u>Distance, miles</u>
T	12,000 and below	25
L	Below 18,000	40
H	Below 18,000	40
H	14,500 - 17,999	100*
H	18,000 - FL 450	130
H	Above FL 450	100

* Applicable only within the contiguous 48 states.

Development of Base-Line Functional Requirements and Initial System Operating Procedures

In the case where system criteria are being developed to meet performance goals, an initial estimate of the functional performance of each base-line made is required. These estimates will be modified during the synthesis process to meet the STOL mission performance goals.

For each function, it is necessary to develop base-line modes switching logic. The switching between modes can be a function of performance measures not meeting that required for the function, or failure of hardware required for a mode. Since the selection of switching logic involves performing trade-offs between automatic mode selection as opposed to mode selection by the crew, it has been decided that the crew would use the automated modes, if they have confidence in those modes, before switching to a manual mode which involves a higher work load, as discussed in a later section of the report.

Development of initial system operating procedures is dependent upon base-line system configurations, initial estimates of system performance requirements, and man-machine task allocations. In addition, the probable air traffic control operational procedures would be included in the development of initial system operating procedures. For example, it is possible that if area navigation is to be utilized, standards will be established for lateral track separation as well as vertical track separation. If both STOL and CTOL aircraft are utilizing area navigation, it is possible that specific tracks would be established for each class of vehicles as a function of their cruise and terminal area speed (ref. 9). In defining the base-line functional requirements and initial system operating procedures, it is useful to define a base-line STOL avionics configuration.

Base-Line Avionics Configuration. - The base-line avionics configuration that was selected for the study was taken from the Federal Aviation Administration's Federal Aviation Regulations (FAR) related to certification of aircraft and their operation in various weather conditions. Table 9 is based on data extracted from FAR Parts 25.1303 and 121.303 (refs. 5 and 6). This table lists the avionics and other equipment required for IFR (instrument flight rule) dispatch. Table 10 was extracted from FAA Advisory Circular 120-20 (ref 16) and lists the airborne equipment requirements for Categories I and II operations. On the basis of these data, Table 11 has been prepared as a definition of the baseline STOL avionics to be considered in the initial simulation. This table lists the subsystems, the number of subsystems required, and the measurements the subsystems provide, classified as direct or indirect. Note that the table does not assume a specific configuration for the avionics. That is, the interconnection of hardware and software is not specified since the degree of redundancy in the STOL

TABLE 9. EQUIPMENT REQUIRED FOR IFR DISPATCH
(FAR PARTS 25.1303 and 121.303)

<u>SUBSYSTEM</u>	<u>NUMBER REQUIRED</u>
AIR DATA	
STATIC PRESSURE SENSOR	2
FREE-AIR TEMPERATURE INDICATOR	1
AIRSPEED INDICATOR	2
ALTIMETER	2
VERTICAL SPEED INDICATOR	2
CLOCK WITH SWEEP SECOND HAND	1
ATTITUDE/HEADING REFERENCE	
MAGNETIC COMPASS	1
VERTICAL GYROSCOPE (ARTIFICIAL HORIZON)	2
VERTICAL GYROSCOPE - INDEPENDENT	1
SLIP-SKID (TURN-AND-BANK)	1
DIRECTIONAL GYROSCOPE	1
COMMUNICATION	
VHF VOICE (TWO-WAY)	2
VOR RECEIVER	2
DME RECEIVER	1
ILS RECEIVER	1
MARKER BEACON RECEIVER	1
ADF RECEIVER	1
AIRBORNE WEATHER RADAR*	1
AIRCRAFT LIGHTING	
INSTRUMENT LIGHTS	
POSITION LIGHTS	
ANTICOLLISION LIGHT	
LANDING LIGHTS	2
ELECTRICAL	
INDEPENDENT GENERATOR & DISTRIBUTION	2
BATTERY	
ENGINE INSTRUMENTS	
COCKPIT VOICE RECORDER	
LANDING GEAR AURAL WARNING	

*MUST BE OPERATING SATISFACTORILY IF CURRENT WEATHER REPORTS INDICATE WEATHER CONDITIONS THAT CAN BE DETECTED WITH AIRBORNE WEATHER RADAR MAY REASONABLY BE EXPECTED ALONG ROUTE TO BE FLOWN.

TABLE 10. AIRBORNE EQUIPMENT REQUIREMENTS
CATEGORIES I AND II*

MINIMUM REQUIREMENTS	CAT I (TURBOJET ONLY)	CAT II (ALL AIRCRAFT)
SINGLE FLIGHT DIRECTOR 1/ OR SINGLE AUTOMATIC APPROACH COUPLER 2/	REQUIRED	MINIMUM REQUIREMENT - TWO- ENGINE PROPELLER AIRCRAFT ONLY.
INSTRUMENT FAILURE WARNING SYSTEM	OPTIONAL 3/	REQUIRED PLUS FLIGHT CREW ASSIGNMENTS AND PROCEDURES SPECIFIED IN NOTE 3/ BELOW.
DUAL ILS AND GLIDE SLOPE RECEIVERS	NOT REQUIRED (N.R.)	REQUIRED
SINGLE FLIGHT DIRECTOR WITH DUAL DISPLAYS 1/ AND SINGLE AUTOMATIC APPROACH COUPLER 2/ OR TWO INDEPENDENT FLIGHT DIRECTOR SYSTEMS	N.R.	REQUIRED
EQUIPMENT FOR IDENTIFICATION OF DECISION HEIGHT	N.R.	REQUIRED. CAN BE: (1) RADAR ALTIMETER, OR (2) INNER MARKERS.
MISSED APPROACH ATTITUDE GUIDANCE	N.R.	REQUIRED. CAN BE: (1) ATTITUDE GYROS WITH CALIBRATED PITCH MARKINGS, OR (2) FLIGHT DIRECTOR PITCH COMMAND, OR (3) COMPUTED PITCH COMMAND.
AUTO THROTTLE SYSTEM	N.R.	REQUIRED ALL TURBOJETS IF OPER- ATIONS BASED ON DUAL FLIGHT DIRECTORS. ALSO REQUIRED ANY AIRCRAFT USING SPLIT AXIS COUPLERS IF APPLICANT CAN'T SHOW IT DOES NOT SIGNIFICANTLY REDUCE PILOT WORKLOAD.
RAIN REMOVAL EQUIPMENT	N.R.	REQUIRED

- 1/ SINGLE AXIS FLIGHT DIRECTORS IF BASIC GLIDE SLOPE INFORMATION
DISPLAYED ON SAME INSTRUMENT.
- 2/ SPLIT AXIS ACCEPTABLE.
- 3/ IF IMPROVED FAILURE WARNING SYSTEM NOT PROVIDED FOR CAT I OPERATIONS
APPLICANT MUST ESTABLISH FLIGHT CREW PROCEDURES AND DUTY ASSIGNMENTS
TO PROVIDE IMMEDIATE DETECTION OF ESSENTIAL INSTRUMENT AND EQUIPMENT
FAILURES. SUCH PROCEDURES AND ASSIGNMENTS ARE REQUIRED FOR CATEGORY
II OPERATIONS.

* SOURCE: FAA ADVISORY CIRCULAR 120-29, SEPT. 25, 1970.

TABLE 11. BASE-LINE STOL AVIONICS

Subsystem	Number Required	Measurement	
		Direct	Indirect.
Air Data			
Pitot-Static	2	P_s, P_t	q_c
Free-Air Temperature Sensor	1	T_m	
Airspeed Indicator	2		V_{IAS}
Barometric Altimeter	2		h_{MSL}
Vertical Speed Indicator	2		h_{MSL}
Angle of Attack Sensor	1	α_M	
Attitude/Heading Reference			
Magnetic Compass	1	MAG HDG	
Vertical Gyroscope	2	θ, θ	
Vertical Gyroscope - Independent	1	θ, θ	
Slip-Skid (Turn/Bank)	1	θ	
Directional Gyroscope	1	HDG	
Clock With Sweep Second Hand	1	Time	
Communication			
VHF Voice (Two-Way)	2		
VOR Receiver	2	θ_s	
DME Receiver	2	ρ_s	
MLS Receiver	2	AZ, EL, R	
Marker Beacon Receiver	1	Fix	
ADF Receiver	1	BRC	
ATC Transponder (4096 Code, Mode 3A)	1		
Digital Data Link (Two-Way)	2		
Autopilot			
Flight Control Computer			
Rate Gyroscopes			
Accelerometers			
Actuators			

TABLE 11. (Continued)

Subsystem	Number Required	Measurement	
		Direct	Indirect
Autothrottle Servo			
Transducers			
Information Presentation			
IPS Display	2		
Mode Selection Switches			
Flight Director Display (ADI)	2		
Flight Director Display (HSI)	2		
Radio Magnetic Indicator	2		
Status Indicators			
Information Management			
Digital Computer	1		
Radar Altimeter	1	h _{AGL}	
Electrical			
Independent Generator & Distribution	2		
Battery			
Auxiliary Power Unit (APU)	1		
Recorders			
Flight Data	1		
Cockpit Voice	1		
Weather Radar	1		

avionics will be a function of the desired system reliability for each of the flight phases. In some cases, a triple redundant configuration might be desirable, in other flight phases a duplicate system with fail operational capability might be suitable, and in other flight phases, a simplex system might be acceptable. Since the variation in system configuration with flight phase can be handled in an integrated system with the proper design of the system hardware and software, the various modes for each of the subfunctions related to the function of concern will indicate the operational configurations available. These configurations are discussed in terms of the system functions for the various flight phases in the succeeding paragraphs.

The base-line system configuration can be represented by the block diagram depicted in Figure 29. This block diagram, while quite general, assumes an understanding of the various subfunctions and modes for each of the system functions discussed in later sections of this report. Note that the radio navigation aids are included under the communication system, whereas state measurements sensors provide primarily self-contained measurements based upon the complete absence of any external (ground-based, airborne, or satellite) measurements.

The computer listing of the input data representing the baseline STOL avionics and EBF aircraft is shown in Figure 30. The aircraft and avionics systems are broken into 50 sections with one candidate subsystem shown under each section. These sections form the hardware and are identified and grouped by the ATA 100 system. The Air Transport Association (ATA) has utilized a listing of aircraft systems by ATA number for a number of years. Table 12 presents the listing of the ATA 100 system by number and by identifying system for the subsystems considered to be the primary subsystems of the aircraft. In addition, the ATA uses a more detailed breakout of the various systems by assigning a second set of digits to each ATA system. This breakout for the avionics is given in Table 13. Note that Section 1 of Figure 30 lists the EBF STOL and the nonavionics ATA systems that are not listed in other sections. Candidate 1 includes the ATA systems which correspond with those given in Table 13. The first data item, the weight, is the weight of those ATA systems for the EBF 100 passenger STOL. This weight was extracted from Reference 2.

Data item 2 (MTBF) is the required MTBF for these ATA systems if the desired probability of nonfailure is 99.8% for a one-hour flight, which is the duration of the longest leg of the route network being flown. Note that no mean-time-to-repair, minimum-time-to-repair or maximum-time-to-repair is listed for Data Items 3, 4, and 5 for the subsystems. In addition, no peaking factor is given. Data item 7, duplication, is a cross reference to other sections, which might use the same equipment. If there is no duplication, the data value of zero is used. Data Item 8 is the number required

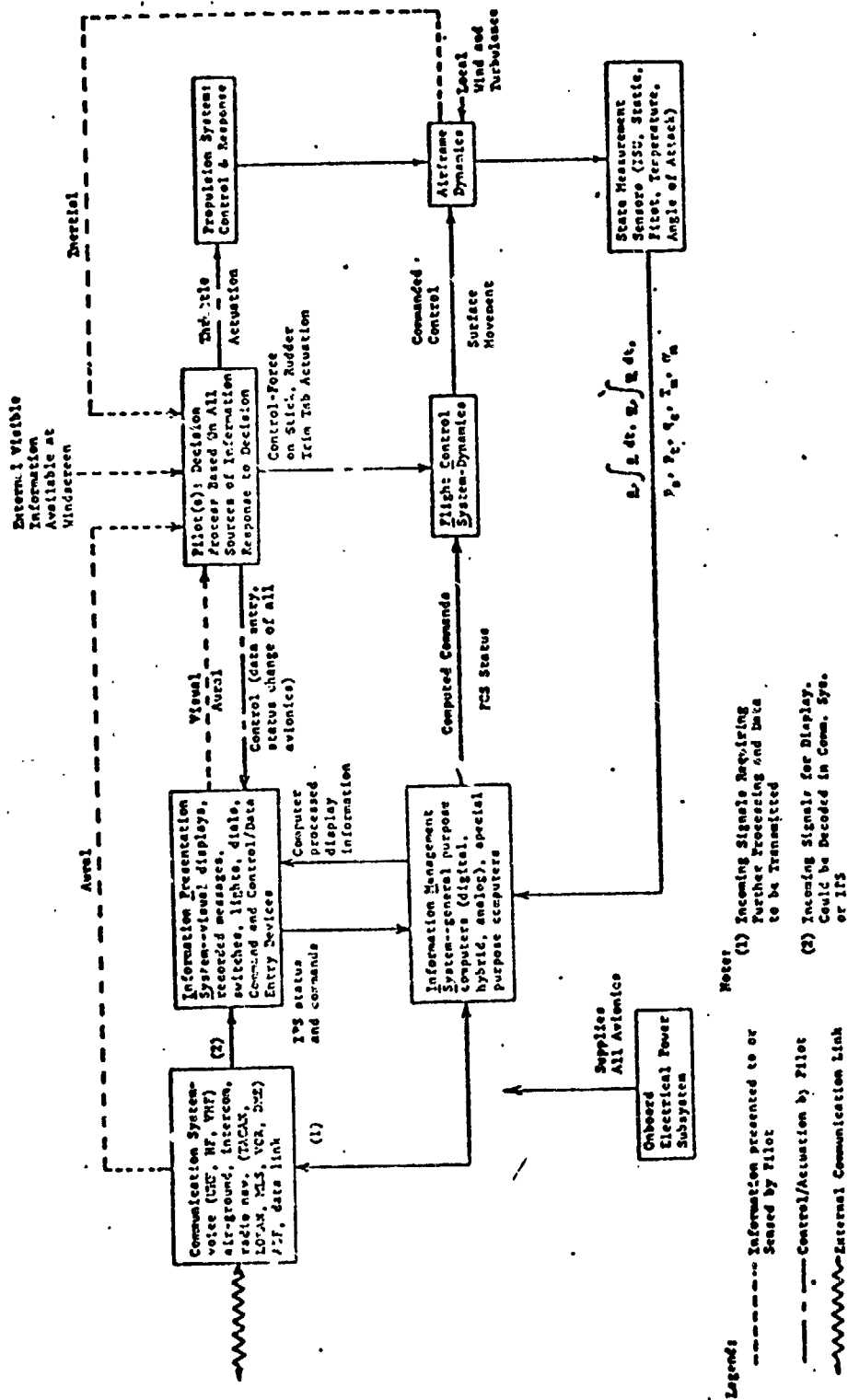


FIGURE 29. BLOCK DIAGRAM DEPICTING MAJOR ELEMENTS AND INTERACTIONS OF AN ADVANCED STOL AVIONICS SYSTEM

CANDIDATE DATA BANK

1 RBF STOL/NOHNAVIONICS ATA SYSTEM

ATA 21,25,26,38,35,36,3A,52-57

1 WEIGHT (LBS) 2.500000E+04
 2 MTBF (MPS) 5.150000E+02
 3 MTRF (MIN) 6.000000E+01
 4 MIN.REPAIR TIME (MIN) 0.5*00
 5 MAX.REPAIR TIME (MIN) 4.800000E+02
 6 PEAKING FACTOR 1.000000E+02
 7 DUPLICATION 0.E*00
 8 NO. REQUIRED FOR DISPATCH 1.000000E+00

2 ATA SYSTEMS 72-76,7A-80/ENGINE

ALLISON PD 287-3 ENGINE SYSTEM

1 WEIGHT (LBS) 1.432000E+04
 2 MTBF (MPS) 2.000000E+03
 3 MTRF (MIN) 6.000000E+01
 4 MIN.REPAIR TIME (MIN) 0.5*00
 5 MAX.REPAIR TIME (MIN) 4.800000E+02
 6 PEAKING FACTOR 1.000000E+02
 7 DUPLICATION 0.E*00
 8 NO. REQUIRED FOR DISPATCH 1.000000E+00

3 ATA SYSTEM 27-37, VOICE COM

VHF VOICE TRANSCIVER

1 WEIGHT (LBS) 2.340000E+01
 2 MTBF (MPS) 3.400100E+03
 3 MTRF (MIN) 1.000000E+01
 4 MIN.REPLACE TIME (MIN) 5.000000E+00
 5 MAX.REPLACE TIME (MIN) 2.000000E+01
 6 PEAKING FACTOR 1.425000E+01
 7 DUPLICATION 0.E*00
 8 NO. REQUIRED FOR DISPATCH 2.000000E+00

4 ATA SYSTEM 7A-12, DME RCVR 1

DME RECEIVER 1

1 WEIGHT (LBS) 2.500000E+01
 2 MTBF (MPS) 1.000000E+03
 3 MTRF (MIN) 1.000000E+01
 4 MIN.REPLACE TIME (MIN) 5.000000E+00
 5 MAX.REPLACE TIME (MIN) 2.000000E+01
 6 PEAKING FACTOR 1.425000E+01
 7 DUPLICATION 5.000000E+00
 8 NO. REQUIRED FOR DISPATCH 1.000000E+00

5 ATA SYSTEM 34-44, DME RCVR 2

DME RECEIVER 2

1 WEIGHT (LBS) 2.500000E+01
 2 MTBF (MPS) 1.000000E+03
 3 MTRF (MIN) 1.000000E+01
 4 MIN.REPLACE TIME (MIN) 5.000000E+00
 5 MAX.REPLACE TIME (MIN) 2.000000E+01
 6 PEAKING FACTOR 1.425000E+01
 7 DUPLICATION 5.000000E+00
 8 NO. REQUIRED FOR DISPATCH 1.000000E+00

FIGURE 30. LISTING OF INPUT DATA FOR STOL AIRCRAFT AND ONBOARD SYSTEMS

6 ATA SYSTEM 34-35, VOR RCVR 1

I VOR RECEIVER 1

1	WTGHT(LBS)	5.4000000E+00	5	MAX.REPLACE TIME(MIN)	2.0000000E+01
2	WTGHT(LBS)	1.0000000E+03	6	PEAKING FACTOR	1.4625000E+01
3	WTGHT(LBS)	1.0000000E+01	7	DUPLICATION	7.0000000E+00
4	MIN.REPLACE TIME(MIN)	5.0000000E+00	8	NO. REQUIRED FOR DISPATCH	1.0000000E+00

7 ATA SYSTEM 34-35, VOR RCVR 2

I VOR RECEIVER 2

1	WTGHT(LBS)	5.4000000E+00	5	MAX.REPLACE TIME(MIN)	2.0000000E+01
2	WTGHT(LBS)	1.0000000E+03	6	PEAKING FACTOR	1.4625000E+01
3	WTGHT(LBS)	1.0000000E+01	7	DUPLICATION	7.0000000E+00
4	MIN.REPLACE TIME(MIN)	5.0000000E+00	8	NO. REQUIRED FOR DISPATCH	1.0000000E+00

8 ATA SYSTEM 34, COMPUTER

I RNAY COMPUTER

1	WTGHT(LBS)	4.4000000E+01	5	MAX.REPLACE TIME(MIN)	4.0000000E+01
2	WTGHT(LBS)	5.0000000E+02	6	PEAKING FACTOR	1.4625000E+01
3	WTGHT(LBS)	2.0000000E+01	7	DUPLICATION	0.2500
4	MIN.REPLACE TIME(MIN)	1.0000000E+01	8	NO. REQUIRED FOR DISPATCH	1.0000000E+00

9 ATA SYSTEM 34-35, BARO ALT

I BAROMETRIC ALTIMETER

1	WTGHT(LBS)	1.0000000E+00	5	MAX.REPLACE TIME(MIN)	2.0000000E+01
2	WTGHT(LBS)	1.0691000E+03	6	PEAKING FACTOR	1.4625000E+01
3	WTGHT(LBS)	1.0000000E+01	7	DUPLICATION	0.2500
4	MIN.REPLACE TIME(MIN)	5.0000000E+00	8	NO. REQUIRED FOR DISPATCH	2.0000000E+00

10 ATA SYSTEM 34-35, AIRSPEED IND

I AIRSPEED INDICATOR

1	WTGHT(LBS)	9.0000000E+00	5	MAX.REPLACE TIME(MIN)	2.0000000E+01
2	WTGHT(LBS)	1.0691000E+03	6	PEAKING FACTOR	1.4625000E+01
3	WTGHT(LBS)	1.0000000E+01	7	DUPLICATION	0.2500
4	MIN.REPLACE TIME(MIN)	5.0000000E+00	8	NO. REQUIRED FOR DISPATCH	2.0000000E+00

FIGURE 30. (CONTINUED)

1 WEIGHT(LBS) 9.3700000E+02 5 MAX.REPLACE TIME(MIN) 1.0000000E+02
 2 WTFR(MRS) 1.2000100E+04 6 PEAKING FACTOR 1.4625000E+01
 3 MTT(LB/MI(MIN) 5.3000000E+01 7 DUPLICATION 0.E+00
 4 MIN.REPLACF TIME(MIN) 2.5000000E+01 8 NO. REQUIRED FOR DISPATCH 2.0000000E+00

37 ATA SYSTEM 24, POWER STORAGE

1 WEIGHT(LBS) 8.4000000E+01 5 MAX.REPLACE TIME(MIN) 3.2000000E+01
 2 WTFR(MRS) 1.6000000E+04 6 PEAKING FACTOR 1.4625000E+01
 3 MTT(LB/MI(MIN) 1.6000000E+01 7 DUPLICATION 0.E+00
 4 MIN.REPLACF TIME(MIN) 8.0000000E+00 8 NO. REQUIRED FOR DISPATCH 1.0000000E+00

38 ATA SYSTEM 24, APU

1 WEIGHT(LBS) 7.9200000E+02 5 MAX.REPLACF TIME(MIN) 8.0000000E+01
 2 WTFR(MRS) 2.4000000E+04 6 PEAKING FACTOR 1.4625000E+01
 3 MTT(LB/MI(MIN) 4.9000000E+01 7 DUPLICATION 0.E+00
 4 MIN.REPLACF TIME(MIN) 2.0000000E+01 8 NO. REQUIRED FOR DISPATCH 1.0000000E+00

39 ATA SYSTEM 27-35, FLT RECORDER

1 WEIGHT(LBS) 4.0000000E+01 5 MAX.REPLACE TIME(MIN) 2.0000000E+01
 2 WTFR(MRS) 2.0000000E+03 6 PEAKING FACTOR 1.4625000E+01
 3 MTT(LB/MI(MIN) 1.2000000E+01 7 DUPLICATION 0.E+00
 4 MIN.REPLACF TIME(MIN) 6.0000000E+00 8 NO. REQUIRED FOR DISPATCH 1.0000000E+00

40 ATA SYSTEM 27-35, VOICE RECORD

1 WEIGHT(LBS) 1.4000000E+01 5 MAX.REPLACE TIME(MIN) 2.0000000E+01
 2 WTFR(MRS) 2.0000000E+03 6 PEAKING FACTOR 1.4625000E+01
 3 MTT(LB/MI(MIN) 1.0000000E+01 7 DUPLICATION 0.E+00
 4 MIN.REPLACF TIME(MIN) 5.0000000E+00 8 NO. REQUIRED FOR DISPATCH 1.0000000E+00

41 ATA SYSTEM 34, HAZARD AVOID

1 WEIGHT(LBS) 1.4000000E+01 5 MAX.REPLACE TIME(MIN) 2.0000000E+01
 2 WTFR(MRS) 2.0000000E+03 6 PEAKING FACTOR 1.4625000E+01
 3 MTT(LB/MI(MIN) 1.0000000E+01 7 DUPLICATION 0.E+00
 4 MIN.REPLACF TIME(MIN) 5.0000000E+00 8 NO. REQUIRED FOR DISPATCH 1.0000000E+00

PROXIMITY WARNING INDICATOR

FIGURE 30. (CONTINUED)

1 WEIGHT(LBS) 4 3.500000E+03
 2 WTRF(MPS) 5 1.000000E+03
 3 MTDPLR(MIN) 6 1.500000E+01
 4 MIN.REPLAC TIME(MIN) 7 8.000000E+00

5 MAX.REPLACE TIME(MIN) 8 3.200000E+01
 6 PEAKING FACTOR 9 1.462500E+01
 7 DUPLICATION 10 0.E+00
 8 NO. REQUIRED FOR DISPATCH 11 1.000000E+00

42 ATA SYSTEM 34 ALTITUDE ALERT
 1 WEIGHT(LBS) 2 2.000000E+00
 2 WTRF(MPS) 3 3.000000E+03
 3 MTDPLR(MIN) 4 1.000000E+01
 4 MIN.REPLAC TIME(MIN) 5 5.000000E+00

5 MAX.REPLACE TIME(MIN) 6 2.000000E+01
 6 PEAKING FACTOR 7 1.462500E+01
 7 DUPLICATION 8 0.E+00
 8 NO. REQUIRED FOR DISPATCH 9 1.000000E+00

43 ATA SYSTEM 35 LANDING GEAR
 1 WEIGHT(LBS) 2 5.985000E+03
 2 WTRF(MPS) 3 5.750000E+02
 3 MTDPLR(MIN) 4 1.000000E+02
 4 MIN.REPLAC TIME(MIN) 5 4.500000E+01

5 MAX. REPLACE TIME(MIN) 6 0.400000E+02
 6 PEAKING FACTOR 7 1.000000E+02
 7 DUPLICATION 8 0.E+00
 8 NO. REQUIRED FOR DISPATCH 9 1.000000E+00

44 ATA SYSTEM 36 LIGHTS
 1 WEIGHT(LBS) 2 3.950000E+02
 2 WTRF(MPS) 3 5.750000E+03
 3 MTDPLR(MIN) 4 1.000000E+01
 4 MIN.REPLAC TIME(MIN) 5 9.000000E+00

5 MAX. REPLACE TIME(MIN) 6 3.000000E+01
 6 PEAKING FACTOR 7 1.462500E+01
 7 DUPLICATION 8 0.E+00
 8 NO. REQUIRED FOR DISPATCH 9 1.000000E+00

45 ATA SYSTEM 37 FLIGHT CONTROLS
 1 WEIGHT(LBS) 2 4.342000E+03
 2 WTRF(MPS) 3 1.000000E+03
 3 MTDPLR(MIN) 4 3.000000E+01
 4 MIN.REPLAC TIME(MIN) 5 1.500000E+01

5 MAX. REPL CE TIME(MIN) 6 0.000000E+01
 6 PEAKING FACTOR 7 1.462500E+01
 7 DUPLICATION 8 0.E+00
 8 NO. REQUIRED FOR DISPATCH 9 1.000000E+00

46 ATA SYSTEM 38 FUEL SYSTEM
 1 WEIGHT(LBS) 2 8.926000E+02
 6 PEAKING FACTOR 7 1.462500E+01

FIGURE 20. (CONTINUED)

47 AT-22-1/30/50 AMP. CNTRL. EQUIP

2	WTRP (MRS)	4.8000000E+03	7	DUPLICATION	0.E+00
3	MITOLPUL (M)	3.0000000E+01	8	NO. REQUIRED FOR DISPATCH	1.0000000E+00
4	MIN. REPLACE TIME (MIN)	1.5000000E+01	9	MAX. MISSION FUEL (LBS)	2.1000000E+04
5	MAX. REPLACE TIME (MIN)	6.0000000E+01	10	RESERVE FUEL REQUIRED (LBS)	2.5000000E+03

1 AFCS AMPLIFIER COMPUTER

1	WEIGHT (LBS)	3.7200000E+03	5	MAX. REPLACE TIME (MIN)	0.0000000E+00
2	WTRP (MRS)	1.2500000E+03	6	PEAKING FACTOR	1.4425000E+01
3	MITOLPUL (M)	3.0000000E+01	7	DUPLICATION	0.E+00
4	MIN. REPLACE TIME (MIN)	1.5000000E+01	8	NO. REQUIRED FOR DISPATCH	2.0000000E+00

48 ATA 22-22 AUTOPILOT ACTUATORS

1 AFCS AUTOPILOT ACTUATORS

1	WEIGHT (LBS)	2.1800000E+01	5	MAX. REPLACE TIME (MIN)	0.0000000E+00
2	WTRP (MRS)	1.4800000E+03	6	PEAKING FACTOR	1.4625000E+01
3	MITOLPUL (M)	3.0000000E+01	7	DUPLICATION	0.E+00
4	MIN. REPLACE TIME (MIN)	1.5000000E+01	8	NO. REQUIRED FOR DISPATCH	2.0000000E+00

49 ATA 34-22 FLT DIRECTOR DISPLAY

1 STOL FLIGHT DIRECTOR DISPLAY

1	WEIGHT (LBS)	1.0000000E+03	5	MAX. REPLACE TIME (MIN)	0.0000000E+00
2	WTRP (MRS)	1.2500000E+03	6	PEAKING FACTOR	1.4425000E+01
3	MITOLPUL (M)	3.0000000E+01	7	DUPLICATION	0.E+00
4	MIN. REPLACE TIME (MIN)	1.5000000E+01	8	NO. REQUIRED FOR DISPATCH	2.0000000E+00

50 ATA 22-44/43 FIT CNTRL SENSORS

1 AFCS SENSORS

1	WEIGHT (LBS)	7.0000000E+00	5	MAX. REPLACE TIME (MIN)	0.0000000E+00
2	WTRP (MRS)	1.2500000E+03	6	PEAKING FACTOR	1.4425000E+01
3	MITOLPUL (M)	3.0000000E+01	7	DUPLICATION	0.E+00
4	MIN. REPLACE TIME (MIN)	1.5000000E+01	8	NO. REQUIRED FOR DISPATCH	2.0000000E+00

51 WIND DATA

1 WIND DATA
 1 MEAN EAST WIND (KTS) 0.E+00
 2 MEAN WEST WIND (KTS) 0.E+00

FIGURE 30. (CONTINUED)

54 AIRPORT CAPACITY

1 SAC CAPACITY

1 VFR CAPACITY MOVEMENTS/HR = 1.500000E+02 2 IFR CAPACITY MOVEMENTS/HR = 4.000000E+01

2 SNA CAPACITY

1 VFR CAPACITY MOVEMENTS/HR = 1.200000E+02 2 IFR CAPACITY MOVEMENTS/HR = 4.000000E+01

3 SJC CAPACITY

1 VFR CAPACITY MOVEMENTS/HR = 1.200000E+02 2 IFR CAPACITY MOVEMENTS/HR = 4.000000E+01

FIGURE 30. (CONTINUED)

TABLE 12. ATA 100 SYSTEM LISTING

ATA No.	System
21	Air Conditioning
22	Autopilot
23	Communications
24	Electrical Power
25	Equipment/Furnishings
26	Fire Protection
27	Flight Controls
28	Fuel
29	Hydraulic Power
30	Ice and Rain Protection
31	Instruments
32	Landing Gear
33	Lights
34	Navigation
35	Oxygen
36	Pneumatic
38	Water/Waste
49	Airborne Auxiliary Power
52	Doors
53	Fuselage
54	Nacelles/Pylons
55	Stabilizers
56	Windows
57	Wings
72	Engines
73	Engine Fuel and Control

TABLE 12. ATA 100 SYSTEM LISTING
(Continued)

ATA No.	System
74	Ignition
75	Engine Air
76	Engine Controls
77	Engine Indicating
78	Exhaust
79	Oil
80	Starting

TABLE 13. ATA SUBSYSTEM LISTING

ATA No.	System and Subsystem
22	Autopilot
22-10	Amplification
22-20	Actuation
22-30	Controlling
22-40	Indicating
22-50	Sensing
22-60	Coupling
23	Communications
23-20	Very High Frequency (VHF)
23-30	Public Address and Passenger Entertainment
23-40	Interphone
23-50	Audio Integrating
23-60	Static Discharging
23-70	Voice Recorders
24	Electrical Power
24-10	Generator Drive
24-20	AC Generation
24-30	DC Generation
24-40	External Power
24-50	Electrical Load Distribution
29	Hydraulic Power
29-10	Main
29-20	Auxiliary
29-30	Indicating
31	Instruments
31-10	Panel
31-20	Independent Instruments

TABLE 13. ATA SUBSYSTEM LISTING
(Continued)

ATA No.	System and Subsystem
32	Landing Gear
32-10	Main Gear and Doors
32-20	Nose Gears and Doors
32-30	Extension and Retraction
32-40	Wheels and Brakes
32-50	Steering
32-60	Position and Warning
33	Lights
33-10	Flight Compartment
33-20	Passenger Compartment
33-40	Exterior
33-50	Emergency Lighting
34	Navigation
34-10	Air Data Instrumentation
34-20	Attitude and Direction Instrumentation
34-30	Radio Navigation
34-40	Radar Navigation
49	Airborne Auxiliary Power
49-10	Power Plant
49-20	Engine
49-30	Engine Fuel and Control
49-40	Ignition/Starting
49-50	Air
49-60	Engine Controls
49-70	Indicating
49-80	Exhaust
49-90	Oil

for dispatch; in other words this is a single aircraft. Data Items 1 through 8 are similar for all other sections of data. Note that Section 46, ATA system 28, which is the fuel system, included an additional data item, 9, which is the maximum mission fuel that can be loaded as described in Reference 2.

State Estimation Function. - The state estimation function can be provided by either an automatic or manual subfunction. Figure 31 indicates the initial subfunctions and the modes for each of the subfunctions, which will be investigated for the cruise flight phase. It should be noted that the subsystems required for each of the modes are denoted by an x under that mode if the subsystem is to be utilized in that mode. The subsystems listed are given by the section labels listed in Figure 30. It is assumed, as previously stated, that the navigation function would normally utilize the automatic subfunction during all flight phases. In addition, if weather conditions require an instrument approach and landing, one or both MLS receivers and the radar altimeter would be required for that flight phase. This is denoted as the approach/landing navigation subfunction. This subfunction is not illustrated in Figure 31.

Note that all automatic state estimation modes use one or more measurements of bearing (θ) or distance (ρ). Reference 17 indicates that the principle en route navigation aid that will be provided by FAA will be VORTAC. The improvements to the VORTAC system discussed in reference 17 indicate that modifications to the ground station circuitry will be made to permit handling of 200 aircraft per VORTAC rather than the current 100 aircraft limitation. In addition, the spacing between channels is being reduced to 50 KHz from the present 100 KHz. These two modifications to the VORTAC system appear to be the only major changes FAA plans to upgrade specific facilities that do not provide adequate coverage or quality of radiated signals necessary for area navigation (reference 17).

Note that while Figure 31 lists only the required airborne equipment for the function to be performed, the ground navigation stations providing the measurements must be available. The arrangement of the modes for the automatic navigation subfunction resulted from running ANGCAP for each possible mode and each leg of the flight. In general, the more accurate modes require the largest number of subsystems available and hence have a higher probability of unavailability than do less accurate modes requiring fewer subsystems. Specific results of the ANGCAP simulation for each of the modes is presented in a later section of this report. While additional modes beyond those indicated in Figure 31 are theoretically possible, the results presented later are based upon the FAA required avionics with the addition of an onboard computer for performance of NAV equation solutions and Kalman filter equation solutions.

FUNCTION - STATE ESTIMATION
SUBFUNCTION - AUTOMATIC NAVIGATION

MODES	MODE 1	MODE 2	MODE 3
SUBSYSTEMS REQUIRED			
ATA SYSTEM 34-31: DME RCVR 1	X		X
ATA SYSTEM 34-32: DME RCVR 2	X		X
ATA SYSTEM 34-33: VOR RCVR 1	X		X
ATA SYSTEM 34-34: VOR RCVR 2	X		X
ATA SYSTEM 34: COMPUTER	X		X
ATA SYSTEM 34-10: RADIO ALT	X		X
ATA SYSTEM 34-10: AIRCRAFT IND	X		X

MODES	MODE 4	MODE 5	MODE 6
SUBSYSTEMS REQUIRED			
ATA SYSTEM 34-35: DME RCVR 1		X	
ATA SYSTEM 34-36: DME RCVR 2		X	
ATA SYSTEM 34-37: VOR RCVR 1		X	
ATA SYSTEM 34-38: VOR RCVR 2		X	
ATA SYSTEM 34: COMPUTER	X		X
ATA SYSTEM 34-10: RADIO ALT	X		X
ATA SYSTEM 34-10: AIRCRAFT IND	X		X

MODES	MODE 7	MODE 8
SUBSYSTEMS REQUIRED		
ATA SYSTEM 34-39: DME RCVR 1		X
ATA SYSTEM 34-40: DME RCVR 2		X
ATA SYSTEM 34-41: VOR RCVR 1	X	
ATA SYSTEM 34-42: VOR RCVR 2	X	
ATA SYSTEM 34: COMPUTER	X	X
ATA SYSTEM 34-10: RADIO ALT	X	X
ATA SYSTEM 34-10: AIRCRAFT IND	X	X

FIGURE 31. STATE ESTIMATION FUNCTION SUBFUNCTIONS AND MODES

FUNCTION - STATE ESTIMATION
 SUBFUNCTION - MANUAL NAVIGATION

MODES MODE 1 MODE 2

SUBSYSTEMS REQUIRED

ATA SYSTEM 34-3A. OMF RCVR 1	X	
ATA SYSTEM 34-3B. VMO RCVR 1	X	
ATA SYSTEM 34-15. PARO ALT		X
ATA SYSTEM 33-10. AIRSPEED IND	X	X

FIGURE 31. (CONTINUED)

FUNCTION: STATE ESTIMATION
 SUBFUNCTION: APPROACH/LANDING NAVIGATION

MODES	MODE 1	MODE 2	MODE 3	MODE 4	MODE 5
SUBSYSTEMS PROVIDED					
ATA SYSTEM 34-35: QMF RVR	X				
ATA SYSTEM 34-36: VCO RVR 1	X				
ATA SYSTEM 34: COMPUTER			X	X	X
ATA SYSTEM 34-16: R233 ALT	X				
ATA SYSTEM 34-16: AIR PRESSURE	X				
ATA SYSTEM 34-16: AIR PRESSURE	X				
ATA SYSTEM 34-16: AIR TEMP	X				
ATA SYSTEM 34-16: VERTICAL VEL	X				
ATA SYSTEM 34-16: ALPHA	X				
ATA SYSTEM 34-20: MAG HEADING	X				
ATA SYSTEM 34-20: ATTITUDE REF	X				
ATA SYSTEM 34-20: HEADING REF	X				
ATA SYSTEM 34-30: LANDING AID	X				

FIGURE 31. (CONTINUED)

Command Generation/Execution Functions.-The initial command generation/execution subfunctions and modes implemented in the program are listed in Figure 32. Additional modes are possible and can be added as desired. As with the state estimation function, it is assumed that the automatic guidance/control mode is utilized when available during all phases of flight. Selection of a manual mode by the crew may occur during VFR weather during the final approach. When visual cues are not available, the crew must utilize the automatic guidance/control subfunction as described previously.

Hazard Avoidance Function.-The hazard avoidance function is assumed to have an automatic and manual subfunction. It is assumed that the automatic subfunction would normally be used, with reversion to manual only upon loss of the computer. The hazard avoidance function is very similar to the combination of the state estimation and command generation functions in that the output of sensors measuring the state of the aircraft with respect to potential hazards such as weather, other aircraft, and obstructions to flight such as terrain and natural features, as well as man-made structures, is processed to generate the appropriate command to avoid the hazard. It is assumed that the command generated would be automatically fed into the command execution subsystem if the automatic hazard avoidance subfunction was used. If the manual hazard avoidance subfunction was utilized, it is assumed that the command execution function would also be performed manually. The initial modes for the automatic and manual subfunctions for hazard avoidance are listed in Figure 33. Additional modes are possible and may be added to the code by loading input data.

Communication Function.-The communication function is assumed to have automatic and manual subfunctions. It is assumed that the automatic subfunction would be used normally with reversion to manual only upon loss of the computer processing information received and transmitted via the digital data link. The initial modes for the automatic and manual subfunctions for the communication function are listed in Figure 34. Additional modes are possible by manipulation of input data.

Systems Management Function.-The systems management function is also assumed to have automatic and manual subfunctions. Since the primary purpose of this function is to assess the status of the aircraft subsystems, it is assumed that the automatic subfunction would normally be used with reversion to manual only upon loss of the computer. The initial modes selected for the automatic and manual subfunctions for systems management are listed in Figure 35. Additional modes are possible by specification of input data.

Safe Flight Function.-The safe flight function has only one mode as shown in Figure 36. If any of those hardware fail in flight, an unscheduled landing is mandatory.

FUNCTION - COMMAND GENERATION/EXECUTION
SUBFUNCTION - AUTOMATIC GUIDANCE/CONTROL

MODES MODE 1 MODE 2

SUBSYSTEMS REQUIRED

ATA SYSTEM 24. COMPUTER	X	X
ATA SYSTEM 31. INFO REPRESENT	X	X
ATA 22-10/36/42 AMP. CTRL. COUPL	X	X
ATA 22-20 AUTOPILOT ACTUATORS	X	X
ATA 34-20 FLT DIRECTOR DISPLAY	X	X
ATA 22-40/50 FLT CTRL SENSORS	X	X

FUNCTION - COMMAND GENERATION/EXECUTION
SUBFUNCTION - MANUAL GUIDANCE/CONTROL

MODES MODE 1 MODE 2 MODE 3

SUBSYSTEMS REQUIRED

ATA SYSTEM 24. COMPUTER	X	X	X
ATA SYSTEM 31. INFO REPRESENT	X	X	X
ATA 22-10/36/42 AMP. CTRL. COUPL	X	X	X
ATA 34-20 FLT DIRECTOR DISPLAY	X	X	X
ATA 22-40/50 FLT CTRL SENSORS	X	X	X

FIGURE 32. COMMAND GENERATION/EXECUTION FUNCTION SUBFUNCTIONS AND MODES

FUNCTION - HAZARD AVOIDANCE
SUBFUNCTION - AUTOMATIC HAZARD AVOIDANCE

MODES	MODE 1	MODE 2	MODE 3
SUBSYSTEMS REQUIRED			
ATA SYSTEM 34, COMPUTER	X	X	X
ATA SYSTEM 34-40, RADAR ALT	X	X	X
ATA SYSTEM 34-40, WX PAPER	X	X	X
ATA SYSTEM 34, HAZARD AVOID	X	X	X

MODE 4	MODE 5	MODE 6
SUBSYSTEMS REQUIRED		
ATA SYSTEM 34, COMPUTER	X	X
ATA SYSTEM 34-40, RADAR ALT	X	X
ATA SYSTEM 34-40, WX PAPER	X	X
ATA SYSTEM 34, HAZARD AVOID	X	X

MODE 7
SUBSYSTEMS REQUIRED
ATA SYSTEM 34, COMPUTER
ATA SYSTEM 34-40, RADAR ALT
ATA SYSTEM 34-40, WX PAPER
ATA SYSTEM 34, HAZARD AVOID

FIGURE 13. HAZARD AVOIDANCE FUNCTION SUBFUNCTIONS AND MODES

FUNCTION - HAZARD AVOIDANCE
SUBFUNCTION - MANUAL, HAZARD AVOIDANCE

CODES	MODE 1	MODE 2	MODE 3	MODE 4
SUBSYSTEMS REQUIRED				
ATA SYSTEM 36-40; P&OR ALT	X			
ATA SYSTEM 38-40; WX DAPAR	X			
ATA SYSTEM 34; HAZARD AVOID		X	X	

FIGURE 33. (CONTINUED)

FUNCTION - COMMUNICATION
SUBFUNCTION - AUTOMATIC COMMUNICATION

MODES MODE 1 MODE 2

SUBSYSTEMS REQUIRED

ATA SYSTEM 24. COMPUTER X X
 ATA SYSTEM 23. DATA LINK X X
 ATA SYSTEM 31. INFO PROCESSING X
 ATA SYSTEM 31-10. DATA ENTRY X

FUNCTION - COMMUNICATION
SUBFUNCTION - MANUAL COMMUNICATION

MODES MODE 1

SUBSYSTEMS REQUIRED

ATA SYSTEM 23-26. VOICE COM X

FIGURE 34. COMMUNICATION FUNCTION SUBFUNCTIONS AND MODES

FUNCTION - SYSTEM MANAGEMENT
SUBFUNCTION - AUTOMATIC SYSTEM MANAGEMENT

MODES	MODE 1	MODE 2	MODE 3
SUBSYSTEMS REQUIRED			
ATA SYSTEM 24, COMPUTER		X	
ATA SYSTEM 21, INFO PRESENTATN	X	X	
ATA SYSTEM 21-20, STATUS IND			X

FUNCTION - SYSTEM MANAGEMENT
SUBFUNCTION - MANUAL SYSTEM MANAGEMENT

MODES	MODE 1	MODE 2	MODE 3
SUBSYSTEMS REQUIRED			
ATA SYSTEM 24, COMPUTER		X	
ATA SYSTEM 21, INFO PRESENTATN	X	X	
ATA SYSTEM 21-10, MONF REFLECT	X	X	
ATA SYSTEM 21-20, STATUS IND			X

MODE 4

MODES	MODE 4	MODE 5
SUBSYSTEMS REQUIRED		
ATA SYSTEM 24, COMPUTER		
ATA SYSTEM 21, INFO PRESENTATN	X	
ATA SYSTEM 21-10, MONF REFLECT		X
ATA SYSTEM 21-20, STATUS IND		X

FIGURE 35. SYSTEMS MANAGEMENT FUNCTION SUBFUNCTION AND MODES

FUNCTION - SAFE FLIGHT
SUBFUNCTION - SAFE FLIGHT

MCDES

MODE 1

SUBSYSTEMS REQUIRED

ATA SYSTEM 79-7A-7A-00/ENGINE	X
ATA SYSTEM 90	X
ATA SYSTEM 24, ELECTRIC POWER	X
ATA SYSTEM 27	X

FIGURE 36. SAFE FLIGHT FUNCTION

Implementation of Functions in Monte Carlo Program.-As previously stated, a system function is defined as an operation or action required to conduct the STOL mission. Each function's availability is evaluated at each time step in the Monte Carlo model as described on page 6. Statistics that result due to reversion to a backup mode or loss of a function are computed in the Monte Carlo model. These statistics are represented by some of the mission performance measures previously discussed on pages 56 and 57 and statistics on the number of times each function was lost in a Monte Carlo run. Statistics are also calculated for the number of modes used for each function in a Monte Carlo run.

Man-Machine Task Allocations.-Various attempts have been made to estimate crew performance. Some of the methods used are reviewed in Appendix F. Development and implementation of a valid, human performance model was beyond the scope of this study. An analysis of crew activities was conducted to estimate the information requirements and crew workload over a typical flight leg. The flight leg was divided into three phases characterized by similar system performance requirements. These phases were then analyzed with respect to the base-line operational modes.

A general description of the functional requirements and their effects on crew activities and operational modes was desired. In-depth review of the operations was neither possible nor warranted. In particular, the work-intensive tasks during final approach and landing could not be described in detail since the response characteristics of the aircraft and the guidance/control system have not been defined. Nonetheless, it is assumed that in order for the aircraft to be used in air carrier service, the man-allocated tasks during this phase will be similar to present air carrier requirements in a manual mode and similar to present cruise requirements in an automatic mode.

Takeoff/Climb: After preflight checkout has been accomplished and the aircraft is positioned for takeoff, all engines are run at or near full power. When indicated airspeed has increased to V_1 the vehicle is rotated to takeoff attitude. The vehicle becomes airborne shortly after rotation as a result of aerodynamic and augmented lift.

Initial climbout follows a steep flight path; the steepness of the flight path is influenced by requirements for increasing forward speed, while maintaining a safe angle of attack along with any noise abatement or ATC procedures.

Transition from takeoff to climb configured flight is accomplished by increasing airspeed through the simultaneous reduction of augmented lift and decreasing of the steepness of the flight path. Engine thrust remains near maximum during the transition. Pitch attitude is varied in order to establish a zero degree or positive flight path angle while

avoiding a stall angle of attack. Engine thrust is reduced after the vehicle has accelerated to a speed which allows stable aerodynamic control. The vehicle is flown from this point as a conventional aircraft.

A time line chart of anticipated system control requirements for the takeoff is presented in Figure 37.

Cruise: During this phase, the vehicle is flown at a constant Mach and altitude. Crew activities, therefore, involve navigation, fuel management, maintaining a guard against other aircraft, and monitoring of automatic equipment. Table 14 summarizes conventional information requirements during the cruise phase.

The crew activities range from a solely monitoring function utilizing an autopilot under altitude hold to a control function, if no autopilot is used, or to guidance/control if the crew must generate guidance commands from the navigation instruments. Workload over these operations varies from very little to moderate.

Final Approach/Landing: The transition to final approach may be fully automatic or manual depending on the terminal guidance system utilized. The microwave landing system together with an airborne computer may generate the curved approach guidance paths needed. In addition, an autopilot may be developed to automatically steer the aircraft on the desired flight path. However, since horizontal turns and vertical maneuvers are critically dependent on power setting, flap setting, aircraft weight, and center of gravity, etc., all of which are flight dependent, it is unlikely that the initial flights will be fully automatic. In this case, manual vectoring or area navigation may be used to obtain navigation information from which the crew must guide and control the aircraft to the final approach. In this case, workload is at its peak.

The last maneuver to final approach is an alignment with the runway centerline. Preceding the letdown, the vehicle follows a level flight path with a forward velocity slightly greater than stall speed. The approach is initiated from a ground clearance altitude of approximately 1000 feet. Engine power settings and pitch attitude are varied in order to maintain a level flight path.

Descent to the runway threshold is initiated by lowering the nose of the aircraft. Indicated airspeed is maintained at a minimum value during the descent along the steep glide path. Pitch attitude changes furnish the primary vehicle control for holding a desired letdown path. Power setting changes and thrust changes are minimized during the letdown.

Final deceleration preceding touchdown is accomplished by flaring the aircraft to a predetermined pitch attitude when the vehicle is over

Control Parameter	Events		
	Takeoff Roll	Rotation Climbout	Transition
Pitch attitude			
Roll attitude.			
Yaw.			
Heading.			
Ground clearance altitude.			
Altitude rate.			
Angle of attack.			
Indicated airspeed			
Power setting.			
Gross weight			

FIGURE 37 . TIME LINE HISTORY OF ANTICIPATED SYSTEM CONTROL ACTIVITY DURING TAKEOFF

TABLE 14. INFORMATION REQUIREMENTS FOR CRUISE PHASES

Flight Control	Navigation
Pitch attitude	Current position
Roll attitude	Destination position
Yaw	Bearing to destination
Turn rate	Distance to destination
Barometric altitude	Ground speed
Altitude rate	
Mach	
Heading	
Engine performance data	

Fuel Management
Fuel quantity
Fuel flow rate
Distance to destination
Ground speed

the runway threshold. After touchdown, all engines are reduced to idle power.

A time line chart of anticipated control activity during the landing is presented in Figure 38.

Commonalities Among Mission Phases: Table 15 summarizes controlled parameters common to pilot control activities involved in performing the mission phases. By combining controlled parameters in this fashion, some idea may be obtained regarding information which must be provided or provided for in the pilot's cockpit area.

Several of the mission phases appear to be characterized by common system control requirements for many of the flight control parameters. Short field maneuvers closely approximate conventional takeoff and landing. Although the STOL phases involve steeper letdown and climbout paths, the vehicle must still be aligned with localizer and glide slope during the approach to landing. In both conventional and STOL modes, takeoff is preceded by a takeoff roll, and aerodynamic lift is a major factor contributing to takeoff lift. In both STOL and conventional modes, aerodynamic stall is a major factor in determining the maneuvering envelope. During the cruise phase, conventional and STOL flight modes are identical.

Division of Crew Duties: It is assumed that two persons operate and control all of the subsystems of the STOL aircraft. Table 16 summarizes the basic division of crew duties which are thought to acceptably distribute the activity involved in all flight phases for Category I, or better, weather.

As discussed in reference 18, approach and landing in low visibility weather conditions requires careful analysis to determine the role of the crew. All test pilots who flew low-visibility approaches as reported in reference 18 "agreed that it is absolutely essential that pilots be provided access into the automatic system". In these low visibility conditions, it was suggested that at least one pilot must maintain instrument flight to touchdown, throughout roll-out, and during taxi-in. It was suggested that one pilot maintain instrument flight to touchdown while the other pilot acts as a decision maker, basing his decisions on the information acquired from the instruments displays, independent landing monitor, or visual cues if available. Reference 19 recommended that "the aircraft commander should be the decision maker while the other pilot is responsible for instrument flight". Following this recommendation, Table 17 presents the division of crew duties for Category II or III weather with copilot duties being those of the instrument pilot and the pilot's duties being those of the aircraft commander. It should be noted that this is essentially a reversal of the data presented in Table 16. It is assumed that if the aircraft commander acquired visual cues, he would inform the instrument pilot by calling out

Control Parameter	Mission Segments		
	Transition	Descent	Landing
Pitch attitude			
Roll attitude.			
Yaw.			
Course to runway			
Ground clearance altitude.			
Altitude rate.			
Angle of attack.			
Indicated airspeed			
Range to runway.			
Power setting.			
Gross weight			

FIGURE 38. TIME HISTORY OF ANTICIPATED CONTROL ACTIVITY DURING LANDING

TABLE 15. SUMMATION OF PARAMETERS CONTROLLED
IN THE FLIGHT PHASES

Pitch attitude	Range to waypoint
Roll attitude	Lateral deviation from course
Yaw	Ground speed
Turn rate	Heading relative to wind
Mach	Engine power
Indicated airspeed	Fuel quantity
Angle of attack	Fuel flow rate
Barometric altitude	Distance to destination
Ground clearance altitude	Gross weight
Altitude rate	Center of gravity
Magnetic heading	Angle of sideslip
Present position	
Waypoint position	
Bearing to waypoint	

TABLE 16. DIVISION OF CREW DUTIES FOR CATEGORY I
OR VFR WEATHER

Pilot Duties	Copilot Duties
<u>Flight Control</u>	
Manual control manipulation	Monitoring of primary power and flight instruments
Auto-stabilization	
Auto-pilot mode selection	
<u>Propulsion and Primary Power</u>	
Engine on-off switching	Monitoring propulsion and primary power displays
Thrust magnitude variation	Controlling center of gravity changes
Augmented lift setting	Managing fuel supply
<u>Secondary Power</u>	
Controlling electrical generating equipment	Monitoring electrical hydraulic and pneumatic subsystem displays
Controlling hydraulic pressure subsystems	
Monitoring electrical, hydraulic and pneumatic subsystem displays	
<u>Communication</u>	
Channel and message monitoring	Channel and function selecting for: Communication radios Navigation radios
<u>Navigation</u>	
All flying	All navigational computation Control and interrogation of area navigation computer and other navigational devices

TABLE 17. DIVISION OF CREW DUTIES
FOR CATEGORY II or III
WEATHER APPROACH & LANDING

Pilot Duties	Copilot Duties
<u>Flight Control</u>	
Monitoring of flight instruments	Manual control manipulation
Visual cue search	Auto-stabilization selection
	Autopilot mode selection
<u>Propulsion and Primary Power</u>	
Monitoring propulsion and primary power displays	Thrust magnitude variation
Controlling center of gravity changes	Augmented lift setting
<u>Secondary Power</u>	
Monitoring electrical, hydraulic and pneumatic subsystem displays	Controlling electrical generations and hydraulic pressure subsystems
	Monitoring electrical, hydraulic and pneumatic subsystem displays
<u>Communication</u>	
Channel and function selection for:	Channel and message monitoring
Communication radios	
Navigation radios	
<u>Navigation</u>	
All navigational computation	All flying
Control and interrogation of area navigation computer and other navigational devices	

"Cue". As discussed in reference 18, when the visual cues were sufficient to laterally align the aircraft with the runway centerline, the aircraft commander would call out "Lateral" and assume control at the lateral axis of the aircraft. The instrument pilot would still be assumed to be performing the task of maintaining the instrument flight. When the aircraft commander acquired sufficient references to visually control the aircraft, he should call out "Visual". At this time he could, at his discretion, aid with aircraft control with inputs to both the lateral and longitudinal axis. There was still no transfer of control. If the visual pilot wished to take complete control, he would state, "I have the aircraft", and assume complete control while the instrument pilot relinquishes complete authority. It was anticipated that this command would be executed by the visual pilot only after the aircraft was safely on the runway, at which time he would assume active control for the roll out. The instrument pilot would then be responsible for configuring the aircraft for roll out (ref. 19).

Another important decision that must be made by the pilot in command is whether or not to execute a missed approach. This decision should be made by the visual pilot and executed by the instrument pilot on the verbal command. When a missed approach is executed, the visual pilot should reconfigure the aircraft, leaving the other pilot free to concentrate on the go-around maneuver.

Mode Selection: Mode selection by the crew involves many design trade-offs as discussed in reference 18. As stated in reference 18, "maximum considerations should be given to the number of modes. If too many modes are provided, mode selection may produce confusion during a critical period of flight". It was assumed that both pilots have an independent system "with the ability to drive the autopilot from either, or in some situations, combinations of both". As recognized in reference 18, "an important operational consideration is the method used to display mode selection to the pilot. If two pilots are involved, then each must have intelligence pertaining to the active modes and whether his system (assuming two systems) is functioning correctly and/or operating the automatics. Annunciation should therefore provide three basic types of information. What is the mode? Who has control? What is the level of automaticity serving the mode?" Reference 18 states that "regardless of the level of automaticity, the pilot will be the ultimate decision maker in the man/machine relationship, as long as the aircraft are manned. Therefore, he must be provided adequate means to evaluate systems performance and take corrective action when required". The reference further states that predictive information should be displayed and an independent monitoring system must be available to "help the pilot assess aircraft performance".

Base-line Modes Switching Logic. - As previously stated, for each function it is necessary to develop base-line modes switching logic. The switching between modes could be a function of performance measures not

meeting those required for the function, or failure of hardware required for a mode. In essence, for those functions such as navigation, the base-line modes switching logic could be only a function of performance measures not meeting those required for the functions if it was possible to improve the performance by switching to a better mode. The priority of modes has been ordered on the basis that the mode with best performance is preferred. The higher the mode number, the lower the performance. For these reasons, the case would not arise in which switching to a better mode would be possible unless the mode being utilized was manually selected and a lower numbered mode was actually operational but not selected. In other words, the only possibility of selecting a mode with better performance would be the case where an automatic mode is available but the crew has elected to operate with a manual mode. The program always uses the automatic subfunction unless the user selects a manual subfunction. The switching between modes for the automatic subfunction is performed by determination of the availability of the subsystems required for each mode. If all subsystems or all modes are available, the first mode is used. As previously stated, when a failure is detected, the system functions are searched to determine the effect of the failure mode. The flight then continues normally, reverts to a backup mode of operation, or in event of a failure of a complete function, performs an unscheduled landing.

While the primary mode switching logic implemented in the program is based upon the assumption of utilizing the automatic subfunction and switching to back-up modes as failures occur, it is possible to modify the switching logic to include mode selection by the crew. This requires modelling the decision process which the crew has been trained to use to fly the aircraft. In effect, since this is an advanced aircraft for which the avionics systems requirements are to be established, this would require designing the crew decision logic and implementing it in the program, a task clearly beyond the scope of this study. As discussed in reference 19, the need exists to reverse the trend toward increased number of switches, dials, and displays that add to the pilot's workload in the task of mode selection. Further study of the crew selection decision logic, design, and implementation of that logic for the STOL should be a high priority task and should be performed in the immediate future.

System Operating Procedures.-The primary system operating procedures implemented in the program include the ATC procedures and rules that were followed in generating the nominal flight path of the STOL aircraft. In addition it has been assumed, as discussed in a later section of this report, that the dispatch requirements in terms of the minimum equipment list must be met or the aircraft cannot be dispatched on the next leg of the flight. As previously discussed in the airport model, certain ground services such as fueling and loading the passengers are assumed to be performed in series, while other ground services such as deplaning and loading and unloading of cargo are assumed to be performed in parallel with the loading

of fuel. A basic operating procedure implemented is that replacement of required subsystems which have failed is begun as soon as the subsystem failure is detected and the aircraft is on the ground.

Other system operating procedures included in the program are a function of the performance of the navigation, guidance, and control program. For example, it is possible to command heading changes or being ascent or descent of the aircraft from a waypoint as a function of either estimated position along track, estimated time, or estimated bearing to a VORTAC station. The actual procedure used for flight path guidance has significant implications, as discussed in Appendix E.

In addition, as discussed in Appendix E, the selection of the common path length is a function of a microwave landing system coverage, the navigation, guidance, and control contributions to the crosstrack and altitude deviations at nominal acquisition of the microwave landing system when that system is required, and the performance of the aircraft. It is possible to increase the length of the common path and thereby increase the time spent flying within the coverage of the microwave landing system. In the process of increasing the common path length, the overall capacity of the airport may have been reduced.

The sample results presented in a later section of this report suggest that certain operating procedures are better than others. For example, if the crew wishes to minimize crosstrack deviations, it appears from the results that this can best be done by command heading changes as a function of bearing. This results in trading off the smaller crosstrack deviations for greater time along track deviations. Definitive conclusions should not be drawn from any of the results presented in the later section since extensive exercise cases were beyond the scope of the study. The various trade-offs between system operating procedures may yield definitive data as to the worth of the various operating procedures when sufficient exercise cases are run.

Details of Information Flow With STOL OPS

The STOL OPS program is modular in its construction. Each module is a subprogram which, to a large degree, stands by itself except for specific input and output parameters that permit communication with the other modules. The individual modules may be categorized into the four basic groups described below.

Input.-The input subprograms read data describing the avionics subsystems, functions, airports, navigation aids, scheduled flights, waypoints, and aircraft performance. These data are organized and stored for access by other program modules.

Nominal Flight.-The powered-lift STOL performance model, described in Appendix B, is used to generate the nominal flight profiles for the scheduled flights defined by the input data. The following profile is used to simulate the aircraft operation:

1. Maximum power climb, at takeoff airspeed, to 1500 feet above the runway
2. Level flight acceleration to 250 knots indicated airspeed
3. Climb to 10,000 feet at constant indicated air speed (250 knots)
4. Level flight acceleration to cruise velocity
5. Climb to cruise altitude at constant Mach number
6. Level flight cruise at constant Mach number
7. Constant Mach number descent to 10,000 feet
8. Decelerate to 250 knots indicated airspeed
9. Descent to approach altitude at constant indicated airspeed
10. Decelerate to approach velocity
11. Descent along specified glideslope to runway.

The principal outputs provided by the nominal trajectory simulation are time of flight and fuel consumed.

Monte Carlo.-There are six major Monte Carlo modules: Preflight, Taxi-Out, Takeoff, Climb, En Route, Landing. A detailed description of these routines is shown in Figures 39 through 44.

Output.-The output module prints the results of the Monte Carlo evaluation. The output is divided into three groups: (1) statistics for

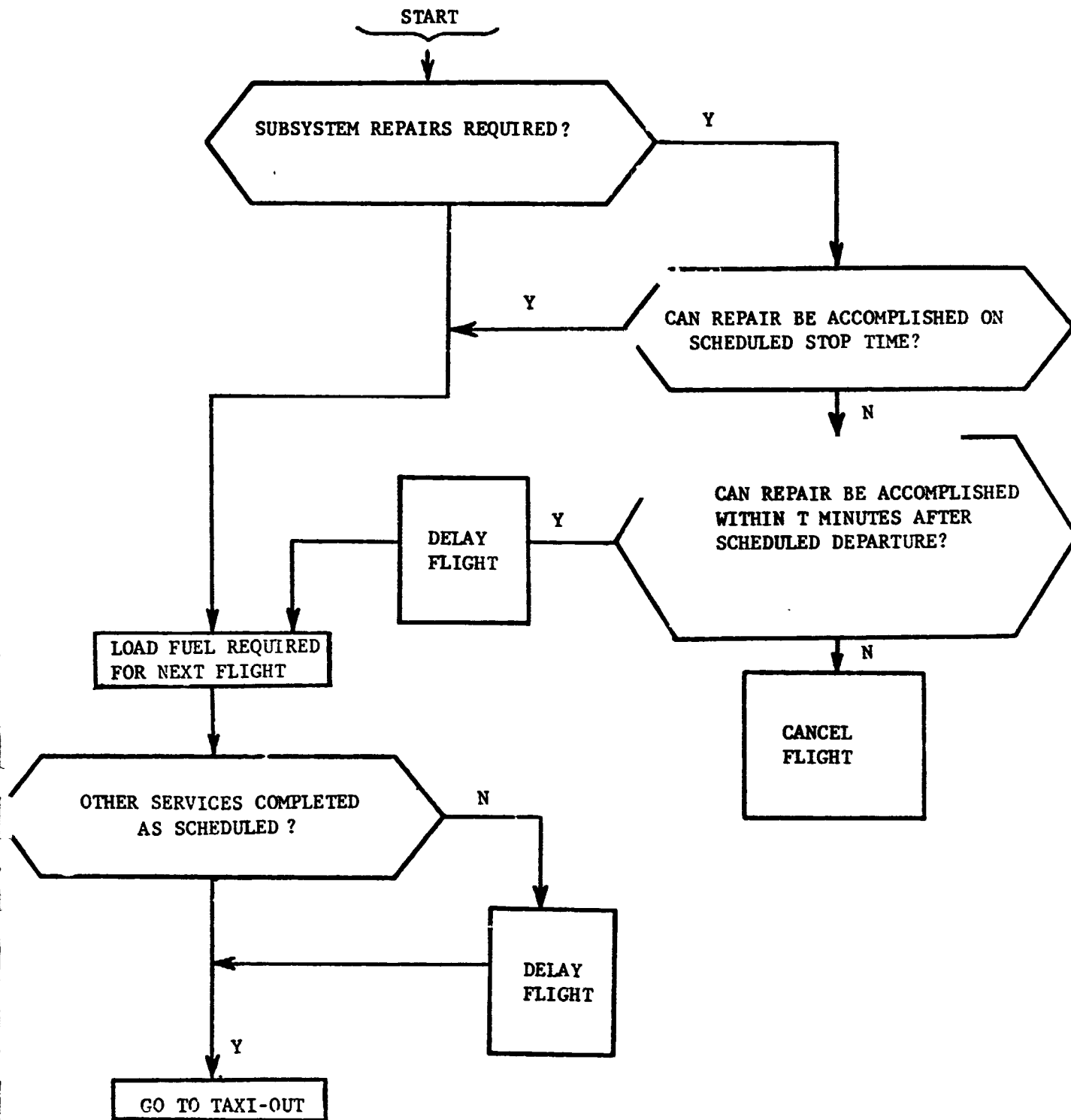


FIGURE 39. PREFLIGHT MONTE CARLO ROUTINE

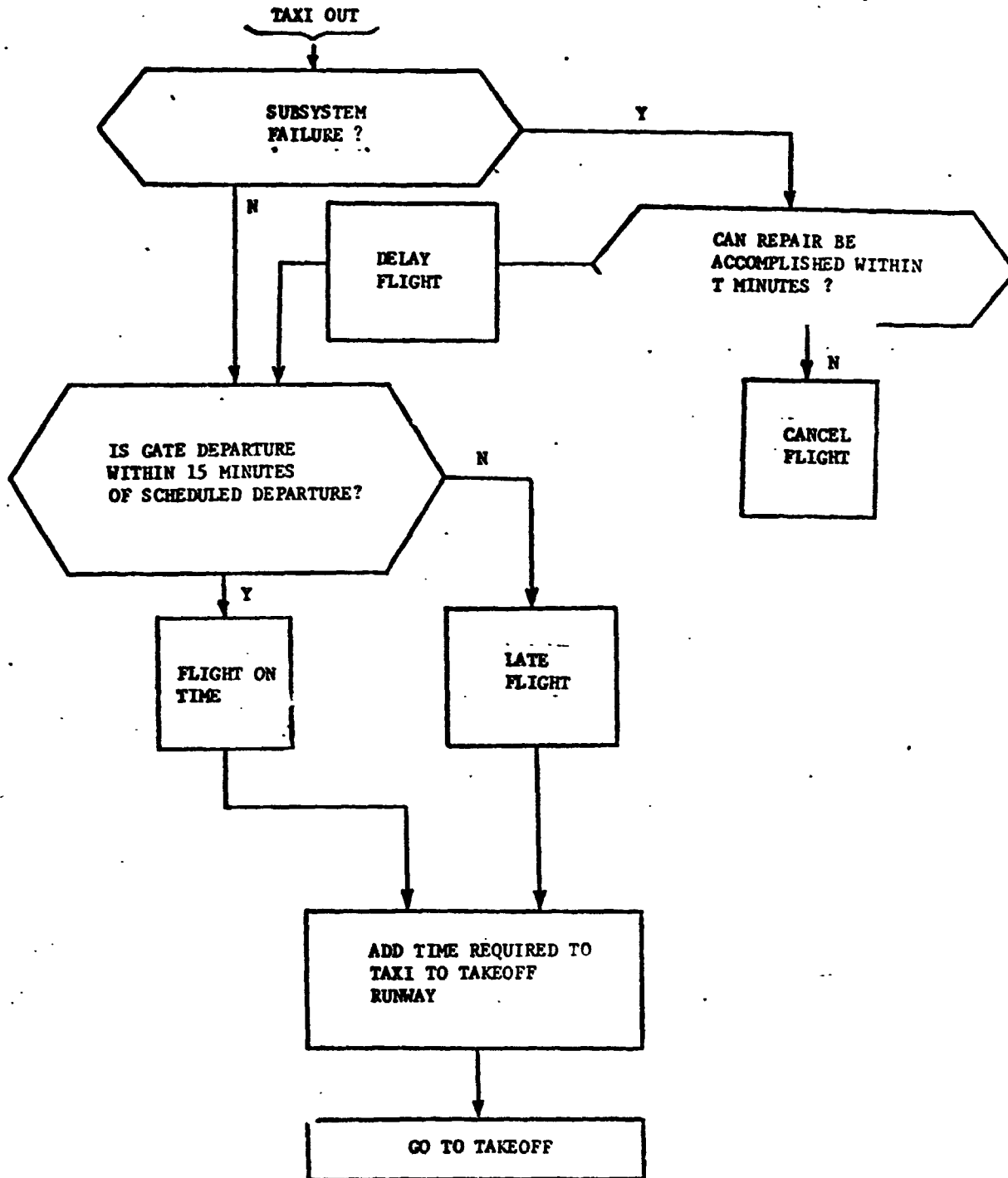


FIGURE 40. TAXI OUT MONTE CARLO ROUTINE

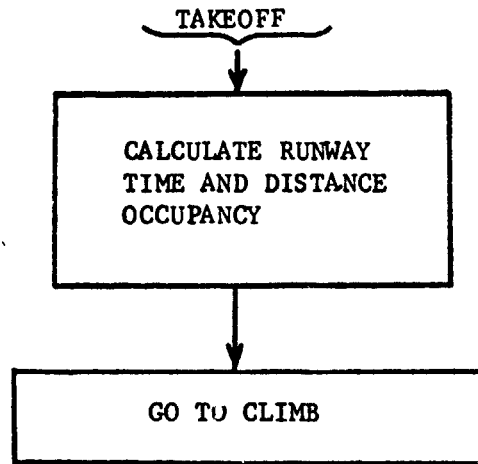


FIGURE 41. TAKEOFF MONTE CARLO ROUTINE

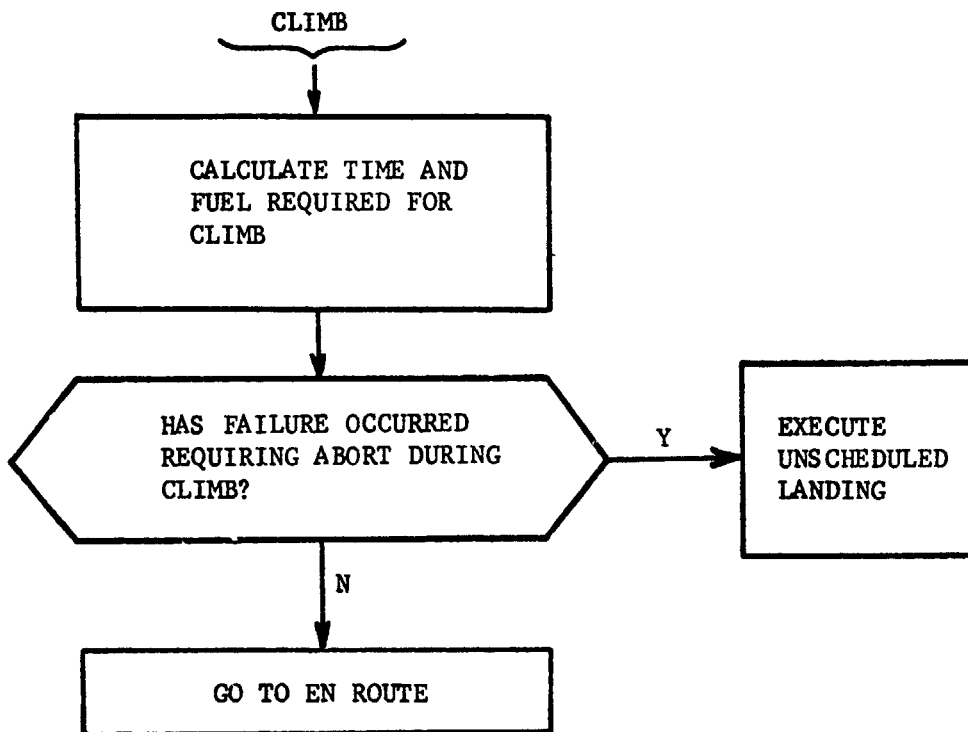


FIGURE 42. CLIMB MONTE CARLO ROUTINE

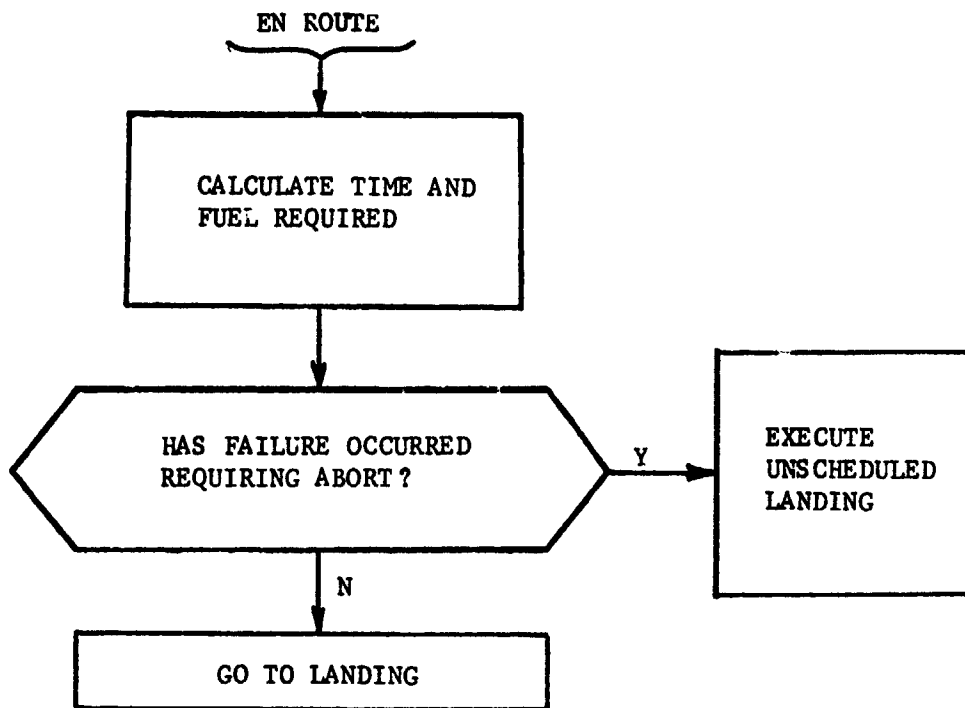


FIGURE 43. EN ROUTE MONTE CARLO ROUTINE

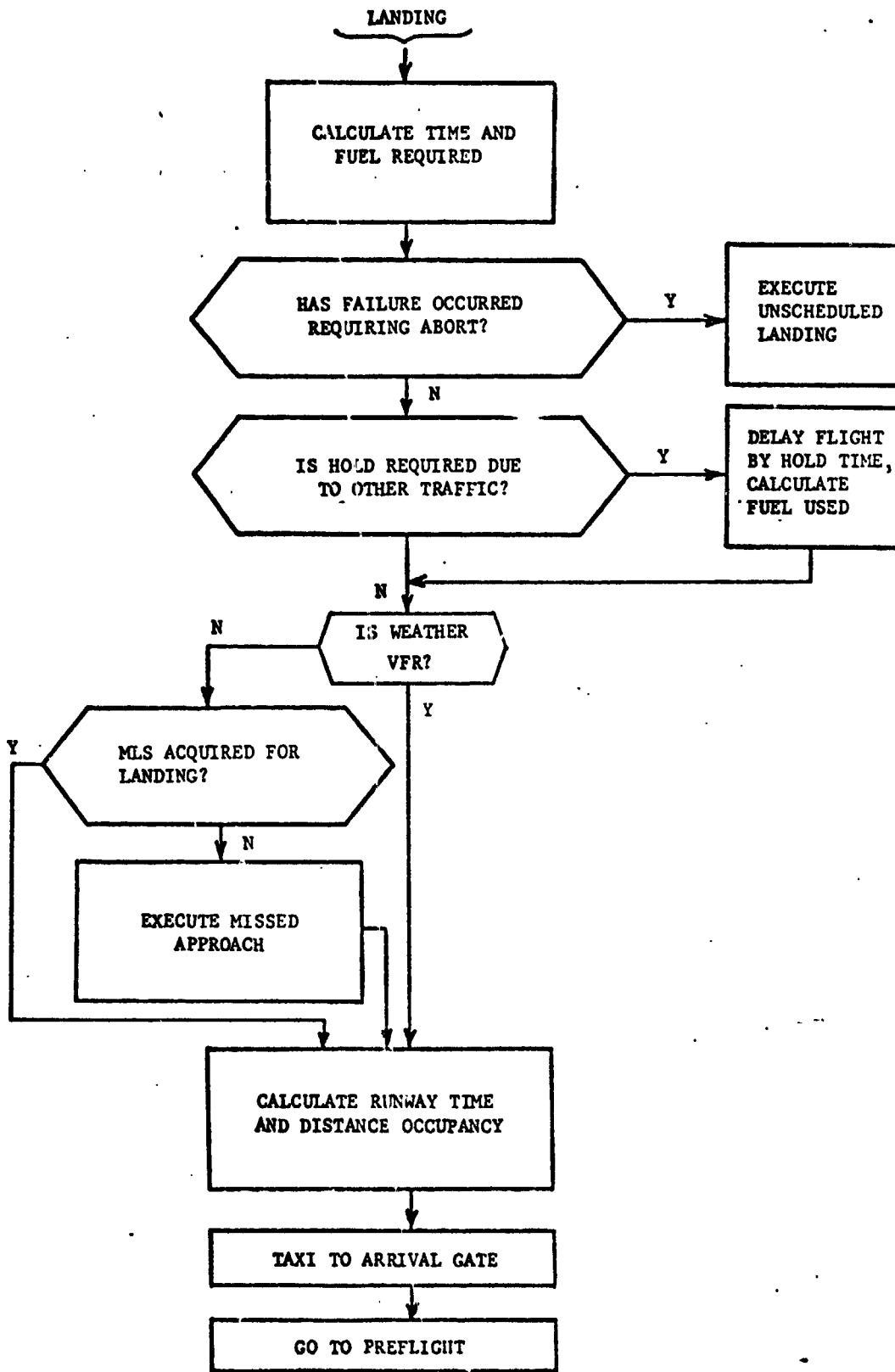


FIGURE 44. LANDING MONTE CARLO ROUTINE

random variables, (2) number of occurrences of specific events, and (3) percent of flights using each mode of each subfunction.

Figure 45 shows the output for variables. The first three columns list the number of samples obtained, the mean value of the variable, and the standard deviation of the variable. The maximum and minimum values that occur during the Monte Carlo evaluation are listed in the next two columns. The last four columns show how many times a specific maximum or minimum is exceeded during the evaluation.

Figure 46 shows the output for specific events, and Figure 47 shows the mode utilization.

Output may be requested for the leg between each airport pair for each flight, totals of all flights for each leg, totals for all legs of each flight, and totals for all flights and all legs.

TOTALS FOR ALL TRIPS AND ALL LC'S

STATISTICS FOR 63 MONTE CARLO TRIALS

	NO. SAMPLES	MEAN	STANDARD DEVIATION	MAXIMUM VALUE	MINIMUM VALUE	CONSTRAINT NUMBER	MAXIMUM	MINIMUM	EXCEEDED
						NO.			
EQUIPMENT REPAIR TIME (MIN)	60	1.03990E+01	0.5E+00	1.04990E+01	1.01990E+01	0	1.20000E+02	-1.00000E+20	0
FUEL LOADING TIME (MIN)	60	1.73325E+01	4.31705E+00	2.06120E+01	7.75619E+00	0	1.00000E+20	-1.00000E+20	0
PASSENGER LOADING TIME (MIN)	60	1.04883E+01	1.80405E+00	1.46152E+01	6.64565E+00	0	1.00000E+20	-1.00000E+20	0
CARGO LOADING TIME (MIN)	60	1.05664E+01	1.93604E+00	1.46806E+01	6.22963E+00	0	1.00000E+20	-1.00000E+20	0
GROUND SERVICE TIME (MIN)	60	2.76709E+01	4.53135E+00	3.42649E+01	1.56202E+01	55	2.00000E+01	5.00000E+00	0
FUEL LOADED (LB)	60	7.27967E+03	1.83585E+03	8.65737E+03	3.27440E+03	0	1.00000E+20	-1.00000E+20	0
INITIAL FUEL LOAD (LJ)	60	9.47271E+03	2.4243E+03	1.11613E+04	6.10359E+03	0	1.00000E+20	-1.00000E+20	0
INITIAL TAKEOFF WEIGHT (LB)	60	1.08876E+05	2.40243E+03	1.13565E+05	1.05587E+05	0	1.00000E+20	-1.00000E+20	0
GATE DEPARTURE DELAY (MIN)	60	4.91659E+01	1.10592E+00	4.94348E+01	0.2E+00	0	1.50000E+01	-1.00000E+20	0
TAKEOFF DELAY (MIN)	60	3.22127E+01	1.10064E+00	9.80328E+01	-3.98315E+00	0	1.00000E+20	-1.00000E+20	0
TAKEOFF RUNWAY OCCUPANCY (MIN)	60	1.87534E+01	0.2E+00	1.87534E+01	1.87534E+01	0	1.00000E+20	-1.00000E+20	0
TAKEOFF RUNWAY DISTANCE (FT)	60	9.49564E+02	0.2E+00	9.49564E+02	9.49564E+02	0	1.00000E+20	-1.00000E+20	0
INITIAL FLIGHT TIME (MIN)	60	4.71668E+01	1.83997E+01	6.45105E+01	2.02096E+01	0	1.00000E+20	-1.00000E+20	0
LANDING TIME (MIN)	60	5.80288E+00	1.86325E+00	7.54301E+01	2.02096E+01	0	1.00000E+20	-1.00000E+20	0
LANDING RUNWAY OCCUPANCY (MIN)	60	8.44305E+01	4.34178E+01	1.40737E+02	-9.01537E+01	0	1.00000E+20	-1.00000E+20	0
LANDING RUNWAY DISTANCE (FT)	60	2.26683E+03	4.6248E+02	3.30000E+03	9.51000E+02	0	1.00000E+20	-1.00000E+20	0
GATE ARRIVAL DELAY (MIN)	60	6.09529E+00	2.17583E+00	2.27551E+01	-1.25091E+01	0	0.2E+00	-1.00000E+20	0
FUEL CONSUMED (LB)	60	6.86443E+03	2.46626E+03	9.66172E+03	3.32322E+03	0	1.00000E+20	-1.00000E+20	0
FUEL REMAINING (LB)	60	2.59224E+03	2.28703E+02	2.88065E+03	1.49151E+03	0	1.00000E+20	-1.00000E+20	0

FIGURE 45. MONTE CARLO VARIABLES

STATISTICS FOR 69 MONTE CARLO TRIALS

EVENT	OCCURRENCES	EVENT	OCCURRENCES
STATE ESTIMATION LOST	0	COMMAND GENERATION LOST	0
HAZARD AVOIDANCE LOST	0	COMMUNICATION LOST	0
SYSTEM MANAGEMENT LOST	0	SAFE FLIGHT LOST	0
UNSCHEDULED LANDING	0	WAKENAKE FAILURE	1
FAILURE IN SECTIONS 1-10	0	FAILURE IN SECTIONS 11-20	0
FAILURE IN SECTIONS 21-30	0	FAILURE IN SECTIONS 31-40	0
FAILURE IN SECTIONS 41-50	1	CANCELLED FLIGHT	0
GATE DEPARTURE	60	DISPATCH RELIABILITY	60
SCHEDULED FLIGHT TIME EXCEEDED	7		

FIGURE 46. MONTE CARLO EVENTS

MODES USED (PER CENT)

MODE	1	2	3	4	5	6	7	8
STATE ESTIMATION	100.0	0.0	0.0	0.0	0.0	0.0	0.0	0.0
AUTOMATIC NAVIGATION	100.0	0.0	0.0	0.0	0.0	0.0	0.0	0.0
COMMAND GENERATION/EXECUTION	100.0	0.0	0.0	0.0	0.0	0.0	0.0	0.0
AUTOMATIC GUIDANCE CONTROL	100.0	0.0	0.0	0.0	0.0	0.0	0.0	0.0
HAZARD AVOIDANCE	100.0	0.0	0.0	0.0	0.0	0.0	0.0	0.0
AUTOMATIC HAZARD AVOIDANCE	100.0	0.0	0.0	0.0	0.0	0.0	0.0	0.0
COMMUNICATION	100.0	0.0	0.0	0.0	0.0	0.0	0.0	0.0
AUTOMATIC COMMUNICATION	100.0	0.0	0.0	0.0	0.0	0.0	0.0	0.0
SYSTEM MANAGEMENT	100.0	0.0	0.0	0.0	0.0	0.0	0.0	0.0
AUTOMATIC SYSTEM MANAGEMENT	100.0	0.0	0.0	0.0	0.0	0.0	0.0	0.0
SAFE FLIGHT	100.0	0.0	0.0	0.0	0.0	0.0	0.0	0.0
SAFE FLIGHT	100.0	0.0	0.0	0.0	0.0	0.0	0.0	0.0

FIGURE 47. MONTE CARLO MODE USAGE

SAMPLE RESULTS FROM APPLICATION OF STOL OPS TO CANDIDATE STOL SYSTEM CONFIGURATION

ANGCAP Results

A detailed description of the aircraft navigation, guidance, and control analysis program (ANGCAP) is presented in Appendix E. A discussion of the detailed output for one leg of the route network is provided for the automatic navigation subfunction, Mode 1. The sample results from all cases of ANGCAP are summarized below. No conclusions are drawn since the analysis performed with ANGCAP is merely to demonstrate the operation of the program and provide the needed information for operation of the Monte Carlo program.

Figure 48 is a sample portion of one page of ANGCAP output during the flight from San Jose to Sacramento. This page is one of many discussed in detail in Appendix E. The output shown indicates that the aircraft has been flying 8 minutes and that it has been 120 seconds since the last update using VOR/DME Stations 5 and 6 listed earlier in Figure 25. Nine states are computed in the program: position in terms of magnetic east and north cartesian coordinates, altitude bias, velocity bias in magnetic east and north coordinates, and range and angle bias to each of the VOR/DME stations. The data in the columns are the standard deviations of each of the nine states. The rows present the following information: the true error and the error that would be estimated by an onboard Kalman filter. Since the real world and filter model agree in this run, these values are identical with the true error. The nominal trajectory information at that time is given in terms of magnetic east and north positions and altitude, velocity, magnetic heading, and flight path angle. The σ deviations in the actual and estimated states are given in terms of time along track, crosstrack position, and altitude. The σ control effort listed is a function of the option selected by the user for control of the aircraft as discussed in Appendix E. In this case, cross-track steering is the only control option being utilized.

The next line of data gives measurements of range and bearing to station 5 and station 6. That is, the range at this time is 25.52 nautical miles to station 5 with a bearing of 159.54° . The range to Station 6 is 24.04 nautical miles with a bearing of -114.27° . These measurements are processed using a Kalman update. As a result of this update, the nine states true and filter estimate of error are updated and the actual- and estimated-state σ deviations are updated as well as the σ control effort. Note that no change in nominal has resulted. Also note that no change in the actual state σ deviations has resulted.

TIME 8:00 MIN. 120.0 SEC. SINCE LAST UPDATE VOR/DME STATION NO. 5 VOR/DME STATION NO. 6
 CASE 1 EAST-POS. NORTH-POS. ALT. RIAS VE-BIAS VN-BIAS RANGE BIAS ANGLE BIAS RANGE BIAS ANGLE BIAS
 NAUT. MILES NAUT. MILES FEET FEET/SEC FEET/SEC NAUT. MILES DEGREES NAUT. MILES DEGREES
 TRUE ERROR 0.839 6.882 50.000 52.197 51.914 0.134 0.617 0.612
 FILTER ESTIMATE OF ERROR 0.839 6.882 50.000 52.197 51.914 0.134 0.617 0.612

NOMINAL TRAJECTORY ONE SIGMA DEVIATIONS ESTIMATED STATE ONE SIGMA CONTROL EFFORT
 POSITION VELOCITY ACTUAL STATE
 -102.08 NM EAST 250.00 KNOTS 57.85 SECONDS 0.00 KNOTS
 96.12 NM NORTH 46.19 DEGREES 1.71 NM CROSS TRACK 3.21 DEGREES
 10536.08 FT ALTITUDE 182.45 FT ALTITUDE 170.27 FT ALTITUDE 0.00 DEGREES

MEASUREMENTS OF RANGE-1 = 25.52 THETA-1 = 190.54 RANGE-2 = 24.44 THETA-2 = 114.27

KALMAN UPDATE
 TIME 8:05 MIN. 6.0 SEC. SINCE LAST UPDATE VOR/DME STATION NO. 5 VOR/DME STATION NO. 6
 CASE 1 EAST-POS. NORTH-POS. ALT. RIAS VE-BIAS VN-BIAS RANGE BIAS ANGLE BIAS RANGE BIAS ANGLE BIAS
 NAUT. MILES NAUT. MILES FEET FEET/SEC FEET/SEC NAUT. MILES DEGREES NAUT. MILES DEGREES
 TRUE ERROR 0.169 0.140 50.000 29.751 29.443 0.130 0.550 0.544
 FILTER ESTIMATE OF ERROR 0.169 0.140 50.000 29.751 29.443 0.130 0.550 0.544

NOMINAL TRAJECTORY ONE SIGMA DEVIATIONS ESTIMATED STATE ONE SIGMA CONTROL EFFORT
 POSITION VELOCITY ACTUAL STATE
 -102.49 NM EAST 257.00 KNOTS 57.85 SECONDS 0.00 KNOTS
 96.12 NM NORTH 46.19 DEGREES 1.14 NM CROSS TRACK 4.67 DEGREES
 10536.08 FT ALTITUDE 187.45 FT ALTITUDE 175.25 FT ALTITUDE 0.00 DEGREES

FIGURE 48. SAMPLE PORTION OF ONE PAGE OF ANGCAP OUTPUT DURING FLIGHT FROM SAN JOSE TO SACRAMENTO

Further description of the complete output for this flight leg is provided in Appendix E.

Figure 49 is a summary of the cases made for this run of ANGCAP. The case number is merely used for identification purposes in processing the data further using the plotting code or the Monte Carlo code. The update type designation of 1 indicates a Kalman update, whereas an update type designation of 2, as in Case 6, denotes a position-fix update, as discussed in Appendix E. The update frequency selected was the same for the sample cases. The measurements combined with the air data information are denoted by the number of VOR and DME receivers for the particular leg flown. For example, Case 1 results in the use of 2 VOR's and 2 DME's, providing measurements of ρ/θ , for leg 1. At the end of a flight, the b deviations or dispersions in the actual state are 153.9 seconds along track, 0.38 n. mi. crosstrack, and 50 feet in altitude. The b deviations or dispersions in the estimated state are 152.88 seconds along track, 0.27 n. mi. crosstrack, and 0 foot in altitude. The final line of printing is the probability of acquiring the microwave landing system for a 90° intercept with a 2 n. mi. common path as described in Appendix E.

Similar information is provided for each of the cases run. Leg 1 is the leg of the route network from San Jose to Sacramento Executive, leg 2 is the route leg from Sacramento Executive to Santa Ana, and leg 3 is the route leg from Santa Ana to San Jose.

Graphs of the actual- and estimated-state b deviations can be drawn using the data for each output point of Figure 48 for each leg of the route network. Since the entire route network is flown four times in the schedule used for the sample runs, this could consume very many man-hours. Typically, to plot the b deviations in the actual and estimated states requires 2 man-hours for each case for each leg.

To avoid this expense, the plotting routine has been utilized to plot the crosstrack (lateral deviation) for the route network referenced to a magnetic east and north cartesian coordinate system. It is possible to plot the nominal flight track as depicted in Figure 50. This plot is for an IFR approach in Category I or worse weather conditions. Note that this plot is different from the VFR flight path given in Figure 19. In addition, it is possible to plot more than one parameter for the route network as shown in Figure 51. For example, Figure 52 is a plot for one round trip around the route network of the actual lateral deviation, 3σ , and a 4 n. mi. airway width for the RNAV mode using a Kalman update of one VOR bearing measurement and DME measurements to two different VORTAC's. Case 2 corresponds to Case 2 in Figure 49 for the flight leg from San Jose to Sacramento. Case 8 corresponds to Leg 2 in Figure 49 from Sacramento (SAC) to Orange County and Case 14 corresponds similarly to Leg 3 from Orange County (SNA) to San Jose (SJC). Use of this plot routine presents the information that would be obtained by hand plotting the output for those cases as a function

SUMMARY OF CASES FOR AMESBC OF 82/19/73 AT 091101

CASE	UPDATES TYPE FREQ (SEC)	RECEIVERS		LEG	ACTUAL DISPERSIONS			ESTIMATE DISPERSIONS			
		VDR	DME		A.T. (SEC)	X.T. (NM)	ACT. (FT)	ACT. (SEC)	X.T. (NM)	ACT. (FT)	
1	1	120.00	2	1	153.19	0.38	50.00	142.84	0.27	0.00	0.05802
2	1	120.00	1	2	151.24	0.38	50.00	152.95	0.27	0.00	0.06117
3	1	120.00	2	1	153.16	0.38	50.00	152.84	0.27	0.00	0.06100
4	1	120.00	0	2	160.00	0.78	50.00	154.49	0.47	0.01	0.22805
5	1	120.00	1	1	152.73	0.39	50.00	152.37	0.27	0.00	0.06503
6	2	120.00	1	1	162.00	0.43	50.00	161.98	0.31	0.00	0.08178
7	1	120.00	2	2	170.26	0.39	49.68	170.15	0.29	0.01	0.06222
8	1	120.00	1	2	176.29	0.39	49.62	170.19	0.29	0.00	0.06233
9	1	120.00	2	2	170.84	0.39	49.65	170.71	0.29	0.02	0.05533
10	1	120.00	0	2	164.83	1.87	49.45	164.01	0.36	0.02	0.37557
11	1	120.00	1	2	170.91	0.40	49.65	170.78	0.29	0.00	0.05570
12	2	120.00	1	1	177.21	0.43	50.00	171.25	0.36	0.00	0.03174
13	1	120.00	2	3	202.52	0.35	49.95	202.45	0.31	0.01	0.06372
14	1	120.00	1	2	202.53	0.35	49.56	202.49	0.31	0.03	0.06371
15	1	120.00	2	3	202.50	0.35	49.62	202.31	0.31	0.04	0.05555
16	1	120.00	0	2	202.77	1.12	49.68	201.21	1.02	0.01	0.29557
17	1	120.00	1	3	202.43	0.35	49.63	202.36	0.31	0.05	0.06593
18	2	120.00	1	3	218.58	0.39	50.00	218.18	0.33	0.00	0.05506

Note: Update type 1 = Kalman Update
 Update type 2 = Position Fix Update

FIGURE 49. SUMMARY OF RESULTS OUTPUT FROM ANGCAP KALMAN FILTER UPDATE

USING FORM (1) ρ/θ , ρ/θ , (2) ρ/θ , ρ , (3) ρ/θ , θ , (4) ρ , ρ ,

(5) ρ , θ , EXTERNAL MEASUREMENTS AND POSITION FIX UPDATE

(6) USING ρ/θ , EXTERNAL MEASUREMENTS

NOMINAL AIRCRAFT PATH CASE 1 7 13

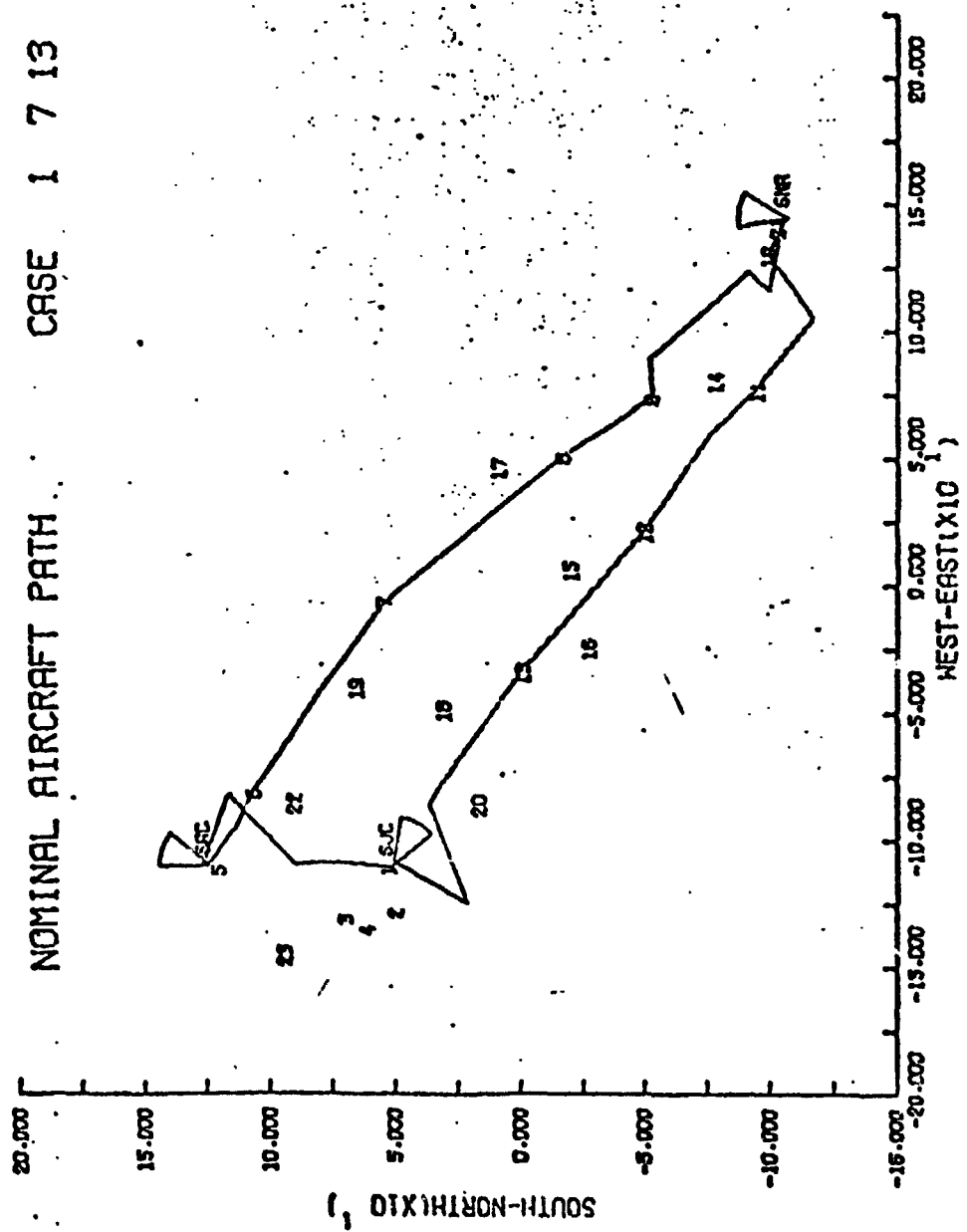


FIGURE 50. NOMINAL GROUND TRACK OF IFR FLIGHT PATH FOR CASES 1, 7, AND 13 OF FIGURE 49.

NOMINAL AIRCRAFT PATH
 ESTIMATED LATERAL DEVIATION
 CASE 1 7 13
 3 SIGMAS

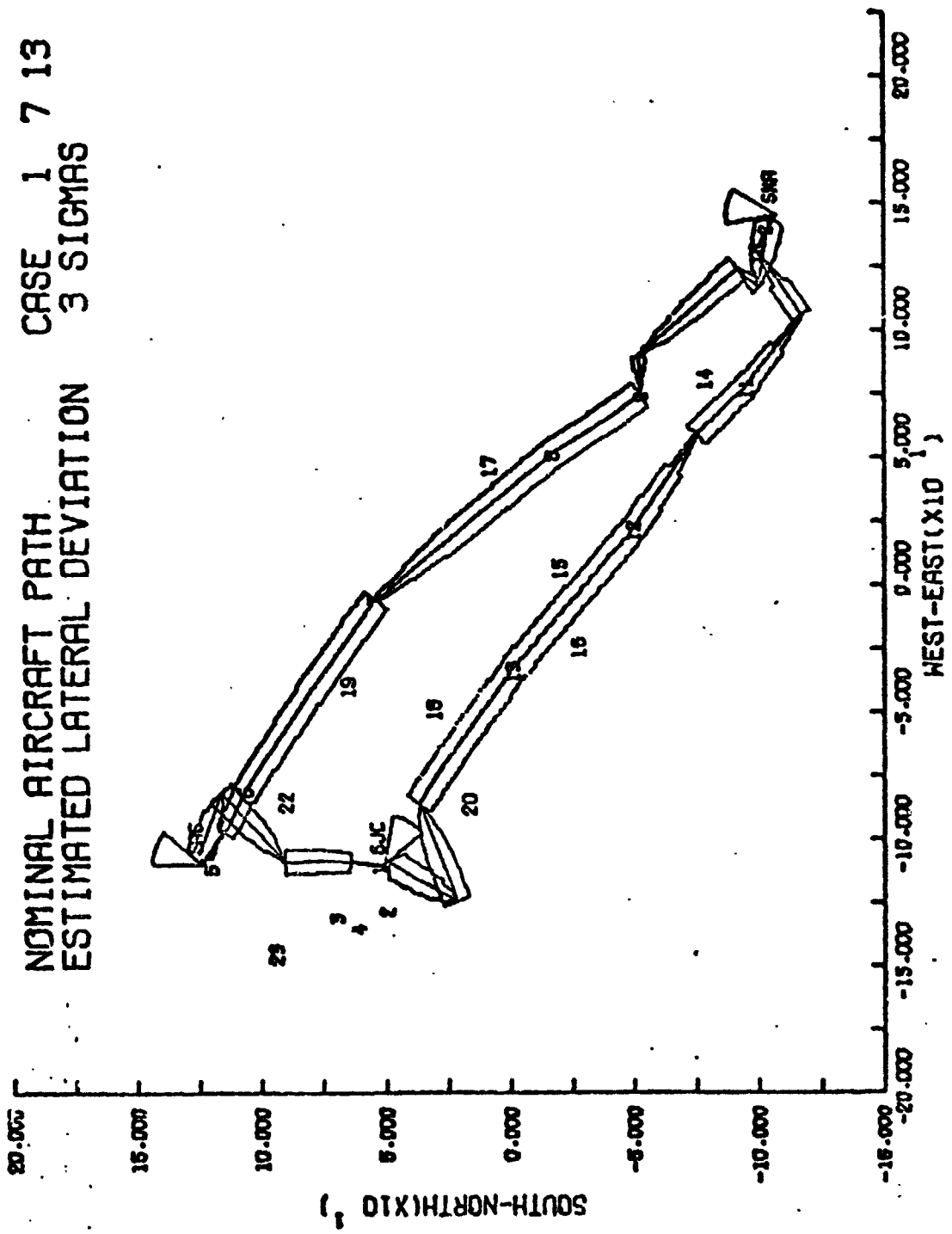


FIGURE 51. NOMINAL GROUND TRACK OF IFR FLIGHT PATH AND ESTIMATED CROSS-TRACK DEVIATION FOR KALMAN FILTER UPDATE USING ρ/θ , ρ/θ EXTERNAL MEASUREMENTS

AIRWAY, 4 NM. WIDE
 ACTUAL LATERAL DEVIATION

CASE 2 8 14
 3 SIGMAS

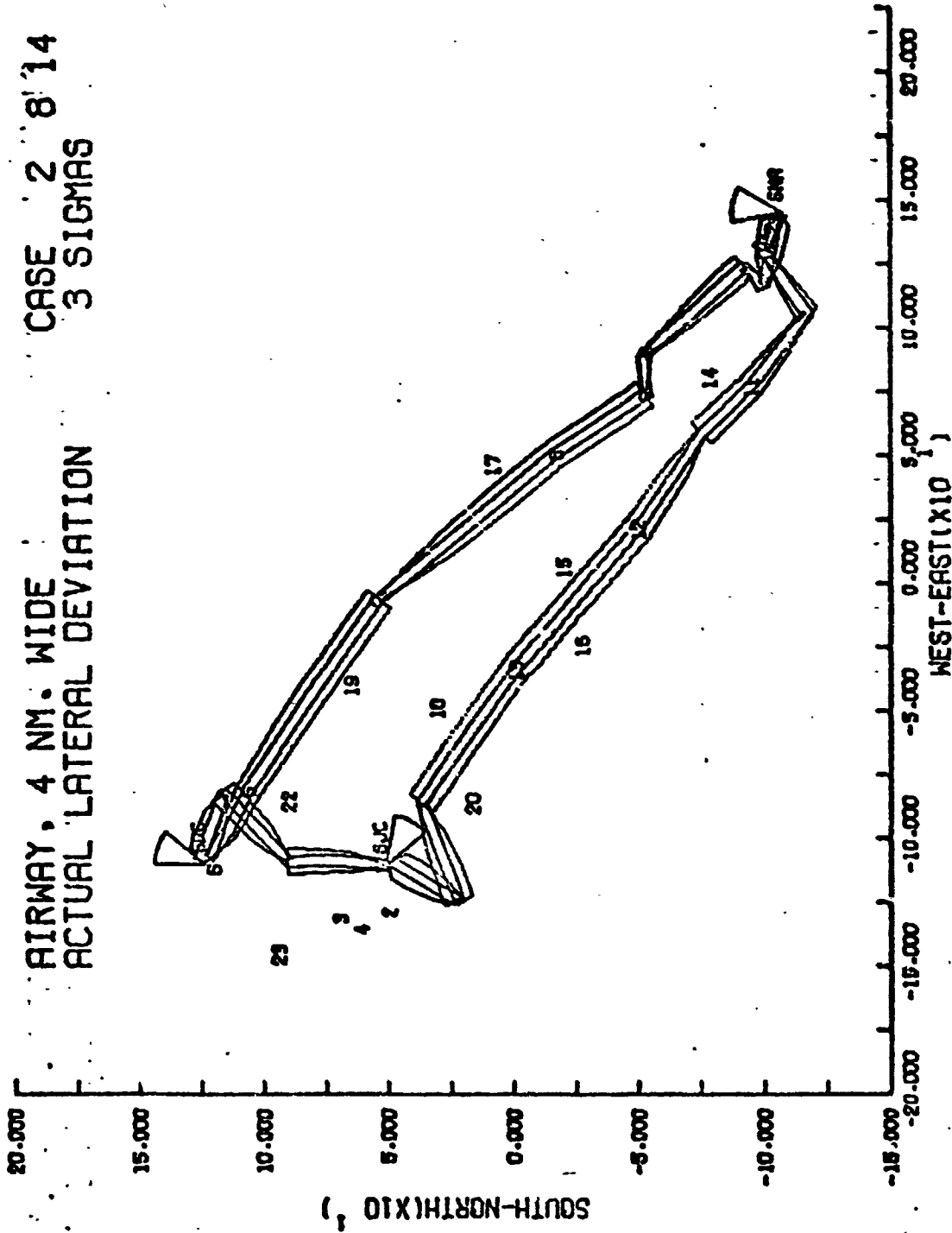


FIGURE 52. PLOT OF 4 NM. AIRWAY WIDTH AND 3 σ CROSSTRACK ACTUAL DEVIATION FOR KALMAN FILTER UPDATE USING p/θ , p MEASUREMENTS

of time for each flight leg. It should be noted that the plots portray a 40° azimuth coverage for the MLS about its heading and a range of 20 n.mi. at each airport, i.e., SC-117 Configuration G.

Figure 53 is a plot of the estimated crosstrack deviation (3σ) and the nominal aircraft flight path for the Kalman filtered update using ρ/θ , θ measurements.

Figure 54 is a plot of the crosstrack actual 3σ deviations for a Kalman filter update using ρ , ρ measurements and the 4 n.mi. airway width. Comparison with Figure 52 reveals that the 3σ lateral deviations are, in general, greater than they were using the ρ/θ , ρ measurements.

Figure 55 presents a similar plot for a Kalman filter update using ρ/θ measurements, except in this case the nominal type flight track is plotted rather than the 4 n.mi. airway width.

Figure 56 is a similar plot except in this case the position fix update was used for the ρ/θ measurements rather than a Kalman filter update. Comparison with Figure 55 reveals the smoothing effect that the Kalman filter has in processing the same measurements.

Figure 57 provides a summary similar to that in Figure 49 for the measurements noted. The total of different measurement and update combinations for each leg was 11.

Figure 58 is a plot of the nominal IFR flight path and the estimated crosstrack 3σ deviation for a Kalman filter update using the bearing measurement to two different VORTAC.

Figure 59 is a plot of the actual and estimated crosstrack 3σ deviations for a position fix update using a single bearing measurement.

Figure 60 is a plot of the 4-n.mi. airway width and the actual 3σ deviation for a Kalman filter update using a single range measurement.

Figure 61 is a plot of the 4-n.mi. airway width and a crosstrack actual 1σ deviation using no external measurements. Note that the scale on the deviation is one-third that of the previous plots. This is comparable to flying using air data and heading only. As expected, the actual cross track deviation uncertainty increases as a function of distance from each airport.

Additional results could be plotted for the various cases run, but since extensive exercise cases were beyond the scope of the contract, additional plots were not made. Furthermore, the complete listing of output for all of these runs is not included in the report. Since the objective was to merely demonstrate the use of the ANGCAP program, no definitive conclusion should be drawn from these results.

NOMINAL AIRCRAFT PATH CASE 3 9 15
 ESTIMATED LATERAL DEVIATION 3 SIGMAS

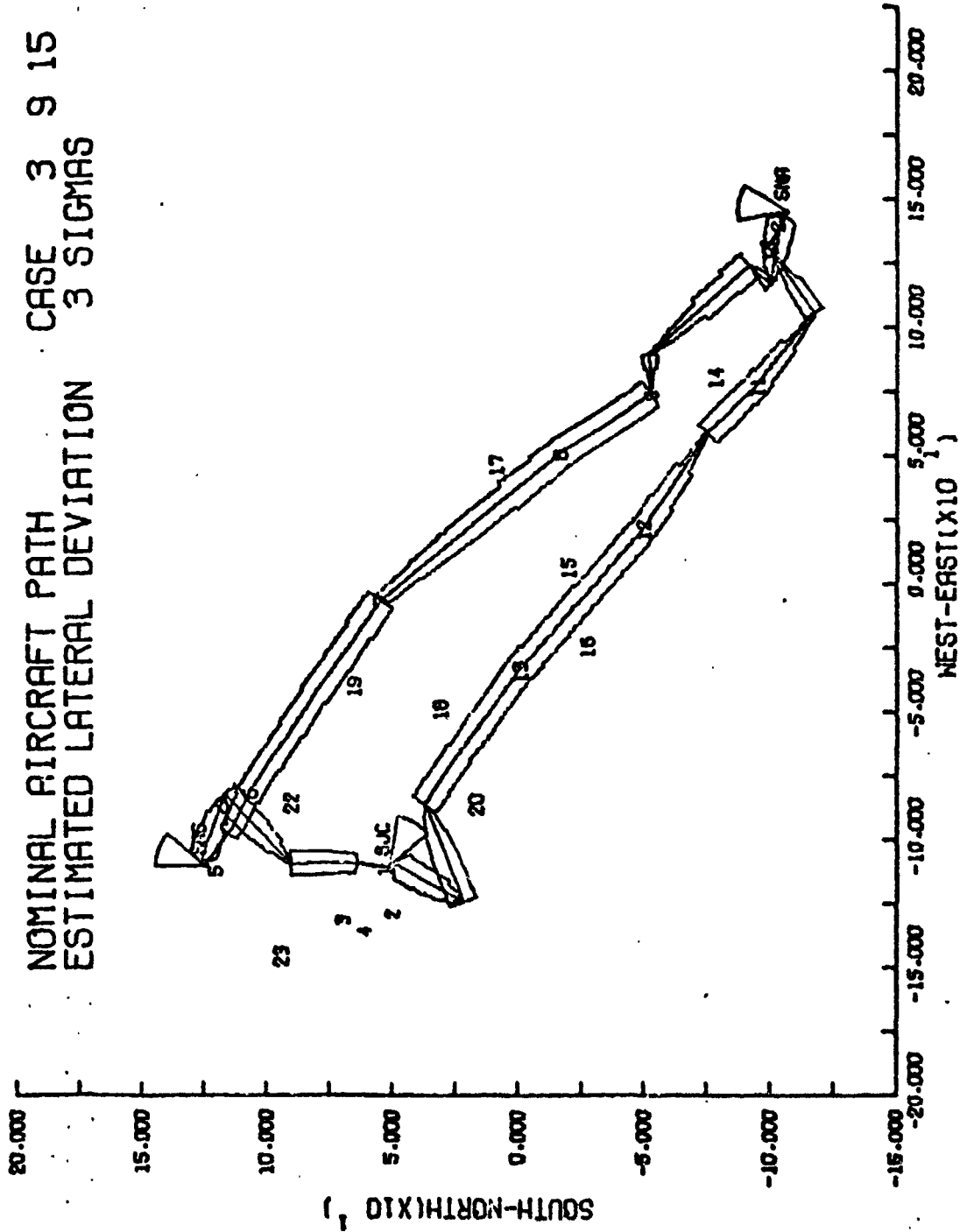


FIGURE 53. PLOT OF NOMINAL IFR FLIGHT PATH AND 3 σ ESTIMATED CROSTRACK DEVIATION FOR KALMAN FILTER UPDATE USING ρ/θ , θ MEASUREMENTS

AIRWAY, 4 NM. WIDE
 ACTUAL LATERAL DEVIATION

CASE 4 10 16
 3 SIGMAS

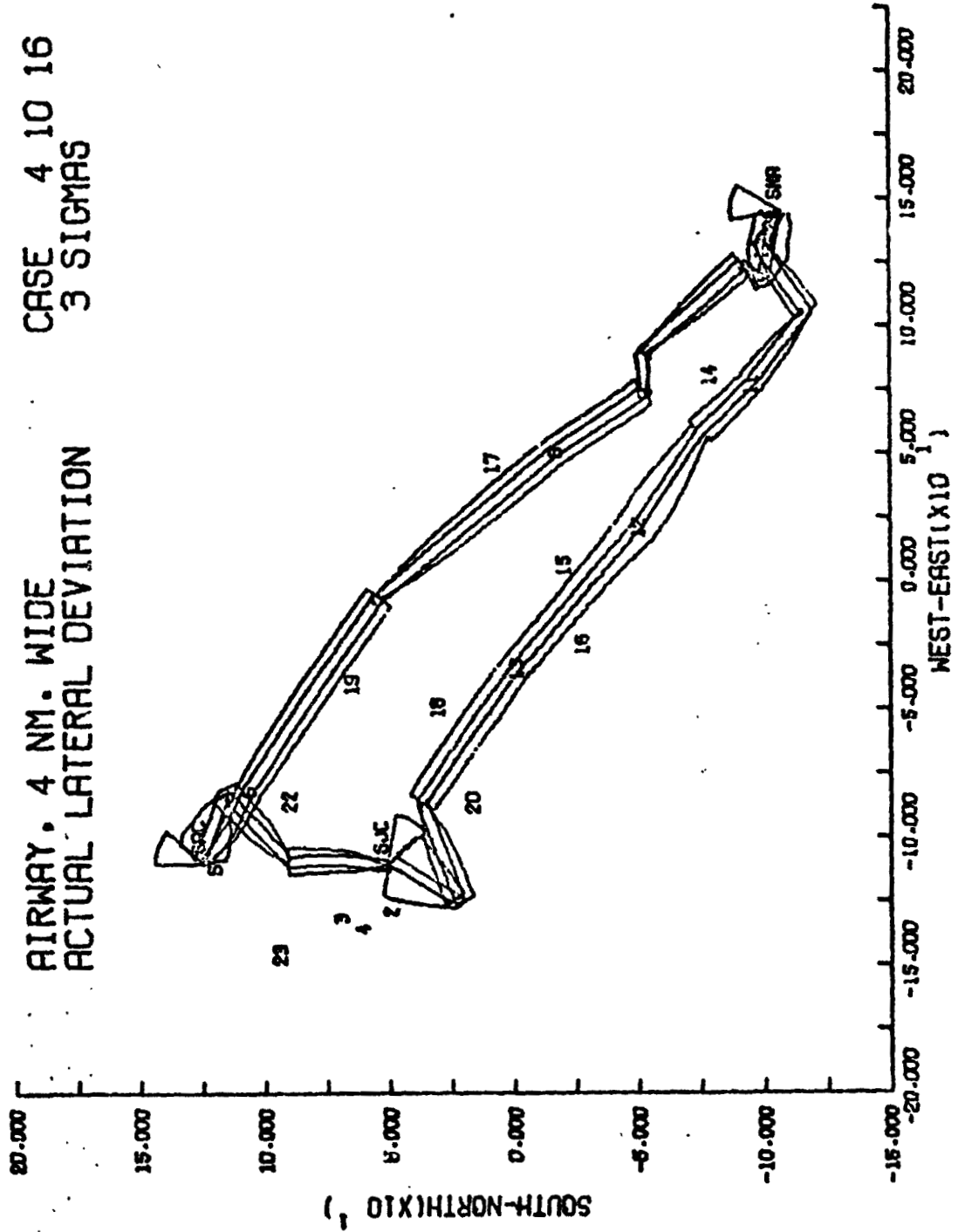


FIGURE 54. PLOT OF 4 N.MI. AIRWAY WIDTH AND 3- σ ACTUAL CROSSTRACK DEVIATION FOR KALMAN FILTER UPDATE USING ρ , ρ MEASUREMENTS

NOMINAL AIRCRAFT PATH
 ACTUAL LATERAL DEVIATION

CASE 5 11 17
 3 SIGMAS

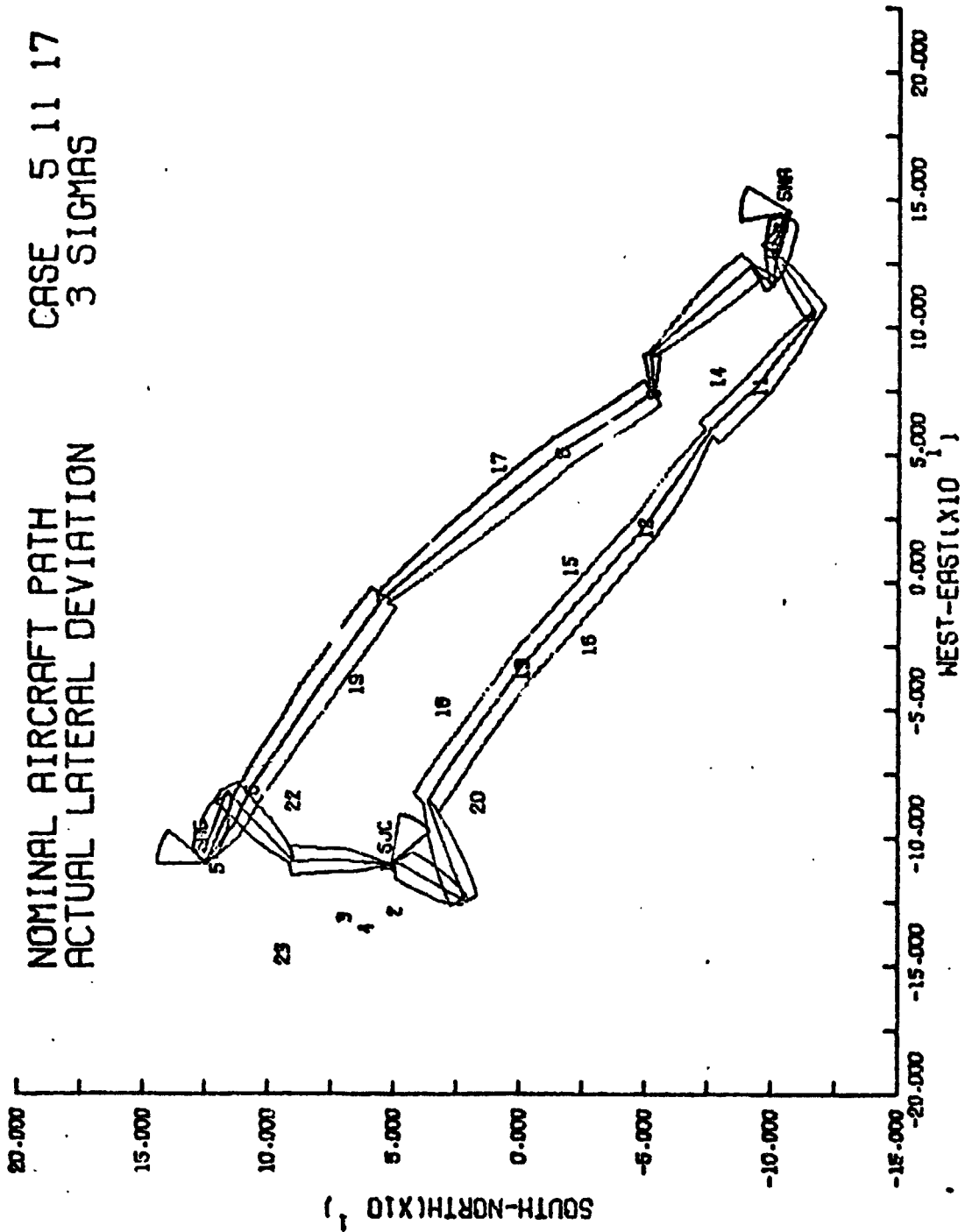


FIGURE 55. PLOT OF NOMINAL IFR FLIGHT PATH AND 3 σ ACTUAL CROSSTRACK DEVIATION FOR KALMAN FILTER UPDATE USING ρ/θ MEASUREMENTS

NOMINAL AIRCRAFT PATH
 ESTIMATED LATERAL DEVIATION

CASE 6 12 18
 3 SIGMAS

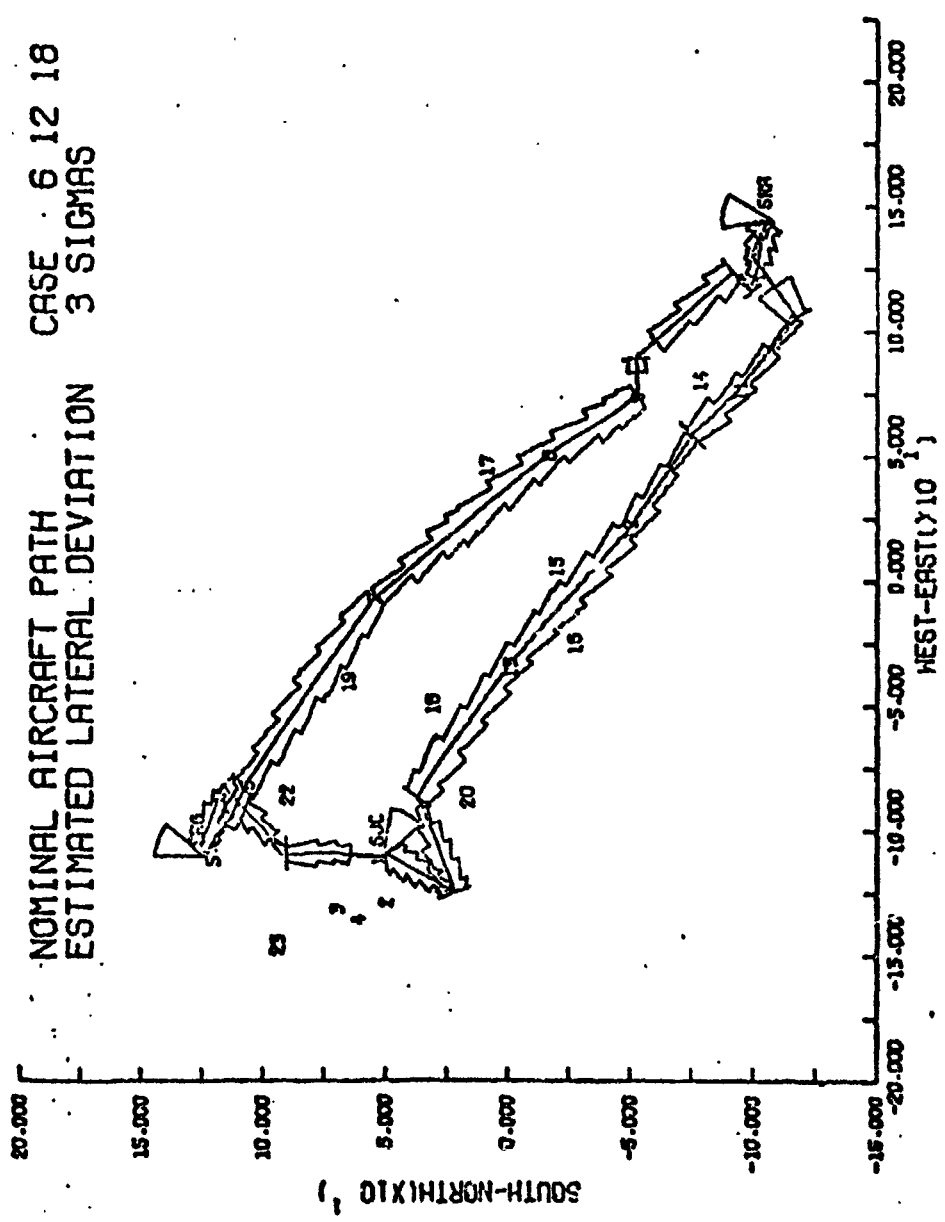


FIGURE 56. PLOT OF NOMINAL IFR FLIGHT PATH AND 3 σ ESTIMATED CROSSTRACK DEVIATION FOR POSITION FIX UPDATE USING ρ/θ MEASUREMENTS

SUMMARY OF CASES FOR AMESJCS OF 02/15/73 AT 152009

CASE	UPDATES TYPE FREQ(SFC)	VOR	RECEIVERS OME	LEG	ACTUAL DISPERSIONS			ESTIMATE DISPERSIONS				
					A.T.(SEC)	X.T.(NM)	ALT.(FT)	A.T.(SEC)	X.T.(NM)	ALT.(FT)		
1	1	120.00	2	0	1	161.19	1.34	50.00	159.11	0.38	0.00	0.3290764
2	2	120.00	1	0	1	344.92	6.22	50.00	245.56	0.50	0.00	0.4619699
3	1	120.00	0	1	1	126.07	0.88	50.00	118.22	0.59	0.00	0.2489069
4	2	120.00	0	1	1	178.97	3.99	50.00	192.77	0.60	0.00	0.4404004
5	2	120.00	0	0	1	349.49	9.71	50.00	0.00	0.00	0.00	0.4755167
6	1	120.00	2	0	2	192.31	0.61	50.00	180.10	0.35	0.00	0.1648885
7	2	120.00	1	0	2	334.98	0.78	50.00	299.89	0.62	0.00	0.2238511
8	1	120.00	0	1	2	158.40	1.89	49.69	167.77	0.37	0.00	0.7768571
9	2	120.00	0	1	2	187.61	2.65	50.00	182.67	0.35	0.00	0.4113053
10	2	120.00	0	0	2	557.55	15.77	50.00	0.00	0.00	0.00	0.4849787
11	1	120.00	2	0	3	235.52	1.05	50.00	235.93	0.78	0.00	0.2376782
12	2	120.00	1	0	3	628.92	7.25	50.00	434.97	1.08	0.00	0.4671595
13	1	120.00	0	1	3	166.07	1.22	49.65	164.11	1.12	0.01	0.3130719
14	2	120.00	0	1	3	408.87	8.83	50.00	212.49	1.83	0.00	0.4732044
15	2	120.00	0	0	3	591.92	16.44	50.00	0.00	0.00	0.00	0.4955961

FIGURE 57. SUMMARY OF RESULTS OUTPUT FROM ANGCAP FOR KALMAN FILTER
 UPDATE USING (1) θ , θ and (3) ρ EXTERNAL MEASUREMENTS AND
 POSITION FIX UPDATE USING (2) θ , (4) ρ , AND (5) NO
 EXTERNAL MEASUREMENTS

NOMINAL AIRCRAFT PATH CASE 1 7 13
 ESTIMATED LATERAL DEVIATION 3 SIGMAS

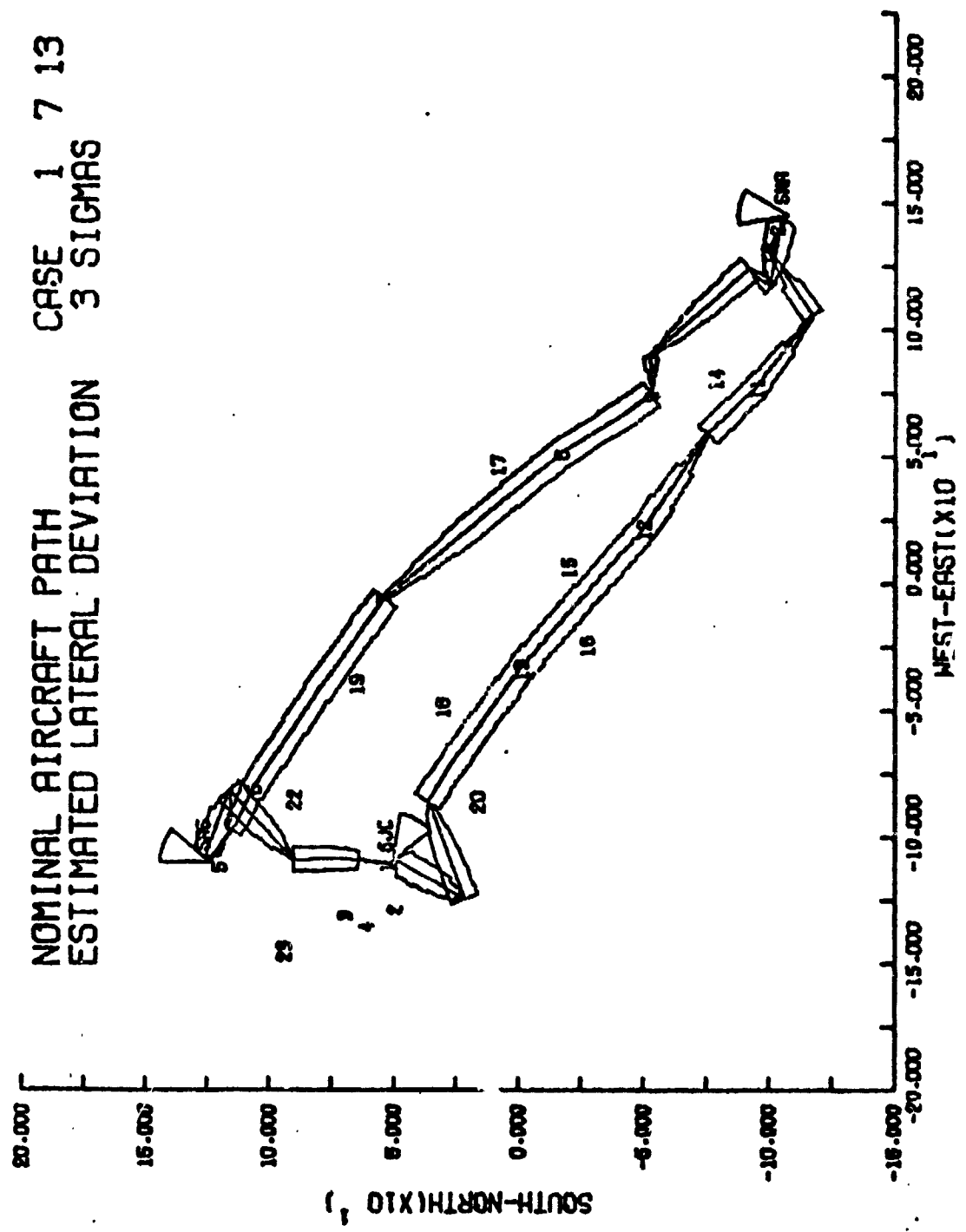


FIGURE 58. PLOT OF NOMINAL IFR FLIGHT PATH AND 3 σ ESTIMATED CROSSTRACK DEVIATION FOR KALMAN FILTER UPDATE USING, θ, θ MEASUREMENTS

SOUTH-NORTH (X10⁴)
 WEST-EAST (X10⁴)
 ACTUAL LATERAL DEVIATION CASE 2 7 12
 ESTIMATED LATERAL DEVIATION 3 SIGMAS

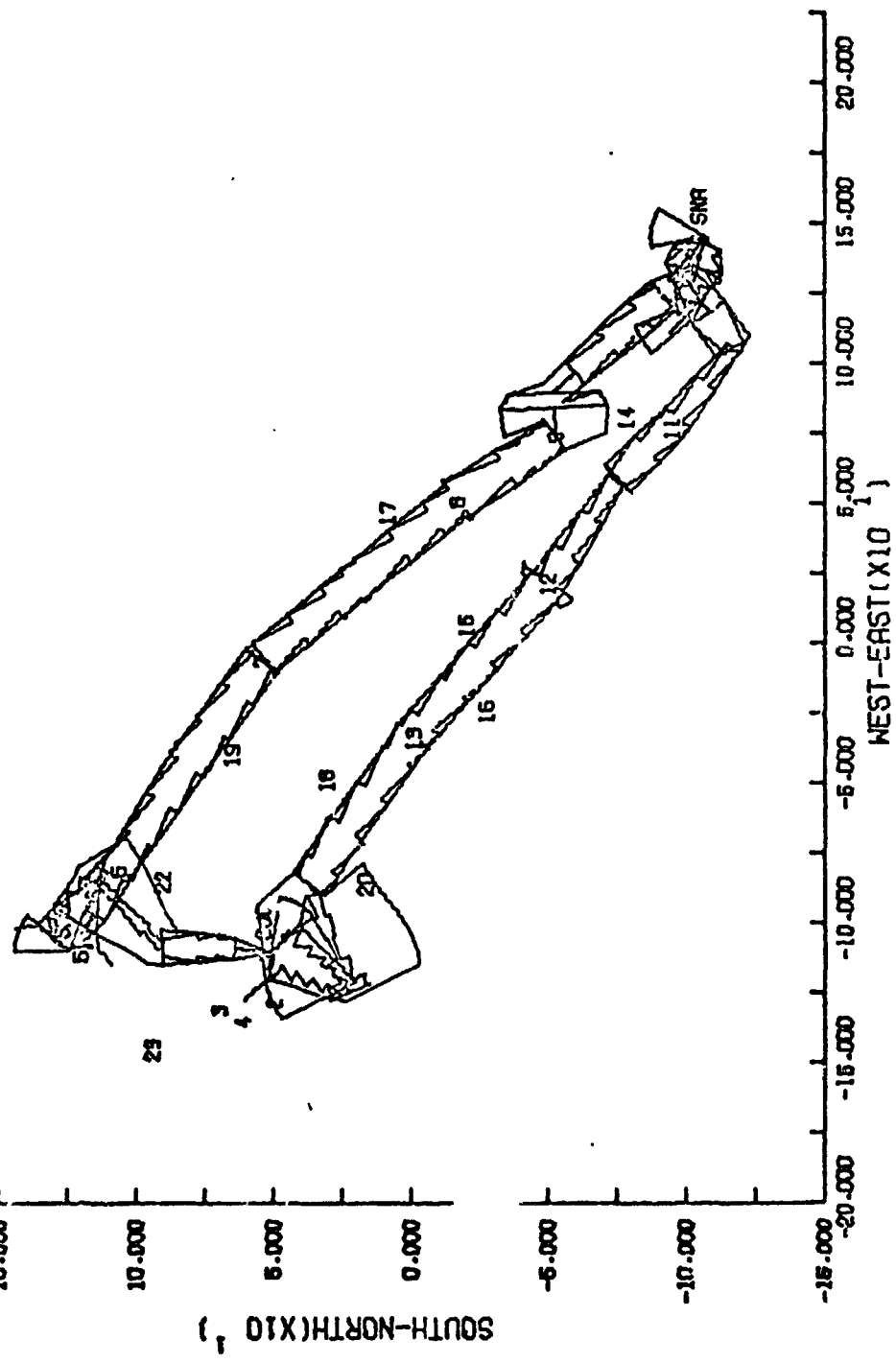


FIGURE 59. PLOT OF 3σ ACTUAL AND ESTIMATED CROSTRACK DEVIATIONS FOR POSITION FIX UPDATE USING θ MEASUREMENT

AIRWAY, 4 NM. WIDE
 ACTUAL LATERAL DEVIATION

CASE 3 8 13
 3 SIGMAS

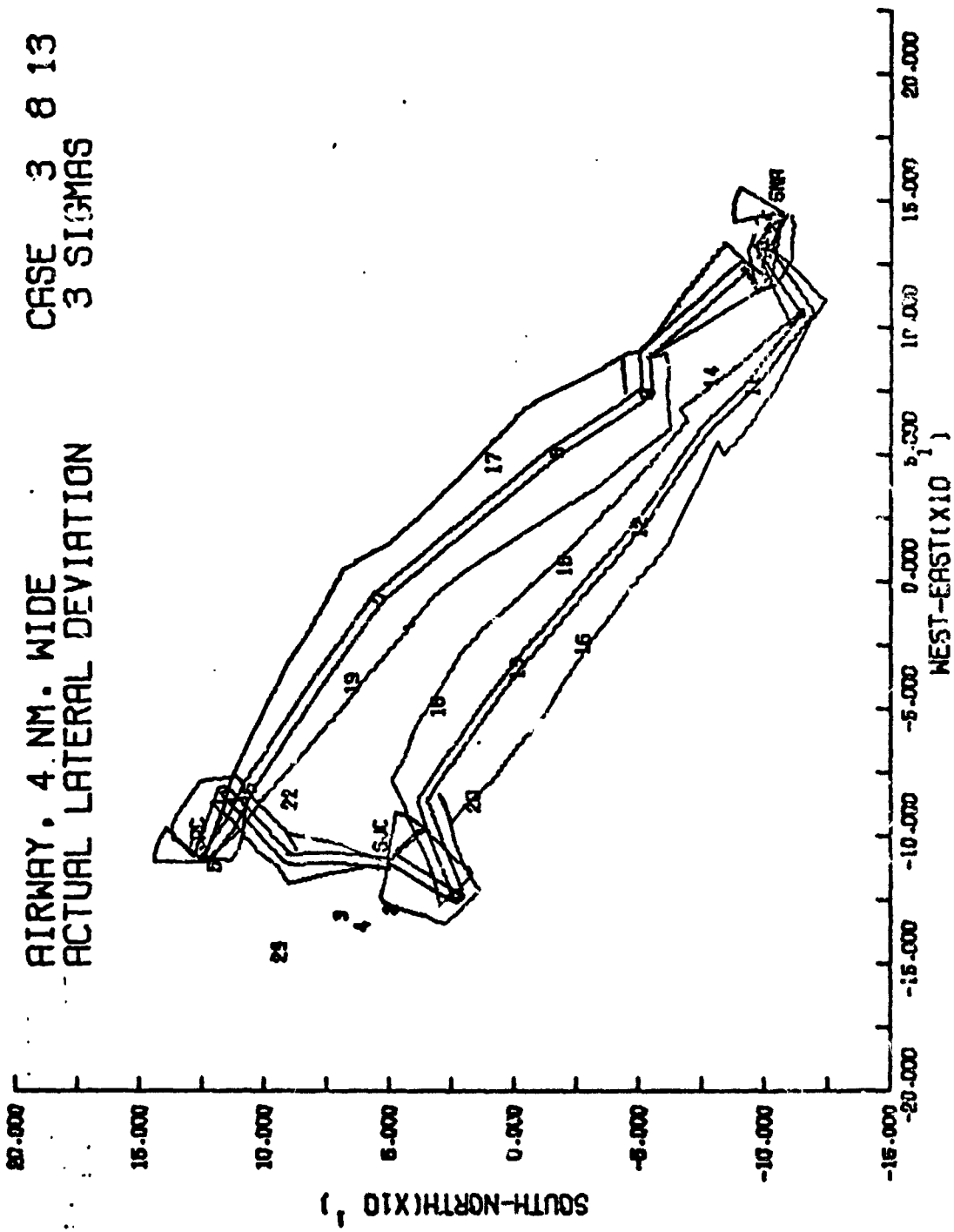


FIGURE 6C. PLOT OF 4 N.M. AIRWAY WIDTH AND 3 σ ACTUAL CROSSTRACK DEVIATION FOR KALMAH
 FILTER UPDATE USING P MEASUREMENT

AIRWAY, 4 NM. WIDE
 ACTUAL LATERAL DEVIATION

CASE 5 10 15
 1 SIGMA

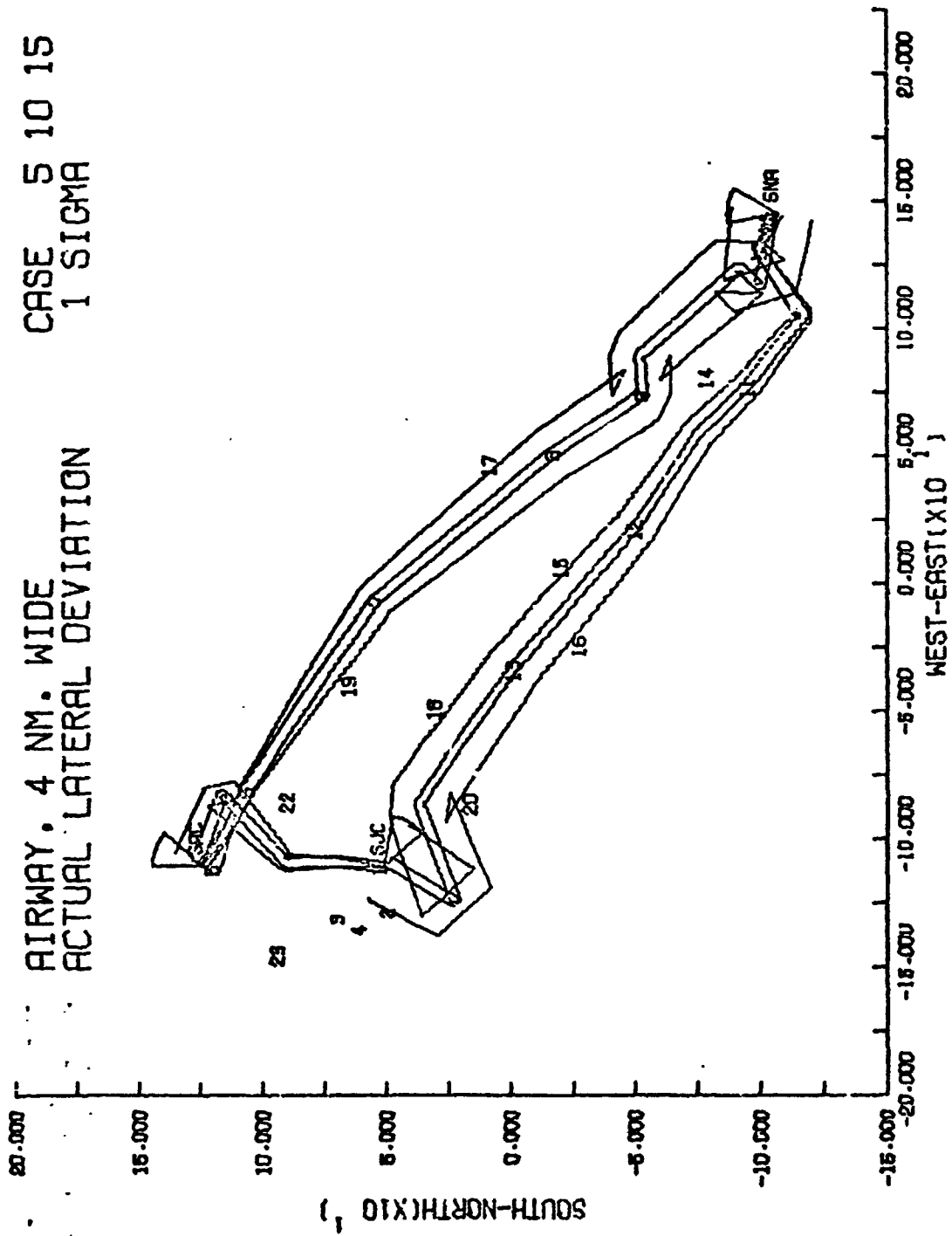


FIGURE 61. PLOT OF 4 NM WIDE AIRWAY WIDTH AND 1 σ ACTUAL CROSSLACK DEVIATION USING NO EXTERNAL MEASUREMENTS

STOL OPS Monte Carlo Results

To demonstrate the use of the STOL OPS program, four examples were run:

- (1) Nominal demonstration run using data presented in previous sections
- (2) Nominal with winds aloft set to zero
- (3) Nominal with IFR weather occurring 100 percent of the time
- (4) Nominal with capacity at SNA increased to 140 movements per hour, MTBF of flight controls increased to 2000 hours.

Case 1. - Figure 62 shows results for all trips between each airport pair and totals for all flights. The E_{xxx} beside each decimal number indicates a power of 10, for example

$$\begin{aligned} 6.1E + 02 &= 6.1 \times 10^2, \\ &= 610 . \end{aligned}$$

The simulation consisted of 250 Monte Carlo evaluations of four successive round trips from SJC to SAC, SAC to SNA, and SNA to SJC. Thus a total of 1000 scheduled flights between each airport pair was evaluated.

The results presented in Figure 62(a) can be interpreted as follows. Of the 1000 scheduled flights from SJC to SAC, 51 (or 5.1 percent) required equipment repair prior to departure with a mean repair time of 41.938 minutes, a maximum repair time of 346.835 minutes, and a minimum repair time of 0.869 minute. A maximum constraint time of 120 minutes was specified, after which time a flight cancellation was assumed. This constraint was exceeded 3 times out of the 51 occurrences. A minimum constraint time of 15 minutes was specified. The value given for the number of times is the number of samples for which repair required less than 15 minutes. This constraint was exceeded 18 times out of the 51 occurrences.

Fuel was loaded 975 times out of 1000 scheduled flights with the values for time involved and constraints exceeded giving a similar interpretation to that for equipment repair. The termination of a Monte Carlo evaluation by a cancelled flight or unscheduled landing causes the program to recycle to the beginning of the next day. Therefore, if the first flight on the day is cancelled, the program does not consider the remaining flights that day, either as cancellations or as being flown. The 25 flights not accounted for are the result of this.

Passengers and cargo were also loaded 975 times out of 1000 flights, and with the values are given for time involved and constraints exceeded.

The results for ground service time are given for 974 of the 1000 scheduled flights. This indicates that one flight out of 975 did not complete ground servicing in time to avoid being cancelled. While the maximum ground service time is only 111 minutes, the flight probably arrived so late that the combination of the late arrival and ground servicing resulted in cancellation. The ground service time includes all ground servicing except repair. Results for fuel weight loaded and the initial fuel load for 975 flights of the 1000 scheduled are given on the next two lines.

The results for initial takeoff weight for 974 out of 1000 scheduled flights are given on the next line.

The results for gate departure delay time are given for the 974 flights that departed of the 1000 scheduled flights. This indicates that 26 out of 1000 flights, or 2.6 percent of the time, the complete schedule could not be completed due to cancelled flights and unscheduled landings. No value was given for a minimum constraint and therefore no results are printed. A maximum constraint of 10 minutes past scheduled gate departure time was exceeded by 579 out of 974 flights that departed.

Takeoff holds were experienced by 648 out of the 974 flights that departed the gate and the results given. The mean hold time due to all causes was 2.2 minutes with a maximum hold of 15.5 minutes. The maximum constraint of 4 minutes was exceeded by 87 of the 649 flights.

Takeoff delays were evaluated for all of the 974 flights that departed the gate with a mean delay of 30.7 minutes. At least one flight departed 1.34 minutes early as indicated by the negative minimum value. The maximum takeoff delay was 281.54 minutes. The minimum constraint indicates 156 flights experienced no takeoff delays.

Takeoff runway occupancy time and distance results are given on the next two lines. These values are deterministic results from Subroutine ARCFT (Appendix B) for the takeoff weight given earlier.

A mean landing hold time of 0.638 minute was experienced by 287 out of 1000 scheduled arriving flights at SAC. The maximum holding time was 2.57 minutes.

Total flight time for the 972 flights arriving at SAC from SJC was 21.44 minutes mean with a maximum of 36.07 minutes. At least one flight had a flight time of 12.46 minutes. Two flights that departed SJC for SAC made unscheduled landings due to loss of a required function.

The minimum constraint number indicates 267 flights experienced no landing delay. Landing delays greater than 10 minutes were experienced by 556 flights.

The output variables starting at equipment repair and extending through takeoff runway distance are associated with the departure airport while the remaining variables are associated with the arrival airport.

The landing runway-occupancy time and distance results are given next. It should be noted that results for minimum runway occupancy time and distance are a function of the aircraft touchdown conditions (weight, velocity), deceleration, and turnoff velocity, whereas the landing runway occupancy time is a function of these factors and the airport's geometry. In other words, the minimum runway occupancy values are those due to reaching turnoff velocity after touchdown while the landing runway occupancy and distance include taxi to the nearest taxiway intersection after deceleration to turnoff velocity.

The gate arrival delay time is referenced to the scheduled gate arrival time as discussed previously. As noted previously, the mean gate departure delay at SJC was 30.66 minutes, whereas the mean gate arrival delay at SAC is 28.67 minutes which indicates that most flights would arrive on time at SAC if they departed SJC on time. Of the 972 flights arriving at SAC, 742 exceeded the scheduled gate arrival time.

Mean fuel consumed was 3648.5 pounds with a maximum fuel consumption of 5740.2 lb. A constraint value on fuel consumption was not loaded but can be done so at user option. Fuel remaining had a minimum value of 606.4 pounds which corresponds to the maximum fuel usage flight. Mean fuel remaining was 2698.2 pounds.

The event tabulation in Figure 62a lists the number of occurrences at each of the specific events. Of these 1000 flights, none of the avionics functions were lost. The safe flight function was lost two times out of the 1000 scheduled flights, resulting in two unscheduled landings. Forty hardware failures occurred.

Due to limitations imposed by computer storage, subsystem failure counts were divided into groups of 10. The event failure in Sections 1-10 indicates how many times any of the first 10 subsystems failed. It is interesting to note that of the 40 hardware failures shown for flights between SJC and SAC,

NOMINAL DEMONSTRATION CASE
 TOTALS FOR ALL TRIALS FROM SJC TO SAC
 STATISTICS FOR 1700 MONTE CARLO TRIALS

	NO. SAMPLES	MEAN	STANDARD DEVIATION	MAXIMUM VALUE	MINIMUM VALUE	CONSTRAINT MAXIMUM	NUMBER OF TIMES EXCEEDED	MINIMUM	NO.
EQUIPMENT REPAIR TIME (MIN)	51	4.19300E+01	6.45205E+01	3.44835E+02	8.69175E-01	1.20000E+02	3	1.50000E+01	18
FUEL LOADING TIME (MIN)	975	9.52200E+00	3.86799E+00	1.85110E+01	3.72923E+00	1.50000E+01	240	1.00000E+01	494
PASSENGER LOADING TIME (MIN)	975	9.92994E+00	3.98834E+00	1.50276E+01	2.83504E+00	1.50000E+01	9	5.00000E+00	0
CARGO LOADING TIME (MIN)	975	1.00575E+01	1.99011E+00	1.89974E+01	4.52514E+00	1.50000E+01	5	5.00000E+00	3
GROUND SERVICE TIME (MIN)	974	2.04497E+01	7.36720E+00	1.11099E+02	8.65445E+00	2.00000E+01	406	5.00000E+00	0
FUEL LOADED (LBS)	975	3.99927E+09	1.37345E+03	6.14663E+03	1.57173E+03	1.00000E+20	0	-1.00000E+20	0
INITIAL FUEL LOAD (LBS)	975	6.34643E+09	4.00549E+03	6.34643E+03	4.34437E+03	1.00000E+20	0	-1.00000E+20	0
INITIAL TAKEOFF FLIGHT (LBS)	974	1.04353E+09	7.92492E+02	1.04353E+09	1.25789E+05	1.00000E+20	0	-1.00000E+20	0
GATE DEPARTURE DELAY (MIN)	974	3.00000E+00	3.57244E+01	2.02480E+02	9.6E+00	1.00000E+01	579	0.1E+00	0
TAKEOFF HOLD TIME (MIN)	974	2.20179E+00	2.06934E+00	1.50000E+01	5.00000E-01	4.00000E+00	47	-1.00000E+20	0
TAKEOFF DELAY (MIN)	974	3.07867E+01	3.53644E+01	2.81541E+02	-1.33943E+00	1.00000E+01	581	0.1E+00	156
TAKEOFF RUNWAY OCCUPANCY (SEC)	974	1.01244E+01	0.8E+00	1.81264E+01	1.01264E+01	1.00000E+20	0	-1.00000E+20	0
TAKEOFF RUNWAY DISTANCE (FT)	974	5.12744E+02	0.8E+00	5.12744E+02	5.12744E+02	1.00000E+20	0	-1.00000E+20	0
LANDING HOLD TIME (MIN)	972	6.38377E-01	3.54304E-01	2.57143E+00	4.28571E-01	4.00000E+00	0	-1.00000E+20	0
TOTAL FLIGHT TIME (MIN)	972	2.14615E+01	2.53547E+00	4.24612E+01	1.24612E+01	1.00000E+20	0	-1.00000E+20	0
LAUNCHING TIME DELAY (MIN)	972	2.74563E-01	3.53144E-01	2.74563E-01	-0.22617E+00	1.00000E+01	586	0.1E+00	27
MIN. RUNWAY OCCUPANCY (SEC)	972	1.02185E+01	5.82826E-01	1.21982E+01	8.37115E+00	1.00000E+20	0	-1.00000E+20	0
MIN. RUNWAY OCCUPANCY (FT)	972	8.68121E+02	7.95274E+01	1.15374E+03	6.32449E+02	1.00000E+03	0	-1.00000E+03	972
LANDING RUNWAY OCCUPANCY (SEC)	972	1.32444E+02	1.77304E+00	1.97401E+02	1.25941E+02	6.00000E+01	972	3.00000E+01	6
LANDING RUNWAY DISTANCE (FT)	972	4.99525E+03	3.79949E+03	6.99525E+03	4.99525E+03	1.00000E+20	0	-1.00000E+20	0
GATE ARRIVAL DELAY (MIN)	972	2.86745E+01	3.53145E+01	2.86745E+01	-0.88720E+00	0.1E+00	742	-1.00000E+20	0
FUEL CONSUMED (LBS)	972	3.64846E+09	3.44674E+02	5.74020E+09	2.36249E+03	1.00000E+20	6	-1.00000E+20	0
FUEL REMAINING (LBS)	972	2.69817E+09	3.44674E+02	3.69815E+09	4.86429E+02	1.00000E+20	0	-1.00000E+20	281

STATISTICS FOR 1700 MONTE CARLO TRIALS

EVENT	OCCURRENCES	EVENT	OCCURRENCES
STATE ESTIMATION LOST	0	COMMAND GENERATION LOST	0
HAZARD AVOIDANCE LOST	0	COMMUNICATION LOST	0
SYSTEM MANAGEMENT LOST	0	SAFE FLIGHT LOST	2
UNSCHEMULED LANDING	2	HARDWARE FAILURE	40
FAILURE IN SECTIONS 1-11	7	FAILURE IN SECTIONS 11-20	3
FAILURE IN SECTIONS 11-20	8	FAILURE IN SECTIONS 31-40	12
FAILURE IN SECTIONS 41-50	10	CANCELLED FLIGHT	3
GATE DEPARTURE	974	DISPATCH RELIABILITY	438
SCHEDULED FLIGHT TIME EXCEEDED	70	DIVERT TO ALTERNATE AIRPORT	17
MISSED APPROACH	1	IFR WEATHER	17
MLS FAILURE	0	HOLD FOR TAKEOFF CLEARANCE	648
HOLD FOR LANDING CLEARANCE	287		

FIGURE 62(a) EXAMPLE OF STOL OPS RESULTS FOR NOMINAL DEMONSTRATION CASE

a required function was lost only twice. If back-up modes were available for the safe flight function, it is possible that the unscheduled landings would not have occurred.

The three cancelled flights resulted from exceeding the 120-minute constraint previously discussed for equipment repair.

As previously discussed, 974 of the scheduled 1000 flights departed the gate. The dispatch reliability, previously defined as the number of scheduled flights departing within 15 minutes of the scheduled gate departure time, is given as 438, a 43.8% dispatch reliability.

The scheduled flight time was exceeded by 70 of the flights from SJC to SAC. No flights were diverted to an alternate airport in this example. There was one missed approach in all the 1000 scheduled flights flown, 972. Category I, or worse, weather, labeled as IFR, existed for 17 of the flights. There were no failures of the MLS. Holds for take-off clearance totaled 648 and holds for landing clearance totaled 287.

Figure 62(b) presents a summary of the modes used for each function for the 1000 scheduled flights from SJC to SAC. The state estimation function used the automatic navigation subfunction Mode 1 100% of the time and reverted only to Mode 3 which was used 0.2% of the time. Since Mode 2 was not used, this indicates a failure of a DME receiver rather than a VORTAC which would have caused reversion to Mode 5. The state estimation subfunction of approach/landing navigation, Mode 1, was used 1.7% of the time. Reversion to the other modes of this subfunction did not occur.

Similarly, the command generation/execution functions operated only in Mode 1 of the automatic guidance/control subfunction.

The hazard avoidance function operated in the automatic hazard subfunction using Mode 1 100% of the time and reverting to Mode 3 for 1% of the time. Examination of this subfunction in Figure 33 indicates that both the radar altimeter and weather radar failed.

The communication function operated in Mode 1 of the automatic communication subfunction 100% of the time and did not revert to a backup mode or subfunction.

The system management function operated in mode 1 of the automatic system-management subfunction and reverted to the manual system-management subfunction, Mode 4, for 0.2% of the time. Examination of Figure 35 indicates that a computer failure would cause this reversion sequence.

The safe flight function has only one subfunction and mode and therefore operated in Mode 2 100% of the time with no reversion possible.

NOMINAL DEMONSTRATION CASE	MODES USED (PER CENT)							
	1	2	3	4	5	6	7	8
STATE ESTIMATION	100.0	0.0	0.0	0.0	0.0	0.0	0.0	0.0
AUTOMATIC NAVIGATION	100.0	0.0	0.0	0.0	0.0	0.0	0.0	0.0
APPROACH/LANDING NAVIGATION	100.0	0.0	0.0	0.0	0.0	0.0	0.0	0.0
COMMAND REFORMATION/EXECUTION	100.0	0.0	0.0	0.0	0.0	0.0	0.0	0.0
AUTOMATIC GUIDANCE/CONTROL	100.0	0.0	0.0	0.0	0.0	0.0	0.0	0.0
HAZARD AVOIDANCE	100.0	0.0	0.0	0.0	0.0	0.0	0.0	0.0
AUTOMATIC HAZARD AVOIDANCE	100.0	0.0	0.0	0.0	0.0	0.0	0.0	0.0
COMMUNICATION	100.0	0.0	0.0	0.0	0.0	0.0	0.0	0.0
AUTOMATIC COMMUNICATION	100.0	0.0	0.0	0.0	0.0	0.0	0.0	0.0
SYSTEM MANAGEMENT	100.0	0.0	0.0	0.0	0.0	0.0	0.0	0.0
AUTOMATIC SYSTEM MANAGEMENT	100.0	0.0	0.0	0.0	0.0	0.0	0.0	0.0
MANUAL SYSTEM MANAGEMENT	0.0	0.0	0.0	0.0	0.0	0.0	0.0	0.0
SAFE FLIGHT	100.0	0.0	0.0	0.0	0.0	0.0	0.0	0.0
SAFE FLIGHT	100.0	0.0	0.0	0.0	0.0	0.0	0.0	0.0

FIGURE 62 (b). (CONTINUED)

Similar interpretations of the results can be made by the reader for the 1000 scheduled flights from Sacramento (SAC) to Santa Ana (SNA) by referring to Figures 62(c) and (d). The results for the 1000 scheduled flights from SNA to SAC are summarized in Figures 62(e) and (f).

The results for the totals of all flights around the route network, 3000 scheduled flights, are shown in Figures 62(g) and (h). The large number of takeoff and landing holds are due to the traffic at SNA and its capacity as can be seen by examining the statistics for each individual leg of the route network. By referring to Figure 23 it can be seen that the number of operations per hour at SNA is over 120 for the three round trips before the last of the day. As can be seen in Figure 30, SNA has a VFR capacity of 120 movements per hour, which clearly indicates that the airport is overloaded.

The sensitivity to operational procedures is also shown in Figure 62. For example, Figure 62(h) indicates that 2065 flights exceeded the maximum gate departure delay constraint of 10 minutes, while the dispatch reliability indicates the 1019 flights departed within 15 minutes after the scheduled gate departure time. This indicates that of the 2965 flights that departed the gate, 840 departed within 0 to 10 minutes of scheduled time, and another 179 departed between 10 and 15 minutes of scheduled time. If dispatch reliability were defined at 10 minutes after scheduled departure time and increased 50% to 15 minutes, a 21.3% increase over the number of aircraft defined as dispatched at 10 minutes results.

Case 4, described later, illustrates the sensitivity to the operational environment that results from increasing the capacity at SNA.

Case 2.-Figure 63 also illustrates the sensitivity to the operational environment since no en route winds were included. Comparison of the total flight time statistics for Cases 1 and 2 shows that the winds assumed had little effect on the flight schedule.

Case 3.-Figure 64 shows the results obtained for operations during IFR weather only. The improvement in schedule reliability for this case occurs because of the reduced traffic at SNA for IFR conditions. Notice the missed approaches are 161 with 22 flights diverted to alternate airports.

Case 4.-Figure 65 shows the results for an assumed capacity of 140 movements per hour at SNA and an increased MTBF of 2000 hours for the flight controls. The improved capacity shows that the mean takeoff/land holding times for all flights have been reduced from 6 to 8 minutes for Case 1 to about 2 minutes. In addition, the total number of holds exceeding 4 minutes was reduced from 1062 to 361 out of 3000 flights.

The increased MTBF for flight controls was used to illustrate an expected sensitivity to technology improvement and hence a decrease in the number of losses of the safe flight function. However, the actual results show

MINIMAL DEMONSTRATION CASE
 TOTALS FOR ALL TOIPS FROM SAC TO SMA
 STATISTICS FOR 100 MONTE CARLO TRIALS

	NO. SAMPLES	MEAN	STANDARD DEVIATION	MAXIMUM VALUE	MINIMUM VALUE	CONSTRAINT MAXIMUM	NUMBER TIMES EXCEEDED	MINIMUM	NO.
EQUIPMENT REPAIR TIME (MIN)	53	3.74818E+01	6.49064E+01	3.51256E+02	5.19498E+00	1.20000E+02	3	1.50000E+01	19
FUEL LOADING TIME (MIN)	971	2.06459E+01	8.46365E+01	2.54660E+01	1.76278E+01	1.50000E+01	971	1.00000E+01	0
PASSENGER LOADING TIME (MIN)	971	1.00218E+01	2.62329E+01	1.54902E+01	3.80549E+00	1.50000E+01	5	5.00000E+00	0
CARGO LOADING TIME (MIN)	0	1.01857E+01	1.96284E+01	1.66284E+01	3.44849E+00	1.50000E+01	4	5.00000E+00	3
GROUND SERVICE TIME (MIN)	971	3.11899E+01	4.80399E+01	1.07713E+01	2.37492E+01	2.00000E+01	969	1.00000E+00	0
FUEL LOADED (LB)	971	4.68325E+01	3.64714E+02	1.07797E+04	7.40282E+03	1.00000E+20	0	-1.00000E+20	0
INITIAL FUEL LOAN (LB)	971	1.13442E+04	2.42701E+03	1.13462E+04	1.13462E+04	1.00000E+20	0	-1.00000E+20	0
INITIAL TAKEOFF WEIGHT (LB)	969	1.10789E+04	3.09068E+02	1.10789E+04	1.10789E+04	1.00000E+20	0	-1.00000E+20	0
GATE DEPARTURE DELAY (MIN)	969	3.52033E+01	3.55937E+01	2.49039E+02	6.5400E+00	1.00000E+01	657	0.5000E+00	0
TAKEOFF HOLD TIME (MIN)	261	6.27259E+01	3.46274E+01	2.14294E+02	4.28571E+01	1.00000E+01	657	0.5000E+00	0
TAKEOFF DELAY (MIN)	969	3.24459E+01	3.55511E+01	2.85117E+02	-2.92690E+00	1.00000E+01	662	0.5000E+00	109
TAKEOFF RUNWAY OCCUPANCY (SEC)	969	1.01288E+01	0.8E+00	1.01288E+01	1.01288E+01	1.00000E+20	0	-1.00000E+20	0
TAKEOFF RUNWAY DISTANCE (FT)	969	5.17764E+02	0.8E+00	5.17764E+02	5.17764E+02	1.00000E+20	0	-1.00000E+20	0
LANDING HOLD TIME (MIN)	730	1.54899E+01	1.46870E+01	1.92000E+02	5.00709E+01	4.00000E+00	519	-1.00000E+20	0
TOTAL FLIGHT TIME (MIN)	967	7.32864E+01	1.78781E+01	2.54443E+02	5.19395E+01	1.00000E+20	0	-1.00000E+20	0
LANDING TIME DELAY (MIN)	967	4.09825E+01	3.43276E+01	2.61269E+02	-1.21279E+01	1.00000E+20	777	0.5000E+00	56
MIN. RUNWAY OCCUPANCY (SEC)	967	9.94542E+01	1.66015E+02	1.49005E+02	-7.00193E+01	1.00000E+20	0	-1.00000E+20	0
MIN. RUNWAY OCCUPANCY (FT)	967	6.46709E+02	1.84757E+02	1.97840E+03	-2.11919E+01	2.00000E+03	0	1.50000E+03	964
LANDING BINNAY OCCUPANCY (SEC)	967	3.13117E+01	3.89447E+01	5.94538E+01	2.02962E+01	6.00000E+01	0	3.00000E+01	139
LANDING BINNAY DISTANCE (FT)	967	1.57403E+03	3.13284E+03	2.77269E+07	1.56929E+03	1.00000E+20	0	-1.00000E+20	0
GATE ARRIVAL DELAY (MIN)	967	3.64371E+01	3.43245E+01	2.77269E+07	-1.61943E+01	0.5000E+00	862	-1.00000E+20	0
FUEL CONSUMED (LB)	967	1.03677E+04	2.48307E+03	3.58047E+04	7.45113E+03	1.00000E+20	0	-1.00000E+20	0
FUEL REMAINING (LB)	967	1.01049E+03	2.48307E+03	3.97803E+03	-2.44185E+04	1.00000E+20	0	2.50000E+03	718

STATISTICS FOR 100 MONTE CARLO TRIALS

EVENT	OCCURRENCES	EVENT	OCCURRENCES
STATE ESTIMATION LOST	0	COMMAND GENERATION LOST	0
HAZARD AVOIDANCE LOST	0	COMMUNICATION LOST	0
SYSTEM MANAGEMENT LOST	0	SAFE FLIGHT LOST	2
UNSCHEMULED LANDING	2	HARDWARE FAILURE	90
FAILURE IN SECTIONS 1-10	18	FAILURE IN SECTIONS 11-20	9
FAILURE IN SECTIONS 21-30	6	FAILURE IN SECTIONS 31-40	30
FAILURE IN SECTIONS 41-50	27	CANCELLED FLIGHT	3
RATE OF PARTURE	969	DISPATCH RELIABILITY	388
SCHEDULED FLIGHT TIME EXCEEDED	592	DIVERT TO ALTERNATE AIRPORT	0
MISSED APPROACH	1	IFR WEATHER	24
MLS FAILURE	0	HOLD FOR TAKEOFF CLEARANCE	261
HOLD FOR LANDING CLEARANCE	730		

FIGURE 62 (c). (CONTINUED)

NOMINAL DEMONSTRATION CASE

	MODES USED (PER CENT)							
	1	2	3	4	5	6	7	8
STATE ESTIMATION	100.0	0.0	0.0	0.0	0.0	0.0	0.0	0.0
AUTOMATIC NAVIGATION	100.0	0.0	0.0	0.0	0.0	0.0	0.0	0.0
APPROACH/LEAVING NAVIGATION	2.0	3.0	0.0	0.0	0.0	0.0	0.0	0.0
COMMAND REFORMATION/RECU/COM	100.0	0.0	0.0	0.0	0.0	0.0	0.0	0.0
AUTOMATIC GUIDANCE/CONTROL	100.0	0.0	0.0	0.0	0.0	0.0	0.0	0.0
HAZARD AVOIDANCE	100.0	0.0	0.0	0.0	0.0	0.0	0.0	0.0
AUTOMATIC HAZARD AVOIDANCE	100.0	0.0	2.4	0.1	0.0	0.0	0.0	0.0
COMMUNICATION	100.0	0.0	0.0	0.0	0.0	0.0	0.0	0.0
AUTOMATIC COMMUNICATION	100.0	0.0	0.0	0.0	0.0	0.0	0.0	0.0
SYSTEM MANAGEMENT	100.0	0.0	0.0	0.0	0.0	0.0	0.0	0.0
AUTOMATIC SYSTEM MANAGEMENT	0.0	0.0	0.0	0.0	0.0	0.0	0.0	0.0
MANUAL SYSTEM MANAGEMENT	0.0	0.0	0.0	0.0	0.0	0.0	0.0	0.0
SAFE FLIGHT	100.0	0.0	0.0	0.0	0.0	0.0	0.0	0.0
SAFE FLIGHT	100.0	0.0	0.0	0.0	0.0	0.0	0.0	0.0

FIGURE 62(d). (CONTINUED)

NOMINAL DEMONSTRATION CASE
 TOTALS FOR ALL TRIPS FROM SMA TO SJC
 STATISTICS FOR 1000 MONTE CARLO TRIALS

	NO. SAMPLES	MEAN	STANDARD DEVIATION	MAXIMUM VALUE	MINIMUM VALUE	CONSTRAINT MAXIMUM	CONSTRAINT MINIMUM	NUMBER OF TIMES EXCEEDED
EQUIPMENT REPAIR TIME (MIN)	80	3.54612E+01	5.71322E+01	3.34161E+02	4.17810E+00	1.20000E+02	1.50000E+01	4
FUEL LOADING TIME (MIN)	963	2.44691E+01	5.87376E+00	8.59425E+01	1.77541E+01	1.50000E+01	1.00000E+01	0
PASSENGER LOADING TIME (MIN)	963	1.00161E+01	1.95437E+00	1.63725E+01	1.91444E+00	1.50000E+01	5.00000E+00	6
CARGO LOADING TIME (MIN)	963	1.00161E+01	1.95437E+00	1.61205E+01	2.68287E+00	1.50000E+01	5.00000E+00	4
GROUND SERVICE TIME (MIN)	962	3.51142E+01	7.78957E+00	1.40785E+02	2.11315E+01	2.00000E+01	5.00000E+00	962
FUEL LOADED (LB)	963	1.03613E+04	2.44659E+03	3.59105E+04	7.45422E+03	1.00000E+02	-1.00000E+20	0
INITIAL FUEL LOAD (LR)	963	1.13913E+04	0.5E+00	1.17915E+04	1.13913E+04	1.00000E+02	-1.00000E+20	0
INITIAL TAKEOFF WEIGHT (LR)	962	1.17995E+04	4.48064E+02	1.17995E+04	1.17995E+04	1.00000E+02	-1.00000E+20	0
GATE DEPARTURE DELAY (MIN)	962	4.72721E+01	3.44410E+01	3.05450E+02	0.5E+00	1.00000E+01	0.5E+00	0
TAKEOFF HOLD TIME (MIN)	990	1.24308E+01	1.61919E+01	1.36509E+02	0.5E+00	1.00000E+01	0.5E+00	0
TAKEOFF DELAY (MIN)	962	5.32291E+01	3.67366E+01	3.02757E+02	-3.10232E+00	1.00000E+01	-1.00000E+20	0
TAKEOFF RUNWAY OCCUPANCY (SEC)	962	1.01264E+01	0.5E+00	1.01264E+01	1.01264E+01	1.00000E+01	0.5E+00	24
TAKEOFF RUNWAY DISTANCE (FT)	962	5.12764E+02	0.5E+00	5.12764E+02	5.12764E+02	1.00000E+02	-1.00000E+20	0
LANDING HOLD TIME (MIN)	485	1.30229E+00	1.49559E+00	7.50000E+00	5.00000E-01	1.00000E+00	-1.00000E+20	0
LANDING TIME DELAY (MIN)	961	2.33411E+01	4.41620E+00	7.24544E+01	4.58423E+01	1.00000E+00	-1.00000E+20	0
MIN. RUNWAY OCCUPANCY (SEC)	961	4.57234E+01	3.67870E+01	2.94064E+02	-1.47232E+01	1.00000E+01	0.5E+00	34
MIN. RUNWAY OCCUPANCY (FT)	961	1.06912E+01	2.44417E+00	2.07444E+01	2.26449E+00	1.00000E+01	-1.00000E+20	0
LANDING RUNWAY OCCUPANCY (SEC)	961	9.62245E+02	3.59982E+02	2.76627E+03	1.02591E+02	2.00000E+03	1.00000E+03	898
LANDING RUNWAY DISTANCE (FT)	961	3.26228E+01	7.43055E+00	5.54691E+01	1.52145E+01	6.00000E+01	3.00000E+01	298
GATE ARRIVAL DELAY (MIN)	961	1.70257E+03	3.02532E+02	3.06707E+03	1.63248E+03	1.00000E+02	-1.00000E+20	0
FUEL CONSUMED (LR)	961	4.78393E+01	3.67814E+01	2.92207E+02	-1.08834E+01	0.5E+00	-1.00000E+20	0
FUEL REMAINING (LR)	961	8.28249E+03	5.93809E+02	1.09324E+04	6.57123E+03	1.00000E+02	-1.00000E+20	0
	961	3.18877E+03	5.93809E+02	4.89053E+03	1.05940E+03	1.00000E+02	2.50000E+03	123

STATISTICS FOR 1000 MONTE CARLO TRIALS

EVENT	OCCURRENCES	EVENT	OCCURRENCES
STATE ESTIMATION LOST	0	COMMAND GENERATION LOST	0
HAZARD AVOIDANCE LOST	0	COMMUNICATION LOST	0
SYSTEM MANAGEMENT LOSS	0	SAFE FLIGHT LOST	0
UN-SCHEDULED LANDING	1	HARDWARE FAILURE	81
FAILURE IN SECTIONS 1-17	20	FAILURE IN SECTIONS 11-20	31
FAILURE IN SECTIONS 18-28	10	FAILURE IN SECTIONS 31-40	3
FAILURE IN SECTIONS 29-38	17	CANCELLED FLIGHT	5
RATE OF PARTIALS	962	DISPATCH RELIABILITY	193
SCHEDULED FLIGHT TIME EXCEEDED	195	OBJECT TO ALTERNATE AIRPORT	0
MISSSED APPROACH	0	IFR WEATHER	19
MLS FAILURE	0	HOLD FOR TAKEOFF CLEARANCE	690
HOLD FOR LANDING CLEARANCE	485		

FIGURE 62(e) (CONTINUED)

NOMINAL DEMONSTRATION CASE	MODES USED (PER CENT)						
	1	2	3	4	5	6	7
STATE ESTIMATION	100.0	0.2	0.1	0.0	0.0	0.0	0.0
AUTOMATIC NAVIGATION	2.0	0.0	0.0	0.0	0.0	0.0	0.0
APPROACH LANDING NAVIGATION	100.0	0.0	0.0	0.0	0.0	0.0	0.0
COMMAND GENERATION/EXECUTION	100.0	0.0	0.0	0.0	0.0	0.0	0.0
AUTOMATIC GUIDANCE/CONTROL	100.0	0.0	0.0	0.0	0.0	0.0	0.0
HAZARD AVOIDANCE	100.0	0.2	2.2	0.0	0.0	0.0	0.0
AUTOMATIC HAZARD AVOIDANCE	100.0	0.0	0.0	0.0	0.0	0.0	0.0
SYSTEM MANAGEMENT	100.0	0.2	0.0	0.0	0.0	0.0	0.0
AUTOMATIC SYSTEM MANAGEMENT	0.0	0.0	0.0	0.0	0.0	0.0	0.0
MANUAL SYSTEM MANAGEMENT	0.0	0.0	0.0	0.0	0.0	0.0	0.0
SAFE FLIGHT	100.0	0.0	0.0	0.0	0.0	0.0	0.0

FIGURE 62(F). (CONTINUED)

NOMINAL DEMONSTRATION CASE
 TOTALS FOR ALL TRIPS AND ALL LEGS
 STATISTICS FOR 300 MONTE CARLO TRIALS

	NO. SAMPLES	MEAN	STANDARD DEVIATION	MAXIMUM VALUE	MINIMUM VALUE	CONSTRAINT MAXIMUM	NUMBER OF VIOLATIONS	MINIMUM	NO.
EQUIPMENT REPAIR TIME (MIN)	184	3.78940E+01	6.24191E+01	3.51256E+02	8.69175E+01	1.20000E+02	10	1.50000E+01	68
FUEL LOADING TIME (MIN)	200	1.89432E+01	7.54700E+00	4.57525E+01	3.73932E+00	1.50000E+01	2184	1.00000E+01	494
PASSENGER LOADING TIME (MIN)	200	1.00042E+01	1.49202E+00	1.62725E+01	1.91444E+00	1.50000E+01	17	5.00000E+00	20
CARGO LOADING TIME (MIN)	200	1.08645E+01	1.97955E+00	1.40978E+01	2.68272E+00	1.50000E+01	15	5.00000E+00	19
GROUND SERVICE TIME (MIN)	200	2.05505E+01	9.28172E+00	1.11092E+02	8.65555E+00	2.00000E+01	2337	5.00000E+00	19
FUEL LOAD (LBS)	200	7.67853E+03	3.16974E+03	3.54103E+04	1.57473E+03	1.00000E+02	0	-1.00000E+02	0
INITIAL FUEL LOAD (LBS)	200	9.68933E+03	2.39843E+03	1.19918E+04	6.34643E+03	1.00000E+02	0	-1.00000E+02	0
INITIAL TAKEOFF WEIGHT (LBS)	200	1.09182E+05	2.39844E+03	1.10795E+05	1.05750E+05	1.00000E+02	0	-1.00000E+02	0
RATE DEPARTURE DELAY (MIN)	200	3.74747E+01	3.72560E+01	3.45846E+02	6.4E+01	1.00000E+02	2645	0.0E+00	0
TAKEOFF HOLD TIME (MIN)	1599	6.44573E+00	1.20057E+01	1.35500E+02	4.28511E+01	4.00000E+00	505	0.0E+00	0
TAKEOFF DELAY (MIN)	200	3.81720E+01	3.72560E+01	3.27572E+02	-3.10272E+00	1.00000E+01	2074	0.0E+00	288
TAKEOFF RUNWAY OCCUPANCY (SEC)	200	1.01248E+01	0.5E+00	1.81258E+02	1.01248E+01	1.00000E+01	0	-1.00000E+01	0
TAKEOFF RUNWAY OCCUPANCY (SEC)	200	5.12748E+00	0.4E+00	5.12748E+02	5.12748E+00	1.00000E+01	0	-1.00000E+01	0
LANDING HOLD TIME (MIN)	200	8.22484E+00	1.48344E+01	1.92000E+02	1.01248E+01	1.00000E+01	0	-1.00000E+01	0
LANDING TIME DELAY (MIN)	200	5.02943E+01	2.41747E+01	1.76000E+02	4.15712E+01	1.00000E+01	557	-1.00000E+01	0
MIN. RUNWAY OCCUPANCY (SEC)	200	3.94415E+01	3.72837E+01	1.443E+02	1.27472E+01	1.00000E+01	0	-1.00000E+01	0
MIN. RUNWAY OCCUPANCY (FT)	200	1.02908E+01	1.76002E+01	2.74446E+01	-1.47272E+01	1.00000E+01	2289	0.0E+00	357
LANDING RUNWAY OCCUPANCY (SEC)	200	4.91373E+02	2.42707E+02	2.74627E+03	-2.71181E+01	1.00000E+01	12	1.50000E+01	216
LANDING RUNWAY OCCUPANCY (FT)	200	4.57145E+01	4.76000E+01	1.37601E+02	1.52185E+01	6.00000E+01	972	3.00000E+01	637
RATE ARRIVAL DELAY (MIN)	200	2.74332E+01	1.59018E+01	4.99525E+01	1.56924E+01	1.00000E+01	0	-1.00000E+01	0
FUEL CONSUMED (LBS)	200	3.77471E+01	3.59740E+01	2.92201E+02	-1.68334E+01	0.0E+00	2518	-1.00000E+01	0
FUEL REMAINING (LBS)	200	7.39874E+01	3.17547E+01	4.82053E+03	-2.44185E+04	1.00000E+02	0	-1.00000E+02	0

STATISTICS FOR 300 MONTE CARLO TRIALS

EVENT	OCCURRENCES	EVENT	OCCURRENCES
STATE ESTIMATION LOST	0	COMMAND GENERATION LOST	0
HAZARD AVOIDANCE LOST	0	COMMUNICATION LOST	0
SYSTEM MANAGEMENT LOST	0	SAFE FLIGHT LOST	4
UN SCHEDULED LANDING	5	HARDWARE FAILURE	218
FAILURE IN SECTIONS 1-11	45	FAILURE IN SECTIONS 12-24	14
FAILURE IN SECTIONS 25-38	24	FAILURE IN SECTIONS 39-43	14
FAILURE IN SECTIONS 44-63	54	CANCELLED FLIGHT	1
RATE DEPARTURE	200	DISPATCH RELIABILITY	1.12
SCHEDULED FLIGHT TIME EXCEEDED	457	DIVERT TO ALTERNATE AIRPORT	0
MISSION ABORT	2	IFR WEATHER	60
MIS FAILURE	0	HOLD FOR TAKEOFF CLEARANCE	1599

FIGURE 62(g). (CONTINUED)

NOMINAL DEMONSTRATION CASE	MODES USED (PER CENT)							
	1	2	3	4	5	6	7	8
STATE ESTIMATION	100.0	0.0	0.0	0.0	0.0	0.0	0.0	0.0
AUTOMATIC NAVIGATION	100.0	0.0	0.0	0.0	0.0	0.0	0.0	0.0
APPROACH/LANDING NAVIGATION	2.1	0.0	0.0	0.0	0.0	0.0	0.0	0.0
COMMAND GENERATION/EXECUTION	100.0	0.0	0.0	0.0	0.0	0.0	0.0	0.0
AUTOMATIC GUIDANCE/CONTROL	100.0	0.0	0.0	0.0	0.0	0.0	0.0	0.0
WZARD AVOIDANCE	100.0	0.0	0.0	0.0	0.0	0.0	0.0	0.0
AUTOMATIC WZARD AVOIDANCE	100.0	0.0	1.9	0.0	0.0	0.0	0.0	0.0
COMMUNICATION	100.0	0.0	0.0	0.0	0.0	0.0	0.0	0.0
AUTOMATIC COMMUNICATION	100.0	0.0	0.0	0.0	0.0	0.0	0.0	0.0
SYSTEM MANAGEMENT	100.0	0.0	0.0	0.0	0.0	0.0	0.0	0.0
AUTOMATIC SYSTEM MANAGEMENT	0.0	0.0	0.0	0.0	0.0	0.0	0.0	0.0
MANUAL SYSTEM MANAGEMENT	0.0	0.0	0.0	0.0	0.0	0.0	0.0	0.0
SAFE FLIGHT	100.0	0.0	0.0	0.0	0.0	0.0	0.0	0.0
SAFE FLIGHT	100.0	0.0	0.0	0.0	0.0	0.0	0.0	0.0

FIGURE 62(h). (CONTINUED)

NOMINAL DEMONSTRATION CASE - NO. WINDS		TOTALS FOR ALL TRIES AND ALL LEGS		STATISTICS FOR 300 MANIF CARLO TRIALS					
		NO. SAMPLES	MEAN	STANDARD DEVIATION	MAXIMUM VALUE	MINIMUM VALUE	CONSTRAINT NUMBER	TIMES EXCEEDED	NO.
							MAXIMUM	MINIMUM	
EQUIPMENT REPAIR TIME (MIN)		164	3.8449E+01	6.7752E+02	5.6476E+02	9.8311E+01	1.2000E+02	0	55
FUEL LOADING TIME (MIN)		2875	1.9240E+01	7.6137E+00	9.9433E+01	2.7970E+00	1.5000E+01	162	494
PASSENGER BOARDING TIME (MIN)		2875	1.0001E+01	7.0522E+00	1.7224E+01	3.4013E+00	1.5000E+01	15	21
CARCO LOADING TIME (MIN)		2875	0.8939E+01	1.9954E+00	1.8464E+01	3.3139E+00	1.5000E+01	19	13
GROUND SERVICE TIME (MIN)		2871	2.9130E+01	9.4907E+00	1.1783E+02	1.0445E+01	2.0000E+01	2793	0
FUEL LOADED (LBS)		2875	7.8710E+03	3.1977E+03	4.1445E+04	1.1747E+03	1.0000E+02	0	0
INITIAL FUEL LOAD (LBS)		2875	9.6999E+03	2.3802E+03	1.1791E+04	6.3464E+03	1.0000E+02	0	0
INITIAL TAKEOFF WEIGHT (LBS)		2870	1.0914E+04	2.3796E+03	1.1775E+04	1.0775E+03	1.0000E+02	0	0
GATE DEPARTURE DELAY (MIN)		2870	3.6541E+01	3.9441E+01	1.1500E+02	6.2857E+01	1.0000E+01	1913	0
TAK-OFF HOLD TIME (MIN)		1491	6.0880E+00	1.2428E+01	1.1500E+02	4.2857E+01	1.0000E+01	456	0
TAK-OFF DELAY (MIN)		2870	3.7469E+01	3.9542E+01	3.8435E+02	-7.1102E+00	1.0000E+01	1825	367
TAK-OFF RUNWAY OCCUPANCY (SEC)		2870	1.0124E+01	0.4700	1.1126E+01	-7.1102E+00	1.0000E+01	0	0
TAK-OFF RUNWAY DISTANCE (FT)		2870	5.1274E+02	0.2200	5.1274E+02	1.0124E+01	1.0000E+02	0	0
LANDING HOLD TIME (MIN)		1448	8.5735E+00	1.5989E+01	2.3450E+02	5.1274E+02	1.0000E+02	0	0
TOTAL FLIGHT TIME (MIN)		2861	5.0294E+01	2.4327E+01	2.8031E+02	4.2857E+01	4.0000E+00	552	0
LANDING TIME DELAY (MIN)		2861	3.8009E+01	3.9969E+01	3.8502E+02	1.2364E+01	1.0000E+02	0	0
MIN. RUNWAY OCCUPANCY (SEC)		2861	1.0265E+01	3.2431E+02	1.8291E+01	-1.6755E+01	1.0000E+01	2822	440
MIN. RUNWAY OCCUPANCY (FT)		2861	8.7343E+02	4.4204E+02	8.7493E+02	1.0270E+01	1.0000E+02	0	0
LANDING RUNWAY OCCUPANCY (SEC)		2861	6.5552E+01	4.7595E+01	1.3259E+02	4.6724E+02	2.0000E+03	0	261
LANDING RUNWAY DISTANCE (FT)		2861	3.7297E+03	1.6033E+03	4.8958E+03	3.0815E+01	6.0000E+01	960	0
GATE ARRIVAL DELAY (MIN)		2861	3.3984E+01	1.6033E+03	4.8958E+03	1.5692E+03	1.0000E+02	256	0
FUEL CONSUMPTION (LBS)		2861	7.4829E+03	3.2099E+03	3.8703E+02	-1.8787E+03	0.2000	0	0
FUEL REPAIRING (LBS)		2861	2.2940E+03	1.8232E+03	5.1718E+03	-3.0454E+04	1.0000E+02	0	0

STATISTICS FOR 300 MANIF CARLO TRIALS		EVENT OCCURRENCES	
EVENT	OCCURRENCES	EVENT	OCCURRENCES
STATE ESTIMATION LOST	1	COMMAND GENERATION LOST	0
HAZARD AVOIDANCE LOST	0	COMMUNICATION LOST	0
SYSTEM MANAGEMENT LOST	0	SAFE FLIGHT LOST	10
UNSCHEMULED LANDING	9	HARDWARE FAILURE	184
FAILURE IN SECTIONS 1-11	49	FAILURE IN SECTIONS 11-20	12
FAILURE IN SECTIONS 21-33	16	FAILURE IN SECTIONS 31-40	62
FAILURE IN SECTIONS 41-53	45	CARC LLED FLIGHT	19
GATE DEPARTURE	2870	DISPATCH RELIABILITY	1149
SCHEDULED FLIGHT TIME EXCEEDED	780	DIVERT TO ALTERNATE AIRPORT	1
MISSED APPROACH	4	IFR WEATHER	75
WAS FAILURE	0	HOLD FOR TAKEOFF CLEARANCE	1591
HOLD FOR LANDING CLEARANCE	1448		

FIGURE 63(a). EXAMPLE OF STOL OPS RESULTS FOR NOMINAL DEMONSTRATION CASE WITH NO EN ROUTE WINDS

	MODES USED (PER CENT)							
	1	2	3	4	5	6	7	8
STATE ESTIMATION	100.0	0.0	0.0	0.0	0.0	0.0	0.0	0.0
AUTOMATIC NAVIGATION	100.0	0.0	0.0	0.0	0.0	0.0	0.0	0.0
APPROACH/LANDER NAVIGATION	2.6	0.0	0.0	0.0	0.0	0.0	0.0	0.0
COMMAND OPERATING/EXECUTION	100.0	0.0	0.0	0.0	0.0	0.0	0.0	0.0
AUTOMATIC GUIDANCE/CONTROL	100.0	0.0	0.0	0.0	0.0	0.0	0.0	0.0
HAZARD AVOIDANCE	100.0	0.1	1.3	0.1	0.0	0.0	0.0	0.0
AUTOMATIC HAZARD AVOIDANCE	100.0	0.0	0.0	0.0	0.0	0.0	0.0	0.0
COMMUNICATION	100.0	0.0	0.0	0.0	0.0	0.0	0.0	0.0
AUTOMATIC COMMUNICATION	100.0	0.0	0.0	0.0	0.0	0.0	0.0	0.0
SYSTEM MANAGEMENT	100.0	0.0	0.0	0.0	0.0	0.0	0.0	0.0
AUTOMATIC SYSTEM MANAGEMENT	0.0	0.0	0.0	0.0	0.0	0.0	0.0	0.0
MANUAL SYSTEM MANAGEMENT	0.0	0.0	0.0	0.0	0.0	0.0	0.0	0.0
SAFE FLIGHT	100.0	0.0	0.0	0.0	0.0	0.0	0.0	0.0

FIGURE 63(b) (CONTINUED)

NOMINAL DEMONSTRATION CASE - IFR WEATHER 100 PERCENT USE TIME
 TOTALS FOR ALL TRIPS AND ALL LEGS

STATISTICS FOR 3000 MONTE CARLO TRIALS

	NO. SAMPLES	MEAN	STANDARD DEVIATION	MAXIMUM VALUE	MINIMUM VALUE	CONSTRAINT MAXIMUM	NUMBER NO.	TIMES EXCEEDED	MINIMUM	NO.
EQUIPMENT DEPARTURE TIME (MIN)	151	3.35345E+01	4.71946E+01	3.42225E+02	4.42107E+00	1.20000E+02	7	1.50000E+01	50	
FUEL LOADING TIME (MIN)	2750	1.72729E+01	5.37508E+00	2.87935E+01	3.31663E+00	1.50000E+01	2069	1.00000E+01	630	
PASSENGER LOADING TIME (MIN)	2750	1.00513E+01	1.86529E+00	1.40457E+01	2.27478E+00	1.50000E+01	18	5.00000E+00	16	
CARGO LOADING TIME (MIN)	2750	1.00513E+01	2.01952E+00	1.76015E+01	2.61199E+00	1.50000E+01	21	5.00000E+00	16	
GROUND SERVICE TIME (MIN)	2748	2.02315E+01	4.51885E+00	1.18049E+02	9.85993E+00	2.00000E+01	2218	1.00000E+00	0	
FUEL LOADED (LBS)	2750	7.25443E+03	2.56948E+03	1.20933E+04	1.39298E+03	1.00000E+02	0	-1.00000E+20	0	
INITIAL FUEL LOAD (LBS)	2748	4.68004E+03	2.34716E+03	1.13718E+04	6.36633E+03	1.00000E+02	0	-1.00000E+20	0	
INITIAL TAKEOFF WEIGHT (LBS)	2748	1.09004E+05	2.38633E+03	1.10795E+05	1.66757E+04	1.00000E+02	0	-1.00000E+20	0	
GATE DEPARTURE DELAY (MIN)	2743	7.16552E+00	1.35798E+01	1.23675E+02	0.6.00	1.00000E+01	581	0.6.00	0	
TAKEOFF HOLD TIME (MIN)	620	2.23199E+00	1.26537E+00	9.20097E+00	1.76000E+00	4.00000E+00	578	-1.00000E+20	1231	
TAKEOFF DELAY (MIN)	2743	5.25976E+00	1.34506E+01	1.20573E+02	-3.18233E+00	1.00000E+01	512	-1.00000E+20	0	
TAKEOFF RUNWAY OCCUPANCY (SEC)	2743	1.01243E+01	6.8.00	1.11265E+01	1.01200E+01	1.00000E+02	0	-1.00000E+20	0	
TAKEOFF RUNWAY DISTANCE (FT)	2743	5.17246E+02	0.8.00	5.12766E+02	5.12766E+02	1.00000E+02	0	-1.00000E+20	0	
LANDING HOLD TIME (MIN)	2714	2.17328E+00	1.01441E+00	1.50000E+01	1.50000E+01	4.00000E+00	49	-1.00000E+20	0	
TOTAL FLIGHT TIME (MIN)	2714	4.72349E+01	1.85338E+01	4.66422E+01	1.5659E+01	1.00000E+02	0	-1.00000E+20	0	
LANDING TIME DELAY (MIN)	2714	2.86166E+00	1.43894E+01	1.10747E+02	-1.86601E+01	1.00000E+01	524	0.6.00	1595	
MIN. RUNWAY OCCUPANCY (SEC)	2714	1.03170E+01	1.63544E+00	2.14511E+01	7.95151E+01	1.00000E+02	0	-1.00000E+20	0	
MIN. RUNWAY DISTANCE (FT)	2714	4.93949E+02	2.35506E+02	3.12459E+03	2.87557E+01	2.00000E+03	17	1.50000E+03	2633	
LANDING RUNWAY OCCUPANCY (SEC)	2714	6.00136E+01	4.77665E+01	1.37346E+02	1.56494E+01	6.00000E+01	918	3.00000E+01	572	
LANDING RUNWAY DISTANCE (FT)	2714	2.77518E+01	1.59952E+03	4.95225E+03	1.56924E+03	1.00000E+02	0	-1.00000E+20	0	
GATE ARRIVAL DELAY (MIN)	2714	1.27842E+00	1.52900E+01	1.15077E+02	-1.97144E+01	0.6.00	994	0.6.00	0	
FUEL CONSUMED (LBS)	2714	8.92402E+03	2.38595E+04	1.20877E+04	2.22218E+03	1.00000E+02	0	-1.00000E+20	0	
FUEL REMAINING (LBS)	2714	2.70848E+03	7.58181E+02	8.93655E+03	-7.07531E+02	1.00000E+02	0	-1.00000E+20	0	

STATISTICS FOR 3000 MONTE CARLO TRIALS

EVENT	OCCURRENCES	FREQUENCY	OCCURRENCES
STATE ESTIMATION LOST	10	COMMAND GENERATION LOST	0
HAZARD AVOIDANCE LOST	6	COMMUNICATION LOST	0
SYSTEM MANAGEMENT LOST	6	SAFE FLIGHT LOST	9
UNSCHEDULED LANDING	12	HARDWARE FAILURE	173
FAILURE IN SECTIONS 1-10	52	FAILURE IN SECTIONS 11-20	20
FAILURE IN SECTIONS 21-30	21	FAILURE IN SECTIONS 31-40	47
FAILURE IN SECTIONS 41-50	43	CANCELLED FLIGHT	7
GATE DEPARTURE	2743	DISPATCH RELIABILITY	2316
SCHEDULED FLIGHT TIME EXCEEDED	507	DIVERT TO ALTERNATE AIRPORT	22
MISSED APPROACH	61	IFR PFAWHER	2736
MIS FAILURE	15	HOLD FOR TAKEOFF CLEARANCE	689
HOLD FOR LANDING CLEARANCE	517		

FIGURE 64. EXAMPLE OF STOL OPS RESULTS FOR NOMINAL DEMONSTRATION CASE ASSUMING 100% IFR (CATEGORY I OR WORSE) WEATHER

NOMINAL DEMONSTRATION CASE - IER WEATHER - 100 PERCENT OF TIME	MODES USED (PER CENT)							
	1	2	3	4	5	6	7	8
STATE ESTIMATION	100.0	0.0	0.0	0.0	0.0	0.0	0.0	0.0
AUTOMATIC NAVIGATION	98.0	0.0	0.0	0.0	0.0	0.0	0.0	0.0
APPROACH/ARRIVAL NAVIGATION	100.0	0.0	0.0	0.0	0.0	0.0	0.0	0.0
COMMAND VERIFICATION/EXECUTION	100.0	0.0	0.0	0.0	0.0	0.0	0.0	0.0
HAZARD AVOIDANCE	100.0	0.0	0.0	0.0	0.0	0.0	0.0	0.0
HAZARD AVOIDANCE	100.0	0.0	0.0	0.0	0.0	0.0	0.0	0.0
COMPENSATION	100.0	0.0	0.0	0.0	0.0	0.0	0.0	0.0
AUTOMATIC COMMUNICATION	100.0	0.0	0.0	0.0	0.0	0.0	0.0	0.0
SYSTEM MANAGEMENT	0.0	0.0	0.0	0.0	0.0	0.0	0.0	0.0
AUTOMATIC SYSTEM MANAGEMENT	0.0	0.0	0.0	0.0	0.0	0.0	0.0	0.0
MANUAL SYSTEM MANAGEMENT	0.0	0.0	0.0	0.0	0.0	0.0	0.0	0.0
SAFE FLIGHT	100.0	0.0	0.0	0.0	0.0	0.0	0.0	0.0
SAFE FLIGHT	100.0	0.0	0.0	0.0	0.0	0.0	0.0	0.0

FIGURE 64. (CONTINUED)

NOMINAL DEMONSTRATION CASES, SNA CAPACITY INCREASED TO 140 MOVEMENTS PER HOUR
 TOTALS FOR ALL TRIPS AND ALL LEGS

STATISTICS FOR 3:00 MONTE CARLO TRIALS

	NO. SAMPLES	MEAN	STANDARD DEVIATION	MAXIMUM VALUE	MINIMUM VALUE	COUNTING NUMBER TIMES EXCEEDED	MINIMUM	NO.
EQUIPMENT REPAIR TIME (MIN)	175	2.8779E+01	3.8503E+01	3.9140E+02	1.9107E+00	1.2000E+02	1.5000E+01	93
FUEL LOADING TIME (MIN)	2937	1.7199E+01	5.8420E+00	2.9149E+01	3.7552E+00	1.5000E+01	1.0000E+01	698
PASSENGER LOADING TIME (MIN)	2937	1.0044E+01	2.0394E+00	1.5059E+01	3.2272E+00	1.5000E+01	5.0000E+00	17
CARGO LOADING TIME (MIN)	2937	1.0004E+01	1.9334E+00	1.9173E+01	1.7247E+00	1.5000E+01	5.0010E+00	18
GROUND SERVICE TIME (MIN)	2935	2.8103E+01	4.2584E+01	1.1729E+02	1.0324E+01	2.0000E+01	5.0007E+00	0
FUEL LOAD (LBS)	2937	7.2231E+03	2.4530E+03	1.2242E+04	1.5472E+03	1.0000E+02	-1.0000E+20	0
INITIAL FUEL LOAD (LBS)	2935	9.7403E+03	2.3709E+03	1.1414E+04	6.3463E+03	1.0000E+02	-1.0000E+20	0
INITIAL TAKEOFF WEIGHT (LBS)	2935	1.0515E+04	2.3794E+03	1.1714E+04	1.2573E+03	1.0000E+02	-1.0000E+20	0
GATE DEPARTURE DELAY (MIN)	2935	6.2344E+00	1.1918E+01	9.4971E+01	0.5E+00	1.0000E+01	0.5E+00	0
TAKEOFF DELAY (MIN)	2439	1.8841E+00	1.9109E+00	1.2300E+01	5.5951E+01	1.0000E+00	-1.0000E+20	1128
TAKEOFF DELAY (MIN)	2435	4.8861E+00	1.1819E+01	9.5950E+01	3.1232E+00	1.0000E+01	0.5E+00	0
TAKEOFF RUNWAY OCCUPANCY (SEC)	2935	1.0124E+01	0.5E+00	1.1263E+01	1.0124E+01	1.0000E+02	-1.0000E+20	0
TAKEOFF RUNWAY DISTANCE (FT)	2935	5.1274E+02	0.5E+00	5.1274E+02	5.1274E+02	1.0000E+02	-1.0000E+20	0
LANDING HOLD TIME (MIN)	1480	1.9464E+00	2.1647E+00	2.3142E+01	4.2457E+01	4.0000E+00	-1.0000E+20	0
TOTAL FLIGHT TIME (MIN)	2925	4.5901E+01	1.0722E+01	6.6271E+01	1.1772E+01	1.0000E+02	-1.0000E+20	0
LANDING TIME (MIN)	2925	2.9420E+00	1.2443E+01	9.5212E+01	-1.1117E+01	1.0000E+01	0.5E+00	1493
MIN. RUNWAY OCCUPANCY (SEC)	2925	1.8324E+01	1.7484E+00	1.9730E+01	-8.3531E+01	1.0000E+02	-1.0000E+20	0
MIN. RUNWAY OCCUPANCY (FT)	2925	8.9743E+02	2.4550E+02	2.6123E+03	-2.9812E+01	2.0000E+03	1.5000E+03	2818
LANDING RUNWAY OCCUPANCY (SEC)	2925	6.5847E+01	4.7471E+01	1.3706E+02	1.5623E+01	6.0000E+01	3.0000E+01	804
LANDING RUNWAY DISTANCE (FT)	2925	2.7717E+03	1.5944E+03	4.9952E+03	1.5692E+03	1.0000E+02	-1.0000E+20	0
GATE ACTUAL DELAY (MIN)	2925	0.9830E+01	1.2404E+01	9.3361E+01	-1.9428E+01	0.5E+00	1073	0
FUEL CONSUMED (LBS)	2925	4.9377E+03	2.1105E+03	1.2237E+04	2.2540E+03	1.0000E+02	-1.0000E+20	0
FUEL REMAINING (LBS)	2925	2.7406E+03	6.1321E+02	4.4235E+03	-8.5687E+02	1.0000E+02	2.5000E+03	925

STATISTICS FOR 3:00 MONTE CARLO TRIALS

EVENT	OCCURRENCES	EVENT	OCCURRENCES
STAFF ESTIMATION LOST	1	COMMAND INFANTION LOST	0
FLIGHT MANAGEMENT LOST	0	COMMUNICATION LOST	0
SYSTEMS MANAGEMENT LOST	0	SAFE FLIGHT LOST	10
UNSCHEMULED LANDING	9	HARDWARE FAILURE	194
FAILURE IN SECTIONS 1-10	54	FAILURE IN SECTIONS 11-20	11
FAILURE IN SECTIONS 21-30	36	FAILURE IN SECTIONS 31-40	62
FAILURE IN SECTIONS 41-50	41	CANCELLED FLIGHT	5
GATE DEPARTURE	2935	DISPATCH DELIABILITY	2610
SCHEDULED FLIGHT TIME EXCEEDED	597	DIVERT TO ALTERNATE AIRPORT	1
MISSFO APPROACH	2	IFR WEATHER	65
MLS FAILURE	0	HOLD FOR TAKEOFF CLEARANCE	1685
HOLD FOR LANDING CLEARANCE	1488		

FIGURE 65. EXAMPLE OF STOL OPS RESULTS FOR DEMONSTRATION CASE WITH INCREASE OF SNA VFR CAPACITY TO 140 MOVEMENTS/HOUR

NOMINAL PENETRATION CASE. SNA CAPACITY INCREASED TO 140 MOVEMENTS PER HOUR

	MOVES USED (PER CENT)							
	1	2	3	4	5	6	7	8
STAT. ESTIMATION								
AUTOMATIC NAVIGATION	100.0	0.0	0.0	0.0	0.0	0.0	0.0	0.0
PERSONNEL/PILOTING NAVIGATION	0.0	0.0	0.0	0.0	0.0	0.0	0.0	0.0
COMMAND REFORMATION/EXECUTION	100.0	0.0	0.0	0.0	0.0	0.0	0.0	0.0
AUTOMATIC GUIDANCE/CONTROL	100.0	0.0	0.0	0.0	0.0	0.0	0.0	0.0
HAZARD AVOIDANCE								
AUTOMATIC HAZARD AVOIDANCE	100.0	0.0	1.6	0.2	0.0	0.0	0.0	0.0
COMMUNICATION								
AUTOMATIC COMMUNICATION	100.0	0.0	0.0	0.0	0.0	0.0	0.0	0.0
SYSTEM MANAGEMENT								
AUTOMATIC SYSTEM MANAGEMENT	100.0	0.0	0.0	0.0	0.0	0.0	0.0	0.0
MANUAL SYSTEM MANAGEMENT	0.0	0.0	0.0	0.0	0.0	0.0	0.0	0.0
SAFE FLIGHT	100.0							
SAFE FLIGHT								

FIGURE 65. (CONTINUED)

an increase in safe flight losses. This variation is acceptable for a Monte Carlo estimate. The probability of losing safe flight is approximately 10 out of 3000, or 0.003. Figure 3 shows that for $n/N = 0.05$, a factor of 10 larger than above, in excess of 20,000 samples are required for 5% accuracy of the result. A probability of 0.05 implies 150 occurrences out of 3000 totals. The 5% accuracy bound is then 18 occurrences. Thus, a variation of only 5 for 3000 totals and a probability of 0.003 is well within the expected Monte Carlo deviations.

The Monte Carlo results for each round trip and leg of that trip are presented in Appendix G for the cases summarized above.

Examples of Experiments Needed Based on Limited STOL OPS Applications.-

A wide variety of experiments are suggested as a result of the limited cases run. These include: substantiation of the many data values such as the steering time constants used in ANGCAP; Kalman updating using two VORTAC stations, either simultaneously or sequentially; the MLS acquisition operational procedure; etc. Experiments that might be required should not be fully designed without conducting extensive exercise cases of STOL OPS. STOL OPS results can serve as the initial conditions for many experiments. The results of the experiments should be presented in a format similar to STOL OPS results to permit easy comparison.

CONCLUDING REMARKS

The basic goals of this study have been met and exceeded in many cases. The STOL systems simulation model was developed, and computer programs collectively called STOL OPS have been written and checked out. A demonstration of STOL OPS and its use in evaluating STOL avionics configurations, air traffic control procedures, ground based navigation aids, and operational procedures was conducted.

Sample results from the demonstration runs are discussed in the preceding sections of this report. For the nominal run, 96.66% of the scheduled flights were flown. The dispatch reliability of about 34% is entirely unacceptable to an airline and this low value is due primarily to air traffic delays. As illustrated in Figure 62(g), the mean gate delay time is 37.67 minutes. The results indicate that increasing the capacity of SNA by 20 operations per hour as shown in Figure 65(a) reduce the mean gate departure delay to 6.23 minutes yielding an 87% dispatch reliability. In other words, a 16.5% increase in the number of operations per hour at a single airport in the route network results in greater than 250% increase in total dispatch reliability. An increase in the number of movements can come about if the separation between aircraft on the common path is decreased, because of improved navigation, guidance, and control accuracy, air traffic control equipment and procedures, or airport redesign. Definitive conclusions should not be drawn since only limited exercise cases have been run.

It is of interest to note from Figure 64 that for 3000 scheduled operations in instrument weather, 2743 or 91.4% were flown. Of these 2743, 22 were diverted to an alternate airport. Fifteen of these 22 diversions were due to MLS failure. Only 161 flights executed a missed approach; 22 of these were due to MLS failure and 139 to the deviations in final approach resulting in failure to acquire the MLS when it was operational using a 90 degree intercept at a 2-n.mi. common path for the MLS siting and coverage used. More definitive conclusions should not be made without extensive exercise cases being ran.

Finally, it is also of interest to note that the state estimation subfunction always operated in the automatic navigation subfunction Mode 1 with reversion to only Modes 2 and 3. The command generation/execution function always operated in the automatic subfunction (mode 1). Similar observations can be drawn by the reader for the other functions. In general, all data values need to be carefully reviewed and extensive exercise cases run with this and different scenarios prior to drawing definitive conclusions.

RECOMMENDATIONS

The set of computer programs that comprise STOL OPS provide the capability to perform detailed analyses of an externally blown flap STOL aircraft and various avionics configurations. These analyses should include:

- (1) Evaluation of avionics systems concepts
- (2) Evaluation of operation procedures
- (3) Synthesis of avionics system configurations for a variety of mission performance goals
- (4) Repeat of (1) through (3) above for differing operational environments.

A more detailed listing of suggested exercise cases which should be run is given in Table 18. These exercise cases could be conducted under an extension to this contract or at NASA Ames Research Center.

After application of STOL OPS to the suggested exercise cases, a large number of additional tasks should be performed. These tasks, including the exercise task, are listed in Table 19. It is very important that a technological forecast be performed. Results of this forecast of avionics technology would aid in assessing the feasibility of alternative system concepts, identifying potential technological developments and their associated risk, cost, and time required for development.

The demonstration cases whose results are presented herein have suggested that experiments should be designed to substantiate critical data values. These experiments range from the establishment of failure rate data collection and analysis to piloted simulations to determine the adequacy of (1) the time constants used for steering, and (2) the usefulness of the operational procedures such as changing heading as a function of either estimated along track position, time, or bearing to a VORTAC or waypoint, etc.

Additional mathematical models need to be developed to consider performance of all functions and improved models should be developed for models currently being used such as the capacity and weather models. Complete discussion of all tasks recommended in Table 19 is inappropriate until further discussions are held with NASA Ames Research Center concerning the priority of each of the recommended tasks.

TABLE 18. SUGGESTED EXERCISE CASES

-
1. Evaluate Effectiveness of Each Function's Modes
 2. Evaluate MLS Configuration G Siting and Acquisition Probability for Subfunctions/Modes (Single and Parallel Runway Operations)
 3. Evaluate Various Operational Procedures for
 - Fixed Time of Arrival
 - Variable Time of Arrival
 4. Evaluate Other Scenarios
 5. Evaluate Improved Utilization of Aircraft by Reduction of Ground Time and Using Fixed Time of Arrival
 6. Establish Avionics Requirements to Meet Variations in Mission Performance Goals
 7. Investigate by Sensitivity Analysis the Need for Improved Models of Final Approach
 8. Establish Needed Backup Modes for Each System Function in Terms of Reliability, Maintainability, Performance for Specified Mission Performance Goals, and Safety Levels for Each Flight Phase
 9. Investigate Sensitivity of Cross Track Deviations to Steering Time Constant
 10. Evaluate Reduced Constraints Impact and Establish Function Requirements
 - Route Width
 - Common Path Length
-

TABLE 19. SUGGESTED TASKS

-
1. Application of STOL OPS to Suggested Exercise Cases
 2. Perform Technological Forecast and Model Selected Systems
 3. Design Experiments to Substantiate Critical Data Value
 4. Develop and Incorporate Human Performance/Reliability Models
 5. Develop Optimum Reliability/Maintainability Allocation Model for Multimode System
 6. Develop and Incorporate Cost of Ownership/Benefit Model
 7. Synthesize 1980 STOL Avionics for CAT I, CAT II, and CAT III. Establish Systems Criteria for 1980 Mission Performance Goals
 8. Develop Additional State Sensor Error Models and Incorporate in Navigation, Guidance and Control Analysis Program
 9. Develop Augmentor Wing or RTOL Model
 10. Incorporate Various Guidance Law Models
 11. Investigate Alternative MLS Configurations Data Rates by Modeling Closed-Loop Final Approach with EBF
 12. Investigate Need for Surveillance Radar
-

REFERENCES

1. Hitt, Ellis F., Levin, Victor, Brown, Ronald A., et al., "Simulation and Effectiveness Evaluation of Integrated Avionics for Military Aircraft", AFAL TR-70-2, Volume 1.
2. "Study of Quiet Turbofan STOL Aircraft for Short-Haul Transportation", Phase 1 Report, Contract No. NAS2-6994, Douglas Aircraft Company, McDonnell Douglas Corporation, October 1972.
3. "A New Guidance System for Approach and Landing", Document No. DO-148, Prepared by SC 117, Radio Technical Commission for Aeronautics, December 18, 1970.
4. "Criteria for Approving Category I and II Landing Minima for FAR 121 Operations", Advisory Circular 120-129, Federal Aviation Administration, Department of Transportation, September 25, 1970.
5. "Federal Aviation Regulations", Volume VII, Part 121, Department of Transportation, Federal Aviation Administration, June 1970.
6. "Federal Aviation Regulations", Volume III, Part 25, Department of Transportation, Federal Aviation Administration, December 1969.
7. Brunk, H.D., An Introduction to Mathematical Statistics, Ginn and Company, New York, 1958.
8. Bryson, A.E., Jr., and Bobick, J.C., "Improved Navigation by Combining VOR/DME Information and Air Data," J. Aircraft, Vol. 9, No. 6, June 1972, pp. 420-426.
9. "Airline Proposed Applications of Area Navigation in the ATC System", Working Paper, Airline Area Navigation Subcommittee, December 20, 1971.
10. "STOL Traffic Environment and Operational Procedures", R-717, Final Report of Contract NAS 2-6437, Charles Stark Draper Laboratory, Massachusetts Institute of Technology, March 1972.
11. "The National Aviation System Plan, Ten Year Plan 1973 - 1982", 1000.27, Appendix 2, Department of Transportation, Federal Aviation Administration, March 1972.
12. "Report of Department of Transportation Air Traffic Control Advisory Committee", Volumes 1 and 2, Department of Transportation, December 1969.

13. VORTAC Listing, Federal Aviation Administration, NAFEC, 1970.
14. Cochran, J.W., "Air Navigation and Air Traffic Control Facility Performance and Availability(RIS: Sm6040-20)", Federal Aviation Administration, Airway Facilities Service, September 11, 1972.
15. Adams, H. W., "Reliability and Operational Economics of the Next Decade of Jet Transports", Douglas Aircraft Company, McDonnell Douglas Corporation, January 1968.
16. "En Route Air Traffic Control", Handbook 7110.9A, Department of Transportation, Federal Aviation Administration, Air Traffic Service, January 1, 1970.
17. "The National Aviation System Policy Summary", 1000.27, Appendix 1, Department of Transportation, Federal Aviation Administration, March 1972.
18. Carmack, D.L., "Crew Duties, Modes, and Function Study", IPIS-TN-71-4. AD740502, USAF Instrument Pilot Instructor School, Randolph Air Force Base, Texas 78148.
19. Moss, Richard W., et al, "Control of Avionic Subsystems: The Crew Station Management Problem", AFFDL-TR-72-75, AD 741945, Air Force Flight Dynamics Laboratory, 15 March 1972.

APPENDIX A

OPERATIONAL ENVIRONMENT

Airport Model

The airport model is designed to encompass a macroscopic view of an airport's airside activities. This view is similar to being in the cockpit of an aircraft as it performs the various tasks related to its airport airside operation.

General input information for the airport model includes such information as airport latitude, longitude, altitude, and controlled airspace radius as well as information that is needed to describe specific points of interest in the airport; e.g., runway end points, turnoff points, etc. Each of these points is designated by an x and y position relative to an origin (such as the control tower) with the positive x axis east and the positive y axis north.

The runway information includes specific information for each runway such as orientation, length, width, turnoff points, etc. Input data for a typical airport is shown in Figure A-1.

Before each Monte Carlo simulation, the incremental times needed to process the aircraft through segments of the airport are computed and stored for use in the Monte Carlo routine. In this manner, every airport event has a precalculated time associated with it (consisting of a nominal time plus possibly a random component) and the Monte Carlo routine need not compute the time each time the event is processed.

The model considers the following phases:

- (1) Landing
- (2) Taxi into gate area
- (3) Refuel
- (4) Cargo load/unload
- (5) Passenger enplanement
- (6) Taxi out to takeoff runway
- (7) Takeoff.

All airport service times are taken sequentially except cargo loading which is in parallel with refueling.

APPENDIX A

SAN JOSE

*** GENERAL INFORMATION ***

CONE NAME-SJF LATITUDE- 37 20 0.8 LONGITUDE-121 55 0.0 ALTITUDE(FT)- 570. CONTROLLED AIRSPACE RADIUS(NM)- 15.

REFERENCE POINT NO.	1	2	3	4	5	6	7	8	9	10	11	12	13	14	15	16	17	18	19	20	21	22	23	24	25	26	
DISTANCE EAST WRT TOWER	-1050.	-3150.	1050.	-1800.	-2100.	-250.	1588.	150.	-780.	-350.	-3500.	-250.	1500.	700.	700.	1500.	1500.	1500.	-1200.	-2700.	-2400.	-3700.	-3050.	-2400.	2250.	-3500.	
DISTANCE NORTH WRT TOWER	-200.	-400.	-200.	-700.	-1350.	-2850.	-2850.	-350.	-350.	-3500.	-250.	-250.	-150.	-150.	-150.	-150.	-4800.	-4800.	-1000.	-1000.	-1000.	-1000.	-1000.	-1000.	-1000.	-1000.	-1000.
REFERENCE POINT NO.	11	12	13	14	15	16	17	18	19	20	21	22	23	24	25	26	27	28	29	30	31	32	33	34	35	36	
DISTANCE EAST WRT TOWER	400.	-1500.	-500.	180.	700.	700.	1500.	1500.	1500.	1500.	1500.	1500.	1500.	1500.	1500.	1500.	1500.	1500.	1500.	1500.	1500.	1500.	1500.	1500.	1500.	1500.	
DISTANCE NORTH WRT TOWER	-1700.	-550.	-250.	-750.	-1250.	-1250.	-4800.	-4800.	-1000.	-1000.	-1000.	-1000.	-1000.	-1000.	-1000.	-1000.	-1000.	-1000.	-1000.	-1000.	-1000.	-1000.	-1000.	-1000.	-1000.	-1000.	

*** RUNWAY INFORMATION ***

RUNWAY NO. 1	HEADING(DEG)	290.	TAKEOFF CLIMB ALT.(FT)	1500.	TURNOFFS	1	2
REF. PT. 1	LEADING(FT)	3000.	GLIDE SLOPE(DEG)	7.	REFERENCE POINT	5	2
	WIDTH(FT)	40.	COMMON PATH(NM)	2.	TURNOFF VELOCITY(KTS)	20.	20.
RUNWAY NO. 2	HEADING(DEG)	110.	TAKEOFF CLIMB ALT.(FT)	1500.	TURNOFFS	1	2
REF. PT. 2	LEADING(FT)	3000.	GLIDE SLOPE(DEG)	7.	REFERENCE POINT	5	1
	WIDTH(FT)	40.	COMMON PATH(NM)	2.	TURNOFF VELOCITY(KTS)	20.	20.
RUNWAY NO. 3	HEADING(DEG)	300.	TAKEOFF CLIMB ALT.(FT)	1500.	TURNOFFS	1	2
REF. PT. 3	LEADING(FT)	4419.	GLIDE SLOPE(DEG)	7.	REFERENCE POINT	11	10
	WIDTH(FT)	150.	COMMON PATH(NM)	2.	TURNOFF VELOCITY(KTS)	20.	20.
RUNWAY NO. 4	HEADING(DEG)	120.	TAKEOFF CLIMB ALT.(FT)	1500.	TURNOFFS	1	2
REF. PT. 4	LEADING(FT)	4419.	GLIDE SLOPE(DEG)	7.	REFERENCE POINT	9	10
	WIDTH(FT)	150.	COMMON PATH(NM)	2.	TURNOFF VELOCITY(KTS)	20.	20.
RUNWAY NO. 5	HEADING(DEG)	120.	TAKEOFF CLIMB ALT.(FT)	1500.	TURNOFFS	1	2
REF. PT. 5	LEADING(FT)	4900.	GLIDE SLOPE(DEG)	7.	REFERENCE POINT	19	6
	WIDTH(FT)	150.	COMMON PATH(NM)	2.	TURNOFF VELOCITY(KTS)	20.	20.
RUNWAY NO. 6	HEADING(DEG)	300.	TAKEOFF CLIMB ALT.(FT)	1500.	TURNOFFS	1	2
REF. PT. 6	LEADING(FT)	4900.	GLIDE SLOPE(DEG)	7.	REFERENCE POINT	20	21
	WIDTH(FT)	150.	COMMON PATH(NM)	2.	TURNOFF VELOCITY(KTS)	20.	20.

*** MISCELLANEOUS INFORMATION ***

GATE REFERENCE POINT- 1A

TAXIRoute NO. TAXIRoute SEQUENCE

1	1- 6- 7- 16- 9- 5- 2-
2	3- 17- 18- 13- 12- 4- 20-
3	17- 18- 13- 11-
4	17- 26- 17- 16- 7- 8-
5	22- 24- 13- 16- 13- 23- 18-
6	19- 9- 16- 13- 12- 25- 21-

FIGURE A-1. INPUT DATA FOR A TYPICAL AIRPORT

Landing.-This phase of the model covers the aircraft's activities during runway occupancy. A constant deceleration of 10 ft/sec^2 is used to calculate runway distance required to slow down. Once it has been determined that the aircraft has reached a safe turnoff velocity, the aircraft is assumed to turn off onto the nearest taxiway. The distance and time from touchdown to turnoff is calculated for the aircraft.

Taxi Into Gate Area.-On the basis of the turnoff that is chosen, the taxi-in route describes the appropriate taxi path for the aircraft from airport configuration data. The aircraft is assumed to taxi in at a constant velocity.

Refuel.-This routine calculates the time taken to refuel the aircraft by dividing the pounds to be loaded by the fueling rate (lb/sec).

Passenger Enplanement.-This portion of the model calculates the time for passengers to board. A normal distribution with a 10-minute mean value and 2-minute deviation is used for passenger enplanement.

Cargo Load/Unload.-The cargo load phase calculates the time to load/unload baggage and freight. A normal distribution with a 10-minute mean value and a 2-minute deviation is used to determine cargo load time.

Taxi Out to Takeoff Runway.-This phase of the model calculates the time for the aircraft to taxi out to the takeoff runway by methods similar to those described in the taxi-in phase.

Takeoff.-The time incurred during takeoff is calculated here. This will be the runway occupancy time during takeoff.

Weather

At the present time, the probability of VFR weather is input as data. Data from the National Oceanic and Atmospheric Administration showed VFR weather occurring 97.8% of the time at Orange County. Because of lack of information for San Jose and Sacramento, this same value is used for all airports.

Winds aloft are modeled as time correlated, normal random processes. The input data required for both east and west winds are:

- (1) Mean wind
- (2) One-sigma deviation
- (3) Correlation time constant.

The winds are assumed to decrease linearly from the above values at 10,000-ft altitude to zero at the ground surface.

APPENDIX A

Traffic Forecast Development

Ideally the operational environment would be defined by forecasting the total short-haul-transportation-system demand and applying a modal split program to determine the short-haul-air-traffic demand. By utilizing data on the capacity of the aircraft which might serve this demand, estimated load factors, and flight characteristics of the aircraft serving this demand, it would be possible to specifically arrive at the STOL air traffic mix and density for the city pairs making up the route network. Since the operational environment includes not only STOL aircraft but other aircraft it is necessary to determine the aeronautical activity for the airports concern. There is a need to know:

- (1) The type of aircraft users (STOL and CTOL air carriers, scheduled air taxi, general aviation, and military services where applicable)
- (2) Types and volumes of operational activity (aircraft operations, passengers arriving and departing, based aircraft, etc.)
- (3) Aircraft mix (large capacity CTOL transports, STOL transports, smaller commercial, business, and pleasure aircraft).

With regard to the types of airport users, CTOL and STOL air carriers will, respectively refer to all conventional and short-takeoff-type scheduled commercial aircraft other than air taxis. Scheduled air taxis refer to aircraft operators for hire which engage in the scheduled transportation of passengers and/or property, and which generally operate small aircraft less than 12,500 pounds maximum takeoff weight. If desirable, the aircraft can be separated by weight and performance characteristics and included in the various other type categories. General aviation aircraft comprise the segment of civil aviation which encompasses all facets of aviation not mentioned above. These include:

- (1) Unscheduled air taxi services
- (2) Business, (corporate - executive transportation)
- (3) Commercial (aerial application - industrial - special)
- (4) Personal (recreation - flight proficiency)

Military aircraft refers to those aircraft of all the military services utilizing airports serving primarily civil aircraft.

APPENDIX A

Major types of operational activity that should be considered are:

- (1) Aircraft operations (movements)
- (2) Busy hours operation
- (3) Enplaning passengers
- (4) Enplaning and deplaning cargo
- (5) Based aircraft .

Aircraft operations include the total number of landings (arrivals) and takeoffs (departures) from an airport. Busy-hour operations are the total number of aircraft operations which occur at an airport's busiest hour, computed by averaging two adjacent busiest hours of a typically high activity day (ref. A-1). Data on enplaning passengers and air cargo and deplaning cargo can be used to determine ground facility requirements. These data are also of use in determining changes that will occur in aircraft operations due to the introduction of a new type of aircraft to the airport, such as one with a higher weight and capacity. It is assumed that over an extended period of time, the number of deplaning passengers will equal the enplaning ones. Data on based aircraft, which are the total number of active general aviation aircraft which use or may be expected to use an airport as "home base" would be needed if a determination of present or future ground facility requirements were desired.

In order to derive meaningful results from the simulation, at a minimum, the aircraft mix and density should be determined separately for scheduled and unscheduled operations and distributed as a function of time of day for the time period of interest. This would require forecasting the above data. Although such a forecast is outside the scope of work on this study, input data must be available for operation of the program. A preliminary forecast was therefore made for each of the three airports.

Development of 1980 Air Traffic Forecast for San Jose Municipal. - Reference A-2 includes a forecast of aircraft operations in 1980 in terms of itinerant operations for scheduled air carrier and general aviation as well as local operations for general aviation. Military operations, both itinerant and local, are included but are relatively small in number. The percent distribution of these operations by aircraft types is also forecast for 1980. Reference A-3 discussed the traffic distribution between the three San Francisco Bay Area airports. It also forecasts the growth patterns expected for the Bay Region. While a specific percentage of the Bay Region aircraft operations is not forecast for San Jose in 1980, the

APPENDIX A

projection of population for Santa Clara County indicates that it will contain the greatest population in 1980 with the largest percentage increases occurring from 1965 to 1980. These figures indicate that Santa Clara County, the location of San Jose Municipal, will contain over 25 percent of the Bay Area population. While SJC operations made up 5 percent of the total Bay Area traffic and Santa Clara County contained 21 percent of the population in 1966, it is felt that a conservative estimate of the total Bay Area air traffic to be handled by San Jose in 1980 is 15 percent. Reference A-2 reports that 525,000 annual scheduled air-carrier operations are forecast for the San Francisco hub in 1980. Fifteen percent of these operations is 78,750 annual operations at San Jose. On an average daily basis this is about 216. If the same percent distribution by air-carrier group is assumed to apply at all San Francisco Bay airports, then San Jose can be expected to have 79 operations daily with aircraft of over 200 seat capacity, 65 operations of aircraft having a capacity of 122 to 199 seats, and 66 operations by aircraft having 75 to 119 seats. The final air carrier operations would be 8 by aircraft possessing less than 54 seats. It is assumed that the 200 seat (and over) aircraft would be DC-10 or L-1011 type. It is assumed that the 120 to 199-seat-capacity aircraft would be 727 type aircraft. Since it is unlikely that the DC-9 and 737 types of aircraft will be retired by 1980, it is assumed that the 75 to 119 seat capacity aircraft consists of two-thirds DC-9 and 737 type and one-third 100 passenger STOL. The 54-seat (and under) aircraft which provide 8 operations daily at San Jose is assumed to be a DHC-7 type aircraft. The summation of itinerant and local operations by general aviation for the Bay Area equals 5,172,700 annually. In 1970, San Jose handled approximately 14 percent of the general-aviation traffic for the Bay Region. If it is assumed that no additional general aviation airports are built and that San Jose would handle the same percentage of the forecast traffic, the annual general aviation operations at San Jose in 1980 would be 755,595, while would yield a daily average of 2,070 operations. Present daily average operations at San Jose in the peak month are 1,333. Quite clearly the number of general aviation operations will lie somewhere between these two numbers, more likely at the lower end. For this reason, it is assumed that the general aviation operations total 1,364. If it is assumed that the percent distribution is the same as that forecast in reference A-2 for general aviation aircraft for the San Francisco hub, then 5.1 percent of the general aviation operations would be turbine powered and considered to be light twins. This yields 70 turbine-powered aircraft, with the remainder of the 1,364 being all other general-aviation aircraft. It is assumed that the number of general-aviation multiengine aircraft is the same percentage as is presently based at San Jose, i.e., 12 percent. This yields 155 operations by multiengine general-aviation aircraft, which would include those turbine powered. Quite obviously, these numbers are estimates and for the purpose

APPENDIX A

of this forecast, a total of 190 operations by light-twin general-aviation aircraft has been assumed. The balance of the 1,364 are light-single type. Figure A-2 shows the assumed mix and distribution by 5 aircraft types for San Jose in 1980. These numbers are quite subjective and should be considered tentative for the purpose of checking out the program.

Development of 1980 Air Traffic Forecast for Sacramento Executive. -

The forecast for Sacramento Executive, which is shown in Figure A-3, was arrived at by assuming that the aircraft operations for 1980 in the Sacramento hub, as reported in reference A-4, should be provided with air carrier operations divided between Sacramento Metropolitan, the present air carrier served site, and Sacramento Executive on an equal basis. This would provide 35,501 scheduled air carrier operations annually at Sacramento Executive. Assuming the same mix by aircraft types, there would be 7,029 annual operations by aircraft having 120 to 199 seat capacity, 25,951 operations by aircraft having 75 to 119 seat capacity, and 2,521 operations by aircraft having less than 54 seats capacity. This provides the daily average of 19 (120 to 199 seats), 71 (75 to 119 seats), and 7 (less than 54 seats). It is assumed that the capacities falling in the range of 75 to 119 seats are provided by the 46 DC-9 or 737 types of aircraft and 25 STOV aircraft. If the assumption is made that the summation of the itinerant and local general aviation operations is distributed equally on an annual basis between 11 airports in the Sacramento hub, 120,000 annual operations would be conducted at each airport. Reference A-3 indicates that 2.8 percent of these operations are forecast to be turbine-powered aircraft. If it is assumed that turbine-powered aircraft are multiengine, this would indicate 3,360 turbine powered aircraft operations annually at each site, with the remaining 116,640 by all other general aviation aircraft. Figure 8(a) indicates that 10 percent of the based general aviation aircraft at Sacramento Executive are currently multiengine. These multiengine aircraft would include the turbine-powered aircraft. Using this breakdown, 12,000 multiengine aircraft operations would occur on an annual basis and 108,000 single-engine aircraft operations. The annual traffic in 1970 is indicated to be 191,543 itinerant and local operations by general aviation as shown in Figure 8(a). Quite obviously, this number is higher than the number arrived at by taking the forecast for the Sacramento hub and distributing the operations across 11 airports. The peak month operations totaled 20,000 in 1970, as shown in Figure 8(a) for Sacramento Executive. Therefore, it was decided that the distribution of the operations across 11 airports was unrealistic, and it has been assumed that the total operations in 1980 would approximate those of the peak month in 1970, or about 240,000 annual operations by general-aviation aircraft. It was further assumed that 10 percent of these operations were provided by twin engine aircraft and 90 percent by single engine aircraft. Figure A-3 gives the mix and density of aircraft estimated for Sacramento Executive in 1980.

SJC DAILY SCHEDULE OF AIRCRAFT OPERATIONS
1980 TIME FRAME

HOUR OF DAY	DC-8		B-727		LIGHT TWIN		LIGHT SINGLE		STOL		HOURLY TOTAL
	TYPE		TYPE		TYPE		TYPE		TYPE		
6.00-6.59	0.		1.		12.		80.		0.		93.
7.00-7.59	3.		6.		12.		80.		3.		104.
8.00-8.59	7.		9.		12.		80.		4.		112.
9.00-9.59	8.		9.		12.		80.		4.		113.
10.00-10.59	1.		3.		12.		80.		1.		97.
11.00-11.59	7.		7.		12.		80.		2.		108.
12.00-12.59	1.		3.		12.		80.		0.		96.
13.00-13.59	3.		4.		12.		80.		1.		100.
14.00-14.59	2.		3.		12.		80.		0.		97.
15.00-15.59	3.		4.		12.		80.		0.		99.
16.00-16.59	4.		5.		12.		80.		1.		102.
17.00-17.59	8.		10.		12.		90.		3.		113.
18.00-18.59	4.		7.		12.		80.		4.		107.
19.00-19.59	5.		9.		11.		55.		4.		84.
20.00-20.59	8.		10.		10.		35.		2.		65.
21.00-21.59	8.		9.		9.		20.		1.		47.
22.00-22.59	6.		7.		8.		10.		0.		31.
23.00-23.59	0.		1.		6.		4.		0.		11.
DAILY TOTAL	78.		107.		200.		1164.		30.		1579.

APPENDIX A

CLASSIFICATION	APPROACH SPEED
DC-8 TYPE	OVER 119 KTS
B-727 TYPE	100 KTS - 119 KTS
LIGHT TWIN TYPE	80 KTS - 99 KTS
LIGHT SINGLE TYPE	UNDER 80 KTS
STOL TYPE	ALL STOL TRANSPORTS

FIGURE A-2. FORECAST OF 1980 DAILY AIR TRAFFIC OPERATIONS
BY TYPE AND TIME OF DAY FOR SAN JOSE MUNICIPAL (SJC)

SAC DAILY SCHEDULE OF AIRCRAFT OPERATIONS
1980 TIME FRAME

HOUR OF DAY	DC-8 TYPE	B-727 TYPE	LIGHT TWIN TYPE	LIGHT SINGLE TYPE	STOL TYPE	HOURLY TOTAL
6.00-6.59	0.	0.	4.	40.	0.	44.
7.00-7.59	0.	3.	4.	40.	0.	47.
8.00-8.59	0.	6.	4.	40.	5.	55.
9.00-9.59	0.	7.	4.	40.	4.	55.
10.00-10.59	0.	1.	4.	40.	1.	46.
11.00-11.59	0.	6.	4.	40.	2.	52.
12.00-12.59	0.	1.	4.	40.	0.	45.
13.00-13.59	0.	3.	4.	40.	1.	48.
14.00-14.59	0.	2.	4.	40.	1.	46.
15.00-15.59	0.	2.	4.	40.	0.	46.
16.00-16.59	0.	3.	4.	40.	1.	48.
17.00-17.59	0.	7.	4.	40.	3.	54.
18.00-18.59	0.	2.	4.	40.	5.	51.
19.00-19.59	0.	4.	4.	35.	4.	47.
20.00-20.59	0.	7.	4.	20.	4.	33.
21.00-21.59	0.	8.	2.	10.	2.	21.
22.00-22.59	0.	6.	2.	5.	1.	13.
23.00-23.59	0.	0.	2.	2.	0.	4.
DAILY TOTAL	0.	68.	66.	592.	29.	755.

APPENDIX A

CLASSIFICATION	APPROACH SPEED
DC-8 TYPE	OVER 119 KTS
R-727 TYPE	100 KTS - 119 KTS
LIGHT TWIN TYPE	80 KTS - 99 KTS
LIGHT SINGLE TYPE	UNDER 80 KTS
STOL TYPE	ALL STOL TRANSPORTS

FIGURE A-3. FORECAST OF 1980 DAILY AIR TRAFFIC OPERATIONS BY TYPE AND TIME OF DAY FOR SACRAMENTO EXECUTIVE (SAC)

APPENDIX A

Development of 1980 Air Traffic Forecast for Orange County. - Forecasting of the air traffic mix and density at Santa Ana (Orange County Airport) provides a similar choice among various alternatives. Air carrier operations were forecast in reference A-2 for the Los Angeles hub. This indicates a 161 percent increase in air carrier operations from 1970 to 1980. Presently, there are 707 weekly operations at Orange County (ref. A-5), which equals 101 daily operations. A 161 percent increase would yield 163 daily operations at Santa Ana in 1980. Alternatively, in 1970, 8.76 percent of the Los Angeles hub air-carrier operations were conducted at Orange County. The continued growth of the Los Angeles Metropolitan Area will be into the open land, which is toward San Diego, and eastward into the desert and northward. Population in the area around Orange County will increase, and it could be assumed that 10 percent of the Los Angeles hub of air-carrier operations might be conducted at Orange County in 1980. This would yield 185 daily operations. Reference A-6 states that "Orange County and Long Beach airport operations have only slightly increased over 1972 due to public resistance" in 1980. For this reason, it has been assumed that the air-carrier operations that could be provided by 727, 737 and DC-9 types of aircraft will remain close to the present number and that the primary additional operations will be provided by STOL. As indicated in Figure A-4, this yields 102, 727-type air carrier operations and 48 STOL-type operations daily.

General aviation operations can be estimated in a variety of manners. For the Los Angeles area hub, reference A-2 indicates a 229 percent increase for local general aviation from 1970 to 1980 and a 281 percent increase in itinerant general aviation operations from 1970 to 1980. Orange County had 261,446 annual local general-aviation operations in 1970 and 225,407 annual itinerant general-aviation operations for a total of 486,853 general aviation operations annually. The peak-month operations in 1970 were 51,000. If it is assumed that the above percentage increases apply across all airports for the Los Angeles area in 1980, 598,711 annual local general-aviation operations and 634,169 annual, itinerant general-aviation operations could be expected, yielding a total of 1,232,880 annual general-aviation operations in 1980 at Santa Ana. This would yield a daily number of 1,640 local and 1,737 itinerant, giving a sum of 3,377 general-aviation operations daily at Orange County. If it is assumed that the operations should be based upon the percent increase from the present peak month, 4,304 general-aviation operations would occur daily at Orange County in 1980. If one assumed that the operations should be based on an equal distribution between 19 Los Angeles area airports to be utilized by general aviation, the total Los Angeles local operations by general aviation in 1980 would be divided by 19 airports to yield 412,847 annual, local general aviation operations per airport in 1980. Similarly, 273,658 itinerant operations could be expected at each general-aviation airport giving a sum for the local and

SNA DAILY SCHEDULE OF AIRCRAFT OPERATIONS
1980 TIME FRAME

HOUR OF DAY	DC-8		B-727		LIGHT TWIN		LIGHT SINGLE		STOL	
	TYPE		TYPE		TYPE		TYPE		TYPE	
6:00-6:59	0		1		22		90		0	
7:00-7:59	0		6		22		90		4	
8:00-8:59	0		10		22		90		6	
9:00-9:59	0		9		22		90		5	
10:00-10:59	0		3		22		90		2	
11:00-11:59	0		5		22		90		3	
12:00-12:59	0		3		22		90		2	
13:00-13:59	0		4		22		90		1	
14:00-14:59	0		3		22		90		1	
15:00-15:59	0		4		22		90		1	
16:00-16:59	0		5		22		90		2	
17:00-17:59	0		9		22		90		4	
18:00-18:59	0		8		22		90		6	
19:00-19:59	0		10		15		80		5	
20:00-20:59	0		11		10		60		3	
21:00-21:59	0		8		5		40		2	
22:00-22:59	0		7		4		17		1	
23:00-23:59	0		1		3		10		0	

APPENDIX A

CLASSIFICATION	APPROACH SPEED
DC-8 TYPE	OVER 119 KTS
B-727 TYPE	100 KTS - 119 KTS
LIGHT TWIN TYPE	80 KTS - 99 KTS
LIGHT SINGLE TYPE	UNDER 80 KTS
STOL TYPE	ALL STOL TRANSPORTS

FIGURE A-4. FORECAST OF 1980 DAILY AIR TRAFFIC OPERATIONS BY TYPE AND TIME OF DAY FOR ORANGE COUNTY (SNA)

176

APPENDIX A

itinerant of 686,505 general-aviation operation. This yields 1,881 general-aviation operations daily. At Santa Ana, the present daily operations for the peak month would be 1,700. Obviously, the 1980 general-aviation operations at Orange County would then range somewhere from 1,700 to 4,304 daily. Since the possibility of changing the configuration of Orange County airport is quite limited (ref. A-7), it is suggested that the general aviation operations be based initially upon the present peak month, or 1,700 daily general-aviation operations.

APPENDIX A

Airport Capacity Model

A traffic mix model utilizing Poisson distribution queueing theory has been developed. This model is based on work done by Goldman (ref. A-8). The following data are required for each aircraft type, i :

- A_i = arrival rate (landings per unit time)
- D_i = departure rate (takeoffs per unit time)
- C_i = common path length used
- v_i = velocity while on the common path
- T_{Ai} = landing runway occupancy time
- T_{Di} = takeoff runway occupancy time .

In addition, a minimum separation distance, Δ , and separation time, T_s , must be specified. The mix model is used to compute a service rate S^s (operations per unit time).

$$S = 1.0 / \left(T_s + \sum_{i=1}^N \sum_{j=1}^N p_{ij} r_{ij} \right) \quad (A-1)$$

where

- p_{ij} = the probability an operation is of type j following an operation of type i , and
- r_{ij} = the minimum time allowed for an operation of type j to follow an operation of type i
- N = number of aircraft types .

Operation type indices i and j are used to denote aircraft types and landings or takeoffs:

- $1 \leq i \leq N$ denotes a type i landing, and
- $N + 1 \leq i \leq 2N$ denotes a type i takeoff.

A completely random uncorrelated traffic mix is assumed, thus

$$p_{ij} = p_i p_j \quad (A-2)$$

APPENDIX A

where P_i is the probability a single operation is of type i ,

$$P_i = A_i / \sum_{j=1}^N (A_j + D_j) \quad 1 \leq i \leq N, \text{ and}$$

$$P_i = D_{i-N} / \sum_{j=1}^N (A_j + D_j) \quad N+1 \leq i \leq 2N \quad (A-3)$$

The minimum time between operations is computed by

$$r_{ij} = \Delta v_i \quad , (v_i > v_j) \quad 1 \leq i \leq N, 1 \leq j \leq N$$

$$r_{ij} = \Delta / v_i + \text{Min}(C_i, C_j) \cdot \left(\frac{1}{v_i} - \frac{1}{v_j} \right), (v_i < v_j) \quad (\text{landing - landing})$$

$$r_{ij} = T_{Dj-N} \quad 1 \leq i \leq N, N+1 \leq j \leq 2N$$

$$\quad (\text{landing following takeoff})$$

$$r_{ij} = T_{Aj} \quad N+1 \leq i \leq 2N, 1 \leq j \leq N$$

$$\quad (\text{takeoff following landing})$$

$$r_{ij} = T_{Di-N} \quad N+1 \leq i < 2N, n+1 \leq j \leq 2N$$

$$\quad (\text{takeoff - takeoff}) \quad (A-4)$$

With the service rate known, the queue load factor F may be computed as:

$$F = \frac{\sum_{i=1}^N (A_i + D_i)}{S} \quad (A-5)$$

where F is the ratio of total demand rate to total service rate. The mean waiting time, W , is the same for all types sharing the same runway,

$$W = \frac{F}{(1-F)S} \quad (A-6)$$

The above model has been implemented as a separate FORTRAN computer program.

Capacity Model Computer Code. - Sample output of the capacity model is shown in Figure A-5(a) and (b). The data required is shown at the top of

SNA TRAFFIC MIX MODEL

A/C TYPE	LANDINGS/HOUR	VELOCITY	CRUISE PATH	OCC.TIME	TAKEOFFS/HOUR	OCC.TIME	OPERATIONS/HOUR	AUNWAY
VFR	IFR	TKNOT	(NM)	(MIN)	VFR	(MIN)	VFR	IFR
1 STOL	3.00	80.00	1.00	0.25	3.00	0.30	6.00	SHORT
2 LIGHT SING	11.00	70.00	3.00	0.25	11.00	0.30	90.00	SHORT
3 LIGHT TWIN	11.00	90.00	4.00	0.33	11.00	0.67	22.00	LONG
4 9-727	5.00	110.00	5.00	0.50	5.00	1.00	10.00	LONG
TOTAL	30.00				30.00		128.00	60.00
MINIMUM SEPARATION (NM)	1.00	3.00						
SAFETY MARGIN (MIN)	0.75	0.50						

SERVICE (LAND. ONLY/HOUR)	LOAD FACTOR	MEAN WAIT TIME (MINUTES)
VFR	VFR	VFR
SHORT ONLY	0.66036	0.6921
LONG ONLY	0.25519	0.6433
COMBINED	1.20544	0.9979999999
S: 37(LONG)	0.47419	0.48114

SERVICE (T.OFF ONLY/HOUR)	LOAD FACTOR	MEAN WAIT TIME (MINUTES)
VFR	VFR	VFR
SHORT ONLY	0.44000	0.1657
LONG ONLY	0.27228	0.33895
COMBINED	0.71228	0.52562
SHORT(LONG)	0.31609	0.13182

SERVICE (L/TO MIXED/HOUR)	LOAD FACTOR	MEAN WAIT TIME (MINUTES)
VFR	VFR	VFR
SHORT ONLY	1.08018	0.62026
LONG ONLY	0.48456	0.77063
COMBINED	1.59975	1.39628
SHORT(LONG)	0.76104	0.51622

SERVICE (LAND. ONLY/HOUR)	LOAD FACTOR	MEAN WAIT TIME (MINUTES)
VFR	VFR	VFR
SHORT ONLY	0.87745	0.69007
LONG ONLY	0.25518	0.64331
COMBINED	1.20270	1.33767
SHORT(LONG)	0.47346	0.3012

SERVICE (T.OFF ONLY/HOUR)	LOAD FACTOR	MEAN WAIT TIME (MINUTES)
VFR	VFR	VFR
SHORT ONLY	0.44000	0.18667
LONG ONLY	0.27228	0.33895
COMBINED	0.71228	0.52562
SHORT(LONG)	0.31609	0.13182

APPENDIX A

FIGURE A-5(a). EXAMPLE OF CAPACITY MODEL RESULTS FOR SIA

	SERVICE (L/TO MIXED/HOUR)		LOAD FACTOR		MEAN WAIT TIME (MINUTES)	
	VFR	IFR	VFR	IFR	VFR	IFR
SHORT ONLY	89.0	45.2	1.07892	0.61920	99.999999	2.16
LONG ONLY	66.0	41.1	0.48456	0.77863	6.83	5.14
COMBINED	80.1	43.0	1.55843	1.39498	99999999.99	99999999.99
SHORT (LONG)	123.0	54.3	0.76038	0.51549	1.73	1.18

STOL COMMON PATH CHANGED TO 1.5 NM

	SERVICE (LAND. ONLY/HOUR)		LOAD FACTOR		MEAN WAIT TIME (MINUTES)	
	VFR	IFR	VFR	IFR	VFR	IFR
SHORT ONLY	54.4	20.2	0.86247	0.69429	0.12	6.76
LONG ONLY	62.7	24.9	0.25318	0.64331	0.33	4.35
COMBINED	53.0	22.5	1.26818	1.33287	99999999.99	99999999.99
SHORT (LONG)	101.1	29.0	0.47492	0.48216	0.54	1.92

	SERVICE (T.OFF ONLY/HOUR)		LOAD FACTOR		MEAN WAIT TIME (MINUTES)	
	VFR	IFR	VFR	IFR	VFR	IFR
SHORT ONLY	109.1	75.0	0.44000	0.18667	0.43	0.18
LONG ONLY	58.8	47.2	0.27228	0.33895	0.38	0.95
COMBINED	89.9	57.1	0.71228	0.52562	1.65	1.16
SHORT (LONG)	151.9	106.2	0.31609	0.13182	0.18	0.09

	SERVICE (L/TO MIXED/HOUR)		LOAD FACTOR		MEAN WAIT TIME (MINUTES)	
	VFR	IFR	VFR	IFR	VFR	IFR
SHORT ONLY	88.8	45.1	1.08143	0.62131	99999999.99	2.18
LONG ONLY	66.0	41.1	0.48456	0.77863	0.85	5.14
COMBINED	79.9	42.9	1.60167	1.39758	99999999.99	99999999.99
SHORT (LONG)	122.8	54.2	0.78170	0.51695	1.75	1.19

STOL COMMON PATH CHANGED TO 2.0 NM

	SERVICE (LAND. ONLY/HOUR)		LOAD FACTOR		MEAN WAIT TIME (MINUTES)	
	VFR	IFR	VFR	IFR	VFR	IFR
SHORT ONLY	54.2	20.1	0.88518	0.69639	0.55	6.95
LONG ONLY	62.7	24.9	0.25318	0.64331	0.33	4.35
COMBINED	52.9	22.5	1.21542	1.33547	99999999.99	99999999.99
SHORT (LONG)	100.9	29.0	0.47544	0.48317	0.54	1.94

	SERVICE (T.OFF ONLY/HOUR)		LOAD FACTOR		MEAN WAIT TIME (MINUTES)	
	VFR	IFR	VFR	IFR	VFR	IFR
SHORT ONLY	109.1	75.0	0.44000	0.18667	0.43	0.18
LONG ONLY	58.8	47.2	0.27228	0.33895	0.38	0.95
COMBINED	89.9	57.1	0.71228	0.52562	1.65	1.16
SHORT (LONG)	151.9	106.2	0.31609	0.13182	0.18	0.09

	SERVICE (L/TO MIXED/HOUR)		LOAD FACTOR		MEAN WAIT TIME (MINUTES)	
	VFR	IFR	VFR	IFR	VFR	IFR
SHORT ONLY	88.7	45.0	1.08249	0.62236	99999999.99	2.20
LONG ONLY	66.0	41.0	0.48456	0.77863	0.85	5.14
COMBINED	79.9	42.9	1.60239	1.39887	99999999.99	99999999.99
SHORT (LONG)	122.7	54.1	0.78235	0.51768	1.76	1.19

FIGURE A-5(b) (Continued)

C3

APPENDIX A

Figure A-5(a). The model has the capability of analyzing up to ten aircraft types. In the example shown, four types are considered. For each type of aircraft, VFR and IFR demand rates for landings and takeoff are required. For landings, additional information describing approach velocity, common-path usage, and runway-occupancy time are required. For takeoffs, it was assumed that turns after leaving the runway eliminate the need for considering common path conflict. Thus, the only additional takeoff information is the runway occupancy time. In addition, short and long runways are considered, and the appropriate runway length must be indicated for each aircraft type. The minimum separation distance and time requirements are also treated as two distinct values for IFR and VFR conditions in this model. The safety margin is a time interval to allow for growth of dispersion in the along-track position after clearance for landing is given. Since STOL aircraft are of particular interest in this model, the subroutines are written to allow repeated evaluations of the data with changes being made to the STOL common path length. Thus, Figure A-5 (a and b) includes results for STOL common paths from .5 n.mi. to 2 n.mi. in addition to the 1 n.mi. specified in the data at the top of Figure A-5(a). For each STOL common-path assumptions, three blocks of output are produced. These blocks show the service rates, load factors, and mean waiting times for an aircraft assuming that separate runways are available for landings and takeoff or that landings and takeoffs are mixed on the same runway. Within each block, queueing statistics are shown for short and long runways, assuming that the traffic is dispersed between the two runways as indicated in the data. A third line shows the statistics if all operations (short and long) are combined on the long runway. The fourth and final line of each block gives the statistics for the following assumptions:

- (1) All aircraft indicated long use the long runway
- (2) Aircraft indicated as short will use the short runway, and if the long runway is not in use, it will also be used for short runway traffic.

Each line in the output shows, separately for VFR and IFR conditions, the service rate in operations per hour, the load factor (arrival rate over service rate), and the mean waiting time in minutes. If the arrival rate is equal to or greater than the service rate, an infinite queue and infinite waiting time result. These conditions are shown by 999999.99 in the output.

This model may be interpreted in the following way. Consider, for example, the output at the top of Figure A-5(a) (STOL common path equals

APPENDIX A

1 n.mi.) for a STOL aircraft arriving to make a landing with four runways in operation, one each for landing, takeoff, short, and long. Under VFR conditions the mean waiting time would be 8.1 minutes. Under IFR conditions the mean waiting time would be 6.67 minutes. It should be noted that the increased waiting time during visual conditions is due to the higher traffic specified in the data (64 landings per hour rather than 30 landings per hour). This increased traffic during visual conditions results in a longer mean waiting time even though the service rate increases from 20.2 landings per hour to 54.5 landings per hour. At the other extreme, consider the case of landings and takeoffs mixed on the same runway which is handling both short- and long-runway aircraft. Under visual conditions, the combined service rate is 80 operations per hour, while under IFR conditions, it is 43 operations per hour. These are both less than the arrival rates (128 and 60) and result in infinite queues.

The impact of STOL common path length requirements may be investigated using this model. Consider landings only using a short runway, mean waiting time under instrument conditions for a common path length of .5 n.mi. is 6.58 minutes. If the STOL common path length is increased to 2 n.mi, the mean waiting time increases to 6.85 minutes as shown at the bottom of Figure A-5(b).

The Monte Carlo analysis program requires a load factor and service rate under instrument and visual conditions for each airport. These numbers may be extracted from output such as shown in Figure A-5 from the appropriate aircraft operating policies (mixing traffic on runways and data chosen for the appropriate time of day. The results shown in this sample output were taken from forecasts of traffic for the 1980 period during the peak hours of 8:00 to 9:00 a.m.

APPENDIX A

References

- A-1 "Planning the Metropolitan Airport System", AC 150/5070-5, Federal Aviation Administration and Airport Operations Council International, May 1970.
- A-2 "Aviation Demand & Airport Facility Requirement Forecasts for Large Air Transportation Hubs Through 1980", AD 684811, Federal Aviation Administration, Department of Transportation, August 1967.
- A-3 "STOL Passenger Demand Potential in the San Francisco Bay Area 1970-1980", STOL Study, Report No. CI-804-SD-1098, Douglas Aircraft Company, January 1969.
- A-4 "Aviation Demand & Airport Facility Requirements for Medium Air Transportation Hubs Through 1980", Federal Aviation Administration, Airports Service, Department of Transportation, January 1968.
- A-5 Official Airline Guide, North American Edition, Vol. 16, No. 22, Part One, November 15, 1972.
- A-6 "Study of Quiet Turbofan STOL Aircraft for Short-Haul Transportation", Phase 1 Report, Contract No. NAS 2-6994, Douglas Aircraft Company, McDonnell Douglas Corporation, October 1972.
- A-7 "A Program Definition Study for Improvement of Short-Haul Air Transportation", Volume II: Working Papers, Section 2, Airport Development Requirements.
- A-8 Goldman, A. J., "Analysis of a Capacity Concept for Runway and Final Approach Path Airspace", Proceedings of the ION National Air Meeting on Air Traffic Control in the 1970's, 14-16 April 1970, The Institute of Navigation.

APPENDIX B

POWERED LIFT STOL PERFORMANCE MODEL

Nomenclature

The following nomenclature is used in the program listings, equations, and discussion of input data for subroutine ARCFT.

<u>FORTTRAN Name</u>	<u>Equation Symbol</u>	<u>Definition</u>
AFC	C_X	Net axial force coefficient
ALFA		Angle of attack, degrees
ALFL11		Angle of attack, degrees, from Table B-11
ALFT13		Angle of attack, degrees, from Table B-13
ALFT14		Angle of attack, degrees, in Table B-14
ALF12		Angle of attack, degrees, in Table B-12
C	C	Speed of sound, feet per second
CD	C_D	Total drag coefficient
CDO	C_{D_0}	Profile drag coefficient
CD4		Input values of C_{D_0} for Table B-4
CD5		Input values of K_1 for Table B-5
CD6		Input values of K_2 for Table B-6
CL	C_L	Lift coefficient
CLMAX		Maximum lift coefficient
CLR	$C_{L_{Roll}}$	Lift coefficient during takeoff roll
CLR19		Input values of $C_{L_{Roll}}$ for Table B-19
CL1		Maximum C_L input values for Table B-1
CL11		Input values of C_L for Table B-11
CL13		Input values of C_L for Table B-13

APPENDIX B

<u>FORTTRAN</u> <u>Name</u>	<u>Equation</u> <u>Symbol</u>	<u>Definition</u>
CL15		Input values of C_L for Table B-15
CL16		Input values of C_L for Table B-16
CMU	C_μ	Gross thrust coefficient
CMUM		Maximum value of gross thrust coefficient
CMU11		Input values of C_μ for Table B-11
CMU12		Input values of C_μ for Table B-12
CMU13		Input values of C_μ for Table B-13
CMU14		Input values of C_μ for Table B-14
CMU15		Input values of C_μ for Table B-15
CMU19		Input values of C_μ for Table B-19
CMZ	C_{μ_0}	Ram drag coefficient
CM10	(C_{μ_0}/C_μ)	Input values for ratio of ram drag coefficient to gross thrust coefficient for Table B-10
CX	C_X	Net axial force coefficient
CZCM	(C_{μ_0}/C_μ)	Output ratio from Table B-16
DCDH	dC/dH	Gradient of speed of sound with altitude, sec^{-1}
DEL	δ	Atmospheric pressure ratio
DSDH	dS/dH	Gradient of density ratio with altitude, ft^{-1}
---	EAS	Equivalent airspeed, knots
FG	FG	Gross thrust, lb
FGMIN	$F_{G\text{MIN}}$	Minimum value of gross thrust, lb
FL12	$(C_D - C_{\mu_0})$	Gross axial force coefficient from Table B-12
FN	F_N	Net thrust, lb

APPENDIX B

<u>FORTTRAN</u> <u>Name</u>	<u>Equation</u> <u>Symbol</u>	<u>Definition</u>
FNMAX	$F_{N_{MAX}}$	Maximum value of net thrust, lb
FNMIN	$F_{N_{MIN}}$	Minimum value of net thrust, lb
FN2		Output $F_{N_{MAX}}$ from Table B-2, lb
FN3		Output $F_{N_{MIN}}$ from Table B-3, lb
FN7	F_N/δ	Normalized net thrust input values to Table B-7
FS	F_S	Excess thrust error in iteration process, lb
FT14	$(C_D - C_{\mu_0})$	Gross axial force coefficient output of Table B-14
FXS	F_{XS}	Excess thrust, lb
FXSR	$F_{XS_{REQ}}$	Required value of excess thrust to fly profile, lb
F8		Maximum gross thrust input values to Table B-8, lb
F9		Minimum gross thrust input values to Table B-9, lb
G AFC	$(C_D - C_{\mu_0})$	Gross axial force coefficient
GAM	γ	Flight path angle, positive for climb, radians
GLIM		Limiting acceptable takeoff acceleration, g's
H2		Altitude input values to Table B-2, ft
IF		Flap position indicator, integer
ICL		Indicator for C_L exceedance, integer
K1	K_1	$\partial C_D / \partial C_L$
K2	K_2	$\partial C_D / \partial C_L^2$
M	M	Mach number
MI		Flight mode indicator, integer
M1		Mach number values for input to Table B-1
M2		Mach number values for input to Table B-2

APPENDIX B

M4		Mach number values for input to Table B-4
M7		Mach number values for input to Table B-7
PHI	φ	Bank angle, in radians
Q	Q	Dynamic pressure, lb/ft ²
RHO	ρ	Atmospheric density, slugs/ft ³
S	S	Wing area, ft ²
SIGMA	σ	Atmospheric density ratio
TP	$\sqrt{\theta}$	Square root of absolute temperature ratio
V	V	True airspeed, ft/sec
VDOT	\dot{V}	Rate of change of true airspeed, ft/sec ²
VWDOT	\dot{V}_W	Head-on component of wind gradient, ft/sec ²
V8		True airspeed input values for Table B-8
V9		True airspeed input values for Table B-9
V10		True airspeed input values for Table B-10
W	W	Aircraft gross weight, lb
WDOT	\dot{W}	Fuel flow, lb/hr
WDT	$\frac{\dot{W}}{\delta\sqrt{\theta}}$	Normalized fuel flow input values for Table B-7
---	\dot{W}_N	Normalized fuel flow output of Table B-7

Description

The powered-lift STOL performance model, subroutine ARCFT, is designed to be used as a subprogram to an integration routine for the purpose of generating flight profiles which reflect the performance capability of the aircraft.

The argument list for calling ARCFT is H, V, W, PHI, IF, GAM, VWDOT, VDOT, WDOT, MI. Of these, H, V, W, PHI, IF, VWDOT, and MI are always specified. In addition, GAM may be specified, depending upon the selection of the flight mode indicator, MI, as explained below.

APPENDIX B

The output variables from ARCFT are always VDOT and WDOT. GAM is also an output variable for certain values of MI.

The flap position indicator, IF, is an input integer which denotes one of three possible flap deflections:

IF = 0, flaps up
IF = 1, takeoff flap setting
IF = 2, landing flap setting.

The flight mode indicator, MI, is an assigned integer which specifies one of nine possible operating modes. These are:

MI = 1, maximum thrust with prescribed GAM
MI = 2, maximum thrust climb at constant equivalent
airspeed (EAS)
MI = 3, maximum thrust climb at constant Mach number
MI = 4, minimum thrust with prescribed GAM
MI = 5, minimum thrust descent at constant EAS
MI = 6, minimum thrust descent at constant Mach number
MI = 7, constant EAS on prescribed GAM
MI = 8, constant Mach number on prescribed GAM
MI = 9, takeoff roll.

Any segment of a desired flight profile can be computed using the appropriate operating mode. The following paragraphs describe the manner in which each mode can be used.

If MI = 1 is selected, maximum thrust is determined from stored data as a function of Mach number and altitude and used to accelerate the aircraft along the selected flight path angle. MI = 4 is similar, except that minimum thrust is implied. A special feature has been incorporated into the routine when MI = 4 has been selected and the flaps are deflected (IF = 1 or 2) because of the interrelationship which exists between engine thrust and lift for powered-lift aircraft. If the maximum lift coefficient is insufficient at minimum thrust, additional engine thrust, up to the maximum value, is automatically provided to maintain flight.

If MI = 2 or 3 is selected, maximum available thrust is used while the equivalent airspeed (EAS) or Mach number, respectively, is held constant. In these cases, the flight path angle, GAM, is not specified, but becomes an output variable. The use of MI = 5 or 6 is similar except that minimum thrust is employed.

Setting MI = 7 or 8 implies flight at constant EAS or Mach number, respectively, at a specified flight path angle (which can be zero for level cruise). If the desired path angle is beyond the performance

APPENDIX B

capability of the aircraft, the specified flight path angle is disregarded and maximum performance is computed.

If the ground roll during takeoff is to be computed, MI = 9 is selected. In this case, the fuel flow and acceleration are computed and a check is made to determine whether the aircraft has reached sufficient airspeed for lift-off. If the aircraft cannot become airborne, GAM = 0 is returned. If takeoff speed has been reached, a small nonzero value of GAM is returned as an indicator that another mode should be selected to compute the initial climb. For passenger comfort, it may be desirable to constrain the takeoff acceleration. Consequently, the full-thrust acceleration is disregarded if the input quantity GLIM is exceeded, and the value of GLIM, in g's, is used instead.

As mentioned previously, the flap configuration is determined by the value of the integer, IF. If the flaps are extended (IF = 1 or 2), the use of either MI = 7 or 8 will both result in flight at constant EAS at the specified flight path angle, if within the aircraft's capability. In this case, iteration on angle of attack and engine thrust is required to satisfy the lift coefficient and net axial force requirements for equilibrium. This iteration is automatically performed internally in the routine.

Each time ARCFT is called, a check is made to insure that the required lift coefficient is within the capabilities of the aircraft for the flap position selected. If this condition is not satisfied, the run is aborted.

A flow chart which illustrates the computational logic of ARCFT is presented in Figure B-1*. It may be seen that ARCFT calls another subroutine, ATMS, to provide atmospheric parameters, and two external functions, FULFLO and AFC. Flow charts for these auxiliary routines are presented in Figures B-2*, B-3*, and B-4*, respectively.

FULFLO computes the instantaneous rate of change of weight due to fuel consumption as a function of net thrust, MACH number, atmospheric pressure ratio, and atmospheric temperature ratio.

AFC computes the net axial force coefficient, with flaps in either takeoff or landing configuration, as a function of lift coefficient, gross thrust coefficient, and ram drag coefficient.

* Tables mentioned with flow charts (Figures B-1 through B-4), while not having prefix B-, numerically correspond to those in this appendix, i.e., B-1, etc.

APPENDIX B

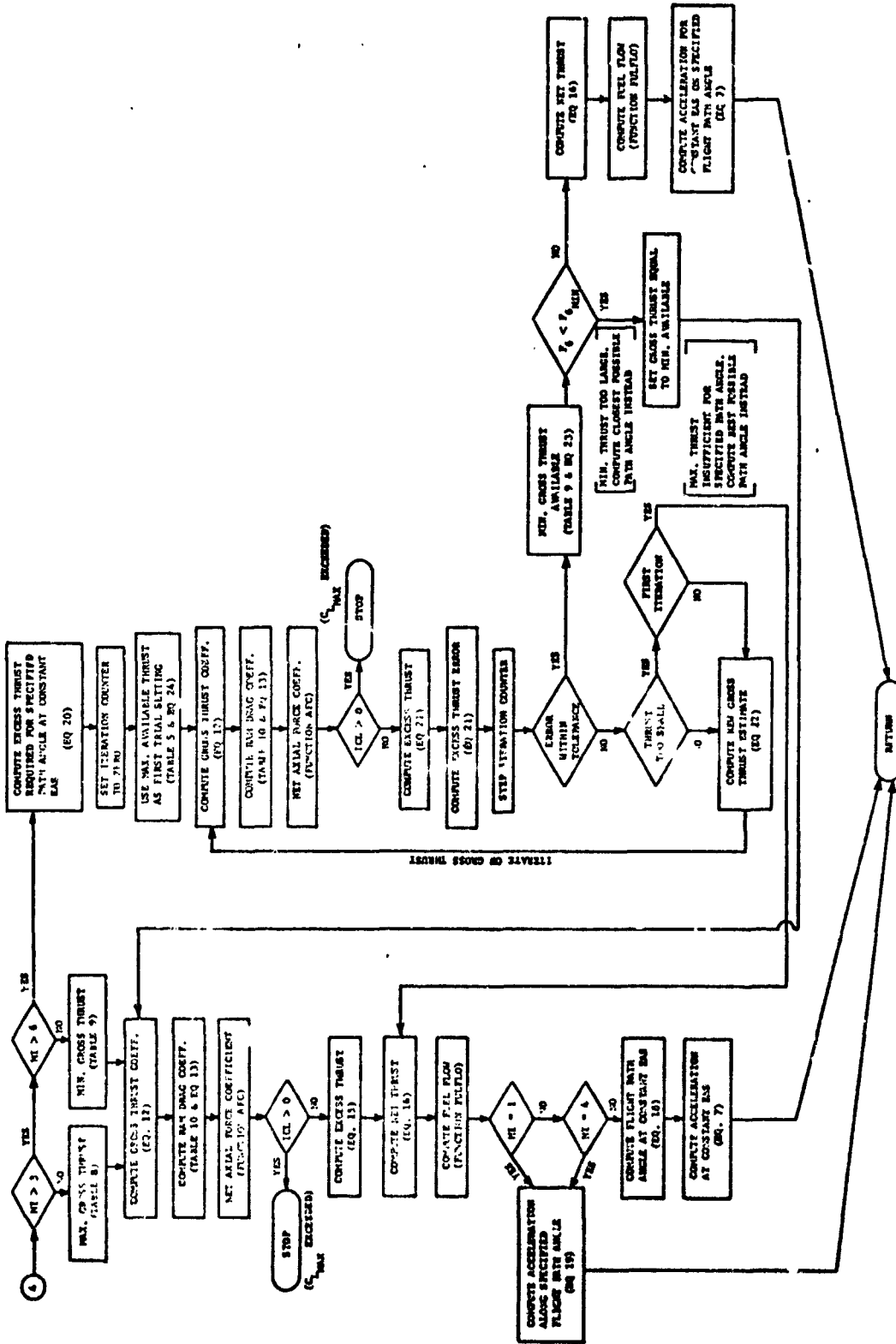


FIGURE B-1. FLOW CHART FOR SUBROUTINE ARCFT (Continued)

APPENDIX B

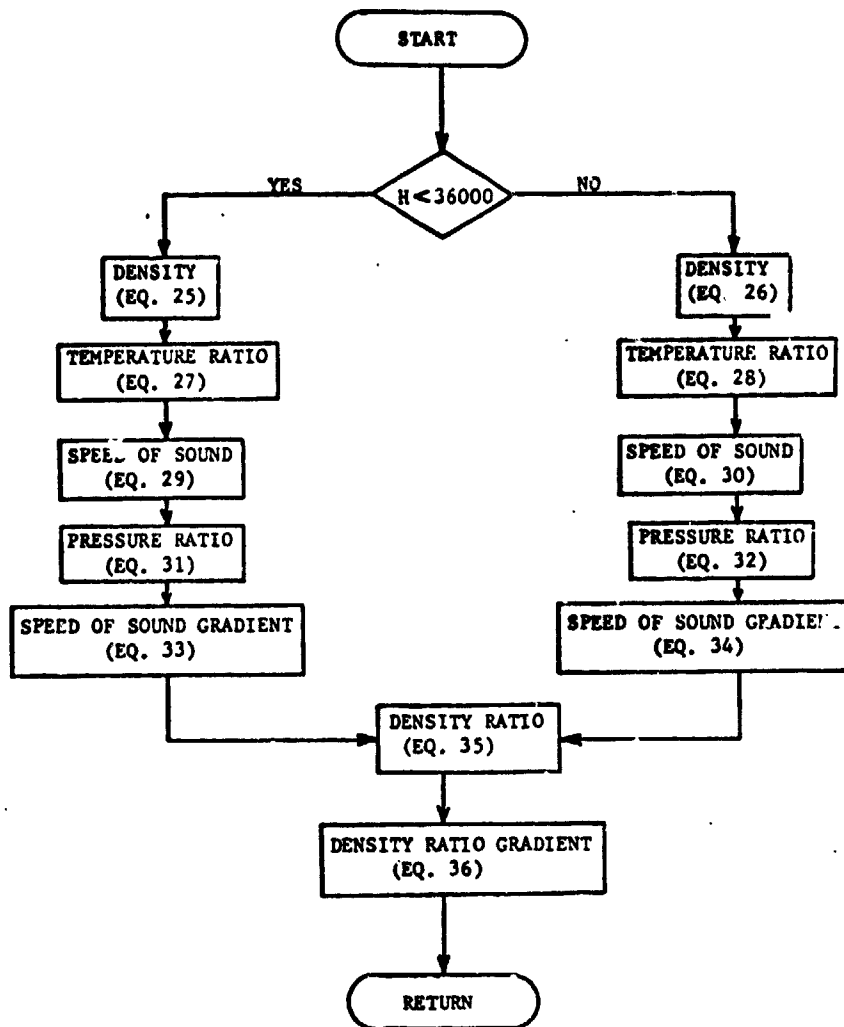


FIGURE B-2. FLOW CHART FOR SUBROUTINE ATMS

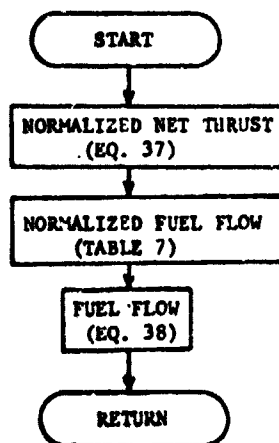
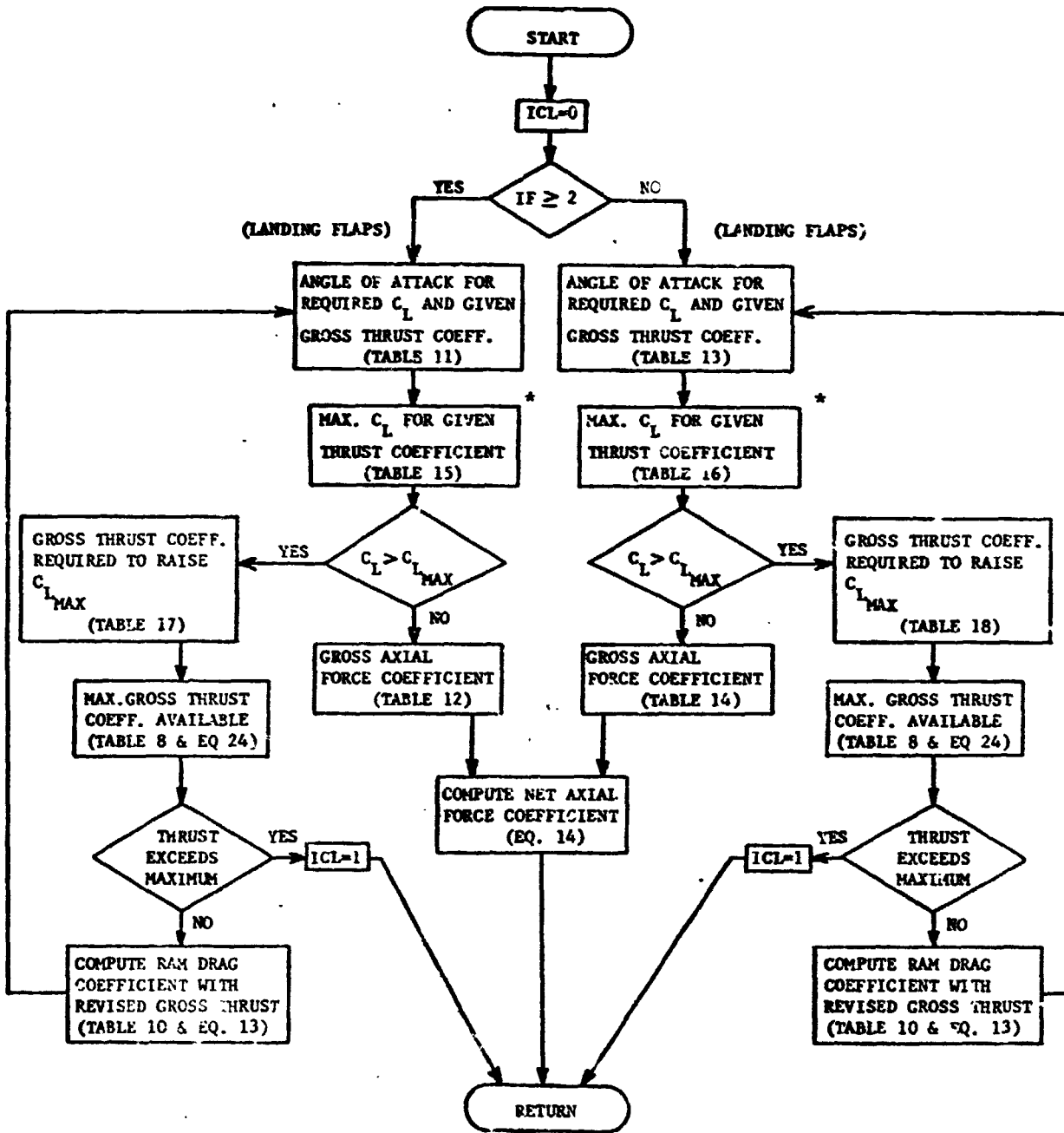


FIGURE B-3. FLOW CHART FOR SUBROUTINE FUEL FLOW

APPENDIX B



* TABLES 11 AND 13 REQUIRE FICTITIOUS COMBINATIONS OF ANGLE OF ATTACK AND C_L TO COMPLETE THE ARRAYS. THE PURPOSE OF TABLES 15 AND 16 IS TO ENSURE THAT THE VALUES BEING USED ARE WITHIN THE LEGITIMATE RANGE.

FIGURE B-4. FLOW CHART FOR FUNCTION AFC

APPENDIX B

All equations and data tables are identified by number on the flow charts. The data tables are listed in the succeeding section, while the equations are listed below.

Equation 1: Mach number

$$M = \frac{V}{C}$$

Equation 2: dynamic pressure

$$Q = \frac{\rho V^2}{2}$$

Equation 3: required lift coefficient

$$C_L = \frac{W}{QS} \frac{1}{\cos \varphi} \quad (\text{assumes } \cos [\gamma] = 1)$$

Equation 4: drag coefficient, flaps up

$$C_D = C_{D_0} + K_1 C_L + K_2 C_L^2$$

Equation 5: acceleration on specified flight path angle, flaps up

$$\dot{V} = \dot{V}_W + g \left[\frac{F_N - C_D QS}{W} - \sin \gamma \right]$$

Equation 6: flight path angle at constant EAS, flaps up

$$\gamma = \sin^{-1} \left\{ \frac{\dot{V}_W + \frac{g}{W} (F_N - C_D QS)}{g - \frac{V^2}{2\sigma} \left(\frac{d\sigma}{dH} \right)} \right\}$$

Equation 7: acceleration for constant EAS

$$\dot{V} = - \frac{V^2}{2\sigma} \left(\frac{d\sigma}{dH} \right) \sin \gamma$$

APPENDIX B

Equation 8: flight path angle at constant Mach number, flaps up

$$\gamma = \sin^{-1} \left\{ \frac{\dot{v}_W + \frac{g}{W}(F_N - C_D QS)}{g + MV \left(\frac{dC}{dH} \right)} \right\}$$

Equation 9: acceleration at constant Mach number

$$\dot{v} = MV \left(\frac{dC}{dH} \right) \sin \gamma$$

Equation 10: net thrust required for specified flight path angle at constant Mach number

$$F_N = C_D QS + \frac{W}{g} \left\{ \left[g + MV \left(\frac{dC}{dH} \right) \right] \sin \gamma - \dot{v}_W \right\}$$

Equation 11: net thrust required for specified flight path angle at constant EAS

$$F_N = C_D QS + \frac{W}{g} \left\{ \left[g - \frac{V^2}{2\sigma} \left(\frac{dC}{dH} \right) \right] \sin \gamma - \dot{v}_W \right\}$$

Equation 12: gross thrust coefficient

$$C_\mu = \frac{F}{QS}$$

Equation 13: ram drag coefficient

$$C_{\mu_o} = C_\mu \left[\frac{C_{\mu_o}(V)}{C_\mu} \right]$$

Equation 14: net axial force coefficient, flaps down

$$C_X = (C_D - C_{\mu_o}) + C_{\mu_o}$$

APPENDIX B

Equation 15: excess thrust

$$F_{XS} = -C_X QS$$

Equation 16: net thrust, flaps down

$$F_N = (C_{\mu} - C_{\mu_0}) QS$$

Equation 17: acceleration during ground roll

$$\dot{v} = \frac{g}{W} [F_{XS} - \mu (C_{L_{Roll}} QS - W)] \quad \text{(The rolling friction coefficient, } \mu, \text{ is assumed to be 0.02)}$$

Equation 18: flight path angle at constant EAS, flaps down

$$\gamma = \sin^{-1} \left\{ \frac{\dot{v}_W + \frac{g}{W} F_{XS}}{g - \frac{v^2}{2\sigma} \left(\frac{d\sigma}{dH} \right)} \right\}$$

Equation 19: acceleration along specified flight path angle, flaps down

$$\dot{v} = \dot{v}_W + g \left[\frac{F_{XS}}{W} - \sin \gamma \right]$$

Equation 20: excess thrust required for specified flight path angle at constant EAS

$$F_{XS_{REQ}} = \frac{W}{g} \left\{ -\dot{v}_W + \left[g - \frac{v^2}{2\sigma} \left(\frac{d\sigma}{dH} \right) \right] \sin \gamma \right\}$$

Equation 21: excess thrust error

$$F_S = F_{XS} - F_{XS_{REQ}}$$

Equation 22: new gross thrust estimate for iteration

$$F_{G_{NEW}} = F_{G_{OLD}} + \left[\frac{-F_E}{\left(1 - \frac{C_{\mu_0}}{C_{\mu}} \right)} \right]$$

APPENDIX B

Equation 23: min gross thrust available

$$FG_{MIN} = \delta[FG_{MIN}(V)]$$

Equation 24: max gross thrust available

$$FG_{MAX} = \delta[FG_{MAX}(V)]$$

Equation 25: atmospheric density (H < 36000 ft)

$$\rho = 2 \left[.034475 + (.019213H^2 \times 10^{-10}) - (.050381H \times 10^{-5}) \right]^2$$

Equation 26: atmospheric density (H ≥ 36000 ft)

$$\rho = 2 \left[.039078 + (.039227H^2 \times 10^{-10}) - (.072121H \times 10^{-5}) \right]^2$$

Equation 27: atmospheric temperature ratio (H < 36000 ft)

$$\sqrt{\theta} = 1 - .000003695H$$

Equation 28: atmospheric temperature ratio (H ≥ 36000 ft)

$$\sqrt{\theta} = .867$$

Equation 29: speed of sound (H < 36000 ft)

$$C = 1117.1 - .00412776H$$

Equation 30: speed of sound (H ≥ 36000 ft)

$$C = 968.5$$

APPENDIX B

Equation 31: atmospheric pressure ratio ($H < 36000$ ft)

$$\delta = .0003375 \rho C^2$$

Equation 32: atmospheric pressure ratio ($H \geq 36000$ ft)

$$\delta = 316.57\rho$$

Equation 33: speed of sound gradient ($H < 36000$ ft)

$$\frac{dC}{dH} = -.00412776 \rho$$

Equation 34: speed of sound gradient ($H \geq 36000$ ft)

$$\frac{dC}{dH} = 0$$

Equation 35: atmospheric density ratio

$$\sigma = \rho / .00237705$$

Equation 36: atmospheric density ratio gradient

$$\left(\frac{d\sigma}{dH} \right) = (.06 H \times 10^{-8}) - .0000292$$

Equation 37: normalized net thrust

$$F_{ND} = \frac{F_N}{\delta}$$

Equation 38: fuel flow

$$\dot{W} = -\delta \sqrt{\theta} (\dot{W}_N)$$

APPENDIX B

Input Data

The Powered-Lift STOL Performance Model (Subroutine ARCFT) requires the following input data to describe the physical characteristics of the aircraft

Discrete Parameters

<u>Fortran Name</u>	<u>Value in Sample Cases</u>
S	1901.
GLIM	0.33

Data Tables

The numerical designation on the following data tables correspond to those used in the flow charts of Figures B-1, B-2, B-3, and B-4. The subroutine requires that the number of points of each table be as shown below. The FORTRAN name is used for all quantities.

TABLE B-1. MAXIMUM LIFT COEFFICIENT VERSUS MACH NUMBER FOR FLAPS UP

<u>M1</u>	<u>CL1</u>
0	1.05
.5	1.05
.8	0.70

These data were assumed to apply to the sample aircraft.

APPENDIX B

TABLE B-2. MAXIMUM NET THRUST AS A FUNCTION OF MACH NUMBER AND ALTITUDE

H2	FN2 (4 engines)				
	M2				
	0	.2	.35	.60	.8
0	96,680	67,200	52,000	39,600	39,600
5000	80,446	55,190	43,264	32,947	32,947
10000	66,500	46,222	35,776	27,238	27,233
15000	54,584	37,940	29,380	22,374	22,374
20000	44,464	30,906	23,920	18,216	18,216
25000	35,924	24,970	19,344	14,731	14,731
30000	28,767	19,995	15,496	11,801	11,801
36000	21,545	14,975	11,588	8,791	8,791
40000	17,960	12,484	9,672	7,356	7,356

The data are assumed values.

TABLE B-3. MINIMUM NET THRUST AS A FUNCTION OF MACH NUMBER AND ALTITUDE

H2	FN3 (4 engines)				
	M2				
	0	.2	.35	.60	.80
0	9,668	6,720	5,200	4,000	4,000
5000	8,044	5,519	4,326	3,295	3,295
10000	6,650	4,622	3,577	2,724	2,724
15000	5,458	3,794	2,938	2,237	2,237
20000	4,446	3,090	2,392	1,821	1,821
25000	3,592	2,497	1,934	1,473	1,473
30000	2,876	2,000	1,550	1,180	1,180
36000	2,154	1,497	1,189	879	879
40000	1,796	1,248	967	735	735

These are also assumed values and are 10 percent of the maximum thrust values given in Table B-2.

APPENDIX B

TABLE B-4. PROFILE DRAG COEFFICIENT VERSUS MACH NUMBER
FLAPS UP

M4	CD4
0	0.0202
0.60	0.0202
0.63	0.02128
0.65	0.0218
0.68	0.0222
0.70	0.0226
0.74	0.0235
0.76	0.0243
0.78	0.0299
0.80	0.0411

These values and those of Tables B-5 and B-6 were obtained by parabolic drag polar fits to the data of Figure 5-7 of MDC J4199.*

TABLE B-5. $\frac{\partial C_D}{\partial C_L}$ VERSUS MACH NUMBER, FLAPS UP

M4	CD5
0	0.01
0.60	0.01
0.63	0.0023
0.65	-0.001
0.68	-0.001
0.70	-0.001
0.74	-0.001
0.76	-0.001
0.78	-0.032
0.80	-0.0915

* "Study of Quiet Turbofan STOL Aircraft for Short-Haul Transportation, Phase I Report, Volume II", McDonnell Douglas Corporation, October, 1972.

APPENDIX B

TABLE B-6. $\frac{\partial C_D}{\partial C_L^2}$ VERSUS MACH NUMBER, FLAPS UP

M4	CD5
0	0.04
0.60	0.04
0.63	0.054
0.65	0.06
0.68	0.06
0.70	0.06
0.74	0.06
0.76	0.06
0.78	0.12
0.80	0.23

TABLE B-7. NORMALIZED FUEL FLOW AS A FUNCTION OF MACH NUMBER AND NORMALIZED NET THRUST

These data are from Figure 6-19 of MDC J4199 except for extrapolation to zero Mach Number and to FN/δ = 100,000 lb.

M7	WDT (4 engines)								
	FN7								
	8,000	16,000	24,000	32,000	40,000	48,000	56,000	64,000	100,000
0	4,000	6,000	8,000	10,000	12,200	14,400	17,000	20,000	33,500
0.2	5,400	7,560	9,640	12,000	14,520	17,200	20,000	23,000	36,500
0.3	6,600	8,880	11,360	14,000	16,800	19,840	23,120	26,600	40,000
0.4	7,680	10,240	13,000	15,840	18,920	22,400	26,040	30,000	43,000
0.5	9,000	11,640	14,520	17,600	20,920	24,640	28,640	32,000	47,120
0.6	10,200	12,960	15,800	19,200	22,640	26,440	30,400	34,200	51,300
0.7	11,200	14,000	17,000	20,240	23,840	27,720	31,600	35,400	52,500
0.8	12,200	14,800	17,800	21,200	24,720	28,600	32,600	36,400	53,500

APPENDIX B

TABLE B-8. MAXIMUM GROSS THRUST VERSUS TRUE AIRSPEED

These data are adapted from Figure 6-13
of MDC J4199

V8	F8
0	96,680
120	99,854
170	102,245
220	105,949
290	111,809
338	116,966

TABLE B-9. MINIMUM GROSS THRUST VERSUS TRUE AIRSPEED

V9	F9
0	9,668
120	9,985
170	10,224
220	10,595
290	11,181
338	11,696

TABLE B-10. RATIO OF RAM DRAG COEFFICIENT TO GROSS THRUST
COEFFICIENT, AS A FUNCTION OF TRUE AIRSPEED

V10	CM10
0	0
135	0.2218
270	0.4179
338	0.5081

These data were deduced from Figure 6-13 of MDC
J4199 with the assumption that the ratio is independent
of thrust setting and altitude.

APPENDIX B

TABLE B-11. LANDING CONFIGURATION ANGLE OF ATTACK AS A FUNCTION OF LIFT COEFFICIENT AND GROSS THRUST COEFFICIENT

These data are based upon unpublished data corrected for trimmed conditions. Some of the values in the table are fictitious and are tabulated only to complete the array for computer use.

CL11	ALFL 11 CMU 11			
	0	1.08	2.07	3.07
0	-14.6	-20.9	-24.2	-26.0
1	-3.7	-12.8	-17.0	-19.6
2	9.0	-4.7	-9.8	-13.2
2.5	18.0	-8	-6.2	-10.0
3.0	27.0	3.2	-2.6	-6.8
4.0	36.0	12.3	4.5	-0.4
4.5	40.5	18.6	8.0	2.8
5.0	45.0	24.9	11.6	6.0
5.5	49.5	31.2	16.0	9.3
5.75	51.75	34.35	18.7	11.0
6.00	56.0	37.5	22.8	12.8
6.50	60.5	43.8	31.0	16.4
7.0	65.0	50.1	39.2	20.6

TABLE B-12. GROSS AXIAL FORCE COEFFICIENT AS A FUNCTION OF GROSS THRUST AND ANGLE OF ATTACK, LANDING CONFIGURATION

These are based upon unpublished data.

ALF 12	FL 12 CMU 12			
	0	1.08	2.07	3.07
-6	0.32	-0.38	-1.02	-1.7
0	0.29	-0.25	-0.82	-1.4
10	0.41	0.12	-0.30	-0.72
16	0.56	0.41	-0.12	-0.2
20	0.68	0.60	-0.43	0.2
24	0.78	0.80	-0.85	0.58

APPENDIX B

TABLE B-13. TAKE-OFF CONFIGURATION ANGLE OF ATTACK AS A FUNCTION OF LIFT COEFFICIENT AND GROSS THRUST COEFFICIENT

These data are based upon unpublished data, corrected for trimmed conditions. Some of the values in the table are fictitious and are tabulated only to complete the array for computer use.

CL13	ALFT 13 CMU 13			
	0	1.08	2.07	3.07
0	-8.5	-11.3	-11.3	-12.0
1.0	-0.4	-3.4	-5.0	-6.4
2.0	12.7	4.7	1.6	-0.4
3.0	27.4	12.8	8.4	5.5
4.0	42.1	23.0	15.2	11.4
5.0	56.8	35.0	23.3	17.4
5.5	60.0	47.0	30.0	20.6
6.0	60.0	50.0	36.7	24.8
6.25	60.0	50.0	40.0	28.4

TABLE B-14. GROSS AXIAL FORCE COEFFICIENT AS A FUNCTION OF GROSS THRUST COEFFICIENT AND ANGLE OF ATTACK, TAKEOFF CONFIGURATION

These are based upon unpublished data.

ALFT14	FT 14 CMU 14			
	0	1.08	2.07	3.07
-6	0.21	-0.76	-1.64	-2.52
0	0.18	-0.75	-1.60	-2.44
4	0.19	-0.69	-1.50	-2.31
8	0.22	-0.59	-1.36	-2.12
14	0.34	-0.38	-1.08	-1.79
20	0.52	-0.10	-0.70	-1.32
30	0.92	0.51	0.10	-0.38

APPENDIX B

TABLE B-15. MAXIMUM LIFT COEFFICIENT IN THE LANDING CONFIGURATION AS A FUNCTION OF GROSS THRUST COEFFICIENT

Because Table B-11 requires fictitious values to complete the array, it is necessary to establish the maximum legitimate value of lift coefficient

CMU 15	CL 15
0	2.40
1.08	4.60
2.07	6.00
3.07	7.25

TABLE B-16. MAXIMUM LIFT COEFFICIENT IN THE TAKEOFF CONFIGURATIONS AS A FUNCTION OF GROSS THRUST COEFFICIENT

Because Table B-13 requires fictitious values to complete the array, it is necessary to establish the maximum legitimate value of lift coefficient

CMU 15	CL 16
0	2.30
1.08	4.10
2.07	5.30
3.07	6.25

TABLE B-17. GROSS THRUST COEFFICIENT REQUIRED TO ATTAIN SPECIFIED MAXIMUM LIFT COEFFICIENT, LANDING CONFIGURATION

This table is identical to Table 15 except that the independent variable is CL15 and the dependent variable is CMU15. No additional input data are required.

APPENDIX B

TABLE B-18. GROSS THRUST COEFFICIENT REQUIRED TO ATTAIN SPECIFIED MAXIMUM LIFT COEFFICIENT, TAKEOFF CONFIGURATION

This table is identical to Table B-16 except that the independent variable is CL16 and the dependent variable is CMU15. No additional input data are required.

TABLE B-19. LIFT COEFFICIENT DURING GROUND ROLL, IN TAKEOFF CONFIGURATION, AS A FUNCTION OF GROSS THRUST COEFFICIENT

It is assumed that the angle of attack is zero throughout the takeoff roll and ground effects are neglected.

CMU 19	CLR 19
0	0.6
1.08	1.12
2.07	1.50
3.07	1.90

Output

Figure B-5 is one page of output data from one application of subroutine ARCFT. This sample page is part of the climbout, cruise, and initiation of descent from San Jose Municipal to Sacramento Executive. The data presented were defined earlier in this Appendix.

APPENDIX B

TIME (FT)	ALT	LATITUDE GAM-H(DEC)	LONGITUDE GAM-V(DEC)	EAS (KTS) BANK (DEG)	TAS (KTS) WEIGHT(LB)	MACH NO.
0.035	2820.	37.19.32	121.54.42	19.0	99. 25.0	103. 120126.
0.35	3736.	37.19.41	121.54.6	16.8	99. 0.0	105. 119969.
1.3	3736.	37.20.6	121.53.55	0.0	151. 0.0	159. 119890.
1.25	3736.	37.21.2	121.53.32	0.0	250. 0.0	254. 119797.
2.32	10000.	37.25.49	121.51.32	9.2	250. 0.0	291. 119472.
3.15	10000.	37.30.6	121.49.5	0.0	344. 0.0	400. 119279.
2.35	11000.	37.31.54	121.49.0	4.8	337. 0.0	398. 119207.
4.37	11000.	37.36.6	121.46.24	0.0	337. 25.0	398. 119332.
5.33	11000.	37.38.7	121.45.23	8.8	337. 0.0	394. 119032.
5.23	11000.	37.43.28	121.44.37	0.0	337. 0.0	393. 118833.
5.37	10000.	37.46.41	121.44.12	-7.5	344. 0.0	400. 118650.
6.42	10000.	37.50.34	121.42.14	0.0	250. 0.0	291. 118768.
5.7	7720.	37.57.4	121.40.3	-3.1	250. 25.0	291. 118649.

FIGURE B-5. SAMPLE PAGE OF TYPICAL OUTPUT FROM SUBROUTINE ARCFIT

APPENDIX C

AIRCRAFT NAVIGATION ERROR ANALYSIS

This appendix describes, in general terms*, the analysis technique used to determine the state estimation (navigation) errors. The development of the technique follows. It is assumed that a stochastic model of the state transition and the state estimator are known. The models are linearized about a nominal solution. A minimum variance is used to determine the state estimation errors. It is shown that this estimator reduces to the solution of the Kalman-Bucy filter equation.

It is assumed that the state of the system to be estimated can be modelled by the stochastic differential equation

$$\dot{x}(t) = f(x,t) + G(t) w(t)$$

$$y(t) = h(x,t) + n(t),$$

where $x(t)$ is the state of the system, $y(t)$ is the observation of the system, and $w(t)$ and $n(t)$ are continuous time white noise processes; $f(x,t)$ and $h(x,t)$ are the deterministic parts of the system and observation nonlinearities, and $G(t)$ is the coefficient matrix for process noise respectively. The white noise sources are introduced to account for not only the stochastic disturbances, but also the system uncertainties due to nonnominal parameters and unmodelled states.

It is assumed that the state (vector) is Gaussian with known mean and variance, i.e.,

$$E [x_0] = \bar{x}_0$$
$$E \left[\begin{pmatrix} x_0 - \bar{x}_0 \\ (x_0 - \bar{x}_0)^T \end{pmatrix} \right] = P(0) .$$

* The specific formulation used in ANGCAP is discussed in Appendix E.

APPENDIX C

The stochastic inputs, $w(t)$ and $n(t)$, are assumed to be white, Gaussian with zero mean and covariance

$$\begin{aligned} E \left[w(t) w^T(\tau) \right] &= Q(t) \delta(t-\tau) \\ E \left[n(t) n^T(\tau) \right] &= R(t) \delta(t-\tau) \end{aligned}$$

and that

$$E \left[w(t) n^T(\tau) \right] = 0 .$$

It is assumed that a linearization about a nominal solution is possible for small deviations of concern. In practice the linearization would be about the current estimate, whereas in the analysis, the linearization is about a predetermined nominal path. Denote the deviation value of $x(t)$ by $\delta x(t)$, i.e.,

$$\delta x(t) = x(t) - \bar{x}(t) .$$

Similarly the nominal value of $x(t)$ has an associated nominal observation $\bar{y}(t)$ and an observed deviation $\delta y(t)$ such that

$$\delta y(t) = y(t) - \bar{y}(t)$$

and

$$\bar{y}(t) = h(\bar{x}(t)) .$$

Expanding $f(x(t), t)$ and $h(x(t), t)$ in a Taylor series expansion about the nominal solution $\bar{x}(t)$,

$$\begin{aligned} \dot{x}(t) &= \dot{\bar{x}}(t) + \delta \dot{x}(t) \\ &= f(\bar{x}(t), t) + \left. \frac{\partial f}{\partial x} \right|_{\bar{x}(t)} \delta x(t) + o(\delta x(t)) + G(t)w(t) \\ y(t) &= \bar{y}(t) + \delta y(t) \\ &= h(\bar{x}(t), t) + \left. \frac{\partial h}{\partial x} \right|_{\bar{x}(t)} \delta x(t) + o(\delta x(t)) + n(t) , \end{aligned}$$

where

$$\lim_{\delta x(t) > 0} o(\delta x(t)) = 0 .$$

APPENDIX C

Hence

$$\delta \dot{x}(t) = F(t) \delta x(t) + G(t)w(t) + o(\delta x(t)) ,$$

$$\delta y(t) = H(t) \delta x(t) + n(t) + o(\delta x(t)) ,$$

where

$$F(t) = \left. \frac{\partial f}{\partial x} \right|_{\bar{x}(t)}$$

and

$$H(t) = \left. \frac{\partial h}{\partial x} \right|_{\bar{x}(t)} .$$

At this point it is convenient to drop the second order stochastic terms $o(\delta x(t))$ by incorporating their effects in $w(t)$ and $n(t)$. Hence, the more nonlinear the system dynamics f and h , the larger the value of covariance for $x(t)$ and $n(t)$, respectively.

Because $f(\bar{x}(t))$ and $h(\bar{x}(t))$ are predetermined nominal values, it is necessary to determine only the deviations from the nominal in order to determine the total system state. Hence, from this point on, it is assumed that an estimate of the linear (perturbed) state equations is required where $w(t)$ and $n(t)$ incorporate the nonlinear second order dynamics. In addition, for ease of notation, the deviation values $\delta x(t)$ and $\delta y(t)$ are simplified to $x(t)$ and $y(t)$, respectively. This should not cause any difficulty since the total state is the sum of the estimated state plus any nominal state value.

An analogous presentation could be made concerning a process represented by discrete difference equations. However, since the procedure is directly analogous, it will not be done.

The error analysis technique parallels the technique used to determine the errors due to incorrect modelling in Kalman filtering. It will later be shown that the technique is not limited to analyzing Kalman filters. The technique can be used to model any estimation process which can be transformed into the form

$$\frac{dx}{dt} = F(t)x(t) + K(t) [y(t) - H(t)x(t)] ,$$

where $x(t)$ is the state of the system, $y(t)$ is the observation, and F , K , and H are the filter coefficients used to weight the previous

APPENDIX C

state estimates with the present observations. However, for the present, it is assumed that a Kalman filter is being utilized and that the actual errors, due to an incorrect modeling of the Kalman filter, are to be determined. The derivation of this filter is found in reference C-1. The necessary equations are presented below. The analysis of continuous systems and that of discrete systems are presented. For a filter which uses continuous state estimation with discrete updates, the filter analysis is a combination of the two techniques.

Analysis for Continuous Systems

The basic process is described by a first order differential equation in vector form:

$$\frac{dx(t)}{dt} = F(t)x(t) + G(t)w(t) . \quad (C-1)$$

The observation is

$$y(t) = H(t)x(t) + n(t), \quad (C-2)$$

where

$x(t)$ = an n_x vector of states with

$$E [x(0)] = 0$$

$y(t)$ = an n_y vector of observations

$w(t)$ = an n_w vector of stochastic inputs to the process
with

$$E[w(t)] = 0 \quad (C-3)$$

$$E[w(t)w'(\tau)] = Q(t)\delta(t-\tau) \quad (C-4)$$

$\delta(t)$ is the Dirac delta function

$n(t)$ = an n_y vector of the observation noise with

$$E[n(t)] = 0 \quad (C-5)$$

$$E[n(t)n'(\tau)] = R(t)\delta(t-\tau) \quad (C-6)$$

APPENDIX C

$F(t)$, $G(t)$, $H(t)$: $n_x \times n_x$, $n_x \times n_w$, $n_y \times n_x$ matrices respectively, and $E [\]$ is an expected value operator on stochastic variables. It is assumed that the process noise w and observation noise n have no correlation to each other,

$$E[w(t)n'(\tau)] = 0 \quad (C-7)$$

The optimal estimator $x^*(t)$ of $x(t)$ which minimizes $E[\|x^* - x\|^2]$ having the observation $y(t)$ from $t = 0$ to t is described by the following differential equation,

$$\frac{dx^*(t)}{dt} = F(t)x^*(t) + K(t)[y(t) - H(t)x^*(t)] \quad (C-8)$$

where

$$K(t) = P(t)H'(t)R^{-1}(t) \quad (C-9)$$

It is assumed that $R(t)$ is positive definite for $t \geq 0$. The covariance matrix $P(t)$ is defined by

$$P(t) \triangleq E \left[[x^*(t) - x(t)] [x^*(t) - x(t)]' \right] \quad (C-10)$$

and it is obtained as a solution of a matrix Riccati equation

$$\frac{dP(t)}{dt} = F(t)P(t) + P(t)F'(t) - P(t)H'(t)R^{-1}(t)H(t)P(t) + G(t)Q(t)G'(t) \quad (C-11)$$

The initial conditions for Equations (C-8) and (C-11) are, respectively,

$$x^*(0) = 0 \quad (C-12)$$

$$P(0) = E[x(0)x'(0)] \quad (C-13)$$

The optimal estimator described above is based on the correct information of initial conditions, and noise covariances, as well as coefficient matrices. Suppose one designs the estimator on the basis of incorrect information with respect to these quantities:

- (1) Incorrect $P_c(0)$ rather than the correct $P(0)$ (a priori covariance of states)
- (2) Incorrect $Q_c(t)$ rather than the correct $Q(t)$ (covariance of the process noise)

APPENDIX C

- (3) Incorrect $R_c(t)$ rather than the correct $R(t)$
(covariance^c of the observation noise)
- (4) Incorrect $F_c(t)$ rather than the correct $F(t)$
(process matrix)
- (5) Incorrect $G_c(t)$ rather than the correct $G(t)$
(coefficient^c matrix of the process noise)
- (6) Incorrect $H_c(t)$ rather than the correct $H(t)$
(observation^c matrix).

The resultant estimator is no longer an optimal one, but becomes suboptimal. This suboptimal estimator is denoted $x_a^*(t)$ and is described by

$$\frac{dx_a^*(t)}{dt} = F_c(t)x_a^*(t) + K_c(t)[y(t) - H_c(t)x_c^*(t)] \quad , \quad (C-14)$$

where

$$x_c^*(0) = 0 \quad (C-15)$$

$$K_c(t) = P_c(t)H_c'(t)R_c^{-1}(t) \quad (C-16)$$

and the calculated covariance $P_c(t)$ is computed by the same Riccati equation as Equation (C-11), but with the incorrect model specified by elements 1 through 6 in the above listing:

$$\begin{aligned} \frac{dP_c(t)}{dt} = & F_c(t)P_c(t) + P_c(t)F_c'(t) \\ & - P_c(t)H_c'(t)R_c^{-1}(t)H_c(t)P_c(t) \\ & + G_c(t)Q_c(t)G_c'(t) . \end{aligned} \quad (C-17)$$

The actual covariance $P_a(t)$ is defined as the error covariance associated with the suboptimal estimator Equation (C-14), hence,

$$P_a(t) \triangleq E\left\{[x_a^*(t) - x(t)][x_a^*(t) - x(t)]'\right\} . \quad (C-18)$$

This is the covariance to be expected in an estimator when insufficient design parameter data are available. The main purpose of this section is to derive equations describing $P_a(t)$. For this purpose, it is easier to derive a differential equation governing the evolution of $P_a(t)$. Thus, differentiating $P_a(t)$ of Equation (C-18) and exchanging the order of the differentiating operator and the expected-value operator yields

APPENDIX C

$$\begin{aligned} \dot{P}_a(t) = & E \left\{ [\dot{x}_a^*(t) - \dot{x}(t)] [x^*(t) - x(t)]' \right\} \\ & + \left\{ E [x_a^*(t) - x(t)] [\dot{x}_a^*(t) - \dot{x}(t)]' \right\} . \end{aligned} \quad (C-19)$$

However, from Equations (C-1) and (C-14),

$$\begin{aligned} \dot{x}_a^*(t) - \dot{x}(t) = & [F_c(t) - K_c(t)H_x(t)] [x_a^*(t) - x(t)] \\ & + \Delta F(t)x(t) - K_c(t)\Delta H(t)x(t) \\ & + K_c(t)n(t) - G(t)w(t) , \end{aligned} \quad (C-20)$$

where

$$\Delta F(t) = F_c(t) - F(t) \quad (C-21)$$

$$\Delta H(t) = H_c(t) - H(t) . \quad (C-22)$$

Also, $x(t)$ is obtained from Equation (C-1):

$$x(t) = U(t,0)x(0) + \int_0^t U(t,s)G(s)w(s)ds \quad (C-23)$$

where $U(t,s)$ is defined by

$$\frac{\partial U(t,s)}{\partial t} = F(t)U(t,s) \quad (C-24)$$

with

$$U(s,s) = I, \quad t \geq s \geq 0 \quad (C-25)$$

and I is an identity matrix.

Furthermore, $x_a^*(t)$ is derived from Equation (C-14)

$$x_a^*(t) = \int_0^t V_c(t,s)K_c(s)y(s)ds , \quad (C-26)$$

where $V_c(t,s)$ is defined by

$$\frac{\partial V_c(t,s)}{\partial t} = [F_c(t) - K_c(t)H_c(t)]V_c(t,s), \quad t \geq s \geq 0 . \quad (C-27)$$

APPENDIX C

When $\dot{x}^*(t)$ and $x^*(t)$ are substituted into Equation (C-19) together with $\dot{x}(t)$ of Equation (C-1) and its solution $x(t)$ in Equation (C-23), paying attention to the fact that $w(t)$ and $n(t)$ are uncorrelated white noises, the following three differential equations are applicable:

$$\begin{aligned} \frac{dP_a(t)}{dt} = & [F_c(t) - K_c(t)H_c(t)]P_a(t) + P_a(t)[F_c(t) \\ & - K_c(t)H_c(t)]' + [\Delta F(t) - K_c(t)\Delta H(t)]\Lambda(t) \\ & + \Lambda'(t)[\Delta F(t) - K_c(t)\Delta H(t)]' \\ & + K_c(t)R(t)K_c'(t) + G(t)Q(t)G'(t) \end{aligned} \quad (C-28)$$

$$\begin{aligned} \frac{d\Lambda(t)}{dt} = & F(t)\Lambda(t) + \Lambda(t)[F_c(t) - K_c(t)H_c(t)]' \\ & + P_x(t)[\Delta F(t) - K_c(t)\Delta H(t)]' \\ & - G(t)Q(t)G'(t) \end{aligned} \quad (C-29)$$

$$\frac{dP_x(t)}{dt} = F(t)P_x(t) + P_x(t)F'(t) + G(t)Q(t)G'(t), \quad (C-30)$$

where $\Lambda(t)$ and $P_x(t)$ are defined by

$$\Lambda(t) \triangleq E \left[x(t) [x_a^*(t) - x(t)]' \right] \quad (C-31)$$

$$P_x(t) \triangleq E [x(t)x'(t)] . \quad (C-32)$$

The initial conditions for Equations (C-28) through (C-30) are given, respectively, by

$$P_a(0) = P(0) \quad (C-33)$$

$$\Lambda(0) = -P(0) \quad (C-34)$$

$$P_x(0) = P(0) . \quad (C-35)$$

APPENDIX C

The matrix equations can be arranged in a more familiar form as follows. Defining the $2n \times 2n$ matrices,

$$X = \begin{bmatrix} P_a & \Lambda^T \\ \Lambda & P_x \end{bmatrix} \quad (C-36)$$

$$A = \begin{bmatrix} (F_c - K_c H_c) & (\Delta F - K_c \Delta H) \\ 0 & F \end{bmatrix} \quad (C-37)$$

and

$$\Xi = \begin{bmatrix} (K_c R K_c^T + G Q G^T) & -G Q G^T \\ -G Q G^T & G Q G^T \end{bmatrix}, \quad (C-38)$$

equations (C-28), (C-29), and (C-30) can be written as

$$\dot{X} = AX + XA^T + \Xi \quad (C-39)$$

which is a solution of the covariance equation for a process described by

$$\frac{dx}{dt} = Ax + \xi, \quad (C-40)$$

where

$$E[x(0)x^T(0)] = X(0) \quad (C-41)$$

$$E[x(0)] = E[\xi(t)] = 0 \quad (C-42)$$

$$E[\xi(\epsilon)\xi^T(\tau)] = \Xi(\epsilon)\delta(\epsilon - \tau). \quad (C-43)$$

Hence, the computation of the actual mean and covariance for the n^{th} order system described by Equations (C-14) through (C-17) is equivalent to the computation of the mean and covariance for the $2n^{\text{th}}$ order system described by Equations (C-40) through (C-43).

Note that for the calculated Kalman filter gain, K requires the solution of Equations (C-16) and (C-17). If a Kalman filter gain is not used (or is approximated), then the method used for obtaining K must be simulated and P need not be calculated. Hence, the technique is applicable for analysis of all filters satisfying Equation (C-14), as initially proposed.

APPENDIX C

Analysis for Discrete Systems

The technique utilized in the previous section is applied to discrete systems and similar results are derived. Symbols are defined in the same manner as in the continuous systems, and similar assumptions are made concerning modelling errors and noise statistics.

The process and observation equations are respectively,

$$x(k+1) = \phi(k)x(k) + G(k)w(k) \quad (C-44)$$

$$y(k) = H(k)x(k) + n(k) \quad (C-45)$$

The optimal estimate $x^*(k+1)$ given the information $Y(k) = [y(0), y(1), \dots, y(k)]$ is given by

$$x^*(k+1) = \phi(k)x^*(k) + K(k)[y(k) - H(k)x^*(k)], \quad (C-46)$$

where

$$K(k) = \phi(k)P(k)H'(k)[H(k)P(k)H'(k) + R(k)]^{-1} \quad (C-47)$$

$$x^*(0) = 0 \quad (C-48)$$

The covariance matrix $P(k)$ is defined by

$$P(k) \triangleq E \{ [x^*(k) - x(k)][x^*(k) - x(k)]' \} \quad (C-49)$$

and it is governed by the following nonlinear difference equation:

$$P(k+1) = [\phi(k) - K(k)H(k)]P(k)[\phi(k) - K(k)H(k)]' + K(k)R(k)K(k)' + G(k)Q(k)G'(k) \quad (C-50)$$

with

$$P(0) = E[x(0)x'(0)] \quad (C-51)$$

When the incorrect models that are the counterparts in a discrete system of those described earlier are used, the resultant suboptimal estimator $x_a^*(k)$ is computed by

$$x_a^*(k+1) = \phi_c(k)x_a^*(k) + K_c(k)[y(k) - H_c(k)x_a^*(k)] \quad (C-52)$$

with

$$K_c(k) = \phi_c(k)P_c(k)H_c'(k)[H_c(k)P_c(k)H_c'(k) + R_c(k)]^{-1} \quad (C-53)$$

$$x_a^*(0) = 0 \quad (C-54)$$

APPENDIX C

The calculated covariance $P_c(k)$ is

$$P_c(k+1) = [\phi_c(k) - K_c(k)H_c(k)]P_c(k)[\phi_c(k) - K_c(k)H_c(k)]' + K_c(k)R_c(k)K_c'(k) + G_c(k)Q_c(k)G_c'(k) \quad (C-55)$$

The actual covariance associated with this suboptimal estimator $x_a^*(k)$ is defined as

$$P_a(k) \triangleq E\left([x_a^*(k) - x(k)][x_a^*(k) - x(k)]'\right) \quad (C-56)$$

The recurrence equations describing $P_a(k)$ are derived similarly to the continuous case

$$\begin{aligned} P_a(k+1) &= [\phi_c(k) - K_c(k)H_c(k)]P_a(k)[\phi_c(k) - K_c(k)H_c(k)]' \\ &+ [\Delta\phi(k) - K_c(k)\Delta H(k)]\Lambda(k)[\phi_c(k) - K_c(k)H_c(k)]' \\ &+ [\phi_c(k) - K_c(k)H_c(k)]\Lambda'(k)[\Delta\phi(k) - K_c(k)\Delta H(k)]' \\ &+ [\Delta\phi(k) - K_c(k)\Delta H(k)]P_x(k)[\Delta\phi(k) - K_c(k)\Delta H(k)]' \\ &+ K_c(k)R(k)K_c'(k) + G(k)Q(k)G'(k) \end{aligned} \quad (C-57)$$

$$\begin{aligned} \Lambda(k+1) &= \phi(k)\Lambda(k)[\phi_c(k) - K_c(k)H_c(k)]' \\ &+ \phi(k)P_x(k)[\Delta\phi(k) - K_c(k)\Delta H(k)]' \\ &- G(k)Q(k)G'(k) \end{aligned} \quad (C-58)$$

$$P_x(k+1) = \phi(k)P_x(k)\phi'(k) + G(k)Q(k)G'(k) \quad (C-59)$$

where $\Lambda(k)$ and $P_x(k)$ are defined by

$$\Lambda(k) \triangleq E\left[x(k)[x_a^*(k) - x(k)]'\right] \quad (C-60)$$

$$P_x(k) \triangleq E[x(k)x'(k)] \quad (C-61)$$

APPENDIX C

The initial conditions for the recurrence equations [Equations (C-57) through (C-59)] are given by, respectively,

$$P_a(0) = P(0) \quad (C-62)$$

$$\Lambda(0) = P(C) \quad (C-63)$$

$$P_x(0) = P(0) \quad (C-64)$$

The matrices can be arranged in similar fashion as before defining

$$X(k) = \begin{bmatrix} P_a(k) & \Lambda^T(k) \\ \Lambda(k) & P_x(k) \end{bmatrix} \quad (C-65)$$

$$A = \begin{bmatrix} (\phi_c - K_c H_c) & (\Delta\phi - K_r \Delta H) \\ 0 & \phi \end{bmatrix} \quad (C-66)$$

and

$$\Xi = \begin{bmatrix} (K_c R K_c^T + G Q G^T) & - G Q G^T \\ - G Q G^T & G Q G^T \end{bmatrix} \quad (C-67)$$

Equations (C-57 through (C-59) can be written as

$$X(k+1) - A(k)X(k)A^T(k) + \Xi(k) \quad (C-68)$$

APPENDIX C

When analyzing continuous time-discrete data systems, a combination of the two analyses is used. Between data measurements Equations (C-36) through (C-39) are used to propagate the estimate and its covariance with K_e , H_e , ΔH , and R set to zero. At a measurement, Equations (C-65) through (C-68) are used to update the estimate and covariance with Φ_n equal to I , and $\Delta \Phi$, G , and Q set equal to zero.

Measurement Error Models

The previously discussed models for analyzing continuous and discrete systems requires error models for each of the measurement. Various references (refs. C-2 through C-6) were surveyed to determine models previously used to characterize the sources of error observed.

Most present radio navigation aids provide either angle or range measurement (VOR, DME, ILS, MLS). All of the references dictate a common form for the VOR/DME error sources, a random but constant bias, and a time uncorrelated white noise. The references differ, however, in the specific values assigned to the statistical parameters. Since these values are input data, the user may select the value felt to be most representative.

VOR Error Model.-The VOR bearing error is modelled as the sum of a random bias and a white-noise component. The zero mean bias component consists of two independent bias sources, a misalignment of the station radials and an imperfect calibration of the VOR receiver. The white noise component is an approximation to the high frequency (compared to the observation frequency) noise due to multipath errors, polarization errors, receiver sensitivity and other station errors.

Typical rms values of the ground and airborne equipment bias errors are 0.8 and 0.6 degree, respectively. The approximate bias error is thus 1.0 degree, rms. A representative value of the variance and of the high-frequency VOR noise is 1.0 degrees.

DME Error Model.-The DME range error is also modelled as the sum of a random bias and a white noise component. The zero mean bias component consists of the time delays between reception and processing of the DME signals by the ground and airborne equipment. The white noise component is due to pulse distorting errors and receiver generated noise.

APPENDIX C

A typical rms value of the ground and airborne equipment bias errors are 0.1 n.mi. resulting in an aggregate rms bias error of 0.4 n.mi. Representative values of the variance and correlation time of the high frequency DME noise are 0.1 n.mi. and 3.6 seconds.

Air Data System Error Models. - The assumed measurements are

- (1) Static pressure, p_s
- (2) Total, stagnation, or pitot pressure, p_t
- (3) Air temperature, T_m
- (4) Angle of attack, α_m

Dynamic pressure, q_c , is related to static and stagnation pressure as follows:

$$q_c = p_t - p_s \quad (C-69)$$

Mach number M , is defined as

$$M = \frac{V_{TAS}}{a} \quad (C-70)$$

where

V_{TAS} = true airspeed

a = local speed of sound .

The local speed of sound is defined as

$$a = \sqrt{\frac{\gamma p_s}{\rho}} = \sqrt{\gamma g R T_s} \quad (C-71)$$

APPENDIX C

where

γ = specific heat ratio of air = 1.4

ρ = air density

g = gravity

R = constant = 53.3 ft./°R

T_s = free-stream static-air temperature

For compressible flow,

$$p_t = p_s \left[1 + \frac{\gamma-1}{\gamma} \frac{\rho v^2}{2p_s} \right]^{\gamma/\gamma-1} \quad (C-72)$$

Substituting from Equations (C-69) through (C-71) into Equation (C-72), M can be expressed as

$$M = \sqrt{\left[\left(\frac{q_c}{p_s} + 1 \right)^{1/3.5} - 1 \right]} \quad (C-73)$$

The free-stream static-air temperature is defined as

$$T_s = \frac{T_m}{1 + \frac{\gamma-1}{2} \eta M^2} = \frac{T_m}{1 + .2\eta M^2} \quad (C-74)$$

where η = recovery factor of temperature probe

Pressure altitude, h , is derived from the hydrostatic equation

$$dp = -\rho g dh \quad (C-75)$$

If temperature is assumed to vary linearly with altitude (ref. C-7), i.e.,

$$T = T_o - \alpha h \quad (C-76)$$

APPENDIX C

where α = temperature lapse rate, and T_o = standard day sea-level temperatures, then it can be shown that

$$\frac{-dp}{p} = \frac{1}{R} = \frac{dh}{T_o - \alpha h} \quad (C-77)$$

This can be solved to give pressure ratio variation with altitude

$$\frac{p}{p_o} = \left(1 - \frac{\alpha h}{T_o} \right)^{1/\alpha R} \quad (C-78)$$

Solving for h yields

$$h = \frac{T_o}{\alpha} \left[1 - \left(\frac{p}{p_o} \right)^{R\alpha} \right] \quad (C-79)$$

The measured static pressure, p_s , has a correction applied for static defect, S_D , and p in Equation (C-79) is usually taken to be

$$p = p_{s_c} = p_s S_D \quad (C-80)$$

Substituting for p , Equation (C-79) becomes

$$h = \frac{T_o}{\alpha} \left[1 - \left(\frac{p_s S_D}{p_o} \right)^{R\alpha} \right] \quad (C-81)$$

Figure C-1 depicts the usual air data system computations.

In some cases, the computed pressure altitude is corrected for variation of local T_o and p_o from the standard day. This correction is not of interest for the purpose of deriving error models for altitude and true airspeed.

The primary sources of pressure altitude and true airspeed estimation errors are measurement errors, mathematical approximations, and atmospheric conditions being other than the standard day.

APPENDIX C

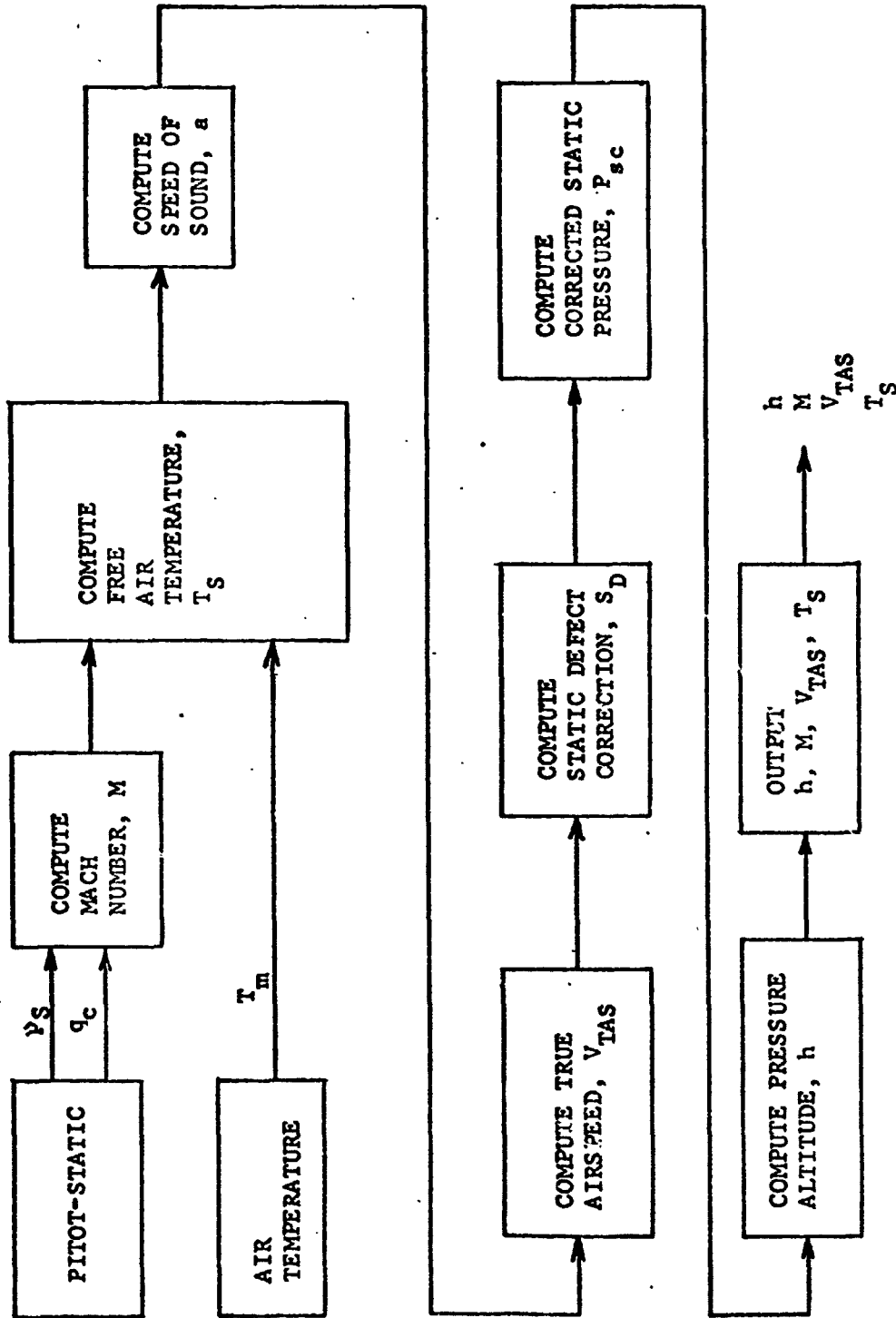


FIGURE C-1. TYPICAL AIR DATA COMPUTATION

APPENDIX C

Examination of Equation (C-81) reveals that the primary errors in altitude are due to:

- (1) Incorrect static pressure measurement p_s , due to installation, transducer, and calibration errors.
- (2) Incorrect static defect correction, S_D , due to mathematical approximation as a function of many variables such as static pressure, dynamic pressure, and angle of attack (references C-6 and C-8),
- (3) Variation of temperature lapse rate from standard day lapse rate (note that lapse rate error would not affect relative vertical spacing of aircraft using barometric altimeters but could cause aircraft descending to impact the terrain),
- (4) Variation of barometric pressure as a function of flight path (uncompensated pressure gradient). The effect of this is the same as entering the wrong local barometric pressure.

The static pressure error has been considered to include both bias (static defect) and random (instrument) components. Nonstandard atmosphere variations are considered to be bias. Table C-1 lists typical models for the error sources and their components.

Reference C-9 assumes the altimeter related errors are:

- (1) Error due to horizontal gradient of pressure
- (2) Nonstandard temperature errors
- (3) Static pressure measurement error
- (4) Instrument error.

If the variation in altimeter error can be determined from the nominal flight path and atmospheric environment, the spatially correlated altimeter errors will be converted to time correlations, thus avoiding introducing additional state variables for the spatial correlation terms. If not, state variables for the spatial correlation terms (such as pressure and temperature lapse rate) must be incorporated into the error model.

APPENDIX C

TABLE C-1. TYPICAL BAROMETRIC ALTIMETER ERROR MODELS

Error (ref. C-10)		Model (ref. C-2)	
Static Pressure			
Bias	1 mbar	$\frac{C_p/3}{(C_p/3)-1}$	$\frac{v_{TAS}^2}{2g}$
Random	0.2% h	$\sqrt{625 \times 10^{-10} h^2 + .25}$ $0 < h \leq 10,000$ ft. $\sqrt{625 \times 10^{-10} h^2 + 100}$ $10,000 < h \leq 100,000$ ft.	
Nonstandard Atmosphere			
Bias	7.5% ρ	$\frac{2 \times 10^{-7} h}{\rho g}$	
Random			

APPENDIX C

The effects of the incorrect sources of T_o , p_o , α , and S_D on the altitude were determined as follows.

Reference C-9 indicates that the effects due to static defect and nonstandard lapse rate, respectively:

$$\Delta h_{SD} = 1.7 \times 10^{-4} \times (\text{velocity in feet/sec}^2)$$

$$\Delta h_{\alpha} = .03 \times (\text{altitude}).$$

It can easily be shown that the error due to an incorrect temperature setting is

$$\Delta h_{\Delta T_o} = \frac{\Delta T_o}{T_o} \times (\text{altitude}).$$

The error in altitude due to an incorrect pressure setting is more difficult to determine. Figure C-2 is a plot of the effect of a 1% error in p_o as a function of altitude. A quadratic curve was fitted to this plot. From this curve, the following altitude error for an incorrect pressure setting was obtained:

$$\Delta h_{\Delta p_o} = 5.7 \frac{\Delta p_o}{p_o} \times (\text{altitude}).$$

Although there can be correlation between the temperature pressure and lapse rate errors it was convenient to assume the errors to be independent. In any case, if the errors are correlated, the results would not differ greatly. From reference C-9, 1 σ values for $\frac{\Delta T_o}{T_o} = .03$ and from reference C-10, a 1 σ value for $\frac{\Delta p_o}{p_o} = .001$.

Hence,

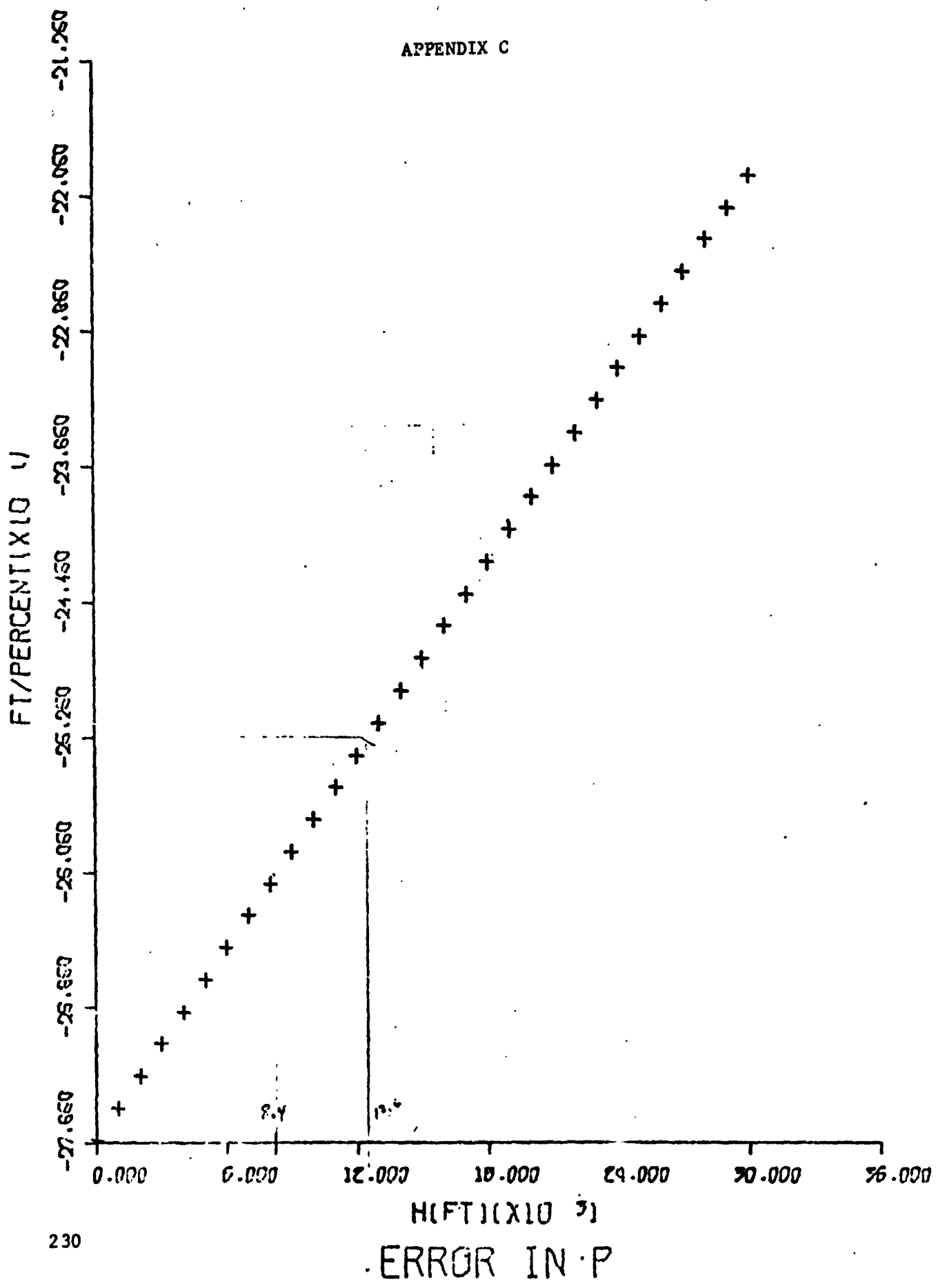
$$\begin{aligned} \Delta h_{\Delta T_o} + \Delta h_{\alpha} + \Delta h_{\Delta p_o} &= [(.03)^2 + (.03)^2 + (.0057)^2]^{1/2} h \\ &= .043 h. \end{aligned}$$

Then utilizing a more conservative sum of error approach between this error and the error due to static defect, the total error Δh is defined to be

$$\Delta h = .047h + 1.7 \times 10^{-4} v^2.$$

The correlation time for altitude errors is much greater than the filter update time. Hence, the error can be modeled as a statistical bias. The program computes the rms error for each phase from the altitude and velocity conditions at the start of each phase.

APPENDIX C



230

ERROR IN P

FIGURE C-2. ERROR IN ALTITUDE VERSUS PRESSURE ERROR

APPENDIX C

True airspeed can be written as

$$V_{TAS} = a M = M \sqrt{\gamma g R T_s} \quad (C-82)$$

The true airspeed can be used in improving the state estimate (refs. C-9 through C-12) for many of the modes of the state estimation function.

The primary sources of error in V_{TAS} are due to:

- (1) Incorrect static, p_s , and dynamic, q_c , pressure measurements due to installation, transducer, and calibration errors (ref. C-13)
- (2) Incorrect temperature measurement, T_M
- (3) Computation errors.

Indicated airspeed, V_{IAS} , is displayed also on the basis of the relation

$$V_{IAS} = \sqrt{\frac{2(p_t - p_s)}{\rho_o}} = \sqrt{\frac{2 q_c}{\rho_o}} \quad (C-83)$$

The navigation procedure normally involves estimating the velocity of the aircraft with respect to the ground. This velocity, V , can be expressed as

$$V = V_{TAS} + V_e \quad (C-84)$$

where V_{TAS} is the onboard estimate using air data measurements and V_e is the error due to the effects of wind, errors in V_{TAS} as previously discussed, and heading errors. Wind effect estimation errors are on the order of 40 knots (rms) en route and 5 to 10 knots (rms) during landing (refs. C-2 through C-5). Hence, the velocity error due to wind is about 10 to 25% of the nominal aircraft velocity. Maximum heading error is limited to 1.5° to 2° and thus contributes less than 3.5% error in nominal velocity. The airspeed error is typically on the order of 1% to 4% (refs. C-11 and C-12). Assuming that the wind, V_{TAS} and heading errors are independent, it can be shown that the rms error for V_e , σ_e , is roughly equal to the rms wind error as follows: using the low rms error for wind variance, σ_w , and the high rms errors for the heading and airspeed errors, σ_h and σ_{TAS} ,

$$\begin{aligned} \sigma_e &= [(\sigma_w^2 + \sigma_h^2 + \sigma_{TAS}^2)]^{1/2} \\ &= [(.1)^2 V^2 + (.035)^2 V^2 + (.04)^2 V^2]^{1/2} \\ &= [(100 + 12 + 16) 10^{-4}]^{1/2} V \\ &= .11V \\ &\sim \\ &= .1V \\ &= \sigma_w \end{aligned}$$

APPENDIX C

Hence, the major source of ground speed error using air data measurements is the wind.

The high frequency winds or gusts cause relatively insignificant deviations from the nominal. Of particular interest, are the (relatively) slow varying winds. Measured data on these winds are relatively nonexistent. The wind is modeled as the sum of two orthogonal (in the horizontal plane) independent, exponentially correlated, random processes. The rms values are on the order of 10% to 20% of aircraft velocity with correlation times on the order of 6 to 15 minutes. Values used for the simulation are 40 knots rms en route and 10 knots rms in the terminal area.

MLS Error Model. - It has been assumed that the microwave landing system would initially be Configuration G of those recommended by SC-117 (ref. C-13). For this system, the error model is that suggested by SC-117, which assumes that the errors are primarily white Gaussian noise with the error in elevation equal to 1.4 feet (2σ), the error in azimuth equal to 11 feet (2σ) and the error in range equal to 20 feet (2σ). Reference C-2 states that the errors are 0.63 milliradian bias and 0.40 milliradian noise (1σ) in azimuth, 0.87 milliradian bias and 0.61 milliradian noise (1σ) in elevation and an assumed bias of 2.0 feet and noise of 20 feet (1σ) for range. Reference C-2 does not state which of the configurations this error model is representative of. For this reason, the previous values from reference C-13 were utilized.

It has been decided that an error model for the radar altimeter is not required since the radar altimeter is primarily used for flare command generation and not in state estimation. Should the use of the radar altimeter change, an error model can be incorporated in the previously discussed state estimation error models.

APPENDIX C

References

- C-1 Nishimura, T., "Modeling Errors in Kalman Filters", NASA CR 11092, June 1970.
- C-2 McGee, L. A., et al, "Navigation for Space Shuttle Approach and Landing using an Inertial Navigation System Augmented by Various Data Sources", Proceedings of the Space Shuttle Integrated Electronics Conference, NASA Manned Spacecraft Center, May 1971.
- C-3 Bryson, A. E., and Bobick, J. C., "Improved Navigation by Combining VOR/DME Information and Air Data", J. Aircraft Vol. 9, No. 6, June 1972, pp. 420-426.
- C-4 Johansen, M., "A Survey of General Coverage Nav aids for V/STOL Aircraft - A VOR/DME Error Model", CR-1588, May 1970, NASA.
- C-5 Hemesath, N. B., "Optimal and Suboptimal Velocity-Aiding for VOR/DME Systems", AIAA Guidance, Control and Flight Mechanics Conference, Santa Barbara, California, August 17-19, 1970.
- C-6 Kayton, M., and Fried, W., Avionics Navigation Systems, J. Wiley and Sons, Inc., New York, N.Y., 1969.
- C-7 Perkins, Courtland D., and Hage, Robert E., Airplane Performance Stability and Control, John Wiley & Sons, Inc., New York (1960).
- C-8 Yarosh, Norman P., et al., "Interface Optimization Investigation", AFAL-TR-67-152, Univac Federal Systems Division, February 1968.
- C-9 Widnall, William S., et al., "Space Shuttle Landing Navigation Using Precision Distance - Measuring Equipment", N 71-35775, Intermetrics, Inc., August 2, 1972.
- C-10 Kriegsman, B. A., and Gustafson, D. E., "Entry Navigation Analyses", Proceedings of the Space Shuttle Integrated Electronics Conference, NASA TM X-58963, Volume I, May 11-13, 1971.
- C-11 Erwin, Ralph L., Jr., "Influence of Flight Dynamics on Terminal Sequencing and Approach Control", Appendix B-5, "Report of Department of Transportation Air Traffic Control Advisory Committee", Volume 2, Appendixes, Department of Transportation, December 1969.
- C-12 Marino, A. S., et al., "Definition and Analysis of Flight Command Functions and Computations", AFFDL-TR-68-145, November 1968.
- C-13 "A New Guidance System for Approach and Landing", Document No. DO-148, Prepared by SC-117, Radio Technical Commission for Aeronautics, December 18, 1970.

APPENDIX D

GUIDANCE/CONTROL FUNCTIONS ANALYSIS

Two basic approaches can be taken to determine the guidance/control errors. The first is to model the open loop equations describing the guidance and control laws and close the loop to obtain the closed loop response. The second is to estimate the closed loop response from observed response data. Since the initial intent of this program is not to obtain and modify guidance/control laws but to determine their effect on the overall system, only the closed loop response is of importance. Additionally, the closed loop response is easier to obtain from field test data. Hence the second approach will be used to model the guidance/control errors.*

The approach is to develop an estimate of the power spectral density of the (assumed stationary Gaussian) process $y(t)$ which is the lateral deviation of an aircraft attempting to follow the guidance commands. This spectral density is designated $\phi(s)$.

The spectrum must satisfy

$$\sigma_y^2 = \frac{1}{2\pi j} \int_{-j\infty}^{j\infty} \phi(s) ds \quad (D-1)$$

This is by no means adequate to determine $\phi(s)$ uniquely. To further define this spectrum, we observe that $y(t)$, the position deviation, must not be excessively large, and furthermore, it must be reasonably smooth. In essence, it is intuitive judgments on these points which permit selection of a model for the spectrum.

The "smoothness of the deviations" may be specified by fixing the average number of times per second which the deviation changes sign. Applying Rice's zero-crossing result (ref. D-1) to this case gives

$$N_0 = \frac{1}{\pi} \left[\frac{\frac{1}{2\pi j} \int_{-j\infty}^{j\infty} s^2 \phi(s) ds}{\sigma_y^2} \right]^{1/2} \quad (D-2)$$

where N_0 is the expected number of sign changes per second.

Equations (D-1) and (D-2) specify two conditions. N_0 and σ_y effectively define ϕ_y since

* The specific formulation used in ANGCAP is discussed in Appendix E.

APPENDIX D

$$\begin{aligned}\sigma_{\ddot{y}}^2 &= \frac{1}{2\pi j} \int_{-j}^j s^2 \bar{\Phi}(s) ds & (D-3) \\ &= N_o^2 \pi^2 \sigma_y^2\end{aligned}$$

by Equation (D-3). The variance of the acceleration is given by

$$\sigma_{\ddot{y}}^2 = \frac{1}{2\pi j} \int_{-j\infty}^{j\infty} s^4 \bar{\Phi}(s) ds \quad (D-4)$$

In order for $\sigma_{\ddot{y}}^2$ to exist, it is necessary for $\bar{\Phi}(s)$ to be of the order of at least s^{-6} for large s . Passing white noise through a third-order dynamic system would give this sort of spectrum. Accordingly, the following form for $\bar{\Phi}$ is proposed:

$$\bar{\Phi}(s) = \frac{1}{|s^2 + \omega_n s + \omega_n^2|^2} \cdot \frac{k^2}{|\tau s + 1|^2} \quad (D-5)$$

The first term is suggested by the pilot using feedback to keep the aircraft on the desired track. It represents a second-order filter, with damping ratio fixed at 1/2. This represents a rather mild tendency to overshoot the desired position. The second term is selected rather arbitrarily to bring the system up to the desired order. $\bar{\Phi}$ may also be expressed as $f(s)f(-s)$ where

$$f(s) = \frac{K}{(s^2 + \omega_n s + \omega_n^2)(\tau s + 1)} \quad (D-6)$$

There are three unknown parameters in this model.

Selecting σ_y^2 , N_o , and $\sigma_{\ddot{y}}^2$ and utilizing equations (D-1), (D-2), (D-4), and (D-5) will define the closed loop frequency response. The values used initially for lateral deviations are

$$\sigma_y = 1500 \text{ feet}$$

APPENDIX D

$$N_o = 1/200 \text{ reversals/second}$$

$$\sigma_y = 1.5 \text{ feet/second}^2$$

Measured data taken from the American Airlines STOL evaluation program (utilizing an MDC-188) form the basis for σ_y and N_o (Ref. D-2). While the standard deviation en route was sometimes slightly greater, this could have been due to increased navigation errors. σ_y is an intuitive guess based upon flight experience and comfort levels. A 2σ value of lateral acceleration greater than 0.1 g is usually rated as irritating and uncomfortable.

Once these values are specified, the definite integrals must be evaluated before the model parameters can be determined. Definite integrals of the form

$$e = \frac{1}{2\pi j} \int_{-j\infty}^{j\infty} e_g(s)e_g(-s)ds \quad (D-7)$$

where

$$e_g(s) = c(s)/d(s) \quad (D-8)$$

$$c(s) = \sum_{k=0}^{n-1} c_k s^k \quad (D-9)$$

and

$$d(s) = \sum_{k=0}^N d_k s^k \quad (D-10)$$

frequently arise in mean square error parameter optimization. The values can be found in references D-3 and D-4 for example.

Using the tables for $N = 3$, the model parameters are found to be

$$\tau = 4.45 \text{ seconds}$$

$$\omega_n = 0.016 \text{ rad/second}$$

$$k = 4.47$$

APPENDIX D

Complete flight data on longitudinal and vertical deviations have not been found. Once these data are specified, the analysis for the longitudinal deviation proceeds as before. However, because longitudinal errors result in altitude errors during ascent or descent, the total error in the vertical plane due to guidance and control become

$$\sigma_z^2 = \sigma_h^2 + \sigma_x^2 \tan^2 \alpha$$

where α is the desired flight path angle and σ_h^2 and σ_x^2 are the altitude and along track guidance/control error variances.

The pilot/aircraft dynamics need not be modelled in as great a detail during the en route phase as in the terminal area. The time span between observed deviations and corrections increases since the need to correct for observed deviations is less acute and the navigation information is more coarse. As a result, the third order system postulated earlier can be greatly simplified with no appreciable degradation in the error analysis.

For the en route phase, the short time constant τ is dropped and the damped oscillatory response is approximated by a time constant defined by the envelope of the oscillatory response. The time constant defining the envelope in the terminal area is equal to

$$\frac{1}{\xi \omega_n} = \frac{1}{.008} = 125 \text{ seconds}$$

For the en route phase, it is postulated that the time constant would be roughly twice this number, possibly a little less. With these guidelines, the steering time constant for the en route phase is 200 seconds.

In order to reduce lateral errors due to external disturbances such as wind, it is important that the steering time constant be short compared to the disturbance time constant. However, too short a time constant requires greater steering efforts, which are not required if the disturbance frequencies are high and their amplitudes low.

APPENDIX D

References

- D-1 Rice, S. O., "Mathematical Analysis of Random Noise", Bell System Technical Journal, Vol. 23, 1944, pp. 282-322 and Vol. 24, 1945 pp. 46-156.
- D-2 MDC-188 (STOL Evaluation Program, MSE Report (October, 1969).
- D-3 Merriam, C. W., III, Optimization Theory and the Design of Feedback Control Systems, McGraw Hill Book Company, New York, 1964.
- D-4 Newton, G. C., Jr., Gould, L. A., and Kaiser, J. F., Analytical Design of Linear Feedback Controls, John Wiley & Sons, New York, 1957.

APPENDIX E

AIRCRAFT NAVIGATION GUIDANCE CONTROL ANALYSIS PROGRAM (ANGCAP) DESCRIPTION AND EXAMPLE OF RESULTS

Program Description

ANGCAP performs error and deviation analysis assuming linear propagation of dispersion from the nominal trajectory. Dispersion propagations are treated by solving in closed form the solution to the Ricatti differential equation for propagation of variance. Three different classes of state vector dispersions are stored internally. These classes are:

- (1) The actual deviation, \underline{d}_a , of the aircraft from the nominal trajectory
- (2) The estimate of the deviation, \underline{d}_e , of the aircraft from the nominal trajectory
- (3) The navigation error, \underline{e} , as predicted by a Kalman filter.

The Class 1 state vector represents true aircraft conditions and should be referred to for computing statistics regarding the aircraft behavior. Class 2 states represent the only information available to the pilot or other control systems. Class 3 states were included to permit evaluation of the accuracy of suboptimal filters. As will be shown in the discussion of the data, statistics describing the error sources are specified both as assumed for the real world and as assumed by the filter. This permits investigating modeling discrepancies for filter stability analysis. Each of the classes of state vector has nine elements:

- 1-3, the aircraft position in a local coordinate system (magnetic east, north, vertical)
- 4-5, random wind velocities in magnetic East and North coordinates;
- 6-9, navigation aid dispersion biases in range and azimuthal measurements.

APPENDIX E

It should be noted that aircraft velocity is not treated directly as a state. It is assumed that the aircraft motion relative to the moving air mass is determined by the steering law. Thus, velocity is wind velocity plus the computed deviations in position times the steering coefficients.

From the state vectors discussed above and their linear statistics (covariances), statistics of a number of important parameters may be computed. For example, some output is presented in crosstrack, along track, and vertical coordinates for more convenient interpretation.

Linear Models. - The state vectors and covariances discussed above are propagated internally in ANGCAP utilizing closed-form formulae for the state transition matrix and additive noise of a linear navigation and control system. The state transition and additive noise matrices are comparable to A and Q in a discrete filter as discussed in Appendix C. The propagation and control model assumes the aircraft is flown in the following manner. The pilot or automatic control system compares the navigation solution to the desired nominal trajectory and makes adjustments to the direction and magnitude of the velocity of the aircraft relative to the random moving atmosphere (winds). These adjustments are made to steer out indicated deviations in along track crosstrack and vertical coordinates utilizing a corresponding set of time constants known as T_{steer} . It is well recognized that the reduction of the dynamics of the aircraft under the control of the pilot or automatic control system to a simple linear first order model ignores many of the problems associated with the design and analysis of such systems. It is felt, however, that this model is sufficiently accurate to represent the controllability of the aircraft for the purposes of establishing dispersions entering the MLS coverage area after the cruise and terminal area operations. It should be realized that this model is entirely insufficient to describe behavior of the aircraft during short periods of critical operation such as final approaches, particularly in the coverage of a MLS system.

Additional features of ANGCAP will be discussed in the following sections describing input data requirements and sample output.

Input Data Description

Figure E-1 shows the input data describing the airports, radio navigation aids, and MLS systems.

Airports are identified by both an index and a three-letter alphabetic code. The position of the airport is entered as a latitude

AIRPORTS	LATITUDE	LONGITUDE	BOUNDRY	COM.PATH	HEADING	MLS TYPE	TERM.NAV.AIDS	EAST	NORTH
1 SAC	38 34 -0.0	121 30 -0.0	15.0	2.0	200.0	4	5	-110.21	123.98
2 SHA	33 36 -0.0	117 50 -0.0	15.0	2.0	190.0	4	19	144.42	-197.39
3 SJC	37 23 -0.0	121 53 -0.0	15.0	2.0	300.0	4	1	-110.47	50.77

RADIO NAVIGATION AIDS

INPUT DATA FROM NAFEC, ANA-251, AND AIRWAY FACILITIES SERVICES, AAF-240

NO.	NAME	CLASS	LATITUDE	LONGITUDE	ELEVATION	MAG.VAR.	EAST	NORTH
1	SAN JOSE	L-VOR/DME	37 21 53.0	121 55 45.0	50.	17.	-111.54	52.42
2	WOODSIDE	L-VOR/DME	37 23 53.0	122 16 49.0	2213.	17.	-128.13	49.59
3	OAKLAND	M-VOR/DME	37 43 33.0	122 17 21.0	10.	17.	-130.63	69.39
4	SAN FRANCISCO	L-VOR/DME	37 36 50.0	122 21 28.0	10.	17.	-134.99	61.07
5	SACRAMENTO	M-VOR/DME	38 26 37.4	121 33 2.0	10.	17.	-111.58	119.97
6	LIVERM	M-VOR/DME	38 4 28.8	121 0 10.1	350.	17.	-80.82	105.97
7	FRESNO	M-VOR/DME	36 53 12.4	119 48 11.0	301.	17.	-6.05	153.74
8	REKERSFIELD	M-VOR/DME	35 29 4.6	119 5 46.9	550.	16.	51.15	-17.12
9	GORHAM (E)	M-VOR/DME	34 48 15.0	118 51 45.0	4239.	16.	74.16	-52.91
10	SEAL BEACH (E)	M-VOR/DME	33 47 30.0	118 3 30.0	30.	16.	130.55	-99.01
11	VENTURA (E)	M-VOR/DME	34 7 0.0	119 3 10.0	500.	16.	77.39	-95.01
12	FELLOAS	L-VOR/DME	35 5 35.2	119 51 52.6	3470.	16.	21.84	-50.32
13	PIREST	M-VOR/DME	36 8 27.2	120 20 50.1	3480.	16.	-33.26	-1.06
14	FILLMORE (E)	M-VOR/DME	34 21 30.0	118 52 45.0	1000.	16.	81.26	-78.13
15	AVENAL	M-VOR/DME	35 38 40.2	119 58 39.4	710.	16.	7.07	-20.01
16	PASO ROBLES	L-VOR/DME	35 40 21.0	120 37 33.7	620.	16.	-23.69	-27.53
17	PORTERVILLE	L-VOR/DME	35 54 47.2	119 1 11.6	580.	16.	47.18	8.53
18	LOS RAMOS	L-VOR/DME	36 42 55.4	120 46 39.4	2400.	17.	-48.09	30.56
19	MERCED	L-VOR	37 13 9.9	120 23 57.3	180.	17.	-39.10	64.78
20	SALINAS	M-VOR/DME	36 39 49.9	121 36 7.4	80.	17.	-85.30	16.30
21	SANTA ANA	L-VOR	33 40 43.2	117 51 45.0	40.	15.	141.98	-103.30
22	STOCKTON	M-VOR/DME	37 50 1.2	121 10 13.3	40.	17.	-84.48	89.80
23	NAPA	L-VOR/DME	38 10 45.9	122 22 19.4	0.	17.	-144.51	93.67

PLS TYPE	ELEVATION (DEG.)	WIDTH (DEG.)	MAX.RANGE (N.M.)
1	CONFIO.D	8.0	30.0
2	CONFIO.E	20.0	20.0
3	CONFIO.F	20.0	30.0
4	CONFIO.G	20.0	20.0
5	CONFIO.I	40.0	20.0
6	CONFIO.K	20.0	20.0

FIGURE E-1. DESCRIPTION OF THE AIRPORTS, RADIO NAVIGATION AIDS, AND MLS SYSTEMS

APPENDIX E

and longitude (degrees, minutes and seconds). The radius to the boundary of the airport's controlled air space is also required. Landing operations are defined by the length (nautical miles) of the common path utilized by STOL aircraft and the runway heading. The MLS type available at that airport is specified by an index. One or two navigation aids (VOR/DME) available for use in the terminal area are specified by indices. For example, airport number 1, Sacramento, has VOR/DME Station Number 5 available in the terminal area. The zero indicates no secondary station is available. For convenience in interpreting the output, the latitude and longitude of each airport is converted into magnetic east and north coordinates (nautical miles) relative to a reference point specified in the data.

Radio Navigation Aids. - As shown in the center of Figure E-1, radio navigation aids are identified by both a numeric index and a label. The class of each station indicates whether VOR and/or DME information is available from that station. The L and H, specifying low or high frequency stations, are not used by the program. The position of each station is specified as a latitude, longitude, and elevation (altitude). Local magnetic variation must also be specified to permit interpreting bearings as magnetic rather than true. For convenience in interpretation of results, the station's latitude and longitude are also converted to east and north coordinates.

Microwave Landing System Definitions. - The coverage of each of the microwave landing system configurations is defined at the bottom of Figure E-1. The coverage is specified by the elevation angle above the horizon (degrees), the width of the beam measured from the center line (degrees), and the maximum range of the beam (nautical miles).

Default Data Values. - Some items of data are stored internally in the program as default values which will be utilized by the code unless an overriding number is specified. To avoid confusion in interpretation of results, each run tabulates all default values contained in the program as shown in Figure E-2. If, in a given run, any of these data were to be changed, the changed values would be shown in the output. The following list defines each of the default data items and its value.

- (1) VAPRCH, 100 knots, the approach velocity of the aircraft for terminal operations prior to a landing.
- (2) THCOMP, 7 degrees, the angle of descent on the common path (glide slope).

APPENDIX E

- (3) BNKANG, 25 degrees, the bank angle for turns in the terminal area.
- (4) THDSCN, 3 degrees, the flight path angle for descent into the terminal area .
- (5) TSTABL, 120 seconds, the time period allowed for stabilization after completing the descent into the terminal area prior to entering the MLS beam.
- (6) HAPRCH, 1000 feet, the approach altitude at which the aircraft enters the MLS beam.
- (7) DMIN, 400 feet, the minimum distance allowable after completing the turn to the final path before beginning the descent on the glide slope,
- (8) TSTRCR, zero, 200 seconds, zero, the steering time constants during cruise.
- (9) TSTRAP, zero, 60 seconds, 60 seconds, the steering time constants during approach maneuvers.
- (10-11) TAUADA and TAUADM, the auto correlation times in seconds for the altimeter, east and north winds during enroute operations and east and north winds in the terminal area. The suffices A or M indicate the values assumed for the actual winds and the values assumed in the Kalman filter model.
- (12-13) SIGADA and SIGADM, the standard deviation of errors associated with the altimeter, east and north winds during enroute operations and east and north winds in the terminal area. Altimeter errors are in feet, and wind errors are in nautical miles per hour.
- (14-15) STNA and STNM, are the white noise error of VOR/DME measurements, actual and model. For example, STNA in Figure E-2 shows that the white noise assumed in the actual stations is 0.1 degree in bearing and 1 n.mi. in range.
- (16-17) STBA and STBM are similar values for the standard deviation of the station bias errors.

APPENDIX E

The program repeats some of the data shown in Figure E-2 in the form of Figure E-3 for more easy interpretation. Figure E-3 shows the altitude and velocity sensing errors from the altimeter and air data system. The locations of the stations to be utilized in a particular leg and their error values are also listed.

En Route Waypoints

En route way points are specified in ANGCAP with data cards identical to those used in STOL OPS. Figure E-4 is a printout of the en route waypoint data and is very similar to the waypoint data printout of STOL OPS. It should be noted that waypoints are specified in terms of a distance and bearing from one of the VOR/DME stations. The other two VOR/DME station indices associated with each waypoint indicate the stations used for navigation when approaching that waypoint. Altitude indicates the altitude at that waypoint and airspeed, the speed approaching the waypoint. The position (distance and bearing) of the last waypoint in each leg is disregarded by the code. Instead, a set of waypoints for terminal area operations is computed from parameters including glide slope angle, common path length, approach speed, approach velocities, etc., as described in the following section.

SHISNAT

(1) VAPRCM = 7.1E+03

(2) TMCOMP = 27.7E+01

(3) INKANG = 3.25E+02

(4) TMO3CN = 5.3E+01

(5) TSTARL = 5.12E+03

(6) MAPRCM = 5.1E+04

(7) DMIN = 5.4E+03

(8) TSTACR = 0.0, 0.2E+03, 0.0

(9) ISTRAP = 1.0, 0.6E+02, 0.6E+02

(10) AUADA = 1.0, 0.36E+03, 0.36E+03, 0.18E+03, 0.18E+03

(11) AUADM = 1.0, 0.36E+03, 0.36E+03, 0.18E+03, 0.18E+03

(12) IGANA = 1.5E+02, 0.4E+02, 0.4E+02, 0.1E+02, 0.1E+02

(13) IGADM = 1.5E+02, 0.4E+02, 0.4E+02, 0.1E+02, 0.1E+02

(14) INA = 1.1E+00, 0.1E+01

(15) THM = 1.1E+00, 0.1E+01

(16) TBA = 0.14E+03, 0.1E+01

(17) THP = 1.14E+00, 0.1E+01

1. END

APPENDIX E

FIGURE E-2. DEFAULT VALUES

NAVIGATION SYSTEM DATA USED IN THIS RUN

ALTITUDE/VELOCITY SENSING ERRORS		ACTUAL		FILTER MODEL	
CROSS	ALTITUDE (FT)	SIG. DEVIATION (F/S)	AUTOCORRELATION TIME (SEC)	SIG. DEVIATION (F/S)	AUTOCORRELATION TIME (SEC)
	50.00	50.00	50.00	50.00	50.00
	67.51	67.51	360. SEC.	67.51	360. SEC.
	67.51	67.51	360. SEC.	67.51	360. SEC.
TERMINAL AREA					
	16.88	16.88	180. SEC.	16.88	180. SEC.
	16.88	16.88	180. SEC.	16.88	180. SEC.

STATION 1 SAN JOSE LOCATION = -117.50 NM EAST, 52.42 NM NORTH, 50. FT ALTITUDE

ACTUAL		FILTER MODEL	
ONE SIGMA ERRORS	BIAS	WHITE NOISE	TOTAL
0-15 RANGE (NM)	0.14	0.10	0.14
VOR BEARING (DEG)	1.00	1.00	1.00

STATION 2 OAKLAND LOCATION = -123.63 NM EAST, 69.39 NM NORTH, 10. FT ALTITUDE

ACTUAL		FILTER MODEL	
ONE SIGMA ERRORS	BIAS	WHITE NOISE	TOTAL
0-15 RANGE (NM)	0.14	0.10	0.17
VOR BEARING (DEG)	1.00	1.00	1.41

STATION 3 SACRAMENTO LOCATION = -117.50 NM EAST, 139.97 NM NORTH, 10. FT ALTITUDE

ACTUAL		FILTER MODEL	
ONE SIGMA ERRORS	BIAS	WHITE NOISE	TOTAL
0-15 RANGE (NM)	0.14	0.10	0.17
VOR BEARING (DEG)	1.00	1.00	1.41

STATION 4 LINCOLN LOCATION = -85.02 NM EAST, 105.97 NM NORTH, 260. FT ALTITUDE

ACTUAL		FILTER MODEL	
ONE SIGMA ERRORS	BIAS	WHITE NOISE	TOTAL
0-15 RANGE (NM)	0.14	0.10	0.17
VOR BEARING (DEG)	1.00	1.00	1.41

APPENDIX E

FIGURE E-3. NAVIGATION ERROR COEFFICIENTS

SCHEDULE										WAYPOINTS			
DEPARTURE AIRPORT	GATE DEPARTURE	TAKEOFF AIRPORT	LANDING AIRPORT	GATE ARRIVAL	DISTANCE (NM)	BEARING (DEG)	VOR/DME STATION	ALTITUDE (FT)	AIRSPEED (KTS)				
SJC					18.	9.	1 1 3	11000.	400.				
					30.	175.	5 1 3	11500.	400.				
					0.	0.	5 5 6	9000.	250.				
SAC					18.	113.	5 5 22	21000.	475.				
					0.	0.	6 6 22	21000.	475.				
					43.	124.	6 6 22	21500.	475.				
					0.	0.	7 7 13	21000.	475.				
					42.	141.	7 7 13	21000.	475.				
					0.	0.	8 8 15	21000.	475.				
SNA					30.	146.	8 8 16	21000.	475.				
					0.	0.	9 9 16	21000.	475.				
					15.	88.	9 9 17	21000.	475.				
					19.	319.	10 10 14	21000.	475.				
					6.	0.	10 10 14	9000.	250.				
SJC					0.	0.	10 10 14	20000.	475.				
					31.	235.	10 10 14	21000.	475.				
					0.	0.	11 11 14	20000.	475.				
					27.	316.	11 11 16	20000.	475.				
					0.	0.	12 12 16	20000.	475.				
					40.	312.	12 12 15	21000.	475.				
					6.	0.	13 13 15	20000.	475.				
					42.	306.	13 13 20	20000.	475.				
					30.	122.	1 1 22	20000.	475.				
					0.	0.	1 1 22	10000.	250.				

APPENDIX E

FIGURE E-4. CRUISE (EN ROUTE) WAYPOINTS

APPENDIX E

Determination of Waypoints For Transition to Final Approach and Landing

As depicted in Figure E-5, successful transition from terminal area approach to final approach along the common path is dependent upon: (1) the location of the waypoint designating the length of the common path, (2) the aircraft performance characteristics, (3) the microwave landing system (MLS) coverage, and (4) the statistics representing position and velocity deviations from nominal at MLS acquisition.

If it is assumed that the pilot desires to have the aircraft stabilized on the extended runway center line at the waypoint designating length of the common path prior to initiating the pitchover, the sequence of maneuvers might be:

- (1) Transition from descent to level flight at desired pitch over altitude for glide slope intercept [designated as (1) in Figure E-5]
- (2) Initiation of turn onto common path [designated as (2) in Figure E-5]
- (3) Complete turn onto common path [designated as (3) in Figure E-5], stabilize, perform sidestep maneuver, stabilize and initiate pitchover to intersect glide slope [designated as (4) in Figure E-5].
- (4) On glide slope on common path [designated as (5) in Figure E-5].

Turn Onto Common Path Maneuver.- Two possibilities exist for the actual turn maneuver. The first assumes the turn is a coordinated turn during which altitude is maintained and the bank angle is limited to a maximum value. For this case, the turn radius, R_T , and rate of turn are a function of velocity, V , bank angle, ϕ , and normal load factor, i.e.,

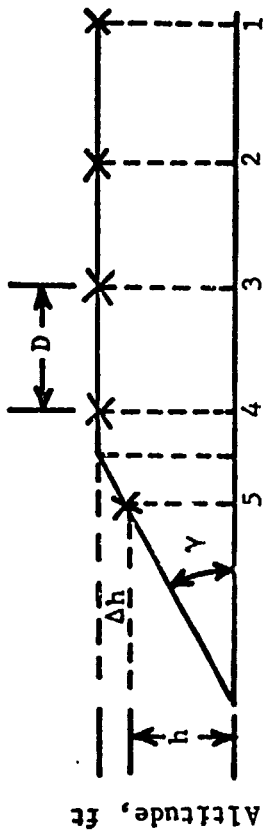
$$L \cos \phi = W$$

$$L \sin \phi = C.F. = \frac{W^2}{gR_T}$$

$$L \sin \phi = \frac{L \cos \phi V^2}{gR_T}$$

$$R_T = \frac{V^2}{g \tan \phi}$$

where L = lift
 W = weight .



Along Track Distance From Touchdown

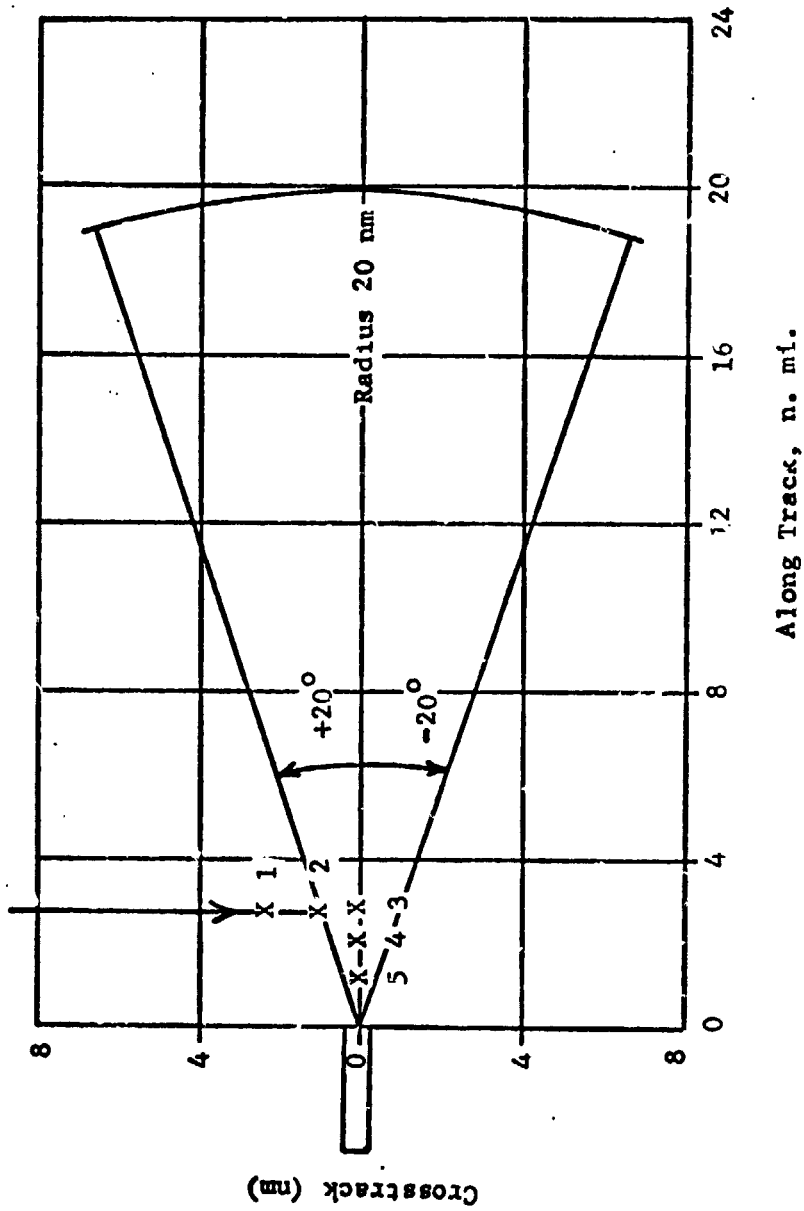


FIGURE E-5. VERTICAL AND HORIZONTAL PLANE FLIGHT PROFILES IN TERMINAL AREA

APPENDIX E

The second case assumes a constant rate of turn is maintained. In this case

$$\frac{MV^2}{R_T} = MV \dot{\psi}$$

$$R_T = \frac{V}{\dot{\psi}}$$

$$\phi = \tan^{-1} \left(\frac{V \dot{\psi}}{g} \right)$$

If the first case is considered with $V = 100$ knots, $g = 32.174 \text{ ft/sec}^2$, and $\phi = 30^\circ$, $R_T \approx 1535 \text{ ft}$. The accepted practice under instrument flight rules is to use a $3^\circ/\text{sec}$ turning rate. For $V = 100$ knots, this yields $R_T = 3226 \text{ ft}$ and $\phi = 15^\circ 22'$. A thorough analysis and experimental program is required to determine which is the better turn maneuver procedure.

Ideally, the point to initiate the turn is a function of the radius of turn, R_T , and the nominal common path intercept angle. Referring to Figure E-6, the horizontal intercept geometry relationships are:

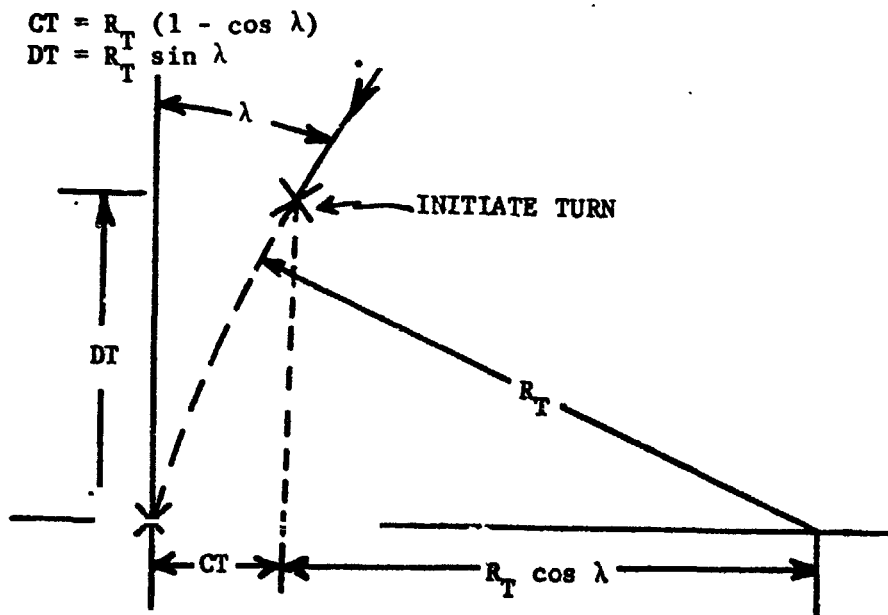


FIGURE E-6. HORIZONTAL INTERCEPT GEOMETRY

APPENDIX E

Table E-1 lists the desired point to initiate the turn referenced downtrack (DT) and crosstrack (CT) from the waypoint on the extended centerline for three turn radii. The crosstrack coverage of the MLS is also given for a 20° azimuth as a function of common path length, L. Figure E-7 is a plot depicting the turn initiation point as a function of intercept angle for $R_T = 1335$ feet.

Sidestep Maneuver. - In setting the length of the common path, designated as waypoint (3) in Figure E-5, an along track distance allowance, D, must be made to permit performing a sidestep maneuver after completing the nominal turn onto the common path. Normal IFR procedures involve stabilizing on the heading of the runway after completing the turn maneuver and then initiating a sidestep maneuver to correct for crosstrack error, y_0 , due to a variety of errors such as:

- (1) Rolling to wings level too early or late compared with the nominal time
- (2) Holding an incorrect bank angle
- (3) Velocity errors when the turn is initiated
- (4) Initiating the turn too soon or late compared with the nominal waypoint for turn initiation.
- (5) Winds

The along track distance, D, the aircraft traverses while performing a sidestep maneuver can be determined as a function of the following parameters:

- (1) V = approach velocity, ft/sec,
- (2) T = time to roll to ϕ , seconds,
- (3) ϕ = bank angle (suggested as 12° in Ref. E-1)
- (4) y_0 = initial crosstrack error to be removed.

The sequence of the sidestep maneuver is depicted in Figure E-6. Let

$$t = \text{duration of each } \phi^\circ \text{ bank turn} = 1/2 \left(\frac{D}{V} - 4T \right).$$

The lateral acceleration during each turn is given by

$$a = g \tan \phi.$$

TABLE E-1. TYPICAL TURN INITIATION COORDINATES
REFERENCED TO COMMON PATH WAYPOINT

R_T , ft	λ , deg	CT, ft	DT, ft	Common Path Length, ft	MLS Crosstrack Coverage
1335	15	45.48	345.52	3040	1106.47
1335	30	178.85	667.50	6080	2212.94
1335	45	391.01	943.99	12160	4425.86
1335	60	667.50	1156.15		
1335	75	989.48	1289.52		
1335	90	1335.00	1335.00		
1535	15	52.30	397.29		
1535	30	205.64	767.50		
1535	45	449.59	1085.41		
1535	60	767.50	1329.35		
1535	75	1137.71	1482.70		
1535	90	1535.00	1535.00		
3226	15	109.91	834.95		
3226	30	432.19	1613.00		
3226	45	944.86	2281.14		
3226	60	1613.00	2793.81		
3226	75	2391.05	3116.09		
3226	90	3226.00	3226.00		

APPENDIX E

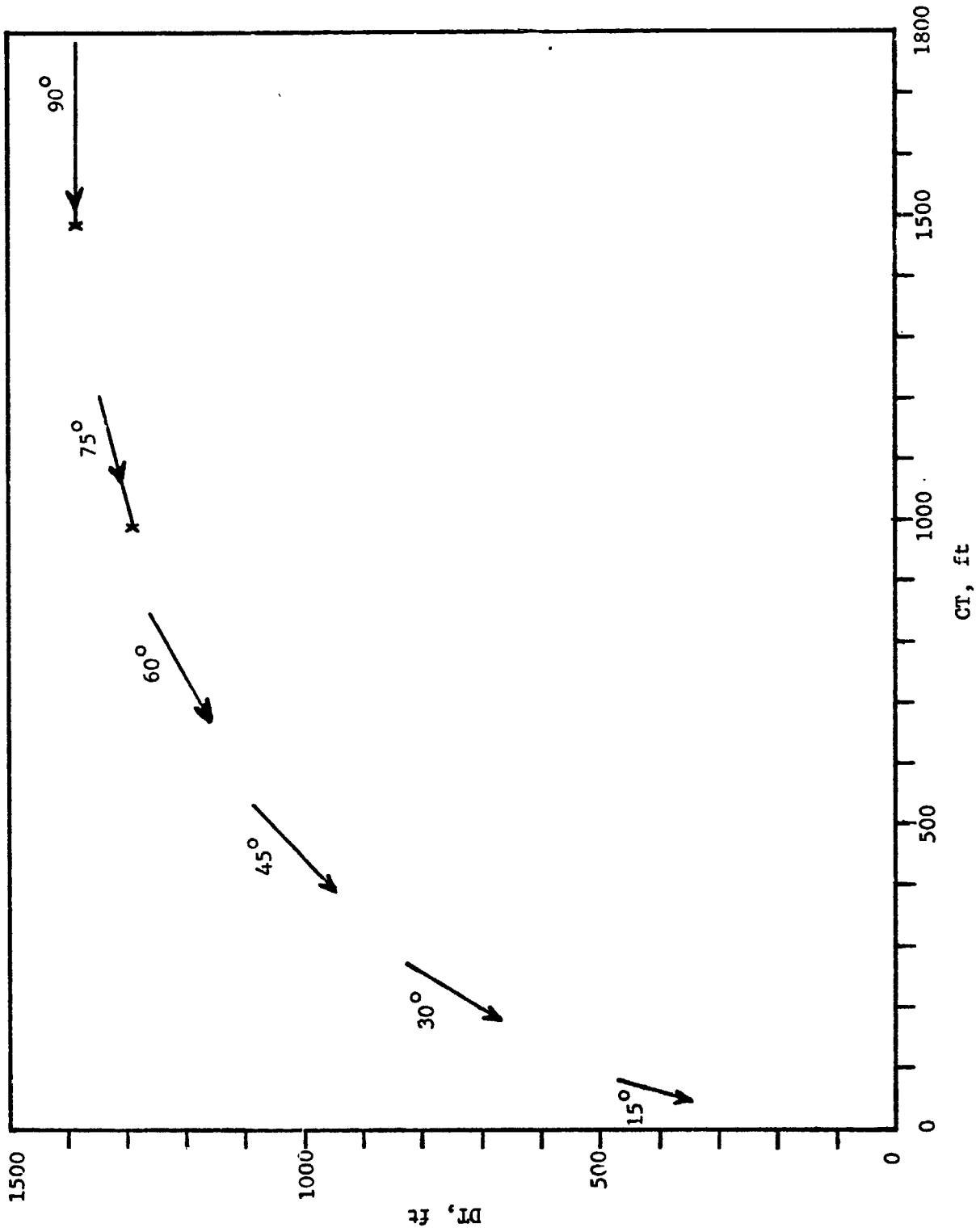
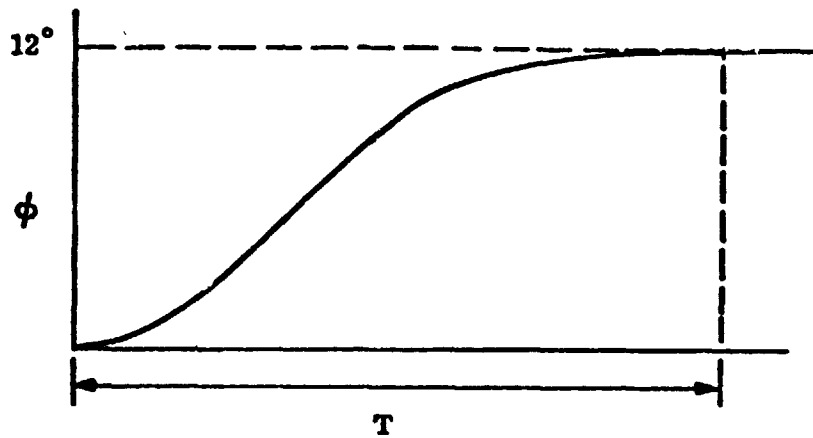
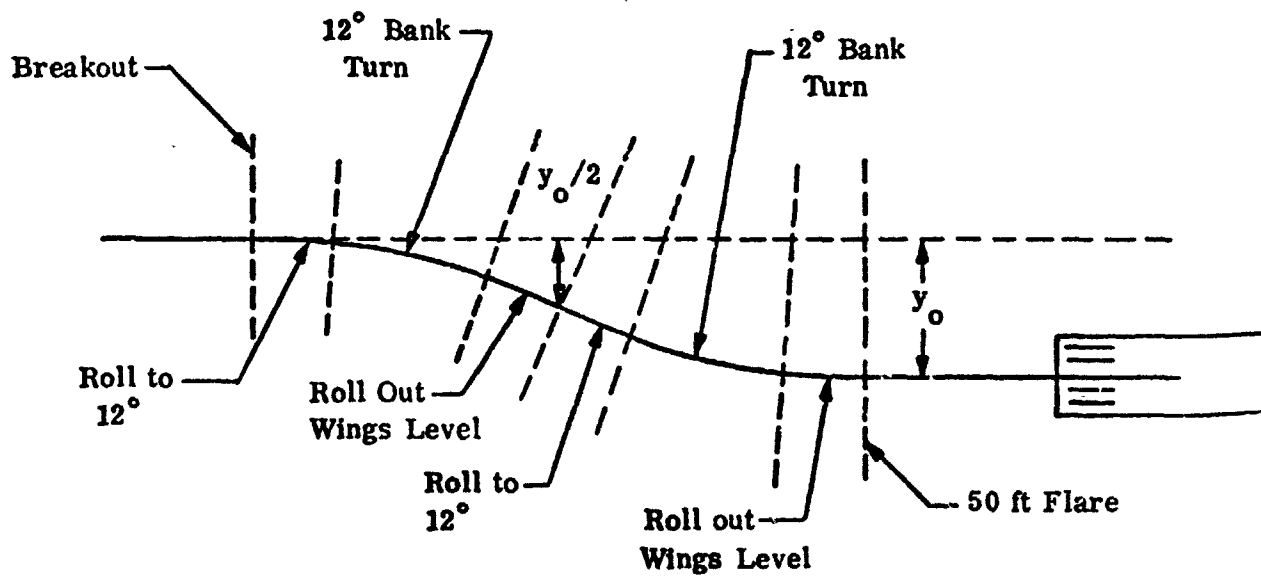


FIGURE E-7. TURN INITIATION HORIZONTAL PLANE COORDINATES FOR $R_T = 1335$ FEET AND INTERCEPT ANGLES SHOWN



a. Generalized Roll Maneuver



b. Components of Corrective S-Turn Maneuver
(Ref. E-1)

FIGURE E-8. SEQUENCE OF SIDESTEP MANEUVER

APPENDIX E

The lateral velocity and distance traveled while the aircraft rolls to \emptyset is negligible.

Hence, the crosstrack error is approximately equal to twice the lateral position gained during each \emptyset roll maneuver, that is

$$y_o \cong 2[1/2 a t^2]$$

$$= g \tan \emptyset (1/4) \left(\frac{D^2}{V^2} - 8 \frac{DT}{V} + 16T^2 \right)$$

$$y_o = \frac{g \tan \emptyset}{4V^2} (D^2 - 8DTV + 16T^2V^2) .$$

Rearranging to solve the required longitudinal distance, D, to correct for an initial lateral displacement error, y_o , yields

$$D^2 - 8DTV + 16T^2V^2 - \frac{4V^2 y_o}{g \tan \emptyset} = 0$$

or

$$D = 4TV + 2V \sqrt{\frac{y_o}{g \tan \emptyset}} .$$

In both constant bank angle and constant rate of turn approaches, pilot induced and wind induced lateral errors of 400 feet can be expected. For example, if $\emptyset = 30^\circ$, T equals 2 seconds, and V equals 100 knots, then D becomes 2934 feet.

The minimum total common path length, L, is given by the sum of the ground distance traversed from pitchover to landing including intercepting the glide slope at altitude, h, plus D, i.e.,

$$L = \frac{Z}{\tan(\text{glide slope angle})} + D = \frac{Z}{\tan \gamma} + D ,$$

where Z = altitude at pitchover initiation.

To be conservative, the effect of stabilization times before, T_B , and after, T_A , the sidestep maneuver should be included as well as the distance traversed toward the runway during the pushover from level flight to the glide slope. In this case,

APPENDIX E

$$L = (Z/\tan \gamma) + D + VT_B + VT_A + VT_P$$

Nominally, T_B and T_A may be equal with a 2-second magnitude, and $T_P = 12$ seconds. For $\gamma = 100$ knots = 168.9 ft/sec, $\gamma = 7^\circ$, $T_B = T_A = 2$ seconds, and $T_P = 12$ seconds

$$VT_B + VT_A + VT_P \approx 676 + 2165 = 2841$$

This value is less than D and, therefore, the equation for determining the length of the common path was selected as

$$L = (Z/\tan \gamma) + D$$

to avoid being overly conservative. Clearly, if an additional term is to be added in the future, it should be VT_P .

To determine whether MLS coverage exists before the initial turn assuming no sidestep or stabilization, consider the case depicted in Figure E-9 for a $7\text{-}1/2^\circ$ glide slope with a 1000-foot minimum altitude. Typical results are given in Table E-2 for various turn radii, R_T .

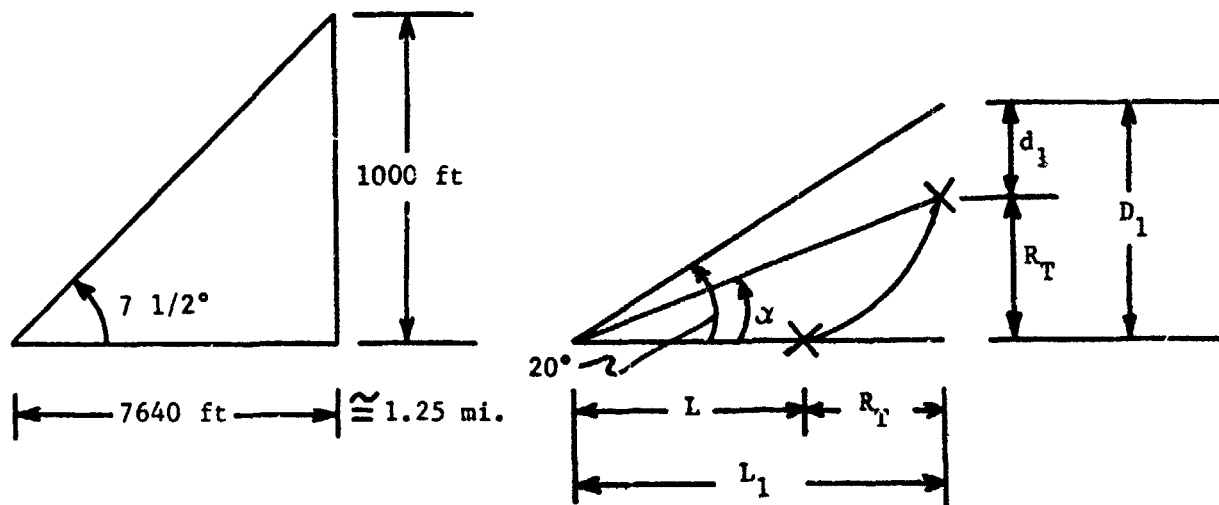


FIGURE E-9. EXAMPLE OF MLS ACQUISITION AND TURN ONTO COMMON PATH

APPENDIX E

TABLE E-2. TYPICAL RESULTS RELATING TURN INITIATION AND MLS ACQUISITION

Radius of turn, ft	1000	2000	3000	4000
Length ($R_T + 7640$), ft	8640	9640	10640	11640
α ($\tan^{-1} \frac{R_T}{R_T + 7640}$), deg	6.5	12	16.40	20
$D_1 = L_1 \tan 20^\circ$, ft	2940	3300	3740	4000 ft
$d_1 = D_1 - R_T$, ft	1940	1300	740	0
$t = \frac{d_1}{V} = \frac{d_1}{169}$, sec	11.5	7.7	4.4	0

Hence, for approaches considered here, the aircraft will always be under MLS coverage prior to turning if it can theoretically transition to the glide slope at 1000 foot altitude .

Pushover Maneuver

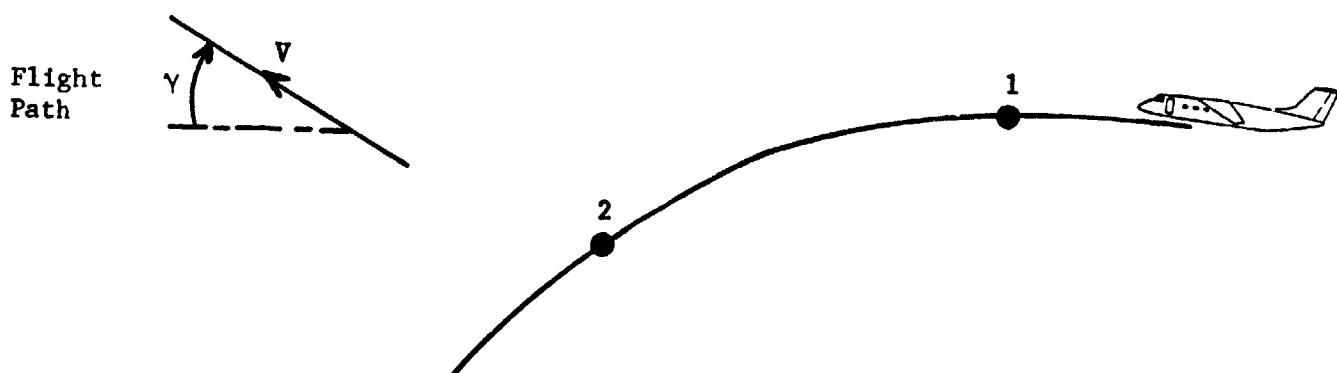


FIGURE E-10. PUSHOVER MANEUVER

As depicted in Figure E-10, assume "pushover" to descent is a constant V maneuver accomplished as follows:

At point "1" a AC_L reduction is abruptly initiated to create a tolerable reduction in load factor n to a value less than 1.0. From that point on, thrust

APPENDIX E

is reduced on a schedule to keep V constant throughout the pushover. Upon reaching the desired descent angle (γ_2), C_L is abruptly increased to reestablish trim at the constant V still being flown. The elapsed time, distance covered, and altitude lost during the maneuver (from point 1 to point 2) is found as follows:

$$\text{Now } mV\dot{\gamma} = L - W \cos \gamma.$$

$$\text{Also, } ng = \frac{L}{m} \text{ or } L = nmg.$$

$$\text{Therefore, } mV\dot{\gamma} = nmg - mg \cos \gamma$$

$$\text{or } \dot{\gamma} = \frac{g}{V} [n - \cos \gamma].$$

Assume γ is always sufficiently small such that $\cos \gamma = 1$.

$$\text{Then } \dot{\gamma} = \frac{g}{V} [n - 1].$$

Let the pushover $n = 0.95$.

$$\text{Then } \dot{\gamma} = -0.05 \frac{g}{V}.$$

The elapsed time for maneuver is (assume $\gamma_1 = 0$)

$$t = \frac{\gamma_2}{\dot{\gamma}} = - \frac{V\gamma_2}{0.05g}.$$

Let $g = 32.174$ and $\gamma_2 = -7^\circ = -0.122$ radians, then

$$t = 0.0759V(\text{sec}).$$

The horizontal distance traveled is

$$x = Vt = 0.0759V^2.$$

Now

$$\ddot{h} = V\dot{\gamma} = V \left\{ \frac{g}{V} [n-1] \right\}$$

$$\text{or } \ddot{h} = g [n-1]$$

$$\text{or, for } n = 0.95$$

$$\ddot{h} = 32.174 [-.05] = -1.609.$$

The altitude loss during the pushover is

$$\Delta h = 1/2 \ddot{h} t^2 = 1/2 (-1.609) (.0759)^2 V^2$$

$$\Delta h = -0.0046 V^2.$$

In summary then, for $\gamma_2 = -7^\circ$,

$$\begin{aligned}t &= 0.0759V \\x &= 0.0759V^2 \\ \Delta h &= -0.0046V^2\end{aligned}$$

Now take the case where $V = 100$ knots = 168.9 ft/sec.
 $V^2 = 28,527$ ft²/sec²

and

$$\begin{aligned}t &\approx 12.82 \text{ seconds} \\x &\approx 2165 \text{ ft} \\ \Delta h &\approx 131 \text{ ft}\end{aligned}$$

If x is included in the common path length input to the program, then

$$L = (h/\tan \gamma) + x + D.$$

Part of x is included if $L = (Z/\tan \gamma) + D.$

Therefore, the program has input $L, D_{\text{MIN}}, Z,$ and $\gamma.$ The program solves for D as follows:

$$D = L - (Z/\tan \gamma) - D_{\text{MIN}}.$$

D_{MIN} could be considered to include that part of x not included by $Z \tan \gamma.$

Therefore, the location of the waypoint to initiate the turn on final is given by

$$\begin{aligned}X &= L + R_T \\Y &= R_T \\Z &= h + \Delta h\end{aligned}$$

referenced to the runway centerline and elevation.

The location of the waypoint denoting the common path length is given by:

$$\begin{aligned}X &= L \\Y &= 0 \\Z &= h + \Delta h\end{aligned}$$

referenced to the runway centerline and elevation.

APPENDIX E

Table E-3 defines the two waypoints for $\gamma = 7^\circ$, $V = 100$ knots, $T = 2$ seconds, $y_0 = 400$ feet, $\theta_{\text{initial}} = 30^\circ$, $\theta_{\text{sidestep}} = 12^\circ$, and $h = 869$ feet.

TABLE E-3. EXAMPLE OF FINAL APPROACH
WAYPOINTS WITH 90° INTERCEPT

<u>Initiate Turn</u>		<u>Common Path</u>
X(ft)	13,614	12,079
Y(ft)	1,535	0
Z(ft)	1,000	1,000
V(knots)	100	100

At this common path length the 20° MLS azimuth and elevation coverages are 4396.4 feet crosstrack and vertical. For $R_T = 1535$, the aircraft would have nominally tracked the MLS for 2861.4 feet which is equivalent to about 17 seconds of flight within the beam.

Approach Waypoints.-ANGCAP computes approach waypoints for the transition from the cruise flight utilizing cruise waypoints to the final approach discussed in the previous section. A 90-degree turn onto the common path is assumed in creating the approach waypoints. Working backwards toward the en route waypoints, a period of level flight for stabilization after descent is used to establish the pull out from the descent. The descent is assumed to be made at the average of the en route and approach velocities. With the descent flight path angle (specified as a parameter in the data), the location of the beginning of the descent from cruise altitude can be computed. With these computations completed, the location of a final en route waypoint along a line 90 degrees from the runway heading and offset by a distance computed from the stabilization time and descent distance is created. This waypoint's position is used as the final waypoint of the en route data.

APPENDIX E

Typical ANGCAP Output

One run of ANGCAP can perform a number of analysis cases. Each case consists of the analysis of a flight from an origin to a destination airport. The analysis is for a specific system configuration defined by the type of update (Kalman or Position Fix) the number of VOR receivers (0, 1 or 2) and the number of DME receivers (0, 1 or 2). The update frequency must also be specified. Experience has shown that a frequency of approximately one update every 2 minutes is sufficient for most analyses. If desired a detailed printout of deviations during cruise operations as shown in Figure E-11 may be obtained. As shown in Figure E-12, a summary is obtained for each case. Finally, a summary of all cases in a run is printed as shown in Figure E-13.

Detailed Cruise Output. - The cruise output is divided into blocks of information at each time during the flight. For example, consider the output of Figure E-11(a). Since errors generated early in the flight have little impact on the final approach values, the analysis of takeoff is very crude. As shown between the two rows of X's near the top of Figure E-11(a), takeoff is analyzed as a discontinuous speed change to the cruise velocity of 400 knots. A flight path is then computed from the coordinates of the originating airport and the first cruise waypoints. During this and all subsequent cruise segments, output is shown before and after each update. For example, consider the output at 4 minutes shown in the middle of Figure E-11(c). Conditions prior to and after the Kalman update are printed. For each time, the first two rows of information are the k values of the true state estimation errors and the values the filter would assume for the errors. These are expressed in the state variables of the problem as labeled. It should be noted that in this run the actual and model values of autocorrelation times and standard deviations of navigation error sources were assumed identical. Thus, these two rows are equal for all blocks. The aircraft's nominal trajectory and the 1σ deviations of the actual state and estimated state are then shown. For ease of interpretation the actual and estimated state dispersions in the down range direction are expressed in terms of time of passage rather than position. Finally the 1σ control effort values are shown. These are obtained by multiplying the estimated state deviations by the controlled gains associated with the parameter T_{steer} . For this run T_{steer} during cruise was specified to be zero with the exception of the crosstrack component. Thus, no control

TIME 0.00 MIN. EAST-POS. NORTH-POS. ALT. BIAS VE-BIAS VN-BIAS
CASE 1 NAUT. MILES NAUT. MILES FEET FEET/SEC FEET/SEC FEET/SEC
TRUE ERROR 0.000 0.000 50.000 67.512 67.512 67.512
FILTER ESTIMATE OF ERROR 0.000 0.000 50.000 67.512 67.512 67.512

MEASUREMENTS OF RANGE-1= 1.97, THETA-1= 147.00, RANGE-2= 27.44, THETA-2= 132.72.
KALMAN UPDATE

TIME 0.00 MIN. EAST-POS. NORTH-POS. ALT. BIAS VE-BIAS VN-BIAS RANGE BIAS ANGLE BIAS
CASE 1 NAUT. MILES NAUT. MILES FEET FEET/SEC FEET/SEC FEET/SEC NAUT. MILES DEGREES NAUT. MILES DEGREES
TRUE ERROR 0.000 0.000 50.000 67.512 67.512 67.512 0.001 0.707 0.001 0.707
FILTER ESTIMATE OF ERROR 0.000 0.000 50.000 67.512 67.512 67.512 0.001 0.707 0.001 0.707

VELOCITY CHANGE OF 400.00 KNOTS
FLIGHT PATH ANGLE CHANGE OF 5.33 DEGREES
HEADING CHANGE OF 5.33 DEGREES
COMMANDED BY NOM. TIME

TIME 0.00 MIN. EAST-POS. NORTH-POS. ALT. BIAS VE-BIAS VN-BIAS RANGE BIAS ANGLE BIAS
CASE 1 NAUT. MILES NAUT. MILES FEET FEET/SEC FEET/SEC FEET/SEC NAUT. MILES DEGREES NAUT. MILES DEGREES
TRUE ERROR 0.000 0.000 50.000 67.512 67.512 67.512 0.001 0.707 0.001 0.707
FILTER ESTIMATE OF ERROR 0.000 0.000 50.000 67.512 67.512 67.512 0.001 0.707 0.001 0.707

NOMINAL TRAJECTORY
VELOCITY 400.00 KNOTS ESTIMATED STATE ONE SIGMA CONTROL EFFORT
-110.47 NM EAST 2.00 SECONDS 0.00 SECONDS 0.00 KNOTS
58.77 NM NORTH 2.00 NM CROSS TRACK 0.00 NM CROSS TRACK 0.00 DEGREES
0.00 FT ALTITUDE 57.00 FT ALTITUDE 0.01 FT ALTITUDE 0.00 DEGREES

TIME 2.00 MIN. EAST-POS. NORTH-POS. ALT. BIAS VE-BIAS VN-BIAS RANGE BIAS ANGLE BIAS
CASE 1 NAUT. MILES NAUT. MILES FEET FEET/SEC FEET/SEC FEET/SEC NAUT. MILES DEGREES NAUT. MILES DEGREES
TRUE ERROR 1.269 1.263 50.000 67.512 67.512 67.512 0.001 0.707 0.001 0.707
FILTER ESTIMATE OF ERROR 1.269 1.263 50.000 67.512 67.512 67.512 0.001 0.707 0.001 0.707

NOMINAL TRAJECTORY
VELOCITY 400.00 KNOTS ESTIMATED STATE ONE SIGMA CONTROL EFFORT
-109.29 NM EAST 11.37 SECONDS 0.00 SECONDS 0.00 KNOTS
64.85 NM NORTH 1.26 NM CROSS TRACK 0.00 NM CROSS TRACK 0.00 DEGREES
7519.41 FT ALTITUDE 914.14 FT ALTITUDE 0.01 FT ALTITUDE 0.00 DEGREES

MEASUREMENTS OF RANGE-1= 11.91, THETA-1= 11.01, RANGE-2= 22.05, THETA-2= 104.73.
KALMAN UPDATE

TIME 6.00 MIN. EAST-POS. NORTH-POS. ALT. BIAS VE-BIAS VN-BIAS RANGE BIAS ANGLE BIAS
CASE 1 NAUT. MILES NAUT. MILES FEET FEET/SEC FEET/SEC FEET/SEC NAUT. MILES DEGREES NAUT. MILES DEGREES

FIGURE E-11(a) SAMPLE OF ANGCAP OUTPUT FOR IEG 1, CASE 1

2:00 MIN. CASE 1
 EAST-POS. NORTH-POS. ALT-RIAS VE-BIAS VN-BIAS RANGE BIAS ANGLE BIAS RANGE BIAS ANGLE BIAS
 NAUT. MILES NAUT. MILES FEET FEET/SEC FEET/SEC NAUT. MILES DEGREES NAUT. MILES DEGREES
 TRUE ERROR 0.114 0.123 50.000 30.274 36.337 0.080 0.606 0.078 0.587
 FILTER ESTIMATE OF ERROR 0.114 0.123 50.000 30.274 36.337 0.080 0.606 0.078 0.587

NOMINAL TRAJECTORY
 VELOCITY 400.00 KNOTS ESTIMATED STATE ONE SIGMA CONTROL EFFORT
 POSITION 19.24 NM EAST 11.31 SECONDS 0.00 KNOTS
 66.05 NM NORTH 1.26 NM CROSS TRACK 3.24 DEGREES
 7519.41 FT ALTITUDE 714.14 FT ALTITUDE 0.00 DEGREES

TIME 2:03 MIN. CASE 1
 EAST-POS. NORTH-POS. ALT-RIAS VE-BIAS VN-BIAS RANGE BIAS ANGLE BIAS RANGE BIAS ANGLE BIAS
 NAUT. MILES NAUT. MILES FEET FEET/SEC FEET/SEC NAUT. MILES DEGREES NAUT. MILES DEGREES
 TRUE ERROR 0.354 0.358 50.000 43.398 43.430 0.080 0.606 0.078 0.587
 FILTER ESTIMATE OF ERROR 0.354 0.358 50.000 43.398 43.430 0.080 0.606 0.078 0.587

NOMINAL TRAJECTORY
 VELOCITY 400.00 KNOTS ESTIMATED STATE ONE SIGMA CONTROL EFFORT
 POSITION 19.72 NM EAST 15.91 SECONDS 0.03 KNOTS
 70.20 NM NORTH 1.44 NM CROSS TRACK 3.60 DEGREES
 11000.00 FT ALTITUDE 1018.65 FT ALTITUDE 997.06 FT ALTITUDE 0.00 DEGREES

MEASUREMENTS OF RANGE-10 14.39 THETA-10 9.00 RANGE-20 22.00 THETA-20 87.88

KALMAN UPDATE

TIME 2:03 MIN. CASE 1
 EAST-POS. NORTH-POS. ALT-RIAS VE-BIAS VN-BIAS RANGE BIAS ANGLE BIAS RANGE BIAS ANGLE BIAS
 NAUT. MILES NAUT. MILES FEET FEET/SEC FEET/SEC NAUT. MILES DEGREES NAUT. MILES DEGREES
 TRUE ERROR 0.121 0.125 50.000 25.193 25.413 0.079 0.538 0.077 0.518
 FILTER ESTIMATE OF ERROR 0.121 0.125 50.000 25.193 25.413 0.079 0.538 0.077 0.518

NOMINAL TRAJECTORY
 VELOCITY 400.00 KNOTS ESTIMATED STATE ONE SIGMA CONTROL EFFORT
 POSITION 19.72 NM EAST 16.20 SECONDS 0.00 KNOTS
 70.20 NM NORTH 1.44 NM CROSS TRACK 3.70 DEGREES
 11000.00 FT ALTITUDE 1015.00 FT ALTITUDE 0.00 DEGREES

FLIGHT PATH ANGLE CHANGE OF -5.33 DEGREES
 COMMANDED BY ALTITUDE

TIME 2:03 MIN. CASE 1
 EAST-POS. NORTH-POS. ALT-RIAS VE-BIAS VN-BIAS RANGE BIAS ANGLE BIAS RANGE BIAS ANGLE BIAS
 NAUT. MILES NAUT. MILES FEET FEET/SEC FEET/SEC NAUT. MILES DEGREES NAUT. MILES DEGREES
 TRUE ERROR 0.121 0.125 50.000 25.193 25.413 0.079 0.538 0.077 0.518
 FILTER ESTIMATE OF ERROR 0.121 0.125 50.000 25.193 25.413 0.079 0.538 0.077 0.518

NOMINAL TRAJECTORY
 VELOCITY 400.00 KNOTS ESTIMATED STATE ONE SIGMA CONTROL EFFORT
 POSITION 19.72 NM EAST 16.20 SECONDS 0.00 KNOTS

FIGURE E-11(b). (CONTINUED)

MEASUREMENTS OF RANGE-1=29.82, THETA-1=174.43, RANGE-2=32.00, THETA-2=119.28.

KALMAN UPDATE

TIME 6.00 MIN.
 CASE 1
 EAST-POS. NORTH-POS. ALT. POS. VE-BIAS VN-BIAS VOR/DME STATION NO. 5 VOR/DME STATION NO. 6
 NAUT. MILES NAUT. MILES FEET FEET/SEC FEET/SEC RANGE BIAS RANGE BIAS ANGLE BIAS ANGLE BIAS
 0.176 0.147 50.000 31.416 30.448 0.134 0.617 0.133 0.612
 TRUE ERROR
 ESTIMATE OF ERROR 0.176 0.147 50.000 31.416 30.448 0.134 0.617 0.133 0.612

NOMINAL TRAJECTORY

POSITION VELOCITY ACTUAL STATE ESTIMATED STATE ONE SIGMA CONTROL EFFORT
 -104.78 NM EAST 250.00 KNOTS 34.65 SECONDS 36.59 SECONDS 0.00 KNOTS
 40.35 NM NORTH 46.10 DEGREES 4.22 NM CROSS TRACK 0.11 NM CROSS TRACK 0.46 DEGREES
 10979.89 FT ALTITUDE 138.76 FT ALTITUDE 129.21 FT ALTITUDE 0.00 DEGREES

TIME 8.00 MIN.
 CASE 1
 EAST-POS. NORTH-POS. ALT. POS. VE-BIAS VN-BIAS VOR/DME STATION NO. 5 VOR/DME STATION NO. 6
 NAUT. MILES NAUT. MILES FEET FEET/SEC FEET/SEC RANGE BIAS RANGE BIAS ANGLE BIAS ANGLE BIAS
 0.829 0.802 50.000 52.197 51.914 0.134 0.617 0.133 0.612
 TRUE EMPOR
 ESTIMATE OF ERROR 0.829 0.802 50.000 52.197 51.914 0.134 0.617 0.133 0.612

NOMINAL TRAJECTORY

POSITION VELOCITY ACTUAL STATE ESTIMATED STATE ONE SIGMA CONTROL EFFORT
 -112.68 NM EAST 250.00 KNOTS 57.85 SECONDS 49.55 SECONDS 0.00 KNOTS
 96.12 NM NORTH 46.19 DEGREES 1.14 NM CROSS TRACK 0.78 NM CROSS TRACK 3.21 DEGREES
 10536.08 FT ALTITUDE 182.43 FT ALTITUDE 170.27 FT ALTITUDE 0.00 DEGREES

MEASUREMENTS OF RANGE-1=25.52, THETA-1=190.54, RANGE-2=24.44, THETA-2=114.27.

KALMAN UPDATE

TIME 8.00 MIN.
 CASE 1
 EAST-POS. NORTH-POS. ALT. POS. VE-BIAS VN-BIAS VOR/DME STATION NO. 5 VOR/DME STATION NO. 6
 NAUT. MILES NAUT. MILES FEET FEET/SEC FEET/SEC RANGE BIAS RANGE BIAS ANGLE BIAS ANGLE BIAS
 0.194 0.140 50.000 29.751 29.443 0.130 0.550 0.130 0.548
 TRUE ERROR
 ESTIMATE OF ERROR 0.194 0.140 50.000 29.751 29.443 0.130 0.550 0.130 0.548

NOMINAL TRAJECTORY

POSITION VELOCITY ACTUAL STATE ESTIMATED STATE ONE SIGMA CONTROL EFFORT
 -102.68 NM EAST 250.00 KNOTS 57.85 SECONDS 50.80 SECONDS 0.00 KNOTS
 96.12 NM NORTH 46.19 DEGREES 1.14 NM CROSS TRACK 1.13 NM CROSS TRACK 4.67 DEGREES
 10536.08 FT ALTITUDE 182.43 FT ALTITUDE 175.25 FT ALTITUDE 0.00 DEGREES

TIME 10.00 MIN.
 CASE 1
 EAST-POS. NORTH-POS. ALT. POS. VE-BIAS VN-BIAS VOR/DME STATION NO. 5 VOR/DME STATION NO. 6
 NAUT. MILES NAUT. MILES FEET FEET/SEC FEET/SEC RANGE BIAS RANGE BIAS ANGLE BIAS ANGLE BIAS
 0.774 0.770 50.000 51.694 51.603 0.130 0.550 0.130 0.548
 TRUE EMPOR
 ESTIMATE OF ERROR 0.774 0.770 50.000 51.694 51.603 0.130 0.550 0.130 0.548

NOMINAL TRAJECTORY

FIGURE E-11(e). (CONTINUED)

POSITION
 04.47 NM EAST
 101.84 NM NORTH
 10092.27 FT ALTITUDE
 VELOCITY
 250.00 KNOTS
 46.19 DEGREES
 -0.51 DEGREES
 ACTUAL STATE
 64.06 SECONDS
 1.57 NM CROSS TRACK
 227.87 FT ALTITUDE
 ESTIMATED STATE
 63.09 SECONDS
 1.37 NM CROSS TRACK
 218.50 FT ALTITUDE
 ONE SIGMA CONTROL EFFORT
 0.00 KNOTS
 5.66 DEGREES
 0.00 DEGREES

MEASUREMENTS OF RANGE-1= 23.50, THETA-1= 140.49, RANGE-2= 16.44, THETA-2= 106.47,

KALMAN UPDATE

TIME
 10.00 MIN.
 CASE 1
 EAST-POS. NORTH-POS. ALT. RIAS VE-RIAS VOR/DVE STATION NO. 5 VOR/DVE STATION NO. 6
 NAUT. MILES NAUT. MILES FEET FEET FEET/SEC FEET/SEC DEGREES DEGREES RANGE BIAS RANGE BIAS
 0.124 0.124 49.999 49.999 29.787 29.787 0.124 0.124 NAUT. MILES NAUT. MILES DEGREES DEGREES
 TRUE ERROR
 0.142 0.142 49.999 49.999 29.787 29.787 0.124 0.124 0.508 0.508
 FILTER ESTIMATE OF ERROR
 0.124 0.124 49.999 49.999 29.787 29.787 0.124 0.124 0.508 0.508

NOMINAL TRAJECTORY

POSITION
 04.47 NM EAST
 101.84 NM NORTH
 10092.27 FT ALTITUDE
 VELOCITY
 250.00 KNOTS
 46.19 DEGREES
 -0.51 DEGREES
 ACTUAL STATE
 64.06 SECONDS
 1.57 NM CROSS TRACK
 227.87 FT ALTITUDE
 ESTIMATED STATE
 64.00 SECONDS
 1.57 NM CROSS TRACK
 222.10 FT ALTITUDE
 ONE SIGMA CONTROL EFFORT
 0.00 KNOTS
 6.47 DEGREES
 0.00 DEGREES

MEASUREMENTS OF RANGE-1= 24.34, THETA-1= 128.49, RANGE-2= 10.09, THETA-2= 80.31,

KALMAN UPDATE

TIME
 12.00 MIN.
 CASE 1
 EAST-POS. NORTH-POS. ALT. RIAS VE-RIAS VOR/DVE STATION NO. 5 VOR/DVE STATION NO. 6
 NAUT. MILES NAUT. MILES FEET FEET FEET/SEC FEET/SEC DEGREES DEGREES RANGE BIAS RANGE BIAS
 0.173 0.173 49.999 49.999 29.371 29.371 0.107 0.107 NAUT. MILES NAUT. MILES DEGREES DEGREES
 TRUE ERROR
 0.124 0.124 49.999 49.999 29.371 29.371 0.107 0.107 0.459 0.459
 FILTER ESTIMATE OF ERROR
 0.106 0.106 49.999 49.999 29.371 29.371 0.106 0.106 0.507 0.507

NOMINAL TRAJECTORY

POSITION
 04.45 NM EAST
 101.84 NM NORTH
 9648.66 FT ALTITUDE
 VELOCITY
 250.00 KNOTS
 46.19 DEGREES
 -0.51 DEGREES
 ACTUAL STATE
 76.27 SECONDS
 1.77 NM CROSS TRACK
 271.75 FT ALTITUDE
 ESTIMATED STATE
 75.42 SECONDS
 1.60 NM CROSS TRACK
 263.79 FT ALTITUDE
 ONE SIGMA CONTROL EFFORT
 0.00 KNOTS
 6.40 DEGREES
 0.00 DEGREES

MEASUREMENTS OF RANGE-1= 24.34, THETA-1= 128.49, RANGE-2= 10.09, THETA-2= 80.31,

KALMAN UPDATE

TIME
 14.00 MIN.
 CASE 1
 EAST-POS. NORTH-POS. ALT. RIAS VE-RIAS VOR/DVE STATION NO. 5 VOR/DVE STATION NO. 6
 NAUT. MILES NAUT. MILES FEET FEET FEET/SEC FEET/SEC DEGREES DEGREES RANGE BIAS RANGE BIAS
 0.173 0.173 49.999 49.999 29.371 29.371 0.107 0.107 NAUT. MILES NAUT. MILES DEGREES DEGREES
 TRUE ERROR
 0.124 0.124 49.999 49.999 29.371 29.371 0.107 0.107 0.459 0.459
 FILTER ESTIMATE OF ERROR
 0.106 0.106 49.999 49.999 29.371 29.371 0.106 0.106 0.507 0.507

NOMINAL TRAJECTORY

POSITION
 04.45 NM EAST
 101.84 NM NORTH
 9648.66 FT ALTITUDE
 VELOCITY
 250.00 KNOTS
 46.19 DEGREES
 -0.51 DEGREES
 ACTUAL STATE
 76.27 SECONDS
 1.77 NM CROSS TRACK
 271.75 FT ALTITUDE
 ESTIMATED STATE
 76.23 SECONDS
 1.77 NM CROSS TRACK
 266.96 FT ALTITUDE
 ONE SIGMA CONTROL EFFORT
 0.00 KNOTS
 7.30 DEGREES
 0.00 DEGREES

MEASUREMENTS OF RANGE-1= 24.34, THETA-1= 128.49, RANGE-2= 10.09, THETA-2= 80.31,

KALMAN UPDATE

TIME
 16.00 MIN.
 CASE 1
 EAST-POS. NORTH-POS. ALT. RIAS VE-RIAS VOR/DVE STATION NO. 5 VOR/DVE STATION NO. 6
 NAUT. MILES NAUT. MILES FEET FEET FEET/SEC FEET/SEC DEGREES DEGREES RANGE BIAS RANGE BIAS
 0.173 0.173 49.999 49.999 29.371 29.371 0.107 0.107 NAUT. MILES NAUT. MILES DEGREES DEGREES
 TRUE ERROR
 0.124 0.124 49.999 49.999 29.371 29.371 0.107 0.107 0.459 0.459
 FILTER ESTIMATE OF ERROR
 0.106 0.106 49.999 49.999 29.371 29.371 0.106 0.106 0.507 0.507

FIGURE E-11(f). (CONTINUED)

FLIGHT PATH ANGLE CHANGE OF -1.40 DEGREES COMMANDED BY ALTITUDE										
TIME	14.92 MIN.	CASE 1	EAST-POS. NAUT. MILES	0.134	NORTH-POS. NAUT. MILES	0.306	VE-BIAS FEET/SEC	49.998	VN-BIAS FEET/SEC	25.583
			TRUE ERROR	0.134		0.306		49.998		25.583
			FILTER ESTIMATE OF ERROR	0.134		0.306		49.998		25.583
NOMINAL TRAJECTORY										
POSITION	116.08 NM NORTH	9000.00 FT ALTITUDE	VELOCITY	250.00 KNOTS	ACTUAL STATE	92.54 SECONDS	ESTIMATED STATE	92.47 SECONDS	ONE SIGMA CONTROL EFFORT	0.00 KNOTS
				46.19 DEGREES		1.86 NM CROSS TRACK		1.85 NM CROSS TRACK		7.63 DEGREES
				-2.12 DEGREES		1372.83 FT ALTITUDE		1370.77 FT ALTITUDE		0.00 DEGREES
VELOCITY CHANGE OF -75.00 KNOTS FLIGHT PATH ANGLE CHANGE OF -0.90 DEGREES HEADING CHANGE OF -116.19 DEGREES COMMANDED BY C.T. POS.										
TIME	14.92 MIN.	CASE 1	EAST-POS. NAUT. MILES	0.134	NORTH-POS. NAUT. MILES	0.306	VE-BIAS FEET/SEC	49.998	VN-BIAS FEET/SEC	25.583
			TRUE ERROR	0.134		0.306		49.998		25.583
			FILTER ESTIMATE OF ERROR	0.134		0.306		49.998		25.583
NOMINAL TRAJECTORY										
POSITION	116.08 NM NORTH	9000.00 FT ALTITUDE	VELOCITY	175.00 KNOTS	ACTUAL STATE	108.82 SECONDS	ESTIMATED STATE	108.78 SECONDS	ONE SIGMA CONTROL EFFORT	0.00 KNOTS
				-70.00 DEGREES		0.30 NM CROSS TRACK		-0.00 NM CROSS TRACK		-0.00 DEGREES
				-3.00 DEGREES		1547.10 FT ALTITUDE		1545.60 FT ALTITUDE		0.00 DEGREES
VELOCITY CHANGE OF -75.00 KNOTS FLIGHT PATH ANGLE CHANGE OF -0.90 DEGREES HEADING CHANGE OF -116.19 DEGREES COMMANDED BY C.T. POS.										
TIME	14.92 MIN.	CASE 1	EAST-POS. NAUT. MILES	0.134	NORTH-POS. NAUT. MILES	0.306	VE-BIAS FEET/SEC	49.998	VN-BIAS FEET/SEC	25.583
			TRUE ERROR	0.134		0.306		49.998		25.583
			FILTER ESTIMATE OF ERROR	0.134		0.306		49.998		25.583
NOMINAL TRAJECTORY										
POSITION	116.08 NM NORTH	9000.00 FT ALTITUDE	VELOCITY	175.00 KNOTS	ACTUAL STATE	108.82 SECONDS	ESTIMATED STATE	108.78 SECONDS	ONE SIGMA CONTROL EFFORT	0.00 KNOTS
				-70.00 DEGREES		0.30 NM CROSS TRACK		-0.00 NM CROSS TRACK		-0.00 DEGREES
				-3.00 DEGREES		1547.10 FT ALTITUDE		1545.60 FT ALTITUDE		0.00 DEGREES
VELOCITY CHANGE OF -75.00 KNOTS FLIGHT PATH ANGLE CHANGE OF -0.90 DEGREES HEADING CHANGE OF -116.19 DEGREES COMMANDED BY C.T. POS.										
TIME	16.00 MIN.	CASE 1	EAST-POS. NAUT. MILES	0.681	NORTH-POS. NAUT. MILES	0.681	VE-BIAS FEET/SEC	49.998	VN-BIAS FEET/SEC	42.808
			TRUE ERROR	0.681		0.681		49.998		42.808
			FILTER ESTIMATE OF ERROR	0.681		0.681		49.998		42.808
NOMINAL TRAJECTORY										
POSITION	117.16 NM NORTH	7999.02 FT ALTITUDE	VELOCITY	175.00 KNOTS	ACTUAL STATE	112.07 SECONDS	ESTIMATED STATE	111.74 SECONDS	ONE SIGMA CONTROL EFFORT	0.00 KNOTS
				-70.00 DEGREES		2.82 NM CROSS TRACK		0.46 NM CROSS TRACK		2.71 DEGREES
				-3.00 DEGREES		1593.04 FT ALTITUDE		1586.78 FT ALTITUDE		0.00 DEGREES
MEASUREMENTS OF RANGE=18 26.94 THETA=18 96.01										
KALMAN UPDATE										
TIME	16.00 MIN.	CASE 1	EAST-POS. NAUT. MILES	0.681	NORTH-POS. NAUT. MILES	0.681	VE-BIAS FEET/SEC	49.998	VN-BIAS FEET/SEC	42.808
			TRUE ERROR	0.681		0.681		49.998		42.808
			FILTER ESTIMATE OF ERROR	0.681		0.681		49.998		42.808
NOMINAL TRAJECTORY										
POSITION	117.16 NM NORTH	7999.02 FT ALTITUDE	VELOCITY	175.00 KNOTS	ACTUAL STATE	112.07 SECONDS	ESTIMATED STATE	111.74 SECONDS	ONE SIGMA CONTROL EFFORT	0.00 KNOTS
				-70.00 DEGREES		2.82 NM CROSS TRACK		0.46 NM CROSS TRACK		2.71 DEGREES
				-3.00 DEGREES		1593.04 FT ALTITUDE		1586.78 FT ALTITUDE		0.00 DEGREES

FIGURE E-11(h). (CONTINUED)

TRUE ERROR	5.141	5.413	49.998	25.910	37.550	0.091	0.380
FILTER ESTIMATE OF ERROR	5.141	5.413	49.998	25.910	37.540	0.091	0.380
NOMINAL TRAJECTORY							
POSITION	ACTUAL STATE			ESTIMATED STATE			ONE SIGMA CONTROL EFFORT
-64.82 NM EAST	132.07 SECONDS			112.02 SECONDS			0.00 KNOTS
117.16 NM NORTH	1.82 NM CROSS TRACK			0.71 NM CROSS TRACK			4.17 DEGREES
7999.02 FT ALTITUDE	1593.04 FT ALTITUDE			1591.42 FT ALTITUDE			0.00 DEGREES
TIME	126.00 SEC. SINCE LAST UPDATE			VOR/ONE STATION NO. 5			
18.00 MIN.	EAST-POS.	NORTH-POS.	ALT.-BIAS	VE.-BIAS	VN.-BIAS	RANGE BIAS	ANGLE BIAS
CASE 1	NAUT.-MILE	NAUT.-MILES	FEET	FEET	FEET/SEC	NAUT.-MILES	DEGREES
	0.749	1.008	49.998	50.021	54.237	0.091	0.380
FILTER ESTIMATE OF ERROR	0.749	1.008	49.998	50.021	54.237	0.091	0.380
NOMINAL TRAJECTORY							
POSITION	ACTUAL STATE			ESTIMATED STATE			ONE SIGMA CONTROL EFFORT
-60.30 NM EAST	126.84 SECONDS			119.82 SECONDS			0.00 KNOTS
119.15 NM NORTH	1.53 NM CROSS TRACK			1.08 NM CROSS TRACK			6.37 DEGREES
6141.40 FT ALTITUDE	1724.46 FT ALTITUDE			1710.55 FT ALTITUDE			0.00 DEGREES
MEASUREMENTS OF RANGE-1= 21.32, THETA-1= 92.21.							
KALMAN UPDATE							
TIME	0.00 SEC. SINCE LAST UPDATE			VOR/ONE STATION NO. 5			
18.00 MIN.	EAST-POS.	NORTH-POS.	ALT.-BIAS	VE.-BIAS	VN.-BIAS	RANGE BIAS	ANGLE BIAS
CASE 1	NAUT.-MILE	NAUT.-MILES	FEET	FEET/SEC	FEET/SEC	NAUT.-MILES	DEGREES
	0.134	0.383	49.998	29.649	37.044	0.091	0.377
FILTER ESTIMATE OF ERROR	0.134	0.383	49.998	29.649	37.044	0.091	0.377
NOMINAL TRAJECTORY							
POSITION	ACTUAL STATE			ESTIMATED STATE			ONE SIGMA CONTROL EFFORT
-90.30 NM EAST	127.94 SECONDS			120.79 SECONDS			0.00 KNOTS
119.15 NM NORTH	1.93 NM CROSS TRACK			1.49 NM CROSS TRACK			8.76 DEGREES
6141.40 FT ALTITUDE	1724.46 FT ALTITUDE			1726.88 FT ALTITUDE			0.00 DEGREES
TIME	120.00 SEC. SINCE LAST UPDATE			VOR/ONE STATION NO. 5			
20.00 MIN.	EAST-POS.	NORTH-POS.	ALT.-BIAS	VE.-BIAS	VN.-BIAS	RANGE BIAS	ANGLE BIAS
CASE 1	NAUT.-MILES	NAUT.-MILES	FEET	FEET/SEC	FEET/SEC	NAUT.-MILES	DEGREES
	0.771	1.004	49.998	51.063	54.059	0.091	0.377
FILTER ESTIMATE OF ERROR	0.771	1.004	49.998	51.063	54.059	0.091	0.377
NOMINAL TRAJECTORY							
POSITION	ACTUAL STATE			ESTIMATED STATE			ONE SIGMA CONTROL EFFORT
-85.78 NM EAST	131.71 SECONDS			130.69 SECONDS			0.00 KNOTS
121.15 NM NORTH	1.81 NM CROSS TRACK			1.52 NM CROSS TRACK			8.94 DEGREES
4233.94 FT ALTITUDE	1901.70 FT ALTITUDE			1884.15 FT ALTITUDE			0.00 DEGREES
MEASUREMENTS OF RANGE-1= 15.86, THETA-1= 85.75.							
KALMAN UPDATE							

FIGURE E-11(1). (CONTINUED)

TIME 20.00 MIN. CASE 1
 EAST-POS. NORTH-POS. ALT. BIAS VE-BIAS VN-BIAS RANGE BIAS ANGLE BIAS
 NAUT. MILES NAUT. MILES FEET FEET/SEC FEET/SEC NAUT. MILES DEGREES
 8.135 8.287 49.998 29.682 32.858 8.89 0.376
 TRUE ERROR 0.135 8.287 49.998 29.682 32.858 8.89 0.376
 FILTER ESTIMATE OF ERROR

NOMINAL TRAJECTORY
 POSITION 175.00 KNOTS VELOCITY
 -95.74 NM EAST 175.00 KNOTS
 121.15 NM NORTH -70.00 DEGREES
 423.94 FT ALTITUDE
 ACTUAL STATE
 131.71 SECONDS
 1.81 NM CROSS TRACK
 1901.70 FT ALTITUDE
 ESTIMATED STATE
 171.66 SECONDS
 1.79 NM CROSS TRACK
 1900.29 FT ALTITUDE
 ONE SIGMA CONTROL EFFORT
 0.00 KNOTS
 10.55 DEGREES
 0.00 DEGREES

TIME 22.00 MIN. CASE 1
 EAST-POS. NORTH-POS. ALT. BIAS VE-BIAS VN-BIAS RANGE BIAS ANGLE BIAS
 NAUT. MILES NAUT. MILES FEET FEET/SEC FEET/SEC NAUT. MILES DEGREES
 0.772 0.921 49.998 51.673 53.644 0.091 0.376
 TRUE ERROR 0.772 0.921 49.998 51.673 53.644 0.091 0.376
 FILTER ESTIMATE OF ERROR

NOMINAL TRAJECTORY
 POSITION 175.00 KNOTS VELOCITY
 -101.27 NM EAST 175.00 KNOTS
 123.14 NM NORTH -70.00 DEGREES
 2476.40 FT ALTITUDE
 ACTUAL STATE
 142.50 SECONDS
 1.91 NM CROSS TRACK
 2591.33 FT ALTITUDE
 ESTIMATED STATE
 142.56 SECONDS
 1.69 NM CROSS TRACK
 2075.32 FT ALTITUDE
 ONE SIGMA CONTROL EFFORT
 0.00 KNOTS
 9.94 DEGREES
 0.00 DEGREES

MEASUREMENTS OF RANGE-1= 15.86, THETA-1= 72.92,
 KALMAN UPDATE

TIME 22.00 MIN. CASE 1
 EAST-POS. NORTH-POS. ALT. BIAS VE-BIAS VN-BIAS RANGE BIAS ANGLE BIAS
 NAUT. MILES NAUT. MILES FEET FEET/SEC FEET/SEC NAUT. MILES DEGREES
 0.148 0.194 49.998 29.774 33.756 0.091 0.376
 TRUE ERROR 0.148 0.194 49.998 29.774 33.756 0.091 0.376
 FILTER ESTIMATE OF ERROR

NOMINAL TRAJECTORY
 POSITION 175.00 KNOTS VELOCITY
 -141.27 NM EAST 175.00 KNOTS
 123.14 NM NORTH -70.00 DEGREES
 2476.40 FT ALTITUDE
 ACTUAL STATE
 1.50 SECONDS
 1.91 NM CROSS TRACK
 2691.33 FT ALTITUDE
 ESTIMATED STATE
 143.46 SECONDS
 1.90 NM CROSS TRACK
 2090.13 FT ALTITUDE
 ONE SIGMA CONTROL EFFORT
 0.00 KNOTS
 11.22 DEGREES
 0.00 DEGREES

TIME 23.54 MIN. CASE 1
 EAST-POS. NORTH-POS. ALT. BIAS VE-BIAS VN-BIAS RANGE BIAS ANGLE BIAS
 NAUT. MILES NAUT. MILES FEET FEET/SEC FEET/SEC NAUT. MILES DEGREES
 0.584 0.651 49.998 48.554 49.962 0.091 0.376
 TRUE ERROR 0.584 0.651 49.998 48.554 49.962 0.091 0.376
 FILTER ESTIMATE OF ERROR

NOMINAL TRAJECTORY
 POSITION 175.00 KNOTS VELOCITY
 -145.44 NM EAST 175.00 KNOTS
 124.67 NM NORTH -70.00 DEGREES
 1000.00 FT ALTITUDE
 ACTUAL STATE
 152.76 SECONDS
 1.91 NM CROSS TRACK
 2242.33 FT ALTITUDE
 ESTIMATED STATE
 152.25 SECONDS
 1.80 NM CROSS TRACK
 2231.49 FT ALTITUDE
 ONE SIGMA CONTROL EFFORT
 0.00 KNOTS
 10.64 DEGREES
 0.00 DEGREES

FIGURE E-11(J). (CONTINUED)

23.54 MIN. CASE 1
 EAST-POS. NORTH-POS. ALT. RFLG VE-BIAS VN-BIAS RANGE BIAS ANGLE BIAS
 NAUT. MILES NAUT. MILES FEET FEET/SEC FEET/SEC NAUT. MILES DEGREES
 0.140 0.140 49.998 16.878 16.878 0.091 0.376
 TRUE ERROR
 FILTER ESTIMATE OF ERROR 0.139 0.139 49.998 16.878 16.878 0.091 0.376
 NOMINAL TRAJECTORY

POSITION VELOCITY
 100.00 FT ALTITUDE 100.00 FT ALTITUDE
 126.67 NM NORTH 100.00 FT ALTITUDE
 125.44 NM EAST 100.00 FT ALTITUDE
 ESTIMATED STATE
 152.81 SECONDS
 1.91 NM CROSS TRACK
 0.00 FT ALTITUDE
 ONE SIGMA CONTROL EFFORT
 0.00 KNOTS
 65.59 DEGREES
 0.00 DEGREES

24.00 MIN. CASE 1
 EAST-POS. NORTH-POS. ALT. RFLG VE-BIAS VN-BIAS RANGE BIAS ANGLE BIAS
 NAUT. MILES NAUT. MILES FEET FEET/SEC FEET/SEC NAUT. MILES DEGREES
 0.159 0.159 49.998 16.878 16.878 0.091 0.376
 TRUE ERROR
 FILTER ESTIMATE OF ERROR 0.159 0.159 49.998 16.878 16.878 0.091 0.376
 NOMINAL TRAJECTORY

POSITION VELOCITY
 100.00 FT ALTITUDE 100.00 FT ALTITUDE
 126.67 NM NORTH 100.00 FT ALTITUDE
 125.44 NM EAST 100.00 FT ALTITUDE
 ESTIMATED STATE
 152.73 SECONDS
 1.20 NM CROSS TRACK
 0.00 FT ALTITUDE
 ONE SIGMA CONTROL EFFORT
 0.00 KNOTS
 41.23 DEGREES
 0.00 DEGREES

MEASUREMENTS OF RANGE-1= 7.33, THETA-1= 47.30.

KALMAN UPDATE
 TIME 24.00 MIN. CASE 1
 EAST-POS. NORTH-POS. ALT. RFLG VE-BIAS VN-BIAS RANGE BIAS ANGLE BIAS
 NAUT. MILES NAUT. MILES FEET FEET/SEC FEET/SEC NAUT. MILES DEGREES
 0.116 0.116 49.998 15.352 15.474 0.091 0.376
 TRUE ERROR
 FILTER ESTIMATE OF ERROR 0.113 0.113 49.998 15.352 15.474 0.091 0.376
 NOMINAL TRAJECTORY

POSITION VELOCITY
 100.00 FT ALTITUDE 100.00 FT ALTITUDE
 126.67 NM NORTH 100.00 FT ALTITUDE
 125.44 NM EAST 100.00 FT ALTITUDE
 ESTIMATED STATE
 152.78 SECONDS
 1.20 NM CROSS TRACK
 0.01 FT ALTITUDE
 ONE SIGMA CONTROL EFFORT
 0.00 KNOTS
 41.38 DEGREES
 0.00 DEGREES

25.54 MIN. CASE 1
 EAST-POS. NORTH-POS. ALT. RFLG VE-BIAS VN-BIAS RANGE BIAS ANGLE BIAS
 NAUT. MILES NAUT. MILES FEET FEET/SEC FEET/SEC NAUT. MILES DEGREES
 0.272 0.272 49.998 16.346 16.387 0.091 0.376
 TRUE ERROR
 FILTER ESTIMATE OF ERROR 0.271 0.271 49.998 16.346 16.387 0.091 0.376
 NOMINAL TRAJECTORY

POSITION VELOCITY
 100.00 FT ALTITUDE 100.00 FT ALTITUDE
 126.67 NM NORTH 100.00 FT ALTITUDE
 125.44 NM EAST 100.00 FT ALTITUDE
 ESTIMATED STATE
 152.88 SECONDS
 0.27 NM CROSS TRACK
 0.00 FT ALTITUDE
 ONE SIGMA CONTROL EFFORT
 0.00 KNOTS
 9.14 DEGREES
 0.00 DEGREES

CASE 1= 3A PLOT POINTS

FIGURE E-11(1). (CONTINUED)

KALMAN UPDATES EVERY 120.0 SECONDS WHEN MEASUREMENTS ARE AVAILABLE

2 VOR RECEIVERS. 2 DME RECEIVERS (VOR/DME-VOR/DME)

TRAJECTORY SUMMARY

TIME (MIN)	PAC (NM)	NORTH (NM)	ALT. (FT)	VEL. (KNOTS)	HDG. (DEG)	FPA. (DEG)	VOR/DME	DME	VOR/DME	DME
0.0-110.67	0.0	0.0	0.0	0.0	0.0	0.0				
2.0-110.72	70.25	11000.0			5.1	5.3	SAN JOSE		OAKLAND	
4.0-110.97	90.09	11000.0			-0.7	0.0	SAN JOSE		OAKLAND	
14.9-111.47	116.08	9000.0			46.2	-0.5	SACRAMENTO		LINDEN	
23.9-115.60	124.67	1000.0			-70.0	-3.0	SACRAMENTO			
25.5-116.61	125.01	1000.0			-70.0	0.0	SACRAMENTO			

92.1 SEC. SINCE LAST UPDATE VOR/DME STATION NO. 5

EAST-POS. NAUT-MILES	NORTH-POS. NAUT-MILES	ALT. BIAS FEET	VE-BIAS FEET/SEC	VN-BIAS NAUT-MILES	RANGE BIAS NAUT-MILES	ANGLE BIAS DEGREES
0.271	0.272	0.498	10.366	0.387	0.091	0.376
FILTER ESTIMATE OF ERROR	0.271	0.272	10.366	0.387	0.091	0.376

NOMINAL TRAJECTORY

POSITION	VELOCITY	ACTUAL STATE	ESTIMATED STATE	ONE SIGMA CONTROL EFFORT
-125.01 NM EAST	100.00 KNOTS	159.10 SECONDS	152.88 SECONDS	0.00 KNOTS
125.01 NM NORTH	-70.00 DEGREES	2.38 NM CROSS TRACK	0.27 NM CROSS TRACK	9.14 DEGREES
1000.00 FT ALTITUDE	0.00 DEGREES	50.00 FT ALTITUDE	0.00 FT ALTITUDE	0.00 DEGREES

MAXIMUM ALLOWABLE DEVIATION TOWARD SUNWAY = 0.50 NM
 PROBABILITY OF MISSED APPROACH=0.05902684

MAXIMUM ONE SIGMA DEVIATIONS

ALONG TRACK	CROSS TRACK	ALTITUDE
153.19	1.91	2240.33
25.54	23.54	23.54

EXECUTION TIME 12.14 SECONDS

FIGURE E-12. SUMMARY OF SAMPLE ANGGAP OUTPUT OF FIGURE E-11

SUMMARY OF CASES FOR AMESBC OF 02/15/73 AT 091101

CASE	UPDATES TYPE FREQ(SEC)	RECEIVERS		LEG	ACTUAL DISPERSIONS			ESTIMATE DISPERSIONS			
		VOR	DME		A.T.(SEC)	X.T.(NM)	ALT.(FT)	A.T.(SEC)	X.T.(NM)	ALT.(FT)	
1	120.00	2	2	1	153.19	0.39	50.56	152.88	0.27	0.00	0.0590266
2	120.00	1	2	1	153.26	0.38	50.25	152.95	0.27	0.00	0.0611980
3	120.00	2	1	1	152.16	0.36	50.20	152.84	0.27	0.00	0.0610055
4	120.00	0	2	1	160.00	0.78	50.56	154.49	0.47	0.01	0.2240584
5	120.00	1	1	1	152.73	0.39	50.25	152.37	0.27	0.00	0.0550326
6	126.00	1	1	1	167.00	0.43	50.56	161.98	0.31	0.00	0.0817853
7	120.00	2	2	2	170.26	0.39	49.88	170.15	0.29	0.01	0.0622205
8	120.00	1	2	2	176.29	0.39	49.42	170.19	0.29	0.00	0.0623248
9	120.00	2	2	2	171.34	0.39	49.65	170.71	0.29	0.00	0.0653221
10	120.00	0	2	2	164.63	1.87	49.65	164.01	0.36	0.02	0.3755734
11	120.00	1	1	2	178.91	0.40	49.65	170.79	0.29	0.00	0.0537340
12	120.00	1	1	2	177.27	0.43	50.56	177.25	0.36	0.00	0.0517460
13	120.00	2	2	3	202.52	0.35	49.95	202.45	0.31	0.01	0.0372228
14	120.00	1	2	3	202.53	0.35	49.66	202.49	0.31	0.03	0.0431128
15	120.00	2	1	3	207.40	0.35	49.62	202.33	0.31	0.04	0.0455388
16	120.00	0	2	3	202.77	1.12	49.64	201.21	1.02	0.01	0.2988701
17	120.00	1	1	3	202.43	0.35	49.63	202.36	0.31	0.05	0.0459369
18	120.00	2	1	3	218.58	0.39	50.56	218.18	0.33	0.00	0.0660688

a. FIVE KALMAN FILTER UPDATES AND ONE POSITION
FIX UPDATE

FIGURE E-13. SUMMARY OF ANGCAP OUTPUT FOR ALL LEGS

SUMMARY OF CASES FOR AMESOKS OF 02/15/73 AT 152009

CASE	UPDATES TYPE F0(F1)F2(F3)	RECEIVERS		LEG	ACTUAL DISPERSIONS			ESTIMATE DISPERSIONS			
		VOP	DME		A.T. (SEC)	X.T. (NM)	ALT. (FT)	A.T. (SEC)	X.T. (NM)	ALT. (FT)	
1	1	120.00	2	0	161.19	1.34	50.00	159.11	0.38	0.00	0.3290766
2	2	120.00	1	1	344.92	6.22	50.00	245.56	0.50	0.00	0.4419699
3	1	120.00	1	1	126.07	0.88	50.00	118.22	0.59	0.00	0.2499949
4	2	120.00	1	1	178.97	3.99	50.00	192.77	0.60	0.00	0.4609406
5	2	120.00	0	0	349.49	9.71	50.00	0.00	0.00	0.00	0.4755147
6	1	120.00	2	2	192.31	0.61	50.00	180.10	0.35	0.00	0.1648895
7	2	120.00	1	2	334.98	0.78	50.00	299.49	0.42	0.00	0.2234511
8	1	120.00	0	1	158.40	1.89	49.69	147.75	0.37	0.00	0.3764471
9	2	120.00	0	2	187.61	2.65	50.00	182.67	0.35	0.00	0.4113083
10	2	120.00	0	2	557.55	15.77	50.00	3.03	0.30	0.00	0.1449781
11	1	120.00	2	3	236.52	1.06	50.00	215.93	0.78	0.00	0.2974792
12	2	120.00	1	0	624.92	7.20	50.00	434.97	1.38	0.00	0.6671595
13	1	120.00	1	3	166.07	1.22	49.65	164.11	1.12	0.01	0.3130719
14	2	120.00	0	3	408.87	8.83	50.00	212.49	1.83	0.00	0.4732044
15	2	120.00	0	3	591.92	16.44	50.00	0.00	0.00	0.00	0.4955961

b. TWO KALMAN FILTER UPDATES AND THREE POSITION FIX UPDATES

FIGURE E-13. (CONTINUED)

APPENDIX E

effort is shown except a 3.94 degree heading change. This heading change represents the action by the pilot to correct for estimated state deviation of 1.53 n.mi. After the update, the actual state deviations have not changed. This is because of a new set of measurement information in no way affects the state of the aircraft. The estimate does not change with the update. Thus, after the update, the improved information results in an estimated crosstrack deviation of 1.57 n.mi. and the resulting control effort increases to 4.05 degrees.

Additional output is shown at each waypoint. Waypoints are treated as potential discontinuities in the velocity of the aircraft. The time at which the velocity change is made on a perturbed mission may be specified by the user. If no specification is made, it is assumed that all heading changes are made when the pilot estimates that he has zero crosstrack error on his new heading. Consider, for example, the velocity change made at 5.91 minutes shown in the center of Figure E-11(d). This is the waypoint where the aircraft begins its descent into the terminal area. As shown between the rows of Xs, this waypoint requires a velocity change of -150 knots, a descent of 5 degrees, and a heading change of 46.9 degrees. Comparing the σ deviation values just prior to and just after the heading change it should be noted that the estimated crosstrack deviations drop to zero. The effect of these deviations map into an increased deviation in along track position.

Velocity magnitude changes are assumed to be made at the same time a heading change is made. If no heading change is commanded at a waypoint with a velocity change, it is assumed that the velocity change is made when the estimated along-track position is at the nominal value. Vertical velocity changes are made in a similar way when level flight is followed by an ascent or descent. If, however, the vertical velocity change is from climbing or descending to level flight, it is assumed that the pilot makes the maneuver when the estimated (barometric altimeter) altitude is at the desired value. For example, when entering the terminal area (shown in Figure E-11(k) at 23.65 minutes into the example, the flight path angle change of 3 degrees is shown commanded by altitude. Thus, the dispersion output at the bottom of Figure E-11(k) shows zero deviation in the estimated state after the pull out from the descent. The actual state deviations are then equal to the altimeter error, 50 feet. It is assumed that the steering time constants are increased after the aircraft enter the terminal area. This represents the tighter control of the aircraft maintained by the pilot when maneuvering in the terminal area and preparing to enter the microwave landing system. Thus, control effort for crosstrack errors (heading corrections) jumps from 37 degrees to 60 degrees after leveling out from the descent. The analysis concludes with the output at the bottom of Figure E-11(l), showing an along-track deviation resulting in time-of-arrival variance of 153.19 seconds with a crosstrack deviation of 0.38 n.mi. and 50-foot altitude deviations. This output is the result for the point where the aircraft is assumed to enter the MLS. As mentioned earlier, the entire run is summarized in Figure E-12. Figure E-12 shows the waypoints, the velocity, heading, and flight path angle of

APPENDIX E

the aircraft between waypoints, and the navigation aids used. The dispersions at the intersection with the MLS are repeated in Figure E-12. If no cruise output had been selected (print option zero), Figure E-12 would be the only output produced. To maintain a check on the analysis during the cruise conditions, the maximum 1σ deviations of the aircraft in the three coordinates (along track, cross-track, and altitude) are summarized. In this particular run, maxima in all three coordinates occurred at 25.54 seconds. Particular attention should be paid to the seemingly large altitude deviation, 2,240 feet. This number is somewhat misleading. 23.54 minutes is the point during the mission when the pull out from descent to approach maneuvering is begun. At this time, the nominal altitude of the aircraft is 1,000 feet. It would be erroneous, however, to assume that because the altitude deviation are 2,240 feet, a high probability of contact with the ground exists. It must be remembered that it was specified that pull out from descent would be made when the altimeter indicated the desired altitude. Thus, for a perturbed run with a lower altitude, pull out would be made earlier and an altitude of 2,240 feet less than nominal would be not reached near the end of the descent. Referring back to the output for 23.54 minutes (at the center of Figure E-11(k)), just prior to the flight path change of 3 degrees, the altitude deviation of 2,239 feet are shown. Since a pull out would be made when the indicated altitude equaled the desired nominal of 1,000 feet, the assumed normal distribution of all errors would be truncated. These large altitude deviations are more reasonably interpreted midday in the descent portion of the flight. For example, at 20 minutes (the bottom of Figure E-11(j)), altitude deviations of 1,901.7 feet are shown with the nominal altitude at 4,284 feet. These deviations occur because it is assumed that the pilot began the descent when his indicated along-track position was at the nominal value for beginning the descent. Since deviations of the estimated along-track position are on the order of 2 minutes, an observer on the ground would note deviations of approximately 1,900 feet in aircraft passing over his head with these statistics.

In addition to the case summary shown in Figure E-12, a summary of all cases in a run, shown in Figure E-13 is produced. Figure E-13 shows the various combinations of system configurations evaluated during this study. The airport pairs considered are indicated by the leg indices 1 through 3. Update types are (1) Kalman filter and (2) position fixes. The probabilities of intersecting the MLS beam with sufficient distance to maneuver prior to descent on the glide slope are shown in the right-hand column of Figure E-13. These numbers are the input to the Monte Carlo analysis from ANGCAP. The Monte Carlo analysis computes on a random basis the modes available in each flight as it enters the MLS. Each mode is then defined in terms of the system configurations shown in Figure E-13 and the appropriate probability of suitable encounter with the MLS is used.

APPENDIX E

References

- E-1 Sullivan, Neil, and Taylor, James K., "Tactical Instrument Landing (TACLAND) System Study", AFFDL-TR-68-22, AD 836650, Bell Aerosystems Company, May 1968.

APPENDIX F

CREW PERFORMANCE

Review of Crew Performance Estimation Methods

Three contractor reports prepared by Bolt, Beranek and Newman, Inc. (BBN) (refs. F-1 through F-3) and one report by Bunker-Ramo have been reviewed (ref. E-4). The Bunker-Ramo approach is basically one of task analysis and workload estimation. It does not lend itself to modeling man in the loop and, hence, is not further discussed.

In general, BBN models the human operator as an optimal controller "subject to his inherent limitations and constraints" (refs. F-1 and F-2). Nonetheless, their representation of the optimal controller is always the linear, quadratic cost, completely observable representation. This framework is said to allow a systematic approach to the modeling of human operators. In contrast, the quasilinear describing function model of the human operator, used by Systems Technology Incorporated (STI), is said to rely "heavily on judgments concerning the closed-loop system structure" (ref. F-2).

It would appear that, in the simple tasks analyzed, the two approaches are equivalent. With the infinite time Kalman filter formulation, the BBN human operator consists of a two-state (second order) estimator with certain gain constants. The STI human operator is also modeled by a second order system. BBN must make judgments concerning the manner in which the human operator weighs his performance index; STI must make value judgments concerning the frequency response of the crossover model they employ. In reality, by modifying the performance index, the frequency response of the operator is altered. This dual nature is even pointed out by BBN when they state that "there is a one-to-one correspondence between g and τ_n , the smaller g , the smaller is τ_n " (ref. F-2). The g is the performance index weight on the derivative of control action; τ_n is the neuromuscular lag time constant.

For multitask assignments, BBN predicts the amount of fixation time per task by minimizing an optimal control problem subject to the length of duration on a particular task. Good agreement is shown for a two-task assignment.

Senders and Carbonnel (also with BBN) predict fixation time as a function of the frequency content of the signal being received (refs. F-5 and F-6). Good agreements have also been reported in this case.

The basic difference between the approach used by BBN and STI appears to be the following: the BBN time domain approach allows one to expand their model in situations where their linear quadratic model does not adequately predict human operator response. The display requirements

APPENDIX F

study indicated that the human operator exhibited no control when the error was small instead of a control directly proportional to the error as predicted by optimal control theory. BBN thus modified their model to account for this dead band instead of just getting an approximate overall linear model (ref. F-3).

In contrast, the STI model has remained relatively fixed over the years. The compensation limitations of the human operator are built into the model. Any gross nonlinearities would defy classical frequency domain analysis. This is not to suggest that the power of the BBN model is necessarily a worthwhile feature. The optimal control model and human operator response are in fairly close agreement if the human operator can perform the task. Hence, the model predicts the most optimistic response for the human operator. Thus, if the optimal control model predicts inferior performance, the human operator will exhibit inferior performance. But, if the optimal control model predicts adequate performance, a judgment must be made whether a well-trained human operator can duplicate this performance. This is especially difficult to determine for higher order plants not dominated by the first and second order characteristics presently studied. The optimal controller can assimilate all the information regarding the plant characteristics, the observed deviations, and the control actions. The human operator has a finite memory time and a limited capability. If the task is too difficult and stress increases, his performance will decrease. Hence, it would appear that the BBN model must be used with care in order to avoid optimistic conclusions.

In contrast to the models above, whose formulation is essentially based on mathematical tractability, several hierarchical models of human operators have been proposed. These models inherently limit the capabilities of the human operator (as the STI model), but the technique is not limited to classical analysis. The models qualitatively postulate the structure of the human operator control laws and then formulate a theory to determine the qualitative amount of action. The models postulate that, at any one time, only one task is actively being controlled. However, a second task may be monitored.

The remaining tasks are placed in a "hold" mode until the operator is finished with the present task and decides to actively control one of the remaining tasks. The next task to be controlled is determined by a decision hierarchy which determines the variable to be controlled and the extent of control based on the system error and the amount of operator stress.

Because of this generality, these models have the potential for modeling the human operator in a more detailed manner. In actuality, none of the hierarchical models investigated has a completely defined decision hierarchy. In addition, the quantitative control laws

APPENDIX F

are arrived at in a somewhat "fuzzy" fashion. Since extensive model matching is needed at the present time, it is difficult to determine whether these models can be used at the present time to predict human operator performance.

Benjamin has used an hierarchical model to describe a human operator in a simple helicopter flying task (ref. F-7). In the simulation, only one control loop was closed at a time, corresponding to the highest level of hierarchy which has error values in the range of concern. The simulated data compared favorably with the real time simulator data.

Wherry has formulated an extensive hierarchical model for simulating aircraft scenarios (ref. F-8). However, except for simple psychomotor tasks, little of the actual theory and even less experimental verification has been accomplished.

In both models, the active control law was formulated as a monotonic function of the error as follows; a deadband region, a step rise, a linear rise, and a saturating limit. There were more than one such curve depending on the amount of pilot stress. The decision hierarchy is based upon vehicle stability considerations.

As one can see, while the above approaches may be intuitively appealing, there are so many variables that it is difficult to determine, from actual experimental data, the values to assign to the variables.

It should be noted, however, that the recent work of BBN has included a deadzone region and is addressing itself to the problem of controlling one task at a time. In addition, reduced state estimation theory may be helpful in modeling the inability of the human operator to optimally estimate all the state variables. Hence, control theoretic aspects may be used to quantify the variables in these hierarchical models. In this way, their full potential could be exploited.

APPENDIX F

REFERENCES

- F-1 Baron, S., et al, "Application of Optimal Control Theory to the Prediction of Human Performance in a Complex Task", Air Force Flight Dynamics Lab, Wright-Patterson Air Force Base, Ohio, AFFDL-TR-69-81 (March, 1970).
- F-2 Kleinman, D., and Baron, S., "Manned Vehicle Systems Analysis by Means of Modern Control Theory", NASA Electronics Research Center, Cambridge, Massachusetts, NAS12-104 (June 26, 1970).
- F-3 Kleinman, D., and Baron, S., "Analytic Evaluation of Display Requirements for Approach to Landing", NASA Ames Research Center, Moffett Field, California, NASA CR-1952 (November, 1971).
- F-4 Finley, D. L., et al, "Human Performance Prediction in Man-Machine Systems, Vol. 1-A Technical Review", NASA Ames Research Center, Moffett Field, California, NASA CR-1614 (August, 1970).
- F-5 Senders, J. W., "The Human Operator as a Monitor and Controller of Multidegree of Freedom Systems", IEEE Trans, on Human Factors in Electronics, Vol. HFE-5, No. 1, pp. 2-5 (September, 1964).
- F-6 Carbonell, J. R., "A Queueing Model of Many-Instrument Visual Sampling", IEEE Trans, on Human Factors in Electronics, Vol. HFE-7, No. 4, pp. 157-164 (December, 1966).
- F-7 Benjamin, P., "A Hierarchical Model of a Helicopter Pilot", Human Factors, Vol. 12, No. 4, pp. 361-374 (August, 1970).
- F-8 Wherry, R. J., "The Development of Sophisticated Models of Man-Machine Systems Performance", Girard W. Levy, Editor, North American Rockwell Corporation, Columbus, Ohio, NR 69H-591 (November, 1969).